

COMBINATORIAL TECHNIQUES IN OPERADIC HOMOTOPY THEORY

KURT STOECKL

ORCID: 0000-0001-5753-5522

Doctor of Philosophy

Submission Date: January 2025

School of Mathematics and Statistics, The University of Melbourne, Victoria, Australia

Submitted in total fulfilment of the degree of Doctor of Philosophy.

ABSTRACT. This thesis consists of the paper "Koszul Operads Governing Props and Wheeled Props", and the joint paper "Diagonals of Permutahedra", with Bérénice Delcroix-Oger, Guillaume Laplante-Anfossi and Vincent Pilaud. These bodies of work are presented alongside a cohesive background, summary, and brief exploration of two problems in their intersection. In the intersection, we discuss feasible methods for constructing tensor products of connected homotopy operadic structures. Secondly, we show that although there is precisely one notion of a shuffle operad up to isomorphism, there are many possible strict notions of shuffle operads.

The first included publication "Koszul Operads Governing Props and Wheeled Props", extends Groebner bases to groupoid coloured operads, to prove the operads whose algebras are props and wheeled props are Koszul. This is accomplished by new biased definitions for (wheeled) props, and an extension of the theory of Groebner bases for operads to apply to groupoid coloured operads. Using the Koszul machine, we define homotopy (wheeled) props, and show they are not formed by polytope based models. Finally, using homotopy transfer theory, we construct Massey products for (wheeled) props, show these products characterise the formality of these structures, and re-obtain a theorem of Mac Lane on the existence of higher homotopies of (co)commutative Hopf algebras.

The second included publication "Diagonals of Permutahedra", provides a systematic enumerative and combinatorial study of geometric cellular diagonals on the permutahedra.

In the first part of the paper, we study the combinatorics of certain hyperplane arrangements obtained as the union of ℓ generically translated copies of the classical braid arrangement. Based on Zaslavsky's theory, we derive enumerative results on the faces of these arrangements involving combinatorial objects named partition forests and rainbow forests. This yields in particular nice formulas for the number of regions and bounded regions in terms of exponentials of generating functions of Fuss-Catalan numbers. By duality, the specialization of these results to the case $\ell = 2$ gives the enumeration of any geometric diagonal of the permutahedron.

In the second part of the paper, we study diagonals which respect the operadic structure on the family of permutahedra. We show that there are exactly two such diagonals, which are moreover isomorphic. We describe their facets by a simple rule on paths in partition trees, and their vertices as pattern-avoiding pairs of permutations. We show that one of these diagonals is a topological enhancement of the Sanbeblidze–Umble diagonal, and unravel a natural lattice structure on their sets of facets.

In the third part of the paper, we use the preceding results to show that there are precisely two isomorphic topological cellular operadic structures on the families of operahedra and multiplihedra, and exactly two infinity-isomorphic geometric universal tensor products of homotopy operads and A-infinity morphisms.

0.1. **Declarations.** I declare that: this thesis comprises only my original work towards the Doctor of Philosophy except where indicated in the preface; due acknowledgement has been made in the text to all other material used; and the thesis is fewer than the maximum word limit in length, exclusive of tables, maps, bibliographies and appendices.

0.2. Preface. The abstract of this thesis contains the abstracts of both constituent publications. Chapter 1 of this thesis, contains no original content, purely providing background and a summary of the content of this thesis. We note that most of the figures used in this chapter were taken or adapted from either the composite papers, personal research statements, or prior talks. Chapter 2 of the thesis contains original content unless otherwise indicated. Chapter 3 of this of thesis consists of publications submitted over the course of my PhD. Chapter 3.1 consists of the paper "Koszul Operads Governing Props and Wheeled Props", which was published by *Advances in Mathematics* in October 2024. The work is a natural amalgamation of existing research until Section 4.2, namely groupoid coloured operads [War22] and Groebner bases for operads [DK10], after which it is original research. Chapter 3.2 consists of the paper "Cellular Diagonals of Permutahedra", which was submitted to *Advances in Mathematics* in January 2024, and is a joint project with B  r  nice Delcroix-Oger, Guillaume Laplante-Anfossi and Vincent Pilaud. The work of this paper is wholly original; however, it makes strong use of the techniques of Laplante-Anfossi [LA22] and Zaslavsky [Zas75]. All authors contributed in part to all sections, however a very rough breakdown of contributions is as follows. Part 1, exploring the combinatorics of (l, n) -braid Arrangements, was mostly contributed by Delcroix-Oger and Pilaud, however the initial mathematics and in particular the $l = 2$ case was worked on by all authors. Part 2, focusing on operadic diagonals of the permutahedra, was mostly contributed by Laplante-Anfossi and myself, however all authors contributed, notably in Sections 4 and 5, of which the later sections directly build on. Part 3, exploring higher algebraic consequences of preceding combinatorics, was largely contributed by Laplante-Anfossi, with contributions including experimental mathematics from all authors. Note, the bibliography of this thesis contains only the citations used in Sections 1-2, and each paper of Section 3 has their own self contained bibliography. I acknowledge the support of, an Australian Government Research Training Program (RTP) Scholarship, and the Australian Research Council Future Fellowship FT210100256.

0.3. **Acknowledgements.** I am indebted to many people for their guidance throughout my PhD. I would like to thank my supervisor Marcy Robertson, for her endless support, insight and commentary. This thesis would not have existed without your help. I would like to thank my prior supervisor Richard Brak, for imparting his love of combinatorics, and for being an all round great person. I would like to thank my collaborators B  r  nice Delcroix-Oger, Guillaume Laplante-Anfossi and Vincent Pilaud. Our project was a highlight of my PhD, and working alongside you has greatly improved my understanding of both mathematics and its communication. I would like to thank my co-supervisors and chair, Jan de Gier, Kari Vilonen, and Paul Zinn-Justin, for their guiding questions and their time.

CONTENTS

0. Preliminaries	1
0.1. Declarations	3
0.2. Preface	4
0.3. Acknowledgements	5
1. Introduction	7
1.1. Background	7
1.2. Summary	10
2. Connections	14
2.1. Tensor Products of Connected Homotopy Operadic Structures	14
2.2. Shuffle Operads	15
3. Included Publications	19
3.1. Koszul Operads Governing Props and Wheeled Props	19
3.2. Cellular Diagonals of Permutahedra	100
References	171

1. INTRODUCTION

1.1. Background. Operadic structures and their representations/algebras use families of graphs to model the composition of functions. Let's consider a concrete example in the case of *operads*, which consist of a sequence of sets of n -ary operations, which compose in a tree like fashion. Let (\mathcal{E}, \boxtimes) be a symmetric monoidal category, such as the category of sets with the Cartesian product (Set, \times) , or the category of vector spaces over a field \mathbb{K} with the tensor product $(Vect, \otimes)$. The most fundamental operad is the *endomorphism operad*. Let X be an object of the monoidal category, a vector space or a set respectively. Then the set of n -ary operations of the endomorphism operad End_X is defined to be $Hom_{\mathcal{E}}(X^{\boxtimes n}, X)$, i.e. the maps of sets from $X^{\boxtimes n} \rightarrow X$, or the linear transformations from $X^{\boxtimes n} \rightarrow X$. These operations can be composed to produce further operations. This operad is of critical importance as it lets us define the algebras of all other operads. To see this, we introduce one further example, the non-symmetric associative operad in (Set, \times)

$$(1) \quad As := F(\bigwedge) / \langle \bigwedge \bigwedge \bigwedge \stackrel{r_1}{=} \bigwedge \bigwedge \bigwedge \rangle = \text{The set of all binary planar trees modulo the relation } r_1.$$

An *algebra* over an operad P , is then defined to be a morphism of operads $A : P \rightarrow End_X$. Informally, A is some kind of generalised functor which realises each abstract operation/tree of P as a concrete operation in End_X . For instance, if X is a set then $A : As \rightarrow End_X$ is a classical monoid in X , as the binary tree with one vertex \wedge is realised as $f : X \times X \rightarrow X$ and r_1 forces f to be associative. Alternatively, if X is a vector space and $\mathbb{K}As$ is the \mathbb{K} -linearisation of As , then $A : \mathbb{K}As \rightarrow End_X$ is an associative algebra.

The descriptive power of this approach is not limited to trees. Two more complicated operadic structures, *properads* and *prop(erads)*, use directed and respectively connected graphs, to model the composition of functions with multiple inputs and multiple outputs. The endomorphism prop(erad) End_X in (\mathcal{E}, \boxtimes) , is defined to have operations with n inputs and m outputs $Hom_{\mathcal{E}}(X^{\boxtimes n}, X^{\boxtimes m})$, and an algebra over a prop(erad) P is again defined to be a morphism of prop(erads) $A : P \rightarrow End_X$. Many familiar algebraic structures are algebras over prop(erads), such as bialgebras, Lie bialgebras and Hopf algebras (Table 1).

Family	An Example Element of Operadic Family		Its Algebras in Vect
	Generators	Relations	
Operads	\wedge	$\bigwedge \bigwedge \bigwedge \stackrel{r_1}{=} \bigwedge \bigwedge \bigwedge$	Associative Algebras
Properads	\wedge, \vee	$\bigwedge \bigwedge \bigwedge \stackrel{r_1}{=} \bigwedge \bigwedge \bigwedge, \bigvee \bigvee \bigvee \stackrel{r_2}{=} \bigvee \bigvee \bigvee, \bigvee \bigwedge \bigwedge \stackrel{r_3}{=} \bigwedge \bigvee \bigvee$	Bialgebras
Props	$\wedge, \vee, \bullet, \circ$	r_1, r_2, r_3 and, $\bigwedge \bigwedge \bigwedge \stackrel{r_4}{=} \bigwedge \bigwedge \bigwedge, \bigvee \bigvee \bigvee \stackrel{r_5}{=} \bigvee \bigvee \bigvee, \bigwedge \bigvee \bigvee \stackrel{r_6}{=} \bigvee \bigwedge \bigwedge, \bigvee \bigwedge \bigwedge \stackrel{r_7}{=} \bigwedge \bigvee \bigvee, \bigwedge \bigwedge \bigwedge \stackrel{r_8}{=} \bigwedge \bigwedge \bigwedge, \bigvee \bigvee \bigvee \stackrel{r_8}{=} \bigvee \bigvee \bigvee$	Hopf Algebras

TABLE 1. Examples of Operadic Structures and their Algebras.

Note, every operad is a properad, and every properad is a prop, but the converse need not hold. For instance, a Hopf algebra is not an algebra over a properad, as disconnected graphs are needed to model the (co)unital and antipodal relations of Table 1. Given their descriptive power, operadic structures and their algebras are ubiquitous in mathematics, for instance arising naturally in the study of deformation theory [AM22], [MV09], differential geometry [MMS09], knot theory [DHR21], [DHR23], and topology [BV06], [WW16].

Perhaps the greatest utility of operadic structures, is how readily they extend to describe relations which only hold up to homotopy. A classical example is that of *path spaces*. If X is a topological space, then $P(X) := \text{Hom}_{\text{Top}}([0, 1], X)$, the set of continuous functions from the interval into X equipped with the compact-open topology, admits a multiplication μ which is only associative up to homotopy. This multiplication takes two different paths with the same start and end point, and composes them into a new path which traverses each sub-path in half the total time.

$$\mu(\mu(e, f), g) = 1/4 \left(\begin{array}{c} \text{1/4} \text{ } \text{1/2} \\ \text{1/2} \end{array} \right) \cong 1/4 \left(\begin{array}{c} \text{1/2} \text{ } \text{1/4} \\ \text{1/4} \end{array} \right) = \mu(e, \mu(f, g)), \text{ where } \mu(p_1, p_2) := \begin{cases} p_1(2t), & 0 \leq t \leq 1/2 \\ p_2(2t - 1), & 1/2 \leq t \leq 1 \end{cases}$$

There are many homotopies which continuously deform $\mu(\mu(e, f), g)$ into $\mu(e, \mu(f, g))$. However, these homotopies can also be continuously deformed into one another, yielding homotopies between homotopies, and so on. Thus, we seek some method to parcel this infinite tower of intricately related higher homotopies.

The A_∞ operad is a *minimal model* for the non-symmetric associative operad $\mathbb{K}As$ (see for instance [LV12]). It is a homotopy associative generalisation of $\mathbb{K}As$, or formally, the smallest possible cofibrant resolution of $\mathbb{K}As$ (up to isomorphism), in the model category of algebraic operads. Alternatively, A_∞ is an operad in the category of differential graded vector spaces $dgVect$, endowed with a morphism of operads $m : A_\infty \rightarrow \mathbb{K}As$ which is both an epimorphism and a quasi-isomorphism. The operad has the explicit form,

$$(2) \quad A_\infty := (F((\mu_n)_{n \geq 1}), d), \text{ where } \mu_n \text{ is a } n\text{-ary operation also denoted } \mu_n = \begin{array}{c} \diagup \quad \diagdown \\ \dots \end{array}.$$

The operation μ_1 encodes a differential, $\mu_2 = \wedge$ corresponds to the generator of As , for $n \geq 3$ each μ_n encodes homotopies via their derivation $\partial(\mu_n)$, and d is a differential that is also *quadratic* (i.e. $d^2 = 0$ and d restricts to $d : E \rightarrow F(E)^{(2)}$ cutting each generator μ_n into a summand of two pieces). Famously, the derivations $\partial(\mu_n)$ are encoded via the associahedra [Sta63]. The associahedron K_n , is a cell complex, which can be realised as a *convex polytope* (the convex hull of a collection of points in \mathbb{R}^n), and whose cells are bijection with planar trees (see Fig. 1).

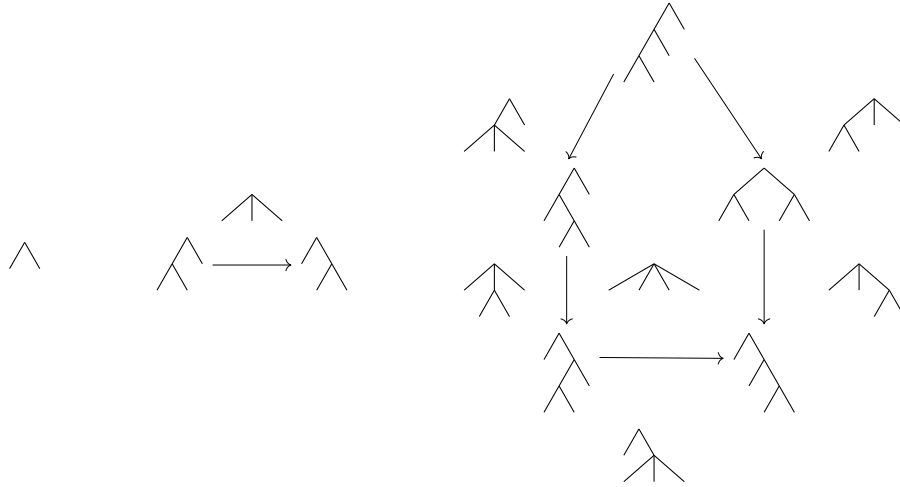


FIGURE 1. From left to right, the associahedra K_1, K_2 and K_3 , with their cells labelled via the bijection to planar trees (see [Sta63] and Appendix C.2.1 of [LV12]).

The boundary operator of the outer cell of K_n yields the derivation of μ_{n+1} , e.g.

$$\partial(\mu_2) = \begin{array}{c} \diagup \quad \diagdown \\ \diagdown \quad \diagup \end{array} - \begin{array}{c} \diagup \quad \diagdown \\ \diagup \quad \diagdown \end{array}, \quad \partial(\mu_3) = \begin{array}{c} \diagup \quad \diagdown \\ \diagdown \quad \diagup \end{array} + \begin{array}{c} \diagup \quad \diagdown \\ \diagup \quad \diagdown \end{array} - \begin{array}{c} \diagup \quad \diagdown \\ \diagdown \quad \diagup \end{array} - \begin{array}{c} \diagup \quad \diagdown \\ \diagup \quad \diagdown \end{array} - \begin{array}{c} \diagup \quad \diagdown \\ \diagdown \quad \diagup \end{array}.$$

How do these encode homotopies? Well, if $\partial(\mu_3) = 0$ then one observes the associativity relation r_1 holds strictly (Eq. (1)). Thus, μ_3 is an obstruction to strict associativity. Each successive μ_n is then an obstruction to a relation in terms of μ_i for $i < n$. Indeed, the dg operad $\mathbb{K}As$ is equivalent to an A_∞ operad in which for all $n \geq 3$ we have that $\partial(\mu_n) = 0$. Thus in general, algebras over the A_∞ operad realise μ_2 as a homotopy associative map $f_2 : X \otimes X \rightarrow X$, and the higher μ_n as homotopies $f_n : X^{\otimes n} \rightarrow X$. The associahedra provides an intrinsically beautiful encoding of all higher homotopies, but there are additional practical reasons to want polytope based quadratic minimal models.

Given two associative algebras A, B it is straightforward to show that their tensor product $A \otimes B$ is also an associative algebra, with an explicit product defined by $\mu(a \otimes b, a' \otimes b') := \mu_A(a, a') \otimes \mu_B(b, b')$. Given two A_∞ algebras A, B , one can reason via abstract nonsense that $A \otimes B$ is an A_∞ -algebra, but explicating the operations is more subtle. However, it turns out that because A_∞ admits a polytope based model, and this polytope admits a known convex realisation, any coherent cellular approximation of the diagonal of this polytope can be used to explicitly construct these higher operations [SU04], [MS06]. Let's briefly unpack this. A *cellular diagonal* of a convex polytope P is a cellular approximation of the thin diagonal $\triangle : P \rightarrow P \times P$ defined by $\triangle(x) := (x, x)$. That is to say, a cellular diagonal is an approximation of \triangle up to homotopy, which agrees on the vertices of $P \times P$, and whose image is a union of cells of $P \times P$.

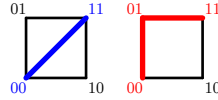


FIGURE 2. The *thin* and a *cellular* diagonal of the interval $[0, 1]$.

A cellular diagonal is said to be *coherent*, if for every face f of P , the restriction to f is also a cellular diagonal. These coherent cellular diagonals induce explicit functorial tensor products of the homotopy structure(s) encoded via the polytope. In essence, the coherence condition induces the necessary coherence in the constructed homotopies. This means that an elegant combinatorial expression for a coherent cellular diagonal of the associahedra, such as the magical formula of [MTTV21], translates into an elegant formula for the tensor product of A_∞ -algebras.

An operad P is said to be *Koszul* if it has a minimal model with a quadratic differential (see around Eq. (2)). There are many other equivalent definitions. Note that by this definition, the (polytope based) quadratic minimal model of $\mathbb{K}As$ shows that it is Koszul. Proving an operad P is Koszul provides many powerful results, including the following.

- It provides an explicit formula for a quadratic minimal model P_∞ , and many equivalent characterisations of P_∞ -algebras (Corollary 7.4.3. and Theorem 10.1.13 of [LV12]). A key feature of these characterisations is the phenomena of Koszul duality. For example, the operad $\mathbb{K}As$ is Koszul self dual, and the operad whose algebras are commutative algebras is Koszul dual with the operad whose algebras are Lie algebras. Hence, an A_∞ -algebra is a codifferential on a cofree coassociative coalgebra, and a L_∞ -algebra, or homotopy Lie-algebra, is a codifferential on a cofree cocommutative coalgebra (Proposition 10.1.12 of [LV12]).
- It provides access to homotopy transfer theory (Theorem 10.3.1 of [LV12]). That is to say, the homotopy retract of any P -algebra has the explicit data of a P_∞ -algebra. For example, the homology of any P -algebra is a P_∞ -algebra. This higher structure in the homology is known as Kaledin classes, it subsumes the Massey products, and completely characterises the formality of the operad [Emp24].
- It provides resolution and rectification results for P -algebras (Proposition 11.4.2, and Theorems 11.4.2 and 11.4.8 of [LV12]). In particular, the homotopy category of dg P -algebras is equivalent to the homotopy category of P_∞ -algebras with ∞ -morphisms

$$Ho(P\text{-alg}) \cong Ho(\infty\text{-}P_\infty\text{-alg}).$$

Any P -algebra can be resolved into a P_∞ -algebra via a generalised bar-cobar resolution, and any P_∞ -algebra can be rectified into a P -algebra. Applying these results to the associative operad $\mathbb{K}As$ recovers the classical bar resolution of associative algebras, and their resolution/rectification results.

We have seen that operads with polytope based quadratic minimal models are both Koszul, and have a feasible method for constructing explicit tensor products of their homotopy algebras. Unfortunately, there are operads which are Koszul and which do not admit polytope based models (such as Theorem 1). Thus, we briefly discuss an alternate method for proving an operad is Koszul. A non-symmetric quadratic operad P is Koszul if its relations can be directed into a convergent rewrite system (see for instance [Lau24]). Let's unpack this. An operad P is said to be quadratic if it admits a presentation in terms of generators and relations $P = F(E)/\langle R \rangle$, where every relation in R is composed of terms using exactly two generators. For instance, $\mathbb{K}As$ is quadratic as the sole relation r_1 has two terms each using two generators Eq. (1). Furthermore, we can direct r_1 to

$$\begin{array}{c} \diagup \quad \diagdown \\ \diagdown \quad \diagup \end{array} \xrightarrow{r_1} \begin{array}{c} \diagup \quad \diagdown \\ \diagup \quad \diagdown \end{array}$$

and this induces a rewrite system R on the set of binary trees, where a pair of binary trees $(T_1, T_2) \in R$ if T_2 is the result of rewriting a subtree of T_1 via r_1 . For instance, every directed arrow (or oriented cell) of Fig. 1 is a rewrite in R . A rewrite system is convergent if all possible rewrites from a common starting point terminate at the same end point. The rewrite system R on $\mathbb{K}As$ is convergent, as every binary tree can be successively rewritten into a tree with no left children. Alternatively, Bergman's Diamond Lemma [Ber78] implies that a terminating rewrite system is convergent if and only if it is locally convergent. Thus, the oriented cells of K_3 in Fig. 1 actually constitute a proof that $\mathbb{K}As$ is Koszul.

In the case of operads, this rewriting approach was first developed in [Hof10] and [DK10]. Where it was shown that a symmetric operad P is Koszul, if an associated non-symmetric shuffle operad P^f admits a quadratic Groebner bases, or equivalently P^f admits a quadratic PBW bases. Here, admitting a bases amounts to checking the convergence of a specific rewrite system as before. The map $-^f$ is a clever way of forgetting the symmetries of an operad whilst conserving the underlying elements. More formally, one of the equivalent characterisations of an operad P being Koszul is that the homology of its bar complex $B(P)$ is concentrated in a particular degree. However, the forgetful functor $-^f$ induces an isomorphism of bar complexes (Section 1.2 of [DK13]), thus

$$(B(P^f) \cong B(P)^f) \Rightarrow (P^f \text{ is Koszul} \iff P \text{ is Koszul}).$$

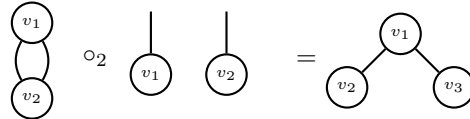
This is why we need only work with the associated non-symmetric shuffle operad P^f .

1.2. Summary. Building from this background, we now informally summarise the essential ideas of the publications present in this thesis. This section is intended to be self-contained given Section 1.1, and complementary to each respective paper.

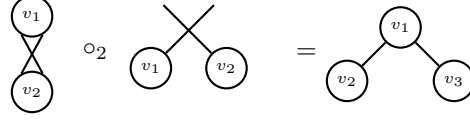
1.2.1. Koszul Operads Governing Props and Wheeled Props. Props, introduced in the uncoloured $dgVect$ case by Adams and Mac Lane ([ML65]), are a symmetric monoidal category whose objects are generated by a free monoid. A wheeled prop, see [MMS09], is a prop with an additional trace operation. Alternatively, as we claimed in Section 1.1, a prop is a set of operations which compose like directed acyclic graphs. One way to formalise this sentence is, there exists a groupoid coloured operad P whose algebras are (coloured) props in Set . The n -ary operations of P are defined to be

$$P\left(\begin{array}{c} \underline{d} \\ \underline{c} \end{array}\right) := \begin{array}{l} \text{The set of directed acyclic graphs with } n \text{ labelled vertices, such that:} \\ \text{the graph has profile } \left(\begin{array}{c} \underline{d} \\ \underline{c} \end{array}\right) \text{ (inputs } \underline{c} \text{ and outputs } \underline{d}\text{); and the } i\text{th vertex has profile } \left(\begin{array}{c} \underline{d}_i \\ \underline{c}_i \end{array}\right). \end{array}$$

Here $\underline{c}, \underline{d}, \underline{c}_i, \underline{d}_i$ are sequences of colours drawn from some underlying set of colours \mathfrak{C} . These sets compose like coloured trees (i.e. we can only perform graftings of matching colours) via graph substitution. That is to say, if we have two graphs, in which the entire profile of the second graph matches the i th vertex of the first graph, then we can substitute the second graph into the i th vertex. For instance,



Assuming all edges are the same colour, and using n to denote the unique sequence of length n drawn from a singleton set, the graphs are respective elements of $P\left(\begin{smallmatrix} (0) \\ (2), (2), (0) \end{smallmatrix}\right), P\left(\begin{smallmatrix} (2) \\ (1), (1), (0) \end{smallmatrix}\right), P\left(\begin{smallmatrix} (0) \\ (2), (1), (1), (0) \end{smallmatrix}\right)$. This operad P , is groupoid coloured in the sense that we can move permutations around in an equivariant fashion. For instance an equivalent way of forming the same graph, under an explicit action of the groupoid, is the following,



In fact, the actions of the groupoid on P completely encodes the equivariance axioms of props. This is advantageous, as P can be shown to admit a quadratic presentation $P \cong F(E)/\langle R \rangle$ where the quadratic relations R consist of all non-equivariant ways of forming all graphs with three vertices, see Fig. 3 for two such relations (or formally Section 6.2 [Sto24]). Note that trying to obtain this presentation without using a groupoid colouring will result in a quadratic unary presentation; see [DV21] for this case for operads.

Essentially the same approach yields a quadratic groupoid coloured operad W whose algebras are wheeled props in *Set*. Thus, if the linearisations of these operads $\mathbb{P} := \mathbb{K}P$ and $\mathbb{W} := \mathbb{K}W$, over a \mathbb{K} field of characteristic 0, could be shown to be Koszul, then the Koszul machine would yield the many powerful results sketched in Section 1.1.

The theory of Koszul duality was first extended to groupoid coloured operads in [War22]. In the same paper, Ward showed that the groupoid coloured operad whose algebras are modular operads is Koszul, before using the Koszul machine to study generalised bar-cobar resolutions, and Massey products of modular operads. Prior to [Sto24], the most general result had been obtained by two different groups of authors.

Theorem 0 ([BM23], [KW23]). The operads governing connected operadic structures

- (1) are Koszul,
- (2) are Koszul self-dual, and
- (3) have minimal models governed by polytopes.

Although their proof methods differed, the common thread of both approaches was using polytopes to parse the minimal models of each operad. Unfortunately, this approach is not feasible for props and wheeled props.

Theorem 1 ([Sto24]). The operads governing props and wheeled props

- (1) are Koszul,
- (2) are not Koszul self-dual, and
- (3) do not have minimal models governed by polytopes.

Thus, the second main result of this paper, which was used to obtain Theorem 1 and can recover Theorem 0, was extending the technique of Groebner bases for operads to groupoid coloured operads.

Theorem 2 ([Sto24]). Let P be a groupoid coloured operad such that the associated coloured shuffle operad $(P^f)_*$ admits a quadratic Groebner basis, then P is Koszul.

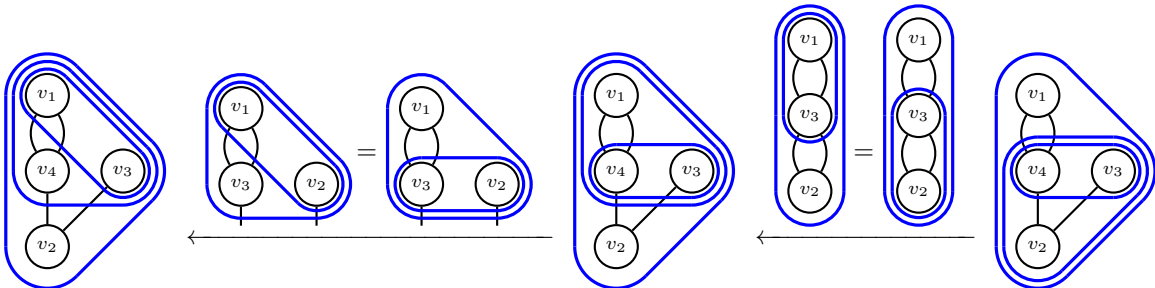


FIGURE 3. Proving that the operad governing props \mathbb{P} is Koszul using Theorem 2 amounts to showing that every labelled directed acyclic graph has a unique minimal nesting (encoding graph substitutions), and every other nesting can be rewritten into it using quadratic relations. Here is one such minimal nesting, and two successive rewrites to it, where the relation corresponding to each rewrite is displayed above the arrow.

The proof of Theorem 2 lies in studying the forgetful functors between groupoid coloured symmetric modules and discrete-coloured non-symmetric modules. As discussed in Section 1.1, the functor $-^f$ from symmetric modules to non-symmetric modules, which forgets the action of the symmetric group, induces an isomorphism of bar complexes. There is a similar forgetful functor $-^{fv}$ from groupoid coloured modules to discrete coloured modules, which forgets the action of the groupoid. In this case, $-^{fv}$ only induces an epimorphism of bar complexes (Section 4.2 of [Sto24]),

$$(B(P^{fv}) \twoheadrightarrow B(P)^{fv}) \Rightarrow (P^{fv} \text{ is Koszul} \Rightarrow P \text{ is Koszul}).$$

However, this is sufficient to prove Theorem 2 given $(P^f)^{fv}$ admits a computable presentation $(P^f)_*$.

1.2.2. Cellular Diagonals of Permutohedra. This joint paper with Bérénice Delcroix-Oger, Guillaume Laplante-Anfossi and Vincent Pilaud, sought to provide a complete combinatorial characterisation of the cellular diagonals of a well known polytope, the permutahedra. Aside from combinatorial interest, it was hoped that studying these diagonals would characterise its induced tensor products of homotopy operads, A_∞ -algebras and A_∞ -morphisms (see sketch of Section 1.1, and [LA22], [LAM23]).

The *permutahedra* $\text{Perm}(n)$, is the convex hull of all permutations in the n th symmetric group, considered as coordinates in \mathbb{R}^n . A common technique in the study of polytopes, is to study associated hyperplane arrangements, in particular their normal fans. Informally, a hyperplane arrangement \mathcal{H} is a set of hyperplanes in \mathbb{R}^d , and the normal fan of $\text{Perm}(n)$ is the braid arrangement \mathcal{B}_n (Definition 1.9 of [DOLAPS23]).

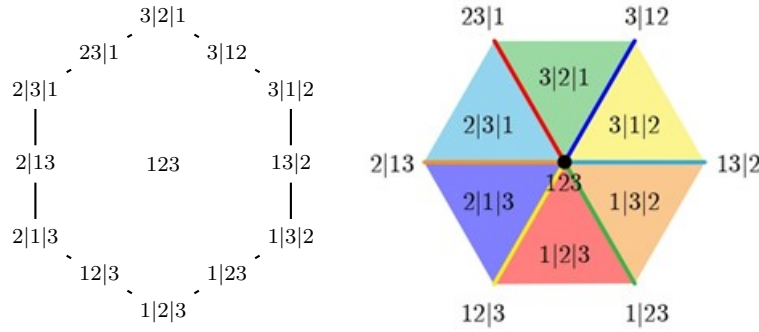


FIGURE 4. A projection of $\text{Perm}(3)$ in \mathbb{R}^2 with faces labelled by ordered partitions (left), and its normal fan, the braid arrangement \mathcal{B}_3 (right). The three hyperplanes, six regions and sole vertex (triple intersection point) of \mathcal{B}_3 are labelled through their duality to $\text{Perm}(3)$.

All possible unions of the regions resulting from $\mathbb{R}^d \setminus \bigcup_{H \in \mathcal{H}} H$ defines what is known as the *face poset*, and all possible intersections of a hyperplane arrangement \mathcal{H} defines what is known as the *flat poset*.

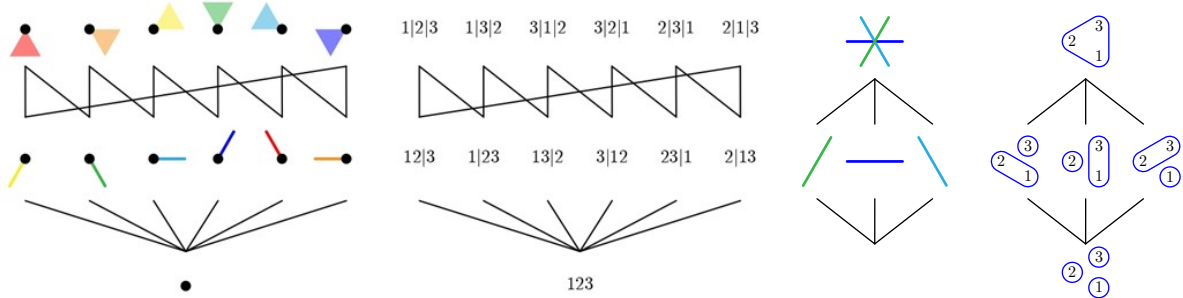


FIGURE 5. The face poset $\text{Fa}(\mathcal{B}_3)$ of the braid arrangement \mathcal{B}_3 where faces are represented as cones (left); $\text{Fa}(\mathcal{B}_3)$ where faces are represented as ordered set partitions (mid left); the flat poset $\text{Fl}(\mathcal{B}_3)$ of the braid arrangement \mathcal{B}_3 where flats are represented as intersections of hyperplanes (mid right); $\text{Fl}(\mathcal{B}_3)$ where flats are represented as set partitions (right).

Crucially, as the normal fan of the permutahedra $\text{Perm}(n)$ is the braid arrangement, the dual of a diagonal of $\text{Perm}(n)$ is a hyperplane arrangement \mathcal{B}_n^2 consisting of two generically translated copies of \mathcal{B}_n (see Fig. 6).

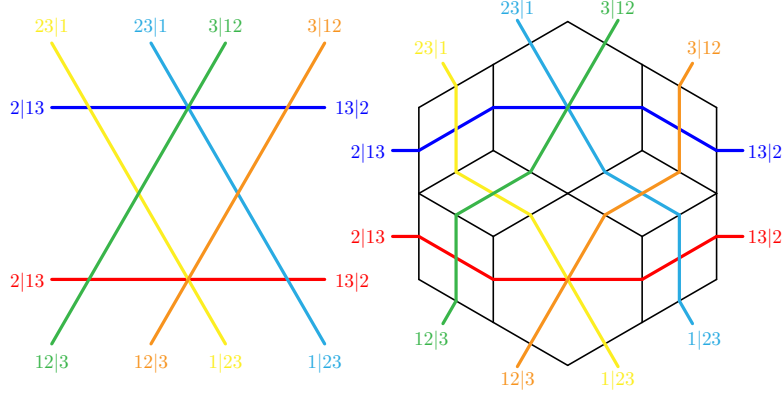


FIGURE 6. The duality between the $(2,3)$ -braid arrangement \mathcal{B}_3^2 (left) and a cellular diagonal of the permutahedron $\text{Perm}(3)$ (right).

By exploiting techniques of [Zas75] we obtained enumeration results for the flat and face posets of \mathcal{B}_n^l , the hyperplane arrangement consisting of l generically translated copies of \mathcal{B}_n . Our most general enumerative result was a Möbius polynomial ([DOLAPS23] Theorem 2.4), which simplified via alternate combinatorial characterisations to elegant formulae for the number of vertices, regions and bounded regions of \mathcal{B}_n^l .

Theorem 3. [DOLAPS23] The number of vertices of the (ℓ, n) -braid arrangement \mathcal{B}_n^ℓ is

$$f_0(\mathcal{B}_n^\ell) = \ell((\ell - 1)n + 1)^{n-2}.$$

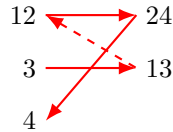
In particular, the outer faces of a cellular diagonal of $\text{Perm}(n)$ are in bijection with pairs (σ, τ) of partitions of $[n]$ whose edge graph forms a bipartite tree. More generally, all faces are in bijection with ordered bipartite forests, see Fig. 7. This combinatorial characterisation was the key to unifying the theory of coherent cellular diagonals of the permutahedra. Prior to this project, there were known to be (at least) two distinct coherent cellular diagonals of the permutahedra Δ^{SU} of [SU04], and Δ^{LA} of [LA22], and these were originally defined via drastically different formulae.

Theorem 4. [DOLAPS23] Let (σ, τ) be a pair of **ordered** partitions of $[n]$ whose edge graph forms a bipartite tree. If for all pairs of adjacent blocks, the directed path between them traverses

- the **maximal** path element **right to left**, then $(\sigma, \tau) \in \Delta^{\text{SU}}$.
- the **minimal** path element **left to right**, then $(\sigma, \tau) \in \Delta^{\text{LA}}$.

Furthermore, $\Delta^{\text{SU}}, \Delta^{\text{LA}}$ and their opposite orders are the only coherent cellular diagonals of permutahedra.

For example, every tree in Fig. 7 respects both the minimal and maximal path conditions (as Δ^{LA} and Δ^{SU} coincide for $n \leq 3$), and $(\sigma, \tau) = ((\{1, 2\}, \{3\}, \{4\}), (\{2, 4\}, \{1, 3\})) \in \Delta^{\text{SU}}$ but not Δ^{LA} as the path between the adjacent blocks $\{3\}, \{4\}$ of σ traverses the minimal path element 1 from right to left.



Given the disparate nature of the original formulae, Theorem 4 can be seen as a topological enhancement of the original Δ^{SU} diagonal [SU04], and a combinatorial enhancement of the original Δ^{LA} diagonal [LA22]. Furthermore, the fact that $\Delta^{\text{SU}}, \Delta^{\text{LA}}$ are the only coherent diagonals (and their cellular images have isomorphic posets), led to following higher algebraic consequences.

Theorem 5 ([DOLAPS23]). There are exactly two geometric universal tensor products of:

- A_∞ -algebras,

- A_∞ -morphisms, and
- homotopy operads.

In each case, both tensor products are ∞ -isotopic.

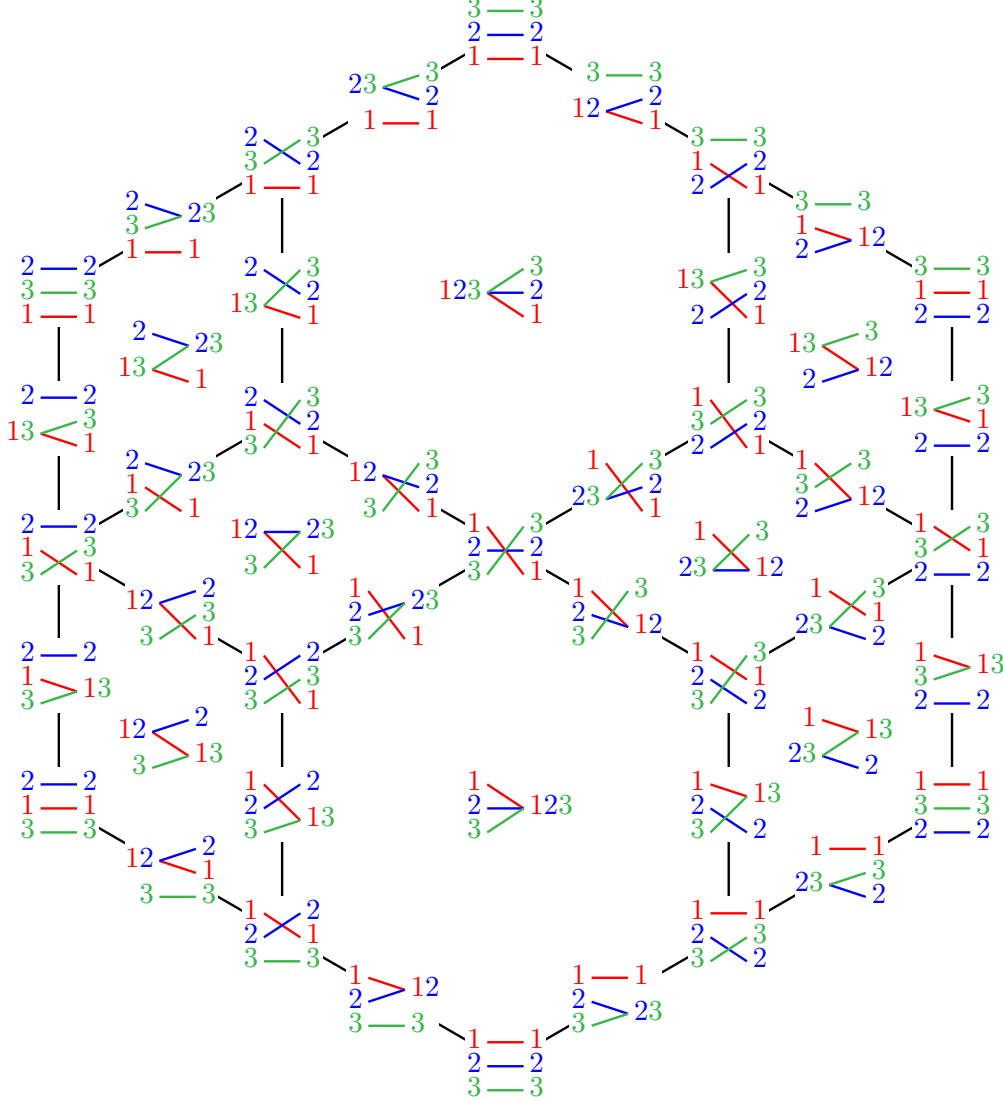


FIGURE 7. The LA (and SU) diagonal of $\text{Perm}(3)$ with faces labelled by ordered bipartite forests.

2. CONNECTIONS

This section briefly explores some natural questions at the intersection of both papers.

2.1. Tensor Products of Connected Homotopy Operadic Structures. This section has benefited greatly from conversations with Guillaume Laplante-Anfossi. In Section 1.1, it was sketched how given an operad P , you can construct an explicit functorial tensor product of P_∞ -algebras if

- P admits a polytope based minimal model P_∞ , and
- the polytope has a known convex realisation.

See [LA22], where the tensor product of homotopy operads is constructed via this general approach. More generally, from Theorem 0 we know there exists polytope based minimal models for all connected operadic

structures, including properads, wheeled properads, cyclic operads and modular operads. Thus, it is natural to seek to use these polytopes to construct tensor products of the homotopy weakened generalisations of all these operadic structures. There are at least two possible pathways to these extensions.

Firstly, we could study these polytopes on a case by case basis. For instance, the appropriate minimal model for the operad governing properads is given by the poset associahedra of [Gal21], which has been realised as a convex polytope in [MPP23] and [Sac23]. Thus as suggested in Remark 7.1.3 of [Sto24], we could mirror the methodology of [LA22] in this particular case.

Alternatively, in [KW23] it was proven that all cubical Feynman categories are Koszul, for instance, the cubical Feynman categories governing connected operadic structures are all Koszul as mentioned in Theorem 0. It is strongly suggested by their methodology, that the associated polytopes of homotopy cubical Feynman categories are operahedra, in particular, projections of the permutahedra (see Section 5.1 of [KW23]). If this is indeed the case, and the projections are the natural projections from de-refinements of normal fans, then Proposition 3.20 of [LA22] immediately yields the diagonals of these polytopes. Alternatively, if this is not true for all cubical Feynman categories, then perhaps the prior cases of interest can be shown to have the necessary projective properties.

It is also natural to hope for non-polytope based methods for explicitly calculating the tensor products of homotopy operadic structures without polytope based models, such as L_∞ -algebras or homotopy (wheeled) props. The author is unaware of any such general extension.

2.2. Shuffle Operads. One of the critical insights in the theory of Groebner bases for symmetric operads is that there exists a good way to forget the symmetries of operads, which enables explicit computation of basis elements. Namely, the forgetful functor $-^f$ from Section 1.1. Symmetric operads are monoids in the monoidal category of symmetric modules with a monoidal composition built from symmetric trees (Mod_Σ, \circ) , and 'shuffle operads' are monoids in the monoidal category of nonsymmetric modules with a monoidal composition built from 'shuffle trees' (Mod, \circ_{sh}) . In essence, the monoidal product \circ_{sh} is defined precisely so that $-^f : Mod_\Sigma \rightarrow Mod$ is strong monoidal with respect to these products. This is desirable, for instance, it yields the isomorphism of bar complexes observed in Section 1.1.

It is natural to wonder, how many choices of monoidal products exist on Mod such that f is strong monoidal? In this section, we show there are infinitely many choices (Proposition 2.2.16), including a minimal or *LA* variant which matches the classical notion of a shuffle operad ([Hof10], [DK10]), and a new maximal or *SU* variant. However, all such choices are isomorphic (Proposition 2.2.15). The findings of this section lie in contrast to Theorem 4, which observed that whilst \triangle^{LA} and \triangle^{SU} are isomorphic, they are also strictly the only coherent cellular diagonals (see Remark 2.2.17).

Note although the theory of this section is described via groupoid coloured operads (to make use of the definitions of [Sto24]), no groupoid actions are used, and the reader may parse these definitions as either (discrete) coloured operads or one coloured operads.

2.2.1. Preliminary Definitions. We start by introducing several notions of shuffle trees, their corresponding monoidal products, and their corresponding type of shuffle operad. We first recall from Definitions 4.13 and 5.2 of [DOLAPS23], that given two non-empty pairwise disjoint subsets $I, J \in [n]$, that

- the *LA* ordering of $\{I, J\}$ was defined to be (I, J) if $\min I < \min J$, and (J, I) otherwise, and
- the *SU* ordering of $\{I, J\}$ was defined to be (I, J) if $\max I < \max J$, and (J, I) otherwise.

These orderings naturally extend to k non-empty pairwise disjoint subsets, and hence induce orderings of vertices of trees. We now describe these orderings on trees with edges coloured by a set of colours \mathfrak{C} .

Definition 2.2.1. Let T be a reduced tree with profile $(\underline{c}; c_0)$ (Definition 2.2.7 of [Sto24], informally a type of tree where: every vertex has at least one input; the inputs of every vertex are ordered by a listing/permutation; and the inputs of the entire tree are ordered by the listing/permutation \underline{c}). For a vertex $v = (v_1, \dots, v_n; v_0)$, for $1 \leq k \leq n$ we let

$$\underline{c}_{v_k} := \{c \in \underline{c} : \text{there exists a directed path from } c \text{ to the } k\text{th input of } v\}.$$

We say that T is one of the following types of shuffle trees, if for every vertex $v = (v_1, \dots, v_n; v_0)$, and for all $1 \leq i < j \leq n$,

- $\min(\underline{c}_{v_i}) < \min(\underline{c}_{v_j})$, then T is a *LA-shuffle tree*.
- $\min(\underline{c}_{v_i}) > \min(\underline{c}_{v_j})$, then T is a *LA^{op}-shuffle tree*.
- $\max(\underline{c}_{v_i}) < \max(\underline{c}_{v_j})$, then T is a *SU-shuffle tree*.
- $\max(\underline{c}_{v_i}) > \max(\underline{c}_{v_j})$, then T is a *SU^{op}-shuffle tree*.

Let \overline{ST}^{LA} denote the set of strict isomorphism classes of *LA* shuffle trees (Definition 2.2.8 of [Sto24]), and let $\overline{ST}_{\vec{v},n}^{LA} \subset \overline{ST}^{LA}$ be those with tree profile \vec{v} and n levels. The *SU* shuffle trees are defined similarly.

Note that \overline{ST}^{LA} is precisely \overline{ST} in Definition 2.2.8 of [Sto24]. There are clear symmetries in these definitions which we now explicate.

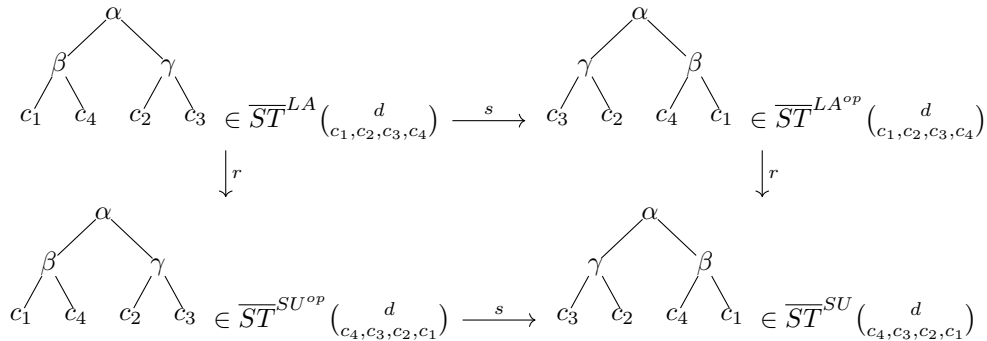
Proposition 2.2.2. *Let T denote the set of reduced trees. Let $r : T \rightarrow T$ denote the map which reverses the order of the final listing of the tree, i.e. $r\vec{v} := r(v_1, \dots, v_m; v_0) := (v_m, \dots, v_1; v_0)$. Let $s : T \rightarrow T$ denote the map which reverses the order of every vertex. Then these maps satisfy the following conditions.*

- The maps r and s are involutive bijections.
- The maps r and s commute.
- The maps r and s preserve levels (height of each vertex).
- The map r restricts to a bijection of,
 - *LA* and *SU^{op}* shuffle trees, and
 - *SU* and *LA^{op}* shuffle trees.
- The map s restricts to a bijection of,
 - *LA* and *LA^{op}* shuffle trees, and
 - *SU* and *SU^{op}* shuffle trees.
- Thus the square of bijections to the right commute.

$$\begin{array}{ccc} \overline{ST}_{\vec{v},n}^{LA} & \xrightarrow{s} & \overline{ST}_{\vec{v},n}^{LA^{op}} \\ \downarrow r & & \downarrow r \\ \overline{ST}_{r\vec{v},n}^{SU^{op}} & \xrightarrow{s} & \overline{ST}_{r\vec{v},n}^{SU} \end{array}$$

Proof. Straightforward from definitions. For the commutativity, observe that the map s preserves the final listing of the tree, and that the map r preserves the listings of every vertex in the tree. \square

Example 2.2.3. Here we illustrate four different height 2 shuffle trees, in bijection under the two maps. For each tree, the listing of each vertex is given by the planar embedding, and the final listing of each tree is indicated by the profile of the set it is contained in, e.g. the top left tree has the final listing $(c_1, c_2, c_3, c_4)^d$. The vertices of the trees are labelled to clarify the bijections, and we stress that r produces a new tree solely by changing the final listing.



Additionally, each type of shuffle tree is a representative of the equivalence class of symmetric trees.

Definition 2.2.4. Let $T \in \overline{ST}_{\vec{v}}$ be a symmetric tree with profile \vec{v} . By Definition 2.2.8 of [Sto24], T is a set of weakly isomorphic trees, i.e. trees which are equal under permuting the listing of the entire tree, and the listing of each vertex. A \vec{v} -*representative* of T is a specific element of this set whose tree listing is also \vec{v} . As each type of shuffle tree uniquely orients every vertex (Definition 2.2.1), we define the *LA*, *SU*, *LA^{op}*, *SU^{op}* *representative* of T to be the unique corresponding shuffle tree with tree profile \vec{v} . Thus, for each type of

shuffle tree (illustrated for LA) we define the *symmetrisation* and *representation* maps,

$$[-] : \overline{ST}_{\vec{v}}^{LA} \rightarrow \overline{\Sigma T}_{\vec{v}}, \quad - *_ {LA} : \overline{\Sigma T}_{\vec{v}} \rightarrow \overline{ST}_{\vec{v}}^{LA}$$

which respectively, reconstructs the weak isomorphism class of each LA shuffle tree, and produces the unique LA \vec{v} -representative of each symmetric tree with profile \vec{v} .

Proposition 2.2.5. *The symmetrisation and representation maps are bijections. Furthermore, as they conserve levels they restrict to bijections*

$$[-] : \overline{ST}_{\vec{v},n}^{LA} \rightarrow \overline{\Sigma T}_{\vec{v},n}, \quad *_ {LA} : \overline{\Sigma T}_{\vec{v},n} \rightarrow \overline{ST}_{\vec{v},n}^{LA}$$

Proof. For each type of shuffle tree, both maps are clearly well-defined and mutual inverses as we can reconstruct any equivalence class from any element, e.g. for any symmetric tree $T = [T_{*_ {LA}}]$. We obtain the restrictions to height n trees, as altering the listing of a vertex does not change its height. \square

Corollary 2.2.6. *Taking composites of representation and symmetrisation maps provides new bijections between the sets of shuffle trees.*

$$\begin{array}{ccc} \overline{ST}_{\vec{v},n}^{LA} & \xrightarrow{[-] *_ {LA^{op}}} & \overline{ST}_{\vec{v},n}^{LA^{op}} \\ & \nwarrow *_ {LA} \quad \nearrow *_ {LA^{op}} & \\ & \overline{\Sigma T}_{\vec{v},n} & \\ & \nwarrow *_ {SU^{op}} \quad \nearrow *_ {SU} & \\ \overline{ST}_{\vec{v},n}^{SU^{op}} & \xrightarrow{[-] *_ {SU}} & \overline{ST}_{\vec{v},n}^{SU} \end{array}$$

(Note: Dashed arrows also connect the outer nodes: $\overline{ST}_{\vec{v},n}^{LA} \xrightarrow{[-] *_ {SU^{op}}} \overline{ST}_{\vec{v},n}^{SU^{op}}$, $\overline{ST}_{\vec{v},n}^{LA^{op}} \xrightarrow{[-] *_ {SU}} \overline{ST}_{\vec{v},n}^{SU}$, and $\overline{ST}_{\vec{v},n}^{LA} \xrightarrow{[-] *_ {SU}} \overline{ST}_{\vec{v},n}^{SU}$.)

Example 2.2.7. Here are the four representations of the symmetrisation of the top left tree of Example 2.2.3.

$$\begin{array}{ccc} \begin{array}{c} \alpha \\ \swarrow \quad \searrow \\ \beta \quad \gamma \\ \swarrow \quad \searrow \quad \swarrow \quad \searrow \\ c_1 \quad c_4 \quad c_2 \quad c_3 \end{array} \in \overline{ST}_{(c_1,c_2,c_3,c_4)}^{LA} & \xrightarrow{s=[-] *_ {LA^{op}}} & \begin{array}{c} \alpha \\ \swarrow \quad \searrow \\ \gamma \quad \beta \\ \swarrow \quad \searrow \quad \swarrow \quad \searrow \\ c_3 \quad c_2 \quad c_4 \quad c_1 \end{array} \in \overline{ST}_{(c_1,c_2,c_3,c_4)}^{LA^{op}} \\ \downarrow [-] *_ {SU^{op}} & & \downarrow [-] *_ {SU} \\ \begin{array}{c} \alpha \\ \swarrow \quad \searrow \\ \beta \quad \gamma \\ \swarrow \quad \searrow \quad \swarrow \quad \searrow \\ c_4 \quad c_1 \quad c_3 \quad c_2 \end{array} \in \overline{ST}_{(c_1,c_2,c_3,c_4)}^{SU^{op}} & \xrightarrow{s=[-] *_ {SU}} & \begin{array}{c} \alpha \\ \swarrow \quad \searrow \\ \gamma \quad \beta \\ \swarrow \quad \searrow \quad \swarrow \quad \searrow \\ c_2 \quad c_3 \quad c_1 \quad c_4 \end{array} \in \overline{ST}_{(c_1,c_2,c_3,c_4)}^{SU} \end{array}$$

Example 2.2.8. Here are the three symmetric binary trees with profile $\binom{d}{c_1,c_2,c_3}$ (see for instance Section 7.6.2 of [LV12] in the uncoloured case), and their four representations. In each square the representations are as follows; the top left is LA , the top right is LA^{op} , bot left is SU^{op} , and bot right is SU .

$$\begin{array}{cccccc} \begin{array}{c} \alpha \\ \swarrow \quad \searrow \\ c_1 \quad c_3 \\ \swarrow \quad \searrow \\ c_1 \quad c_2 \end{array} & \xrightarrow{[-] *_ {LA^{op}}} & \begin{array}{c} \alpha \\ \swarrow \quad \searrow \\ c_3 \quad c_1 \\ \swarrow \quad \searrow \\ c_2 \quad c_1 \end{array} & \xrightarrow{[-] *_ {LA^{op}}} & \begin{array}{c} \alpha \\ \swarrow \quad \searrow \\ c_1 \quad c_2 \\ \swarrow \quad \searrow \\ c_1 \quad c_3 \end{array} & \xrightarrow{[-] *_ {LA^{op}}} & \begin{array}{c} \alpha \\ \swarrow \quad \searrow \\ c_2 \quad c_3 \\ \swarrow \quad \searrow \\ c_3 \quad c_1 \end{array} \\ \downarrow [-] *_ {SU^{op}} & & \downarrow [-] *_ {SU} & & \downarrow [-] *_ {SU^{op}} & & \downarrow [-] *_ {SU} \\ \begin{array}{c} \alpha \\ \swarrow \quad \searrow \\ c_3 \quad c_1 \\ \swarrow \quad \searrow \\ c_3 \quad c_2 \end{array} & \xrightarrow{[-] *_ {SU}} & \begin{array}{c} \alpha \\ \swarrow \quad \searrow \\ c_1 \quad c_2 \\ \swarrow \quad \searrow \\ c_1 \quad c_3 \end{array} & \xrightarrow{[-] *_ {SU}} & \begin{array}{c} \alpha \\ \swarrow \quad \searrow \\ c_2 \quad c_3 \\ \swarrow \quad \searrow \\ c_2 \quad c_1 \end{array} & \xrightarrow{[-] *_ {SU}} & \begin{array}{c} \alpha \\ \swarrow \quad \searrow \\ c_3 \quad c_2 \\ \swarrow \quad \searrow \\ c_1 \quad c_3 \end{array} \end{array}$$

As expected, each family of shuffle tree produces a unique representative of each symmetric tree, i.e. in the LA case we observe that the top-left of each square differs. Note that the representations chosen by the families can coincide, as indicated by the duplicates within squares.

We now construct four related notions of shuffle operads from these four families of shuffle trees.

Definition 2.2.9. Let A_1, \dots, A_n be \mathbb{V} -modules. We define the shuffle monoidal products to be

$$(A_1 \circ_{LA} \dots \circ_{LA} A_n)(\vec{v}) := \coprod_{T \in \overline{ST}_{n, \vec{v}}^{LA}} (A_1 \circ \dots \circ A_n)(T),$$

and so on, altering the underlying set of shuffle trees for each product. Note that $(A_1 \circ \dots \circ A_n)(T)$ (and the symmetric monoidal product for symmetric trees) can be found in Definition 3.1.3 of [Sto24].

Proposition 2.2.10. *Each of the shuffle products above give $\mathbb{V}\text{-Mod}$ a strict monoidal structure with unit*

$$\mathcal{I}(\vec{v}) := \begin{cases} \coprod_{Aut(v)} 1_{\mathcal{E}}, & \vec{v} = (v; v) \text{ for some } v \in Ob(\mathbb{V}) \\ \emptyset, & \text{else} \end{cases}$$

Proof. The LA case is Lemma 3.1.4 of [Sto24]. The proofs for LA^{op} , SU and SU^{op} proceed similarly. \square

Definition 2.2.11. Let $(\mathbb{V}_{\Sigma}\text{-Mod}, \circ)$ denote the monoidal category of reduced symmetric modules with the operadic symmetric monoidal product. Let $(\mathbb{V}\text{-Mod}, \circ_{LA})$ and $(\mathbb{V}\text{-Mod}, \circ_{SU})$ respectively, denote the monoidal category of reduced modules with the LA/SU operadic monoidal product. Then,

- a *symmetric operad* is a monoid in $(\mathbb{V}_{\Sigma}\text{-Mod}, \circ)$,
- a *LA -shuffle operad* is a monoid in $(\mathbb{V}\text{-Mod}, \circ_{LA})$, and
- a *SU -shuffle operad* is a monoid in $(\mathbb{V}\text{-Mod}, \circ_{SU})$.

By definition, a \mathbb{V} -coloured LA -shuffle operad is a \mathbb{V} -coloured shuffle operad of Definition 3.1.5 of [Sto24]. The variants of the standard zoo of equivalent operadic definitions are available for each type of operad, e.g. partial, monadic and so on.

2.2.2. Unique up to Isomorphism But Many Ways to Forget. We now discuss the forgetful functor from symmetric modules to non-symmetric modules, and how it forms the underlying functor of a strong monoidal functor.

Definition 2.2.12. Let $(C, \otimes_C, 1_C)$ and $(D, \otimes_D, 1_D)$ be monoidal categories. A *strong monoidal functor* is a triple consisting of a

- functor $F : C \rightarrow D$,
- an isomorphism $\varepsilon : 1_C \rightarrow F(1_D)$, and
- a set of isomorphisms $\{\mu_{A,B} : F(A) \otimes_D F(B) \rightarrow F(A \otimes_C B)\}_{A,B \in C}$.

respecting well known unitality and associativity conditions (see for instance [ML13]).

Definition 2.2.13. Let $f : \mathbb{V}_{\Sigma}\text{-Mod} \rightarrow \mathbb{V}\text{-Mod}$ denote the *forgetful functor* from the category of reduced symmetric \mathbb{V} -modules to the category of reduced \mathbb{V} -modules, which forgets the underlying action of the symmetric group.

Proposition 2.2.14. *The forgetful functor is a strong monoidal functor from $(\mathbb{V}_{\Sigma}\text{-Mod}, \circ)$ into both $(\mathbb{V}\text{-Mod}, \circ_{LA})$ and $(\mathbb{V}\text{-Mod}, \circ_{SU})$. Formally, if*

$$*_{\Sigma \rightarrow LA} : f(A) \circ_{LA} f(B) \rightarrow f(A \circ B), \text{ and } *_{\Sigma \rightarrow SU} : f(A) \circ_{SU} f(B) \rightarrow f(A \circ B)$$

are the isomorphisms induced by the symmetrisation bijections, e.g. $[-] : \overline{ST}_{2, \vec{v}}^{LA} \rightarrow \overline{\Sigma T}_{2, \vec{v}}$ induces

$$(f(A) \circ_{LA} f(B))(\vec{v}) = \coprod_{T \in \overline{ST}_{2, \vec{v}}^{LA}} (f(A) \circ f(B))(T) \cong f\left(\coprod_{T \in \overline{\Sigma T}_{2, \vec{v}}} (A \circ B)(T)\right) = f((A \circ B))(\vec{v}).$$

Then the following triples are strong monoidal functors.

$$(f, id, *_{\Sigma \rightarrow LA}) : (\mathbb{V}_{\Sigma}\text{-Mod}, \circ, I) \rightarrow (\mathbb{V}\text{-Mod}, \circ_{LA}, I), \text{ and } (f, id, *_{\Sigma \rightarrow SU}) : (\mathbb{V}_{\Sigma}\text{-Mod}, \circ, I) \rightarrow (\mathbb{V}\text{-Mod}, \circ_{SU}, I)$$

Proof. The LA case is well known. For the uncoloured case we direct the reader to Proposition 5.3.3.1 of [BD16] as the proof completely explicates the necessity of the reduced assumption. The groupoid coloured extension is Lemma 3.1.10 of [Sto24]. The SU case follows via a similar argument. \square

Given that the category of strong monoidal functors is closed under composition, we observe that up to isomorphism, there is only one way for f to be a forgetful functor.

Proposition 2.2.15. *Let $(\mathbb{V}\text{-Mod}, \circ', I)$ be a strict monoidal category, such that $(f, id, \mu) : (\mathbb{V}\text{-Mod}_\Sigma, \circ, I) \rightarrow (\mathbb{V}\text{-Mod}, \circ', I)$ is a strong monoidal functor. Then, the composite of strong monoidal functors,*

$$(f, id, \mu) \circ (f, id, \mu) = (id, id, *_{\Sigma \rightarrow LA}^{-1} \circ \mu) : (\mathbb{V}\text{-Mod}, \circ_{LA}, I) \rightarrow (\mathbb{V}\text{-Mod}, \circ', I)$$

is strong monoidal, and clearly an isomorphism.

However, LA and SU shuffle operads are far from strictly unique.

Proposition 2.2.16. *There exist infinitely many strict monoidal categories $(\mathbb{V}\text{-Mod}, \circ', I)$ endowed with a strong monoidal functor $(f, id, \mu) : (\mathbb{V}\text{-Mod}_\Sigma, \circ, I) \rightarrow (\mathbb{V}\text{-Mod}, \circ', I)$.*

Proof. We first provide one explicit counter example that addresses the heart of the issue. Let T be a reduced tree. We say T is an 'odd-even' shuffle tree if every vertex with odd arity is ordered under the LA shuffle condition, and if every vertex with even arity is ordered under the SU shuffle condition, see Definition 2.2.1. One can then mirror Section 2.2.1, defining a set of strict isomorphism classes of 'odd-even' trees, providing unique 'odd-even' representations of every symmetric tree, and defining a monoidal category $(\mathbb{V}\text{-Mod}, \circ_{oe})$ whose monoids are 'odd-even' shuffle operads. One can then show there exists a strong monoidal functor $(f, id, *_{\Sigma \rightarrow oe}) : (\mathbb{V}\text{-Mod}_\Sigma, \circ) \rightarrow (\mathbb{V}\text{-Mod}, \circ_{oe})$. The only real point that requires checking over and above the proof of Proposition 2.2.14, is that $*_{\Sigma \rightarrow oe}$ remains associative. This follows as ordering any one vertex does not change the arity of any other vertex. Thus given any height n tree, one can order all vertices at each level, by any ordering of the levels of that tree, and still obtain the same result. There are many ways to extend this counter example to an infinite family of counter examples, for instance the prior argument holds for any LA/SU partition of \mathbb{N} . □

Remark 2.2.17. The coherent cellular diagonals of the permutahedra \triangle^{LA} and \triangle^{SU} not only admit isomorphic cellular images, but are also strictly the only coherent cellular diagonal alongside their opposites (Theorem 5.13 and 5.15 of [DOLAPS23]). The key additional criterion that forces \triangle^{LA} and \triangle^{SU} to strictly unique is condition (2) of Definition 5.7 of [DOLAPS23], which is informally an extra coherence condition imposed by compatibility with the diagonal. Perhaps, $(f, id, *_{\Sigma \rightarrow LA}) : (\mathbb{V}_\Sigma\text{-Mod}, \circ, I) \rightarrow (\mathbb{V}\text{-Mod}, \circ_{LA}, I)$ and $(f, id, *_{\Sigma \rightarrow SU}) : (\mathbb{V}_\Sigma\text{-Mod}, \circ, I) \rightarrow (\mathbb{V}\text{-Mod}, \circ_{SU}, I)$ are the only such strong monoidal functors which are compatible with some additional Hopf operadic structure? See Section 5.3.3 of [LV12].

Remark 2.2.18. Where do the opposing notions of shuffle trees fit in? Well, if $R : \mathbb{V}\text{-Mod} \rightarrow \mathbb{V}\text{-Mod}$ is the functor which formally reverses each \mathbb{V} -module A , i.e.

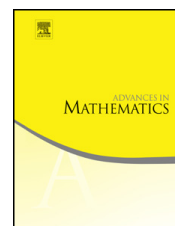
$$R(A)(\vec{v}) := A(r\vec{v}) \text{ with } r\vec{v} := r(v_1, \dots, v_k; v_0) = (v_k, \dots, v_1; v_0).$$

then $R(-)^f = R(-^f)$. Furthermore $R(-^f)$ can be shown to be the underlying functor of a strong monoidal functor from $(\mathbb{V}\text{-Mod}_\Sigma, \circ, I)$ into both $(\mathbb{V}, \circ_{LA^{op}}, I)$ and $(\mathbb{V}, \circ_{SU^{op}}, I)$, by mirroring Proposition 2.2.14.



Contents lists available at ScienceDirect

Advances in Mathematics

journal homepage: www.elsevier.com/locate/aim

Koszul operads governing props and wheeled props

Kurt Stoeckl

School of Mathematics and Statistics, The University of Melbourne, Victoria, Australia



ARTICLE INFO

Article history:

Received 29 August 2023

Received in revised form 16 June 2024

Accepted 22 July 2024

Available online 5 August 2024

Communicated by Ross Street

Keywords:

Operads

Props

Koszul Duality

Gröbner bases

ABSTRACT

In this paper, we construct groupoid coloured operads governing props and wheeled props, and show they are Koszul. This is accomplished by new biased definitions for (wheeled) props, and an extension of the theory of Groebner bases for operads to apply to groupoid coloured operads. Using the Koszul machine, we define homotopy (wheeled) props, and show they are not formed by polytope based models. Finally, using homotopy transfer theory, we construct Massey products for (wheeled) props, show these products characterise the formality of these structures, and re-obtain a theorem of Mac Lane on the existence of higher homotopies of (co)commutative Hopf algebras.

© 2024 The Author(s). Published by Elsevier Inc. This is an open access article under the CC BY license (<http://creativecommons.org/licenses/by/4.0/>).

Contents

1.	Introduction	2
1.1.	Acknowledgments	5
2.	Preliminaries	5
2.1.	Bimodules	5
2.2.	Fundamental graphical definitions	8
3.	Groupoid coloured operads	12
3.1.	Monoidal groupoid coloured operads	12

E-mail address: kstoeckl@student.unimelb.edu.au.

URL: <https://kstoeckl.github.io/>.

<https://doi.org/10.1016/j.aim.2024.109869>

0001-8708/© 2024 The Author(s). Published by Elsevier Inc. This is an open access article under the CC BY license (<http://creativecommons.org/licenses/by/4.0/>).

3.2.	Monadic groupoid coloured operads	16
3.3.	Partial compositions	18
3.4.	Some assumptions	19
3.5.	Tree monomials and presentations of operads	19
3.6.	Koszul groupoid coloured operads	20
4.	Koszul groupoid coloured operads via Groebner bases	22
4.1.	Divisibility, order and Groebner bases for discrete coloured shuffle operads	23
4.2.	The groupoid coloured extension	25
4.3.	Rewriting systems and Groebner bases	32
5.	The operad governing wheeled props	35
5.1.	Wheeled props	36
5.2.	A groupoid coloured quadratic operad	39
5.3.	The shuffle operad	42
5.4.	Ordering the object coloured tree monomials	44
5.5.	The operad governing wheeled props is Koszul	48
6.	The operad governing props	51
6.1.	Props	51
6.2.	A groupoid coloured quadratic presentation	60
6.3.	The shuffle operad	60
6.4.	Ordering the object coloured tree monomials	61
6.5.	The operad governing props is Koszul	63
6.6.	Applying these techniques to other operadic structures	66
7.	Homotopy (wheeled) props	67
7.1.	Nesting models and polytope based techniques	73
7.2.	Homotopy transfer theory	75
8.	Appendix: axioms of an alternate prop	77
	References	78

1. Introduction

Props, introduced by Adams and Mac Lane ([37]), are a type of symmetric monoidal category. Their representations model various (mixed) algebraic and coalgebraic structures including associative, commutative, Lie and Hopf algebras. They arise naturally in the study of deformation theory [1], [42], differential geometry [38], knot theory [11], [12], and topology [7], [56]. Homotopy props arise when one wishes to study variants of the algebraic structures above, which are only weakly associative. For instance, Mac Lane introduced PACTs, a version of homotopy associative props, and used them to identify Massey products of (co)commutative Hopf algebras (Section 7.2). Another example are the cobordism categories of Segal whose morphism spaces are moduli spaces of Riemann surfaces. In these cobordism categories, categorical composition is associative on the associated chain complex, but is only homotopy associative at the space level (e.g. Remark 3.31 of [50]).

Wheeled props are props with an additional non-degenerate bilinear form or “trace” operation. They were introduced by Markl, Merkulov and Shadrin [38], where they used (homotopy) wheeled props to study Batalin–Vilkovisky quantisation formalism in theoretical physics. Wheeled props are also known to arise in invariant theory [16], and they play a key role in the study of universal finite type invariants of virtual and welded

tangles [11]. This is far from a spanning list, and we direct the interested reader to the more complete literature surveys of [24], [35] and [57].

These examples of homotopy (wheeled) props motivate a more systematic study of homotopy associative, or ∞ -props. While there are many known models for ∞ -operads and ∞ -properads in the literature (e.g. [6], [9], [20], [24], [32], [44], [42] etc.) there are currently only a few suggested models for ∞ -props (including [8], [23] and [21]), and ∞ -wheeled props (including [48]). This paper uses the machinery of Koszul duality to provide an algebraic model for homotopy, or ∞ , (wheeled) props.

Over the last 20 years, the Koszul machine has been used to construct homotopy associative versions of many operadic structures. In brief, an operad P is said to be Koszul if, and only if, it admits a minimal model P_∞ with a quadratic differential (Definition 3.6.7). The minimal model P_∞ is characterised by the property that algebras over P_∞ are homotopy (associative) P -algebras. A coloured Koszul operad governing non-symmetric operads was first constructed in [54]. Later in [55], Ward constructed a groupoid coloured operad governing modular operads, and showed it was Koszul. Most recently it has been shown by two different groups of authors ([4], [27]) that the operads governing operadic families living on connected graphs (including operads, dioperads, wheeled properads, etc.) are all Koszul. A common thread unifying the last three papers, is that they all use the theory of convex polytopes, explicitly or implicitly, to interpret the minimal models of the operads.

Our present work, builds on this story with three main results. Firstly, in Sections 5 and 6, we construct groupoid coloured operads \mathbb{W} and \mathbb{P} , governing wheeled props and props respectively. We then prove, in Sections 5.5 and 6.5, that

Theorem 1.0.1. *The groupoid coloured operads \mathbb{W} and \mathbb{P} are Koszul.*

By virtue of the Koszul machine, the associated minimal models \mathbb{P}_∞ (and \mathbb{W}_∞) govern homotopy associative dg-(wheeled) props. Then in Section 7, we provide simple counter examples showing the following.

Theorem (7.1.1). *There exist subcomplexes of \mathbb{W}_∞ and \mathbb{P}_∞ which are **not** isomorphic, as lattices, to the face poset of convex polytopes.*

Consequently, there are no polytope based minimal models for the operads \mathbb{W} and \mathbb{P} . This shows that the previous techniques for proving the operads governing operadic structure are Koszul do not readily extend to (wheeled) props (Remark 7.1.2). Indeed, in order to prove that \mathbb{P} and \mathbb{W} are Koszul we develop a more generally applicable tool. In Section 4.3, we transfer the techniques of Groebner bases for operads ([14], [25]) to groupoid coloured operads with the following result.

Theorem (4.2.13). *Let P be a groupoid coloured operad such that the associated coloured shuffle operad $(P^f)_*$ admits a quadratic Groebner basis, then P is Koszul.*

The proof of this theorem, in Section 4.2, relies on the studying the extent that the forgetful functor $-^{f^\vee}$, from groupoid coloured modules to (discrete-groupoid) coloured modules, fails to be monoidal with respect to the operadic monoidal products on both categories. In particular, given a groupoid coloured shuffle operad P we construct an epimorphism, of groupoid coloured shuffle cooperads, between the bar complexes $B(P^{f^\vee}) \twoheadrightarrow B(P)$ (Proposition 4.2.4). This lets us infer the following.

Proposition (4.2.1). *A groupoid coloured shuffle operad P is Koszul if the coloured shuffle operad P^{f^\vee} is Koszul.*

Thus by obtaining an explicit simple presentation for P^{f^\vee} which we denote P_* (Corollary 4.2.12), we may apply known rewriting techniques for coloured operads ([33], [40]) to prove P is Koszul (Section 4.3). We note that Theorem 4.2.13 can also be applied to prove that the operads governing connected operadic structures are Koszul (Section 6.6). Two less dramatic results that may also be of independent interest, are new biased definitions of (wheeled) props (5.1.2, 6.1.2). Critically, for defining \mathbb{W} and \mathbb{P} , the equivariance axioms of these structures enable a simple canonical form for every composite of operations. Thus, when we translate these equivariance axioms into actions of the groupoid (in Sections 5.2 and 6.2), the operads inherit these simple canonical forms.

The general theory and constructions of this paper can be used for many purposes. For instance, as we now know that \mathbb{W} and \mathbb{P} are Koszul, we can apply the technique of homotopy transfer theory (HTT) to these structures (Section 7.2). As homology is an example of a homotopy retract (over a field of characteristic 0), we are able to construct generalised Massey products. This immediately provides an alternate characterisation of the formality of a wheeled prop (Proposition 7.2.6), and a means of reinterpreting a theorem of Mac Lane as a particular instance of HTT (Section 7.2). In addition, HTT provides an alternate pathway to studying deformations of (wheeled) props (Remark 7.2.9).

Currently, the author is working with Philip Hackney and Marcy Robertson to develop graphical and Segal models for infinity props. It is expected that the nerve functor of [30], from strictly unital algebraic homotopy operads to dendroidal sets, will extend to homotopy props. That is to say, a unital version of an algebraic homotopy prop (i.e. an algebra over \mathbb{P}_∞), will be an example of graphical ∞ -prop (i.e. a graphical set satisfying an inner horn condition). Additionally, it is expected that graphical ∞ -props will be cofibrant objects in the model category of simplicially enriched props [8], [23].

Another area for future work is pursuing combinatorially simpler models for homotopy (wheeled) prop(erad)s. Although homotopy props do not admit a nesting model governed by polytopes, properads do. In particular, the appropriate minimal model for the operad governing properads is given by the poset associahedra of [18] (Remark 7.1.3). This poset has been recently realised as a convex polytope in [39] and [49]. As such, one could define tensor products of homotopy properads by extending the program of [29]. Finally, it is plausible that ‘simpler’ combinatorial models for homotopy (wheeled) props exist. Given

the inclusion of the operad Com into \mathbb{W} and \mathbb{P} (Proposition 7.0.2), an extension of existing graphical models for the coLie cooperad ([51], [52]) might bear fruit.

1.1. Acknowledgments

I would like to thank my supervisor, Marcy Robertson, for countless discussions and her careful review of this paper. I'm very grateful for an early conversation with Ben Ward, in which he suggested that the techniques thus far developed for wheeled props, might also be applicable to props. I would like to thank Guillaume Laplante-Anfossi for many useful conversations, and comments on this paper. I'm thankful to Andrew Sack for pointing out that a subcomplex of the minimal model for the operad governing props violated the diamond condition. I would like to thank both Dominik Trnka and Bruno Vallette for catching errors in an earlier version. Additionally, I would like to thank my referees for their detailed comments, and in particular, for spotting an error in my initial proof of Theorem 4.2.13. Finally, I acknowledge the support of, an Australian Government Research Training Program (RTP) Scholarship, and the Australian Research Council Future Fellowship FT210100256.

2. Preliminaries

Throughout this paper, let \mathcal{E} be a co-complete, closed symmetric monoidal category and let \mathbb{V} be a small groupoid. Informally, we say that a coloured wheeled prop is a \mathfrak{C} -coloured bimodule in \mathcal{E} , together with composition operations that are described by wheeled graphs (11.33 of [57] and Definition 5.1.2). As such, in order to define (wheeled) props, we first need to introduce some preliminaries on bimodules and wheeled graphs. Furthermore, as we will construct a groupoid coloured operad governing wheeled props, we will need to define groupoid coloured bimodules, and their morphisms.

2.1. Bimodules

We first recall the definition of \mathfrak{C} -coloured profiles and introduce notation, which we will use throughout this paper.

Definition 2.1.1 (Section 1.1 of [57]). Let \mathfrak{C} be a non-empty set (of colours) and let Σ_n denote the symmetric group on n letters.

- (1) An element in \mathfrak{C} will be called a **colour**.
- (2) A **\mathfrak{C} -profile of length n** is a finite sequence

$$\underline{c} = (c_1, \dots, c_n)$$

of colours. We write $|\underline{c}| = n$ for the length. The **empty profile**, with $n = 0$, is denoted by \emptyset .

(3) Given two \mathfrak{C} -profiles $\underline{c}, \underline{d}$ and $i \in \{1, \dots, |\underline{c}|\}$ we define the following \mathfrak{C} -profiles

$$\begin{aligned}\underline{c} \circ_i \underline{d} &= (c_1, \dots, c_{i-1}, d_1, \dots, d_{|\underline{d}|}, c_{i+1}, \dots, c_{|\underline{c}|}) \\ (\underline{c}, \underline{d}) &= (c_1, \dots, c_{|\underline{c}|}, d_1, \dots, d_{|\underline{d}|}) \\ \underline{c} \setminus c_i &= (c_1, \dots, c_{i-1}, c_{i+1}, \dots, c_{|\underline{c}|})\end{aligned}$$

(4) For a \mathfrak{C} -profile \underline{c} of length n and $\sigma \in \Sigma_n$, define the left and right actions

$$\sigma \underline{c} = (c_{\sigma(1)}, \dots, c_{\sigma(n)}) \quad \text{and} \quad \underline{c} \sigma = (c_{\sigma^{-1}(1)}, \dots, c_{\sigma^{-1}(n)}).$$

(5) The groupoid of all \mathfrak{C} -profiles with left (resp., right) symmetric group actions as morphisms is denoted by $\mathcal{P}(\mathfrak{C})$ (resp., $\mathcal{P}(\mathfrak{C})^{op}$).

(6) Define the product category $\mathcal{S}(\mathfrak{C}) := \mathcal{P}(\mathfrak{C})^{op} \times \mathcal{P}(\mathfrak{C})$. Its elements are pairs of \mathfrak{C} -profiles and are written either horizontally as $(\underline{c}; \underline{d})$ or vertically as $\begin{pmatrix} \underline{d} \\ \underline{c} \end{pmatrix}$.

A **bimodule** is a functor $P \in \mathcal{E}^{\mathcal{S}(\mathfrak{C})}$ (Definition 10.28 of [57]). We may generalise this definition to a groupoid coloured bimodule as follows.

Definition 2.1.2. Let $\mathcal{W}_k(\mathbb{V}) := \mathbb{V}^k \rtimes \Sigma_k$, where we suppose that Σ_k acts on \mathbb{V}^k from the left, and let $\mathcal{W}(\mathbb{V}) := \coprod_{k \geq 0} \mathcal{W}_k(\mathbb{V})$.

- A \mathbb{V}_Σ -**bimodule** is a functor $P \in \mathcal{E}^{\mathcal{S}(\mathbb{V})}$, where $\mathcal{S}(\mathbb{V}) := \mathcal{W}(\mathbb{V})^{op} \times \mathcal{W}(\mathbb{V})$.
- A \mathbb{V}_Σ -**module** is a functor $P \in \mathcal{E}^{\mathcal{W}(\mathbb{V})^{op} \times \mathbb{V}}$.
- A **non-symmetric** groupoid coloured bimodule, or a \mathbb{V} -bimodule is a \mathbb{V}_Σ -bimodule in which Σ_k acts trivially. Similarly, one can define a non-symmetric \mathbb{V} -module.

In the case that \mathbb{V} is the discrete category of colours, then we recover the definition of a bimodule. In the more general case, we can unpack the definition of a groupoid coloured bimodule to see that it consists of the following data.

- For any pair of profiles, it has an object $P\left(\begin{smallmatrix} \underline{d} \\ \underline{c} \end{smallmatrix}\right) \in \mathcal{E}$.
- A (iso)morphism $\begin{pmatrix} \delta \\ \phi \end{pmatrix} : P\left(\begin{smallmatrix} \underline{d} \\ \underline{c} \end{smallmatrix}\right) \rightarrow P\left(\begin{smallmatrix} \underline{d}' \\ \underline{c}' \end{smallmatrix}\right)$ in $\mathcal{W}(\mathbb{V})$, is equivalently a pair of compatible permutations and isomorphisms $\begin{pmatrix} \delta \\ \phi \end{pmatrix} = ((\begin{smallmatrix} \sigma \\ \tau \end{smallmatrix}), (\begin{smallmatrix} g \\ f \end{smallmatrix}))$, where $(\tau; \sigma) \in \Sigma_{|\underline{c}|} \times \Sigma_{|\underline{d}|}$ and $g : \sigma \underline{d} \rightarrow \underline{d}' \in \mathbb{V}^{|\underline{d}|}, f : \underline{c}' \rightarrow \underline{c} \in \mathbb{V}^{|\underline{c}|}$. Thus, this morphism of $\mathcal{W}(\mathbb{V})$ induces an action of the groupoid coloured module

$$P\left(\begin{smallmatrix} \underline{d} \\ \underline{c} \end{smallmatrix}\right) \xrightarrow{\begin{pmatrix} \delta \\ \phi \end{pmatrix} = ((\begin{smallmatrix} \sigma \\ \tau \end{smallmatrix}), (\begin{smallmatrix} g \\ f \end{smallmatrix}))} P\left(\begin{smallmatrix} \underline{d}' \\ \underline{c}' \end{smallmatrix}\right). \quad (1)$$

We note in particular that, the identity of $\mathcal{W}(\mathbb{V})$ is $((\begin{smallmatrix} id \\ id \end{smallmatrix}), (\begin{smallmatrix} id \\ id \end{smallmatrix}))$ and composition satisfies

$$\left(\begin{pmatrix} \sigma' \\ \tau' \end{pmatrix}, \begin{pmatrix} g' \\ f' \end{pmatrix}\right) \circ \left(\begin{pmatrix} \sigma \\ \tau \end{pmatrix}, \begin{pmatrix} g \\ f \end{pmatrix}\right) = \left(\begin{pmatrix} \sigma'\sigma \\ \tau\tau' \end{pmatrix}, \begin{pmatrix} g'' \\ f'' \end{pmatrix}\right). \quad (2)$$

Here if $g' : \sigma'\underline{d}' \rightarrow \underline{d}''$ and $f' : \underline{c}'' \rightarrow \underline{c}'\tau'$ then g'' and f'' are given by the clear composites

$$\begin{aligned} g'' &: \sigma'\sigma\underline{d} \rightarrow \sigma'\underline{d}' \rightarrow \underline{d}'' \\ f'' &: \underline{c}'' \rightarrow \underline{c}'\tau' \rightarrow \underline{c}\tau\tau'. \end{aligned}$$

Remark 2.1.3. It is straightforward to confirm that our definition of a groupoid coloured module is dual (and isomorphic) to Definition 3.3 of [46] (when restricted to groupoids). We also note that our definition is equivalent to the dual of the definition of a \mathbb{V} -coloured sequence presented in [55] if a very minor error is corrected. In Definition 2.2.1, the (dual) definition of a \mathbb{V} -coloured module is explicitly unpacked (here it is called a \mathbb{V} -coloured sequence, and it is also restricted to the case in which $k > 0$, see Remark 2.3.1 of [55]). However, in this unpacking of the definition, some necessary morphisms are omitted. There are more morphisms acting on \mathbb{V} -coloured modules than those given via the automorphisms of \mathbb{V} (unless \mathbb{V} is skeletal), in particular there are morphisms

$$\begin{pmatrix} v_0 \\ v_1, \dots, v_r \end{pmatrix} \xrightarrow{(\sigma, f_1, \dots, f_r; f_0^{op})} \begin{pmatrix} v'_0 \\ v'_1, \dots, v'_r \end{pmatrix}$$

where $\sigma \in \mathbb{S}_r$, $f_0^{op} : v_0 \rightarrow v'_0$ and $f_i : v_i \rightarrow v'_{\sigma^{-1}(i)}$. This minor misidentification changes none of the results of the paper, this is because the groupoid still acts on a tree T via the automorphism group of the internal edges of T (using Eq. (2) of Definition 2.1.2 to define Eq. (3) of Definition 3.1.2, instead of (2.1) to define (2.4) as in [55]).

Definition 2.1.4. Given two small groupoids \mathbb{U}, \mathbb{V} , and two symmetric monoidal categories \mathcal{D}, \mathcal{E} , let $P \in \mathcal{D}^{\mathcal{S}(\mathbb{U})}$ and $Q \in \mathcal{E}^{\mathcal{S}(\mathbb{V})}$ be two distinct bimodules. A **morphism of bimodules** $h : P \rightarrow Q$ consists of a morphism of groupoids $h_0 : \mathbb{U} \rightarrow \mathbb{V}$, and a sequence of set maps

$$\left\{ P\left(\frac{\underline{d}}{\underline{c}}\right) \xrightarrow{h_1\left(\frac{\underline{d}}{\underline{c}}\right)} Q\left(\frac{h_0(\underline{d})}{(\underline{c})h_0}\right) \right\}_{\left(\frac{\underline{d}}{\underline{c}}\right) \in \text{ob}(\mathcal{S}(\mathcal{E}))},$$

so that all squares of the following form commute.

$$\begin{array}{ccc} P\left(\frac{\underline{d}}{\underline{c}}\right) & \xrightarrow{h_1\left(\frac{\underline{d}}{\underline{c}}\right)} & Q\left(\frac{h_0(\underline{d})}{(\underline{c})h_0}\right) \\ \left((\frac{\sigma}{\tau}), (\frac{g}{f})\right) \downarrow & & \downarrow \left((\frac{\sigma}{\tau}), (\frac{h_0(g)}{(f)h_0})\right) \\ P\left(\frac{\underline{d}'}{\underline{c}'}\right) & \xrightarrow{h_1\left(\frac{\underline{d}'}{\underline{c}'}\right)} & Q\left(\frac{h_0(\underline{d}')}{(\underline{c}')h_0}\right) \end{array}$$

Above, $((\sigma_\tau), (g_f))$ is any action of the \mathbb{U}_Σ -bimodule P given by Eq. (1), and in an abuse of notation we use $h_0(-), (-)h_0$ to denote the morphisms of groupoids $\mathbb{U}^{|\underline{d}|} \rightarrow \mathbb{V}^{|\underline{d}|}$, and respectively $\mathbb{U}^{|\underline{d}|^{op}} \rightarrow \mathbb{V}^{|\underline{d}|^{op}}$, induced by $h_0 : \mathbb{U} \rightarrow \mathbb{V}$. To be explicit $h_0(\underline{d}) := (h_0(d_1), \dots, h_0(d_k))$, and if $g = (g_1, \dots, g_{\underline{d}}) \in \text{Hom}_{\mathbb{V}^{|\underline{d}|}}(\sigma \underline{d}, \underline{d}')$ then $h_0(g) = (h_0(g_1), \dots, h_0(g_{\underline{d}})) \in \text{Hom}_{\mathbb{U}^{|\underline{d}|}}(h_0(\sigma \underline{d}), h_0(\underline{d}'))$.

A morphism h of groupoid coloured operads is said to be

- **full**, if the sequence of set maps are injective,
- **faithful**, if the sequence of set maps are surjective,
- an **epimorphism**, if it is faithful, and the underlying morphism of groupoids is essentially surjective,
- an **isomorphism**, if it is fully faithful and h_0 is an isomorphism of groupoids.

We similarly define and characterise the morphisms of (non-symmetric) groupoid coloured modules. Other familiar types of morphisms are possible, but will not be needed in this text.

We note this definition of a morphism of groupoid coloured bimodules allows for both differing groupoids and differing ambient symmetric monoidal categories. This extension to allow differing groupoids will be essential in the study of particular morphisms of groupoid coloured operads (see Section 4.2 and Proposition 7.0.2). If we specialise Definition 2.1.4 to a fixed groupoid \mathbb{V} and fixed symmetric monoidal category \mathcal{E} , then a morphism of groupoid coloured bimodules is a natural transformation.

2.2. Fundamental graphical definitions

Operations in (wheeled) props are parameterised by wheeled graphs. In this section, we provide a formal definition of a wheeled graph (Definition 2.2.4) and describe when two such graphs are isomorphic (Definition 2.2.5). The definitions of this subsection all stem verbatim from [24] and [57], further related definitions and examples may be found there.

2.2.1. Generalised graphs

Fix an infinite set \mathfrak{F} once and for all.

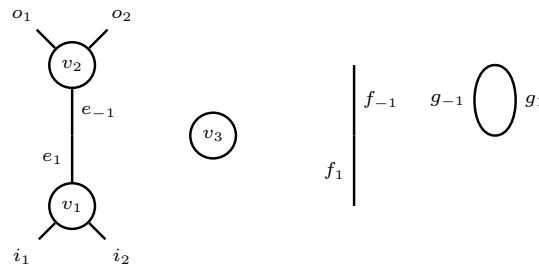
Definition 2.2.1. A **generalised graph** G is a finite set $\text{Flag}(G) \subset \mathfrak{F}$ with

- a partition $\text{Flag}(G) = \coprod_{\alpha \in A} F_\alpha$ with A finite,
- a distinguished partition subset F_ϵ called the **exceptional cell**,
- an involution ι satisfying $\iota F_\epsilon \subseteq F_\epsilon$, and
- a free involution π on the set of ι -fixed points in F_ϵ .

For a given generalised graph G , we unpack this definition and introduce some notation. The elements of $Flag(G)$ are called **flags** (or half edges). Every non-exceptional partition subset of $Flag(G)$ say $F_\alpha \neq F_\epsilon$ is a **vertex**, and if $f \in F_\alpha$ we say the flag f is **adjacent** (or attached) to the vertex. We note it is possible for a vertex to have no adjacent flags, in which case $F_\alpha = \{\emptyset\}$. The exceptional cell F_ϵ then corresponds to flags which are ‘free floating’ in the graph, and are not associated to any vertices. We shall denote the vertices of a graph as $Vt(G)$.

The non-trivial orbits of the involutions are called **edges** of the graph, and the fixed points of the involutions are called **legs** of the graph. Orbits of ι are called **internal edges**, whereas orbits of π are called **exceptional edges**. Note that because the involution π is free on the fixed points of ι , every fixed point of ι is part of an exceptional edge. Non-trivial orbits of flags in F_ϵ are called **exceptional loops**. Finally, the fixed points of ι (there are no fixed points of π) are called **legs** of the graph, these can also be considered exceptional (or ordinary) if they are (not) in F_ϵ .

Example 2.2.2 (1.12 of [57]). Consider the following diagrammatic representation of a generalised graph γ



The underlying partition set of γ is $\{\{i_1, i_2, e_1\}, \{o_1, o_2, e_{-1}\}, \emptyset, \{f_{\mp 1}, g_{\mp 1}\}\}$ with the last element being the exceptional cell. The 2 orbits of the involution ι are $e_{\mp 1}$ and $g_{\mp 1}$, all other flags are fixed points. The involution π has one 2 orbit corresponding to $f_{\mp 1}$ all other flags are fixed. The graph γ has three vertices, a single exception edge with flags $f_{\mp 1}$ and a single exceptional loop with flags $g_{\mp 1}$.

2.2.2. Structures on generalised graphs

We now introduce further structure on generalised graphs in order to define wheeled props. The extra data we introduce is: a colour for each edge; an orientation for each edge; and a labelling of the incoming/outgoing flags of each vertex, as well as labelling of the generalised graph.

Definition 2.2.3. Suppose G is a generalised graph.

- (1) A **colouring** for G is a $Flag(G) \xrightarrow{\kappa} \mathfrak{C}$ that is constant on orbits of both involutions ι and π .
- (2) A **direction** for G is a function $Flag(G) \xrightarrow{\delta} \{-1, 1\}$ such that

- if $\iota x \neq x$, then $\delta(\iota x) = -\delta(x)$, and
 - if $x \in F_\epsilon$, then $\delta(\pi x) = -\delta(x)$.
- (3) For G with direction, an **input** (resp. **output**) of a vertex v is a flag $x \in v$ such that $\delta(x) = 1$ (resp. $\delta(x) = -1$). An **input** (resp., **output**) of the graph G is a leg x such that $\delta(x) = 1$ (resp. $\delta(x) = -1$). For $u \in \{G\} \cup Vt(G)$, the set of inputs (resp. outputs) of u is written as $in(u)$ (resp. $out(u)$).
- (4) A **listing** for G with direction is a choice for each $u \in \{G\} \cup Vt(G)$ of a bijection of pairs of sets,

$$(in(u), out(u)) \xrightarrow{\ell_u} (\{1, \dots, |in(u)|\}, \{1, \dots, |out(u)|\}),$$

where for a finite set T the symbol $|T|$ denotes its cardinality.

Definition 2.2.4. A (\mathcal{C} -coloured) **wheeled graph**, is a generalised graph together with a choice of a colouring, a direction, and a listing. For such a graph G , we may use the colouring, listing, and direction to speak of the profile of the graph and any of its vertices. If $u \in \{G\} \cup Vt(G)$, with $in(u) = \underline{c}$ and $out(u) = \underline{d}$ (treating these as sets ordered by the listing) then we say that u has profile $\left(\frac{\underline{d}}{\underline{c}}\right)$.

A **wheel** of a (directed) wheeled graph is a directed cycle. A **wheel-free** graph is a wheeled graph without any wheels.

A convention: All graphs in this paper will be drawn with their inputs on the bottom and outputs on the top, e.g. the two graphs in Example 2.2.6 each have one vertex with two inputs and no outputs.

2.2.3. Isomorphic graphs

So having defined what a graph is, all that remains is the question of when should two graphs be considered the same.

Definition 2.2.5 (4.1 and 4.15 of [57]). Let G and G' be wheeled graphs.

- A **weak isomorphism** $\varphi : G \rightarrow G'$ is a bijection of partitioned sets that commutes with both involutions and leaves invariant both the colouring and the directions.
- A **strict isomorphism** $\varphi : G \rightarrow G'$ is a weak isomorphism that also leaves invariant the listing.

Example 2.2.6. The following two graphs whose listings are given by the planar embedding are weakly isomorphic, but not strongly isomorphic.



2.2.4. Trees

Operations in operads are parameterised by trees. So, in this section, we specialise the prior definitions of wheeled graphs and their isomorphisms to describe this important type of graph.

Definition 2.2.7. A **tree** is a simply connected graph where every vertex has a single output. We shall refer to the sole output of a tree as the root. We say a tree T with profile $(\underline{c}; d)$ is:

- **reduced** if every vertex has at least one input.
- a **\mathfrak{C} -tree** if it is a reduced tree with a colouring \mathfrak{C} (a key colouring being $ob(\mathbb{V})$).
- **level** if the height of every input leg (leaf) is the same. The height of a leg or vertex of a tree is defined to be the number of vertices on the directed path from it to the root. We say a tree with 0 levels is **empty**.
- a **shuffle** tree if for every vertex v of the tree say with profile $(v_1, \dots, v_n; v_0)$, that for $1 \leq i < j \leq n$ we have that $\min(\underline{c}_i) < \min(\underline{c}_j)$ where $\underline{c}_k = \{c \in \underline{c} : \text{there exists a directed path from } c \text{ to } v_k\}$.
- a **strongly regular** tree if the listing of T is given by performing a depth first search on the tree using the listing of the vertices to determine the order of the exploration of the children. In other words, the inputs of the tree are ordered left to right through embedding the tree into the plane.

Examples of shuffle trees and strongly regular trees are given in Example 3.1.6.

We note that this definition of a $ob(\mathbb{V})$ -coloured tree is the same as Definition 2.3 of [55], with the additional caveat that every internal vertex of the tree has an explicit listing as well. We explicitly refer to these trees as being **object-coloured** to stress that the morphisms of the groupoid are not (yet) involved.

Using the prior definitions of isomorphic graphs, we define the following classes of trees.

Definition 2.2.8. Let,

- $\overline{ST} :=$ weak isomorphism classes of, possibly empty, coloured trees.
- $\overline{RT} :=$ strict isomorphism classes of, possibly empty, coloured strongly regular trees.
- $\overline{ST} :=$ strict isomorphism classes of, possibly empty, coloured shuffle trees.

If we wish to exclude the empty trees, we shall drop the over-line. The subscripts $-_{n,\vec{v}}$ refer to the restrictions of these classes to those trees with n levels and profile \vec{v} .

We note that the notion of an isomorphism of $ob(\mathbb{V})$ coloured trees in [55] (Definition 2.9) is equivalent to that of a weak isomorphism.

3. Groupoid coloured operads

In this section, we present alternate definitions (monoidal and monadic) of variants (symmetric, non-symmetric and shuffle) of groupoid coloured operads, and define what it means for these operads to be Koszul. The necessary theory is a natural amalgamation of shuffle operads ([14], [25]) and groupoid coloured operads ([46], [55]). We note that groupoid coloured operads are a specific instance of category coloured operads [46], and the latter is explicitly related to internal operads [3], and substitutes [17], in [53]. Furthermore, [3] establishes the connection between substitutes [17], regular patterns [19], and Feynman categories [26].

3.1. Monoidal groupoid coloured operads

We start by presenting monoidal definitions of the operads and providing fundamental examples. Our definition of a symmetric groupoid coloured operad is precisely that of Ward's (accounting for Remark 2.1.3). To define our monoids, we will decorate trees with groupoid coloured modules, but because our trees are reduced, we will need the following assumption.

Definition 3.1.1. A groupoid coloured module $A : \mathcal{W}(\mathbb{V})^{op} \times \mathbb{V} \rightarrow \mathcal{E}$ is said to be **reduced** if, for all $v \in \mathbb{V}$, $A(\emptyset, v) = \emptyset$, the terminal object in \mathcal{E} .

For the remainder of this paper, we assume all groupoid coloured modules (symmetric or non-symmetric) are reduced. That is to say, all of our 'operations' have at least one input. We make this assumption to align with the theory of Ward (see Definition 2.35 of [55]). It is also required to establish a monoidal functor between symmetric and shuffle groupoid coloured operads (Lemma 3.1.10).

Recall from Definitions 2.2.4 and 2.2.7 that every vertex w of a tree T has a listing/profile.

Definition 3.1.2 (*The objects $A_\Sigma(T)$ and $A(T)$*). Let A_Σ be a \mathbb{V}_Σ -module, and let A be a \mathbb{V} -module. Let w be a vertex of a $ob(\mathbb{V})$ -tree with profile $(v_1, \dots, v_r; v_0)$ then set

$$A_\Sigma(w) := [\coprod_{\sigma \in S_r} A_\Sigma(v_{\sigma(1)}, \dots, v_{\sigma(r)}; v_0)]_{S_r}$$

$$A(w) := A(v_1, \dots, v_r; v_0)$$

Here $A_\Sigma(w)$ inherits a natural action of $(\prod_i^U Hom_{\mathbb{V}}(-, v_i)) \times Hom_{\mathbb{V}}(v_0, -)$ where \times_i^U is the unordered product, and $A(w)$ inherits a natural action of $(\prod_i Hom_{\mathbb{V}}(-, v_i)) \times Hom_{\mathbb{V}}(v_0, -)$. We also explicitly define our objects for empty trees,

$$A_\Sigma(|_v) = A(|_v) := \prod_{Aut(v)} 1_{\mathcal{E}}$$

with their induced action by $\text{Hom}(-, v) \times \text{Hom}(v, -)$. Let T be a $\text{ob}(\mathbb{V})$ -tree and form the unordered tensor products $\bigotimes_{w \in \text{Vt}(T)} A_\Sigma(w)$ and $\bigotimes_{w \in \text{Vt}(T)} A(w)$. Then any edge E of T with colour v_E , input flag x and output flag y provides the group $\text{Aut}(v_E)$ with an action on this tensor product by acting simultaneously on the vertex connected to x on the left and the vertex connected to y on the right. This action commutes across edges by Eq. (2), and hence provides an action of the group $\prod_{E \in \text{Edges}(T)}^U \text{Aut}(v_E)$ on these tensor products. We let $[-]_{\text{Edges}(T)}$ denote the coinvariants of this action and define,

$$A_\Sigma(T) := [\bigotimes_{w \in \text{Vt}(T)} A_\Sigma(w)]_{\text{Edges}(T)} \quad (3)$$

$$A(T) := [\bigotimes_{w \in \text{Vt}(T)} A(w)]_{\text{Edges}(T)} \quad (4)$$

Definition 3.1.3. For a tree T with n levels, \mathbb{V}_Σ -modules $A_{\Sigma,1}, \dots, A_{\Sigma,n}$, and \mathbb{V} -modules A_1, \dots, A_n , let

$$(A_{\Sigma,1} \circ \dots \circ A_{\Sigma,n})(T) := [\bigotimes_{w \in \text{Vt}(T)} A_{\Sigma,ht(w)}(w)]_{\text{Edges}(T)}$$

$$(A_1 \circ \dots \circ A_n)(T) := [\bigotimes_{w \in \text{Vt}(T)} A_{ht(w)}(w)]_{\text{Edges}(T)}$$

We then define the following symmetric, non-symmetric, and shuffle monoidal products as,

$$(A_{\Sigma,1} \circ \dots \circ A_{\Sigma,n})(\vec{v}) := \coprod_{T \in \Sigma \overline{T}_{n,\vec{v}}} (A_{\Sigma,1} \circ \dots \circ A_{\Sigma,n})(T);$$

$$(A_1 \circ \dots \circ A_n)(\vec{v}) := \coprod_{T \in R \overline{T}_{n,\vec{v}}} (A_1 \circ \dots \circ A_n)(T);$$

$$(A_1 \circ_{sh} \dots \circ_{sh} A_n)(\vec{v}) := \coprod_{T \in S \overline{T}_{n,\vec{v}}} (A_1 \circ \dots \circ A_n)(T).$$

Lemma 3.1.4. Each of the products above give the underlying category a strict monoidal structure with unit

$$\mathcal{I}(\vec{v}) := \begin{cases} \coprod_{\text{Aut}(v)} 1_{\mathcal{E}}, & \vec{v} = (v; v) \text{ for some } v \in \text{Ob}(\mathbb{V}) \\ \emptyset, & \text{else} \end{cases}$$

This (to be proven) lemma provides the following monoidal definitions of operads.

Definition 3.1.5.

- (1) A **symmetric groupoid coloured operad** is a monoid in the category of \mathbb{V}_Σ -modules with the monoidal product given by symmetric composition.
- (2) A **non-symmetric groupoid coloured operad** is a monoid in the category of \mathbb{V} -modules with the monoidal product given by non-symmetric composition.
- (3) A **shuffle groupoid coloured operad** is a monoid in the category of \mathbb{V} -modules with the monoidal product given by shuffle composition.

We now prove Lemma 3.1.4.

Proof. For the symmetric case, we refer the reader to Proposition 3.6 of [46] and Lemma 2.22 of [55] (accounting for Remark 2.1.3). We shall only explicitly prove the shuffle case, and the other cases follow similarly. Let $Vt(T)_n = \{v \in Vt(T) : ht(v) = n\}$, then

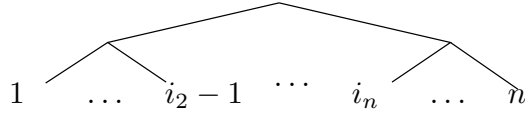
$$\begin{aligned}
& (A_1 \circ_{sh} (A_2 \circ_{sh} A_3))(\vec{v}) \\
&= \coprod_{T \in \overline{ST}_{2, \vec{v}}} (A_1 \circ (A_2 \circ_{sh} A_3))(T) \\
&= \coprod_{T \in \overline{ST}_{2, \vec{v}}} [\bigotimes_{w_1 \in Vt(T)_1} A_1(w_1) \bigotimes_{w_2 \in Vt(T)_2} (A_2 \circ_{sh} A_3)(w_2)]_{Edges(T)} \\
&= \coprod_{T \in \overline{ST}_{2, \vec{v}}} [\bigotimes_{w_1 \in Vt(T)_1} A_1(w_1) \bigotimes_{w_2 \in Vt(T)_2} (\coprod_{T_2 \in \overline{ST}_{2, \vec{w}_2}} (A_2 \circ A_3)(T_2))]_{Edges(T)} \\
&= \coprod_{T \in \overline{ST}_{2, \vec{v}}} [\bigotimes_{w_1 \in Vt(T)_1} A_1(w_1) \bigotimes_{w_2 \in Vt(T)_2} (\\
&\quad \coprod_{T_2 \in \overline{ST}_{2, \vec{w}_2}} [\bigotimes_{w'_1 \in Vt(T_2)_1} A_2(w'_1) \bigotimes_{w'_2 \in Vt(T_2)_2} A_3(w'_2)]_{Edges(T_2)} \\
&\quad)]_{Edges(T)} \\
&= \coprod_{T' \in \overline{ST}_{3, \vec{v}}} [\bigotimes_{w_1 \in Vt(T')_1} A_1(w_1) \bigotimes_{w_2 \in Vt(T')_2} A_2(w_2) \bigotimes_{w_3 \in Vt(T')_3} A_3(w_3)]_{Edges(T')} \\
&= (A_1 \circ_{sh} A_2 \circ_{sh} A_3)(\vec{v})
\end{aligned}$$

The second to last line follows as \mathcal{E} is a closed monoidal category, so we can iteratively commute the colimits and monoidal products. The grouping of the two coproducts into the single coproduct $\coprod_{T' \in \overline{ST}_{3, \vec{v}}}$ is done by the obvious bijection. Similar working shows $((A_1 \circ_{sh} A_2) \circ_{sh} A_3)(\vec{v}) = (A_1 \circ_{sh} A_2 \circ_{sh} A_3)(\vec{v})$ yielding the associativity of the product. The required unitality results are then easily verified, giving the result. \square

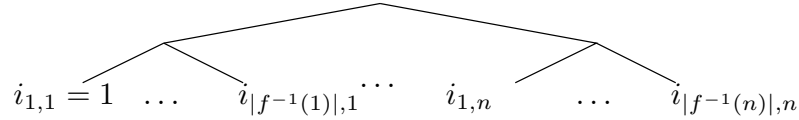
Example 3.1.6. Groupoid coloured operads coloured by a discrete category are coloured operads. This can be seen in the case of $\mathcal{E} = Vect$, the category of vector spaces, by observing that the defined monoidal products are equivalent to those of Definition 1.5 of

[25]. This follows from inspection, however we clarify the following bijections to structures used in their definition.

- A non-decreasing surjection $f : [m] \rightarrow [n]$ is a linear tree of height 2. In particular if $i_n = \min\{i : f(i) = n\}$ then the corresponding linear tree is



- A shuffling surjection $f : [m] \rightarrow [n]$ (i.e. one in which $\min f^{-1}(i) < \min f^{-1}(j)$ for all $i < j$) is a shuffle tree of height 2. In particular if $i_{1,k} < i_{2,k} < \dots < i_{|f^{-1}(k)|,k}$ are the elements of $f^{-1}(k)$ ordered smallest to largest then the corresponding shuffle tree is



We make the following definitions in light of this example.

Definition 3.1.7. We refer to (non-groupoid) coloured operads as **discrete coloured operads**. Given a groupoid \mathbb{V} , a $ob(\mathbb{V})$ -**coloured operad** is a discrete coloured operad with objects/colours $ob(\mathbb{V})$.

Another fundamental example of a groupoid coloured operad is the endomorphism operad.

Definition 3.1.8 (Example 2.15 of [55]). A functor $X : \mathbb{V} \rightarrow \mathcal{E}$ admits a natural extension into a groupoid coloured module End_X . For each profile $(v_1, \dots, v_n; v_0)$

$$End_X(v_1, \dots, v_n; v_0) := Hom_{\mathcal{E}}(X(v_1), \dots, X(v_n); X(v_0))$$

with inherited action of $(\times_i^U Hom_{\mathbb{V}}(-, v_i)) \times Hom_{\mathbb{V}}(v_0, -)$, and the Σ_n action given by permuting the labels. This groupoid coloured module admits the structure of a unital \mathbb{V} -coloured operad with composition given by composition of functions. We call End_X the **endomorphism operad**.

The operad structure of End_X is well-defined, as associativity of functions not only yields associativity of the operadic structure maps, but also compatibility of the structure maps with the action of groupoid on the internal edges. A **morphism** of (groupoid coloured) operads is a morphism of the (groupoid coloured) modules (Definition 2.1.4), which is also compatible with the operadic structure maps.

Definition 3.1.9 (2.3.2 of [55]). Let $X : \mathbb{V} \rightarrow \mathcal{E}$ be a functor and P be a \mathbb{V} -coloured operad. A P -algebra structure on X is a morphism of groupoid coloured operads $P \rightarrow \text{End}_X$.

If this reader at this stage wants a more sophisticated example of a groupoid coloured operad, then it is possible to skip ahead and read Section 5-5.2 which includes a nice example of the equivalence classes induced by the action of the groupoid on internal edges of trees (Example 5.2.1). This later section does use some terminology introduced in the remainder of this section, but should be relatively clear to the reader already familiar with operads. Other examples of groupoid coloured operads include the operad governing props (this is less approachable for technical reasons, but can be found Section 6), and the operad governing modular operads (see Section 3.1 of [55]).

We close this section by noting that there is a natural forgetful functor $-^f$ from \mathbb{V}_Σ -modules to \mathbb{V} -modules, which forgets the action of the group of symmetries.

Lemma 3.1.10. *Given \mathbb{V}_Σ -modules P and Q we have that*

$$(P \circ Q)^f \cong P^f \circ_{sh} Q^f$$

Proof. As the forgetful functor does not touch the underlying coinvariants given by the groupoid, this is an immediate corollary of the corresponding result for discrete coloured operads in [25] (Section 1.7, which is itself a corollary of Proposition 3 of [14]), given we have assumed our modules are reduced (Definition 3.1.1). \square

The forgetful functor is not only straightforward to calculate in practice (for instance see Example 4.3.5, and Section 5.3), but also enables us to characterise when O is Koszul by inspecting O^f (Definition 3.6.7).

3.2. Monadic groupoid coloured operads

In this section, we introduce monadic definitions of our operads and prove their equivalence to the monoidal definitions. In many cases it is more convenient to work with non-unital variants of operads (e.g. Sections 5, 6), and monadic definitions provide a clear path to non-unital variants. We note that our monadic definition of a symmetric groupoid coloured operad is that of [55], and the others are natural alterations.

Definition 3.2.1. We define the following endofunctors

- Let $\mathbb{T}_{\mathbb{V}, \Sigma}, \overline{\mathbb{T}_{\mathbb{V}, \Sigma}} : \mathbb{V}_\Sigma\text{-modules} \rightarrow \mathbb{V}_\Sigma\text{-modules}$ be defined on objects as

$$\mathbb{T}_{\mathbb{V}, \Sigma}(A)(\vec{v}) := \coprod_{T \in \Sigma T} A_\Sigma(T), \quad \overline{\mathbb{T}_{\mathbb{V}, \Sigma}}(A)(\vec{v}) := \coprod_{T \in \Sigma T} A_\Sigma(T)$$

- Let $\mathbb{T}_{\mathbb{V}}, \overline{\mathbb{T}_{\mathbb{V}}} : \mathbb{V}\text{-modules} \rightarrow \mathbb{V}\text{-modules}$ be defined on objects as

$$\mathbb{T}_{\mathbb{V}}(A)(\vec{v}) := \coprod_{T \in RT} A(T), \quad \overline{\mathbb{T}_{\mathbb{V}}}(A)(\vec{v}) := \coprod_{T \in \overline{RT}} A(T)$$

- Let $\mathbb{T}_{\mathbb{V},sh}, \overline{\mathbb{T}_{\mathbb{V},sh}} : \mathbb{V}\text{-modules} \rightarrow \mathbb{V}\text{-modules}$ be defined on objects as

$$\mathbb{T}_{\mathbb{V},sh}(A)(\vec{v}) := \coprod_{T \in ST} A(T), \quad \overline{\mathbb{T}_{\mathbb{V},sh}}(A)(\vec{v}) := \coprod_{T \in \overline{ST}} A(T)$$

Morphisms of \mathbb{V}_{Σ} (and \mathbb{V})-modules are natural transformations, and so they are given by collections of equivariant maps from $A_{\Sigma}(\vec{v}) \rightarrow B_{\Sigma}(\vec{v})$, which induce maps from $A_{\Sigma}(T) \rightarrow B_{\Sigma}(T)$ (and similarly for $A(-)$). Taking the coproduct of these maps specifies the endofunctors on morphisms.

Lemma 3.2.2. *Substitution of trees endows these functors with the structure of a monad.*

Proof. See Definition 2.1.1 of [55] for a definition of substitution of trees, it is straightforward to modify this definition to also track the listings of the internal vertices (as required by Definition 2.2.7). From here, the proofs for $\mathbb{T}_{\mathbb{V},\Sigma}$ and $\overline{\mathbb{T}_{\mathbb{V},\Sigma}}$ are Theorems 2.10 and 2.11 of [55]. The modifications of these proofs to yield the results for the other functors is straightforward. \square

Definition 3.2.3. These yield the following monadic definitions of groupoid coloured operads,

- A symmetric (non-)unital groupoid coloured operad is a algebra over the monad $\overline{\mathbb{T}_{\mathbb{V},\Sigma}}$ (resp. $\mathbb{T}_{\mathbb{V},\Sigma}$).
- A non-symmetric (non-)unital groupoid coloured operad is a algebra over the monad $\overline{\mathbb{T}_{\mathbb{V}}}$ (resp. $\mathbb{T}_{\mathbb{V}}$).
- A shuffle (non-)unital groupoid coloured operad is a algebra over the monad $\overline{\mathbb{T}_{\mathbb{V},sh}}$ (resp. $\mathbb{T}_{\mathbb{V},sh}$).

By this definition, each groupoid coloured operad (of any type) P comes with a morphism $\eta_T : P(T) \rightarrow P(\vec{v})$ for every $ob(\mathbb{V})$ -tree T of profile \vec{v} , this morphism ‘contracts’ the tree.

Lemma 3.2.4. *The unital monadic definitions (Definition 3.2.3) are equivalent to the monoidal definitions (Definition 3.1.5).*

Proof. A sketch of the proof for symmetric operads is given in Theorem 2.2.4 of [55]. The proof is modified in the obvious ways for non-symmetric and shuffle operads. \square

Definition 3.2.5 (2.19 of [55]). An **augmentation** of a unital groupoid coloured operad P is a morphism $P \rightarrow \mathcal{T}$ where \mathcal{T} is the unique unital operad structure on the \mathbb{V} -module given by

$$\mathcal{T}(\vec{v}) := \begin{cases} 1_{\mathcal{E}}, & \vec{v} = (v; v) \text{ for some } v \in Ob(\mathbb{V}) \\ \text{terminal object in } \mathcal{E}, & \text{otherwise} \end{cases}$$

An **augmented operad** is an operad with an augmentation. If \mathcal{E} is an Abelian category, then the augmentation ideal is the kernel of these maps, and we denote it \overline{P} .

Corollary 3.2.6. *An augmented operad P in an Abelian category is isomorphic to \overline{P} .*

Proof. Immediate, but see for instance [34], Proposition 21. \square

3.3. Partial compositions

We will use partial operadic compositions throughout this paper (see [34] for the uncoloured case). Instead of defining partial groupoid coloured operads and proving the equivalence of this definition (which is possible but tedious), we will simply define a partial composition as monadic contractions (3.2.3) of particular trees.

Definition 3.3.1. Let P be a groupoid coloured shuffle operad we define the partial composition

$$P\left(\begin{smallmatrix} d \\ \underline{c} \end{smallmatrix}\right) \otimes P\left(\begin{smallmatrix} c_i \\ \underline{b} \end{smallmatrix}\right) \xrightarrow{\circ_{i,\sigma}} P\left(\begin{smallmatrix} d \\ (\underline{c} \circ_i \underline{b})\sigma \end{smallmatrix}\right)$$

by the contraction map applied to a shuffle tree T with 2 vertices. In particular, for $\alpha \in P\left(\begin{smallmatrix} d \\ \underline{c} \end{smallmatrix}\right)$ and $\beta \in P\left(\begin{smallmatrix} b \\ \underline{a} \end{smallmatrix}\right)$ we define $\alpha \circ_{i,\sigma} \beta$ to be the contraction map η_T applied to the shuffle tree T with: 2 vertices; the root vertex decorated by α ; the lower vertex decorated by β ; the lower vertex connected to the i th input flag of the root; and the listing of the legs of the tree specified by σ . In other words, σ is a **shuffle permutation**, which is to say that

- for $j \leq i$, $\sigma(j) = j$
- $\sigma(i+1) < \sigma(i+1) < \dots < \sigma(i+|\underline{b}|)$
- $\sigma(i+|\underline{b}|+1) < \dots < \sigma(|\underline{c}|+|\underline{b}|-1)$.

We will occasionally use the shorthand \circ_{φ} to refer to a partial composition with i and σ suppressed. We also similarly define partial compositions for symmetric and non-symmetric groupoid coloured operads as the contractions of the obvious trees associated to

$$P\left(\begin{smallmatrix} d \\ \underline{c} \end{smallmatrix}\right) \otimes P\left(\begin{smallmatrix} c_i \\ \underline{b} \end{smallmatrix}\right) \xrightarrow{\circ_i} P\left(\begin{smallmatrix} d \\ \underline{c} \circ_i \underline{b} \end{smallmatrix}\right)$$

3.4. Some assumptions

We now mirror [55] (Assumption 2.28 and above) and make two assumptions for the rest of this paper. Firstly, we assume that $\text{Aut}(v)$ is finite for all $v \in \text{Ob}(\mathbb{V})$. Secondly, we assume that the co-complete and closed symmetric monoidal category used by our operads is $\text{dgVect}_{\mathbb{K}}$, the category of differential graded vector spaces over \mathbb{K} , a field of characteristic 0. The finiteness of $\text{Aut}(v)$ not only allows for summation over automorphism groups as in Ward, but also enables an isomorphism between groupoid coloured shuffle operads and discrete coloured shuffle operads developed in Section 4.2. We restrict to characteristic 0 for the same reasons as Ward, i.e. homotopy transfer theory can be done in characteristic 0 without resolving automorphisms, but this is not the case in characteristic $p > 0$. In particular, the characteristic 0 assumption is needed for a groupoid coloured module to admit its homology as a deformation retract (Proposition 7.2.2).

3.5. Tree monomials and presentations of operads

Tree monomials correspond to the basis elements of free operads, and an understanding of their form is needed for developing Groebner bases for operads. Groupoid coloured tree monomials are equivalence classes of discrete coloured tree monomials under the action of the groupoid, so this work naturally extends Sections 2.2-2.5 of [25].

By the general theory of monads, each of our operads admits a forgetful functor which maps to the underlying \mathbb{V}_{Σ} (or \mathbb{V})-module, and this forgetful functor admits a left adjoint. We shall denote these left adjoints $\overline{F}_{\Sigma}, \overline{F}, \overline{F}_{sh}$ for the unital variants and F_{Σ}, F, F_{sh} for the non-unital variants. If we wish to highlight the underlying groupoid we will use a superscript e.g. $F^{\mathbb{V}}$. A **free groupoid coloured operad** is the image of one of these left adjoints applied to an appropriate groupoid coloured module.

Definition 3.5.1. Let E be a \mathbb{V}_{Σ} (or \mathbb{V})-module, a **groupoid coloured tree monomial** of $F_{\Sigma}(E)$ is of the form $[\bigotimes_{w \in Vt(T)} e_w]_{\text{Edges}(T)}$ (see Definition 3.1.2), where T is a $\text{ob}(\mathbb{V})$ -tree of suitable type for the free operad, and each e_w is in $E(w)$. We can view a groupoid coloured tree monomial as an equivalence class of (discrete) coloured tree monomials (in the sense of Section 2.1 of [25]) under the action of the groupoid on the edges of the tree. A tree monomial has several natural degrees (conserved under this action)

- Its **arity** corresponds to its number of leaves.
- Its **weight** corresponds to the number of internal edges +1, or equivalently the number of constituent generators from E .

We say an element of a groupoid coloured operad is **homogeneous** with respect to a degree if it is a sum of groupoid coloured tree monomials with non-zero coefficients, all

with the same degree. Furthermore, we shall use $F_\Sigma(E)^{(k)}$ to denote the weight k subset of $F_\Sigma(E)$.

We close this section by defining quotient operads, and what we mean by a quadratic presentation.

Definition 3.5.2 (2.5.2 [55]). Given two \mathbb{V} (or \mathbb{V}_Σ)-modules A and I , we say I is a **submodule** of A if it is a subcategory of A . If P is a groupoid coloured operad (of any type) and $I \subset P$ a submodule of appropriate type, we say I is an **ideal** of P if the image of any of the contracting maps η_T of the operad (Definition 3.2.3) applied to a tensor with a factor of I lands back in I .

Definition 3.5.3. If I is an ideal of P , we may form a **quotient operad** P/I with the quotient \mathbb{V} -module and the inherited structure maps. We say an operad P admits a **quadratic presentation** if $P \cong F_\Sigma(E)/R$ and $R \subset F_\Sigma(E)^{(2)}$.

3.6. Koszul groupoid coloured operads

We now introduce what it means for a groupoid coloured operad to be Koszul using the theory of Ward [55], before providing an alternate characterisation through shuffle operads. We briefly recall the necessary definitions of groupoid coloured cooperads, and the bar/cobar complexes, before presenting four equivalent characterisations of when a groupoid coloured operad is Koszul (Definition 3.6.7). Through the theory of shuffle operads we will show that a groupoid coloured symmetric operad O is Koszul when its groupoid coloured shuffle operad O^f is Koszul. This result will enable the Groebner basis machinery developed in Section 4.

3.6.1. Background: cooperads and bar/cobar complexes

We first recall some supporting theory of [55] regarding cooperads and bar/cobar complexes. All definitions in this section are presented for symmetric groupoid coloured operads, but they can be modified in obvious ways to obtain analogous definitions for non-symmetric and shuffle groupoid coloured operads.

Definition 3.6.1 (2.29 [55]). A symmetric groupoid coloured non-unital conilpotent co-operad is a comonoid in the category of \mathbb{V}_Σ -modules with comonoidal product given in Section 2.4.1 of [55].

By the general theory of comonads, a cooperad admits a forgetful functor $F_{\Sigma,c}$ which maps to the underlying \mathbb{V}_Σ -module, and this forgetful functor admits a left adjoint. This allows us to define cofree cooperads, which leads to the following definition of cooperads with a quadratic presentation.

Definition 3.6.2 (2.5.3 [55]). Let R be a homogeneous quadratic ideal of $F_{\Sigma,c}(E)$, then we define a **quadratic cooperad** $Q(E, R)$ as the union of all sub-cooperads of $Q \subset F_{\Sigma,c}(E)$ such that the composite $Q \hookrightarrow F_{\Sigma,c}(E) = F_{\Sigma}(E) \rightarrow F_{\Sigma,c}(E)^{(2)}/R$ vanishes.

A particularly important quadratic cooperad is the Koszul dual cooperad defined as follows.

Definition 3.6.3 (2.5.4 [55]). Let $P \cong F_{\Sigma}(E)/R$ be a quadratic \mathbb{V}_{Σ} operad, then $P^i := Q(sE, s^2R)$.

Where s is the suspension operator in $dgVect$. The suspension operator and its inverse s^{-1} are also used in the bar/cobar constructions. This familiar adjoint pair (see for instance [33] for the uncoloured case) extends naturally to groupoid coloured operads as follows.

Definition 3.6.4 (2.6.1 [55]). Let P be an operad, the **bar** construction of P is $B(P) := (F_c(sP), \partial + d_P)$, i.e. it is the cofree operad generated by the suspension of P whose differential is induced by the operadic composition of P (∂) and the differential of P (d_P).

Definition 3.6.5 (2.6.2 [55]). Let Q be a conilpotent cooperad, the **cobar** construction of Q is $\Omega(Q) := (F(s^{-1}Q), \partial + d_Q)$, i.e. it is the free operad generated by the desuspension of Q whose differential is induced by the cooperadic composition of Q (∂) and the differential of Q (d_Q).

There is a natural grading on these complexes, which simplifies some theory for Koszulness.

Definition 3.6.6. There is a natural grading on the bar (and cobar) complex called the **syzygy degree** induced by the weight gradings of P and $F_c(-)$. In particular, if $a \in F_c(sP)^{(k)} = F(sP)^{(k)}$ then the syzygy degree of a is $w_P(a_1) + \dots + w_P(a_k) - k$.

3.6.2. Koszul characterisations

We now present four equivalent definitions for when a quadratic groupoid coloured operad is Koszul, before making some comments and proving their equivalence.

Definition 3.6.7. A quadratic \mathbb{V}_{Σ} -operad P is **Koszul** if any of the following equivalent definitions hold,

- (1) the inclusion $\zeta_{P^i} : P^i \rightarrow B(P)$ is a quasi-isomorphism.
- (2) the composition $\Omega(P^i) \rightarrow \Omega(B(P)) \rightarrow P$ is a quasi-isomorphism.
- (3) using the syzygy degree $H^n(B(P)) = 0$ for $n \geq 1$.
- (4) the \mathbb{V}_{sh} -operad P^f is Koszul.

Analogous versions of the first three characterisations also hold for non-symmetric and shuffle groupoid coloured operads.

The first characterisation is Definition 2.45 of [55], and the remaining characterisations are ordered by their appearance in the proof below. For the purpose of this paper, the second and the fourth characterisation are the most useful. When P is Koszul we will denote $P_\infty := \Omega(P^i)$. By the second characterisation, P_∞ is a model for P , which by construction is quadratic (and hence minimal). The fourth characterisation is precisely the reason we have developed the theory of groupoid coloured shuffle operads, and this is what will enable the theory of Groebner bases in the subsequent section. We note that [55] has further characterisations of groupoid coloured operads, and many characterisations in the uncoloured case (see for instance 7.9.2 of [33]) admit natural generalisations.

The equivalence of (1) and (2) in Definition 3.6.7 is a consequence of the bar-cobar adjunction, see Lemma 2.44 of [55]. Then, (1) and (3) are equivalent in an obvious extension of the argument of Proposition 7.3.1 of [33], i.e. the inclusion $\zeta_{P^i} : P^i \rightarrow B(P)$ induces an isomorphism $P^i \cong H^0(B(P))$. Finally, (3) and (4) are equivalent through the following proposition.

Proposition 3.6.8 (Proposition 1.4 [15]). *The symmetric bar complex of a groupoid coloured operad P is isomorphic, as a shuffle dg groupoid coloured cooperad, to the shuffle bar complex of P^f , i.e. $B(P)^f \cong B(P^f)$.*

Proof. This proposition immediately extends to the groupoid coloured case as a consequence of f being monoidal (Lemma 3.1.10). \square

So,

$$B(P)^f \cong B(P^f) \implies \forall n, H^n(B(P)^f) \cong H^n(B(P^f))$$

which tells us that,

$$\begin{aligned} H^n(B(P)) = 0 \text{ for } n \geq 1 &\iff H^n(B(P)^f) = 0 \text{ for } n \geq 1 \\ &\iff H^n(B(P^f)) = 0 \text{ for } n \geq 1 \end{aligned}$$

So P is Koszul by Definition 3.6.7.(3), if and only if, P^f is Koszul by Definition 3.6.7.(3).

4. Koszul groupoid coloured operads via Groebner bases

The theory of Groebner bases was first developed for (discrete one-coloured) operads in [14], extending upon the PBW bases of [22], as a useful tool for proving that specific operads are Koszul. In particular, Dotsenko and Khoroshkin proved that if an operad O has a shuffle operad O^f with a quadratic Groebner basis, then O is Koszul. This powerful

tool was extended to discrete coloured operads in [25], and is currently in the process of being extended to dioperads by Khoroshkin. In this section, we develop the theory of Groebner bases for groupoid coloured operads by proving the following theorem.

Theorem (4.2.13). *Let P be a \mathbb{V} -coloured operad such that the associated $ob(\mathbb{V})$ -coloured shuffle operad $(P^f)_*$ admits a quadratic Groebner basis, then P is Koszul.*

We briefly revisit the theory of Groebner bases for discrete coloured operads ([2], [14], [22], and [25]) before extending the theory to groupoid coloured operads in Section 4.2. We then close this section by explicitly establishing a well known equivalence between confluent terminating rewriting systems and Groebner bases. This provides alternate methods for proving that a discrete coloured operad admits a Groebner basis. Later, we use techniques developed in this section to prove that the operads governing wheeled props (Section 5.5) and props (Section 6.5) are Koszul.

4.1. Divisibility, order and Groebner bases for discrete coloured shuffle operads

We start by recalling some necessary definitions and results.

Definition 4.1.1. Given a discrete coloured shuffle operad, a partial ordering \leq of its underlying tree monomials is said to be **admissible** if

$$(\alpha \leq \alpha' \text{ and } \beta \leq \beta') \implies \alpha \circ_{\varphi} \beta \leq \alpha' \circ_{\varphi} \beta'$$

where α, α' and β, β' are pairs of arity homogeneous tree monomials and \circ_{φ} is a shuffle composition. If the order is also total (i.e. all tree monomials are comparable) then we will call it a **total admissible order**.

For the rest of this section, we assume all tree monomials are ordered by a total admissible order. Path lexicographic orders are an example of a total admissible order, and we will construct two such orders in this paper (5.4, 6.4), but see [14] for many additional examples. This total order on tree monomials allows us to identify the largest term with non-zero coefficients of any element of a given shuffle operad. For such an element f , we will denote the largest term by $lt(f)$, and its coefficient by c_f .

Definition 4.1.2. Given two tree monomials α and β , we say that α is **divisible** by β if there exists a subtree T' of α whose corresponding tree monomial is β . As α is divisible by β , a composite of elementary shuffle compositions and generators may be used to form α from β (Proposition 6 of [14]). This yields an operator in tree monomials $m_{\alpha, \beta}$ such that $m_{\alpha, \beta}(\beta) = \alpha$.

Note that we can apply the operator $m_{\alpha, \beta}$ to other tree monomials with the same shape as β . Furthermore, as we have a total admissible order \leq , it must be the case that

if $\gamma < \beta$ then $m_{\alpha,\beta}(\gamma) < m_{\alpha,\beta}(\beta) = \alpha$. Several examples of divisibility, and the induced operators, are provided in Example 4.3.5. With the preceding definitions, we can now define Groebner bases for discrete coloured shuffle operads.

Definition 4.1.3. Let $F_{sh}(E)$ be a free discrete coloured shuffle operad, I an operadic ideal of $F_{sh}(E)$, and G a system of arity homogeneous generators for I . We say G is **Groebner basis** for I if, for all ideal elements $f \in I$, the leading term of f is divisible by the leading term of an element of G . We say G is **quadratic** if $G \subset F_{sh}(E)^{(2)}$.

This is certainly a definition, but we need a practical way to characterise when we have a Groebner basis. To this end, we first discuss reductions and S -polynomials.

Definition 4.1.4. If f, g are two arity homogeneous elements of $F_{sh}(E)$ such that $lt(f)$ is divisible by $lt(g)$, then

$$r_g(f) := f - \frac{c_f}{c_g} m_{lt(f), lt(g)}(g)$$

is called the **reduction of f modulo g** .

The total admissible order on tree monomials implies that $lt(r_g(f)) < lt(f)$, and in Section 4.3, we will interpret a reduction $f \rightarrow r_g(f)$ as a rewrite of f to a smaller element. These reductions may be chained together to provide a unique normal form for every element of the discrete coloured shuffle operad through the following proposition.

Proposition 4.1.5 (Proposition 7 [14]). *If G is a Groebner basis for I and $f \in F_{sh}(E)$ then there exists a unique element $\bar{f} \in F_{sh}(E)$ such that*

- (i) $f - \bar{f} \in I$
- (ii) \bar{f} is a linear combination of tree monomials which have no non-trivial reductions modulo G (i.e. for all g in G , every term of \bar{f} with a non-zero coefficient is not divisible by $lt(g)$). We denote this $f \equiv \bar{f} \bmod G$.

We say that \bar{f} is the **unique normal form** of f .

We now slightly extend the notion of a reduction by defining a S -polynomial.

Definition 4.1.6. We say that two tree monomials α, β have a **common multiple** if there exists a discrete coloured tree monomial γ such that γ is divisible by both α and β . We say that a common multiple is **small** if the corresponding subtrees of α and β in γ overlap.

Definition 4.1.7. Let f and g be two arity homogeneous elements of $F_{sh}(E)$ whose leading terms admit a small common multiple γ . The **S-polynomial** corresponding to γ is defined by

$$s_\gamma(f, g) := m_{\gamma, lt(f)}(f) - \frac{c_f}{c_g} m_{\gamma, lt(g)}(g)$$

We can now give the following equivalent characterisations of Groebner bases for operads.

Proposition 4.1.8 (Theorem 1 [14]). *The following are equivalent.*

- (1) G is a Groebner basis for I
- (2) for all $f \in I$, $f \equiv 0 \pmod{G}$
- (3) for all pairs of elements from G , all their S -polynomials (if defined) are congruent to 0 mod G .

In particular, the third characterisation means we can check we have a Groebner basis by a generalised version of Buchberger's algorithm [14]. This means we can apply this algorithm to check that a discrete coloured operad is Koszul through the following result.

Proposition 4.1.9 (Theorem 3.12 [25]). *A discrete coloured shuffle operad P with a quadratic Groebner basis is Koszul.*

4.2. The groupoid coloured extension

We now extend these techniques to the groupoid coloured case. We point out that the constructions of this section will be clarified in Example 4.2.14.

4.2.1. Forgetting the action of the groupoid

We first show that the Koszulness of a \mathbb{V} -coloured operad P is characterised by the Koszulness of an $Ob(\mathbb{V})$ -coloured shuffle operad. We note that the arguments of this section also apply to symmetric and non-symmetric operads with the obvious modifications to modules and operadic compositions.

Recall from Lemma 3.1.4, that the forgetful functor from \mathbb{V}_Σ -modules to \mathbb{V} -modules is monoidal with respect to the symmetric operadic and shuffle operadic monoidal compositions (Definition 3.1.5). One consequence of this is that the bar complex of a groupoid coloured operad P , and its corresponding shuffle operad P^f are isomorphic as groupoid coloured shuffle cooperads (Proposition 3.6.8),

$$B(P^f) \cong B(P)^f.$$

This result allowed us to infer that P is Koszul, if, and only if, P^f is Koszul (Definition 3.6.7). Thus, instead of studying the Koszulness of \mathbb{V} -coloured symmetric operads, it is sufficient to study the Koszulness of \mathbb{V} -coloured shuffle operads.

There also exists a forgetful functor $-^{f_{\mathbb{V}}}$ from \mathbb{V} -modules to $ob(\mathbb{V})$ -modules, which forgets the action of the groupoid. However, $-^{f_{\mathbb{V}}}$ is not monoidal. Despite this failure, we will show in Proposition 4.2.4, that there exists an epimorphism $B(P^{f_{\mathbb{V}}}) \twoheadrightarrow B(P)$ of groupoid coloured shuffle cooperads. This epimorphism lets us infer one of the two directions.

Proposition 4.2.1. *A \mathbb{V} -coloured shuffle operad P is Koszul if $P^{f_{\mathbb{V}}}$ is Koszul.*

Proof. The epimorphism $B(P^{f_{\mathbb{V}}}) \twoheadrightarrow B(P)$ implies (using syzygy degree, Definition 3.6.6) that,

$$H^n(B(P^{f_{\mathbb{V}}})) = 0 \text{ for } n \geq 1 \implies H^n(B(P)) = 0 \text{ for } n \geq 1.$$

Hence by Definition 3.6.7, if $P^{f_{\mathbb{V}}}$ is Koszul then P is Koszul. \square

The following epimorphism of groupoid coloured shuffle operads will not only let us construct $B(P^{f_{\mathbb{V}}}) \twoheadrightarrow B(P)$, but will eventually lead to a simpler presentation of $P^{f_{\mathbb{V}}}$ in the next subsection. Recall that a morphism of groupoid coloured operads is a morphism of groupoid coloured modules, Definition 2.1.4, which is compatible with the operadic structure maps.

Definition 4.2.2. Let E be a \mathbb{V} -coloured module. We define an epimorphism of groupoid coloured operads,

$$[-] : F_{sh}^{ob(\mathbb{V})}(E^{f_{\mathbb{V}}}) \twoheadrightarrow F_{sh}^{\mathbb{V}}(E).$$

The underlying map of groupoids is the inclusion $[-]_0 : ob(\mathbb{V}) \hookrightarrow \mathbb{V}$. The map of groupoid coloured modules is defined on the basis elements of $F_{sh}^{ob(\mathbb{V})}(E^{f_{\mathbb{V}}})$, and sends each $ob(\mathbb{V})$ -coloured tree monomial T to a \mathbb{V} -coloured tree monomial by adding in the action of \mathbb{V} on the internal edges of T (Definition 3.5.1),

$$[T] := \left[\bigotimes_{w \in \text{Int}(T)} e_w \right]_{\text{Edges}(T)}.$$

Lemma 4.2.3. *The quotient map $[-]$ is indeed an epimorphism of groupoid coloured operads.*

Proof. We first observe that $[-]$ (trivially) respects the trivial action of the groupoid $ob(\mathbb{V})$. Next, we observe that $[\alpha \circ_{\varphi} \beta] = [\alpha] \circ_{\varphi} [\beta]$, as both sides of the equation have

the same action of \mathbb{V} on the internal edge specified by the partial composition \circ_φ . Finally, $[-]$ must be an epimorphism, as the equivalence class corresponding to any groupoid coloured tree monomial in $F_{sh}^\mathbb{V}(E)$ is represented by at least one non-groupoid coloured tree monomial in $F_{sh}^{ob(\mathbb{V})}(E^{f\mathbb{V}})$. (See Lemma 4.2.7 for one method of producing a particular representative.) \square

Proposition 4.2.4. *The quotient map $[-]$ induces an epimorphism $B(P^{f\mathbb{V}}) \twoheadrightarrow B(P)$ of groupoid coloured shuffle cooperads.*

Proof. As in the prior definition, the underlying map of groupoids is the inclusion $ob(\mathbb{V}) \hookrightarrow \mathbb{V}$. Now, recall from Definition 3.6.4, that given a groupoid coloured shuffle operad P , its bar construction is $B(P) = (F_c(sP), \partial + d_P)$, where the differential d_P is the differential induced by the differential of P , and ∂ is the differential induced by the operadic composition of P . Furthermore, the underlying groupoid coloured modules of the cofree cooperad $F_c(sP)$ and $F(sP)$ are equal. Hence,

$$F_c^{ob(\mathbb{V})}(sP^{f\mathbb{V}}) = F^{ob(\mathbb{V})}(sP^{f\mathbb{V}}) \twoheadrightarrow F^\mathbb{V}(sP) = F_c^\mathbb{V}(sP).$$

This composite, which we also denote $[-]$ in a minor abuse of notation, respects the cooperadic structure, i.e. if we let $\Delta^{ob(\mathbb{V})}$ and $\Delta^\mathbb{V}$ denote the partial cooperadic products for $F_c^{ob(\mathbb{V})}(sP^{f\mathbb{V}})$ and $F_c^\mathbb{V}(sP)$ respectively, then $([-], [-]) \circ \Delta^{ob(\mathbb{V})} = \Delta^\mathbb{V} \circ [-]$. This follows as, for $\alpha \in F_c^{ob(\mathbb{V})}(sP^{f\mathbb{V}})$, we observe that $\Delta^{ob(\mathbb{V})}(\alpha) \in \Delta^\mathbb{V}([\alpha])$.

Thus, to conclude the proof, we need only show that $[-]$ commutes with the respective differentials. This is immediate for the differentials induced by the differential of P . For the ∂ (operadic) differentials, we recall from Section 2.6.1 of [55] that for a groupoid coloured operad Q , the differential ∂ of $B(Q)$ is the unique extension of the following cooperad map.

$$F_c(sQ) \longrightarrow F_c(sQ)^{(2)} = F(sQ)^{(2)} \cong s^2 F(Q)^{(2)} \longrightarrow s^2 Q \longrightarrow sQ$$

Where the first map is projection, the second is the operadic structure map, and the final is a shift in degree. Thus if we let $\partial_{ob(\mathbb{V})}$ and $\partial_\mathbb{V}$ denote the ∂ differentials of $B(P^{f\mathbb{V}})$ and $B(P)$ respectively. Then the equation $[-] \circ \partial_{ob(\mathbb{V})} = \partial_\mathbb{V} \circ [-]$, is witnessed by the commutativity of their inducing cooperad maps,

$$\begin{array}{ccccccc} F_c(sP^{f\mathbb{V}}) & \longrightarrow & F_c(sP^{f\mathbb{V}})^{(2)} = F(sP^{f\mathbb{V}})^{(2)} \cong s^2 F(P^{f\mathbb{V}})^{(2)} & \longrightarrow & s^2 P^{f\mathbb{V}} & \longrightarrow & sP^{f\mathbb{V}} \\ \downarrow [-] & & & & & & \downarrow [-] \\ F_c(sP) & \longrightarrow & F_c(sP)^{(2)} = F(sP)^{(2)} \cong s^2 F(P)^{(2)} & \longrightarrow & s^2 P & \longrightarrow & sP \end{array}$$

Thus $[-]$ is a morphism of groupoid coloured modules that also respects the shuffle cooperadic structure, and hence is a morphism of groupoid coloured shuffle cooperads. \square

4.2.2. A simpler presentation

Given a quadratic \mathbb{V} -coloured operad P we now seek a simple quadratic presentation for $P^{f_{\mathbb{V}}}$. Given we have an epimorphism of groupoid coloured operads $[-] : F_{sh}^{ob(\mathbb{V})}(E^{f_{\mathbb{V}}}) \twoheadrightarrow F_{sh}^{\mathbb{V}}(E)$ (Definition 4.2.2). An analogue of the fundamental theorem of homomorphisms implies the composite $[-]^{f_{\mathbb{V}}}$ is an isomorphism of $ob(\mathbb{V})$ -coloured shuffle operads,

$$F_{sh}^{ob(\mathbb{V})}(E^{f_{\mathbb{V}}}) / \langle Ker([-]) \rangle \cong F_{sh}^{\mathbb{V}}(E)^{f_{\mathbb{V}}}. \quad (5)$$

Thus, we seek to characterise $Ker([-])$. Firstly, we show the kernel admits a quadratic presentation.

Definition 4.2.5. Let $[-]_2$ be the restriction to weight two elements (Definition 3.5.1), $[-]_2 := [-]|_{(F_{sh}^{ob(\mathbb{V})})_{(2)}}$.

By direct inspection,

$$Ker([-]_2) = \{\alpha \circ_{\phi} \beta = \alpha' \circ_{\phi'} \beta' : \alpha, \beta, \alpha', \beta' \in E^{f_{\mathbb{V}}} \text{ such that } [\alpha \circ_{\phi} \beta] = [\alpha' \circ_{\phi'} \beta']\}.$$

Lemma 4.2.6.

$$\langle Ker([-]_2) \rangle = \langle Ker([-]) \rangle$$

Proof. Clearly $\langle Ker([-]_2) \rangle \subseteq \langle Ker([-]) \rangle$. Conversely, by Definition 3.1.2, the action of $[-]_{Edges(T)}$ is applied to each internal edge via an unordered tensor product. Thus, as $Ker([-]_2)$ encodes the action of a single internal edge, sequential applications of relations in $Ker([-]_2)$ encode the action across all internal edges. \square

We now seek an explicit presentation of $Ker([-]_2)$.

Lemma 4.2.7. Let P be a \mathbb{V} -coloured operad with a total order on its underlying $ob(\mathbb{V})$ -coloured tree monomials. Every \mathbb{V} -coloured tree monomial T admits a unique minimal representative, which we denote T_* .

Proof. As $Aut(v)$ is finite for all $v \in ob(\mathbb{V})$, every equivalence class $T := [\bigotimes_{w \in Vt(T)} e_w]_{Edges(T)}$ is finite. Therefore, as a total order on a finite set is a well-order, a unique minimal element exists. \square

Remark 4.2.8. It is possible to define a total order on groupoid coloured tree monomials using Lemma 4.2.7. In particular, given two groupoid coloured tree monomials α, β we define $\alpha \leq \beta$ if, and only if, $\alpha_* \leq \beta_*$. One could then define an appropriate notion of an admissible order for groupoid coloured shuffle operads such that this order is admissible. From here, one could directly redevelop the entire theory of Groebner bases for groupoid

coloured shuffle operads. However, the entire point of this section is to circumvent the need to do this.

Corollary 4.2.9. *This defines an injective map $-_*$ from \mathbb{V} -coloured operads to $ob(\mathbb{V})$ -coloured operads.*

Proof. Given a \mathbb{V} -coloured operad P , every $x \in P$ is of the form $x = \sum_i k_i T_i$, where each $k_i \in \mathbb{K}$ and T_i is \mathbb{V} -coloured tree monomial. Thus x_* is given via linearisation, $x_* := \sum_i k_i (T_i)_*$. The map is injective as the equivalence class of any groupoid coloured tree monomial can be reconstructed from any element. \square

Remark 4.2.10. In general, $-_*$ will not be a morphism of groupoid coloured operads, as every morphism of the groupoid \mathbb{V} is mapped to an identity morphism. Thus, if α is an element of a \mathbb{V} -coloured operad which admits a non-trivial action of the groupoid \mathbb{V} , i.e. $\alpha \neq \alpha \cdot v$, then $(\alpha \cdot v)_* \neq \alpha_* \cdot (v_*) = \alpha_* \cdot id = \alpha_*$.

Lemma 4.2.11. *If $F_{sh}^{ob(\mathbb{V})}(E^{f\mathbb{V}})$ is totally ordered, then $\langle Ker([-]_2) \rangle = \langle E_*^2 \rangle$ where*

$$E_*^2 := \{\alpha \circ_\varphi \beta - [\alpha \circ_\varphi \beta]_* : \alpha, \beta \in E^{f\mathbb{V}}\}.$$

Proof. By their respective definitions, it is clear that $\langle E_*^2 \rangle \subseteq \langle Ker([-]_2) \rangle$. In the other direction, if $\alpha \circ_\varphi \beta - \alpha' \circ_{\varphi'} \beta' \in Ker([-]_2)$, then it must be the case that $\alpha \circ_\varphi \beta - [\alpha \circ_\varphi \beta]_*, \alpha' \circ_{\varphi'} \beta' - [\alpha' \circ_{\varphi'} \beta']_* \in E_*^2$ with $[\alpha \circ_\varphi \beta]_* = [\alpha' \circ_{\varphi'} \beta']_*$, and hence $\langle Ker([-]_2) \rangle \subseteq \langle E_*^2 \rangle$. \square

Thus, from Eq. (5), Lemma 4.2.6 and Lemma 4.2.11, we obtain the following simple presentation for $P^{f\mathbb{V}}$.

Corollary 4.2.12. *Let P be a free \mathbb{V} -coloured shuffle operad $P = F_{sh}^{\mathbb{V}}(E)$. Then $P^{f\mathbb{V}}$ is isomorphic as a $ob(\mathbb{V})$ -coloured shuffle operad to,*

$$P_* := F_{sh}^{ob(\mathbb{V})}(E^{f\mathbb{V}}) / \langle E_*^2 \rangle.$$

Let P be a \mathbb{V} -coloured shuffle operad with presentation $P = F_{sh}^{\mathbb{V}}(E) / \langle R \rangle$. Then $P^{f\mathbb{V}}$ is isomorphic as a $ob(\mathbb{V})$ -coloured shuffle operad to,

$$P_* := F_{sh}^{ob(\mathbb{V})}(E^{f\mathbb{V}}) / \langle E_*^2 \sqcup R_* \rangle, \text{ where } R_* := \{[r]_* : r \in R\}.$$

This corollary tells us we can translate the actions of the groupoid into an explicitly computable set of quadratic relations E_*^2 (other non-quadratic encodings of the action of the groupoid are possible such as the invertible unary maps of [3]).

Theorem 4.2.13. *Let P be a \mathbb{V} -coloured operad such that the associated $ob(\mathbb{V})$ -coloured shuffle operad $(P^f)_*$ admits a quadratic Groebner basis, then P is Koszul.*

Proof. If the $ob(\mathbb{V})$ -coloured operad $(P^f)_*$ admits a quadratic Groebner basis, then it is Koszul by Theorem 3.12 of [25]. This implies that P^f is Koszul, through Proposition 4.2.1 and the isomorphism of $(P^f)_*$ with $(P^f)^{f\mathbb{V}}$ given by Corollary 4.2.12. This implies that P is Koszul by Definition 3.6.7.(4). \square

We will later use Theorem 4.2.13 to prove the operads governing wheeled props and props are Koszul (Sections 5.5, and 6.5). For now, we provide a more basic example, clarifying the constructions of this section.

Example 4.2.14. Let \mathbb{V} be the groupoid with three objects a, b, c and a single non-identity isomorphism $f : b \rightarrow c$, and its inverse $f^{-1} : c \rightarrow b$. Let N be the non-symmetric $ob(\mathbb{V})$ -coloured module spanned by a single binary operation

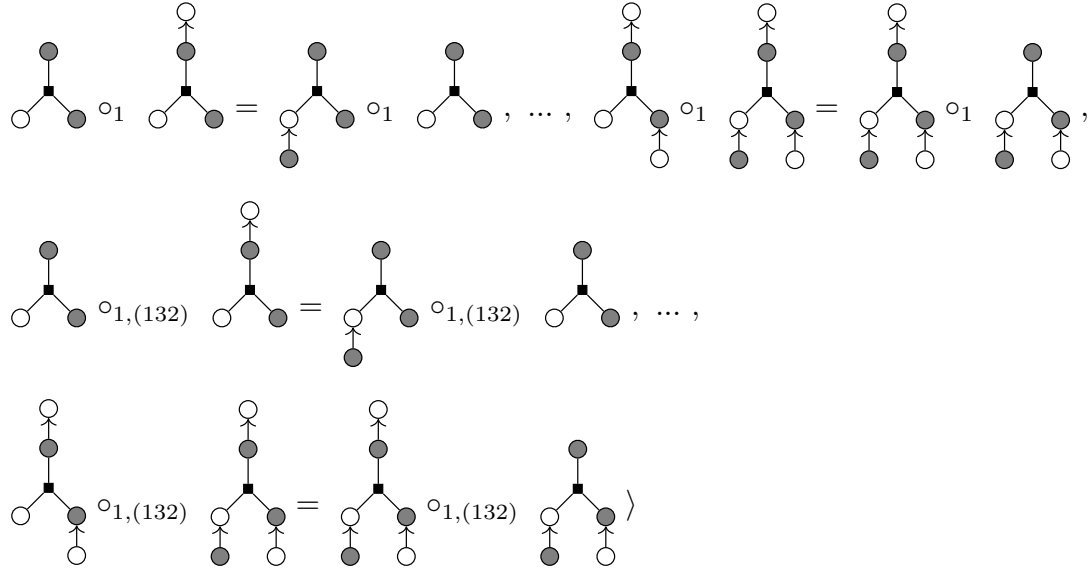
$$N = N\left(\begin{smallmatrix} c \\ b, c \end{smallmatrix}\right) = \langle \text{○} \xrightarrow{\quad} \text{●} \rangle$$

Where we use a white/grey circle to denote a colouring by the object b/c respectively. Given these identifications, we represent the morphisms of \mathbb{V} graphically, the isomorphism $f : b \rightarrow c$ is denoted $\text{○} \longrightarrow \text{●}$, and its inverse $f^{-1} : c \rightarrow b$ is denoted $\text{●} \longrightarrow \text{○}$. Let E be the free non-symmetric \mathbb{V} -module generated by N . In particular, E contains 2^3 elements corresponding to the \mathbb{V} -action on the generator's three flags,

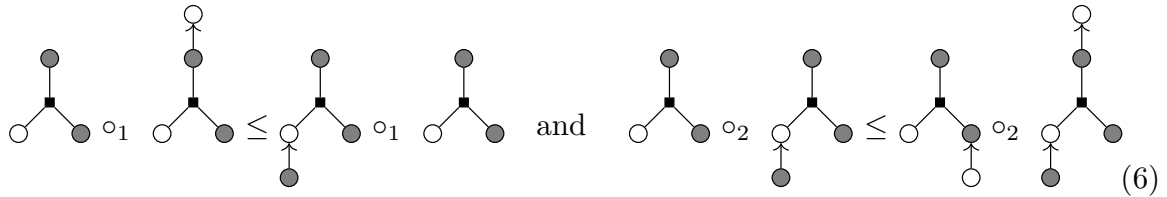
$$E = \langle \text{○} \xrightarrow{\quad} \text{●}, \text{○} \xrightarrow{\quad} \text{●} \xrightarrow{\quad} \text{○}, \text{○} \xrightarrow{\quad} \text{●} \xrightarrow{\quad} \text{○} \xrightarrow{\quad} \text{●}, \text{○} \xrightarrow{\quad} \text{●} \xrightarrow{\quad} \text{○} \xrightarrow{\quad} \text{●} \xrightarrow{\quad} \text{○}, \text{○} \xrightarrow{\quad} \text{●} \xrightarrow{\quad} \text{○} \xrightarrow{\quad} \text{●} \xrightarrow{\quad} \text{○} \xrightarrow{\quad} \text{●}, \text{○} \xrightarrow{\quad} \text{●} \xrightarrow{\quad} \text{○} \xrightarrow{\quad} \text{●} \xrightarrow{\quad} \text{○} \xrightarrow{\quad} \text{●} \xrightarrow{\quad} \text{○}, \text{○} \xrightarrow{\quad} \text{●} \xrightarrow{\quad} \text{○} \xrightarrow{\quad} \text{●} \xrightarrow{\quad} \text{○} \xrightarrow{\quad} \text{●} \xrightarrow{\quad} \text{○} \xrightarrow{\quad} \text{●} \rangle$$

Note that the object $a \in ob(\mathbb{V})$ does not appear in E , as a is disconnected from b and c in \mathbb{V} . The $ob(\mathbb{V})$ -coloured module $E^{f\mathbb{V}}$ contains the same 2^3 elements, but forgets the underlying action of \mathbb{V} . We now consider the $ob(\mathbb{V})$ -coloured shuffle operad $F_{sh}^{ob(\mathbb{V})}(E^{f\mathbb{V}})$. In particular, we assume it admits a total admissible order and compute E_*^2 .

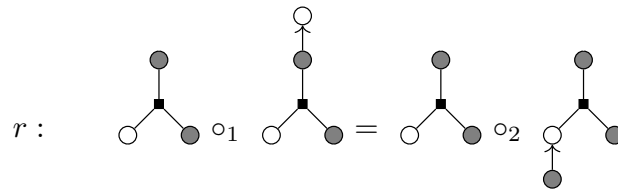
$$E_*^2 = \langle \text{○} \xrightarrow{\quad} \text{●} \circ_2 \text{○} \xrightarrow{\quad} \text{●}, \text{○} \xrightarrow{\quad} \text{●} \circ_2 \text{○} \xrightarrow{\quad} \text{●} \xrightarrow{\quad} \text{○}, \text{○} \xrightarrow{\quad} \text{●} \circ_2 \text{○} \xrightarrow{\quad} \text{●} \xrightarrow{\quad} \text{○} \xrightarrow{\quad} \text{●}, \text{○} \xrightarrow{\quad} \text{●} \circ_2 \text{○} \xrightarrow{\quad} \text{●} \xrightarrow{\quad} \text{○} \xrightarrow{\quad} \text{●} \xrightarrow{\quad} \text{○}, \dots, \text{○} \xrightarrow{\quad} \text{●} \circ_2 \text{○} \xrightarrow{\quad} \text{●} \xrightarrow{\quad} \text{○} \xrightarrow{\quad} \text{●} \xrightarrow{\quad} \text{○} \xrightarrow{\quad} \text{●}, \text{○} \xrightarrow{\quad} \text{●} \circ_2 \text{○} \xrightarrow{\quad} \text{●} \xrightarrow{\quad} \text{○} \xrightarrow{\quad} \text{●} \xrightarrow{\quad} \text{○} \xrightarrow{\quad} \text{●} \xrightarrow{\quad} \text{○}, \text{○} \xrightarrow{\quad} \text{●} \circ_2 \text{○} \xrightarrow{\quad} \text{●} \xrightarrow{\quad} \text{○} \xrightarrow{\quad} \text{●} \xrightarrow{\quad} \text{○} \xrightarrow{\quad} \text{●} \xrightarrow{\quad} \text{○} \xrightarrow{\quad} \text{●} \xrightarrow{\quad} \text{○} \rangle$$



Each row above contains 2^4 equalities corresponding to the (prior) free action of the groupoid on the external flags. Each equality corresponds to an action of \mathbb{V} along an internal edge. We note that this example is particularly simple to compute, because the equivalence class corresponding to each groupoid coloured tree monomial with a single internal edge, contains exactly two elements. Thus, each equation in E_*^2 is independent of the rest, and contains the minimal representative $[-]_*$ with respect to any total admissible order on $F_{sh}^{ob(\mathbb{V})}(E^{f_{\mathbb{V}}})$. If we assume that,

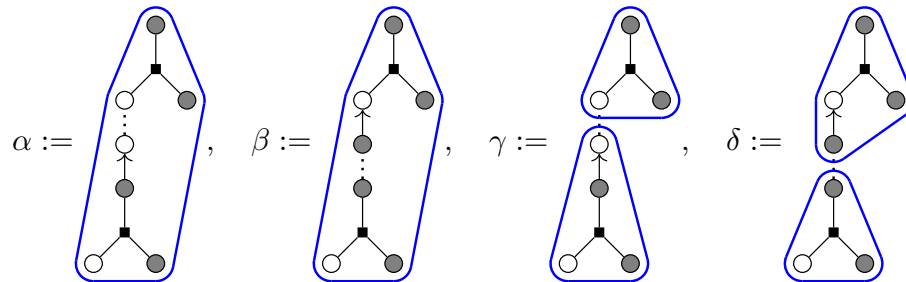


Then the following relation r between groupoid coloured tree monomials in $F_{sh}^{\mathbb{V}}(E) \binom{c}{b,c,c}$,



can be represented by the same pair of elements in $F_{sh}^{ob(\mathbb{V})}(E^{f_{\mathbb{V}}}) \binom{c}{b,c,c}$ (i.e. in an abuse of notation $r_* = r$). So, if R is the \mathbb{V} -coloured module generated by r , i.e. it contains 2^4 basis elements corresponding to the free action of \mathbb{V} on the external flags of r , then R_* will also contain 2^4 elements computed similarly. So we have calculated the constituents of Corollary 4.2.12. In particular, if $P := F_{sh}^{\mathbb{V}}(E)/\langle R \rangle$ then $P^{f_{\mathbb{V}}} \cong P_* := F_{sh}^{ob(\mathbb{V})}(E^{f_{\mathbb{V}}})/\langle E_*^2 \sqcup R_* \rangle$. Note in particular, that whilst P_* has no notion of external actions of \mathbb{V} , that all actions of \mathbb{V} along internal edges are encoded through E_*^2 .

Finally, consider the following four elements of the bar constructions $B(P^{f\vee})$.



Here we denote,

- vertices of bar constructions via blue brackets, which are labelled with elements of $P^{f\vee}$,
- and internal edges of the operad $P^{f\vee}$, and the cooperad $B(P^{f\vee})$, with $\circ \cdots \cdots \circ$, $\bullet \cdots \cdots \bullet$.

We observe through $P^{f\vee} \cong P_*$ and the relations of E_* , i.e. the left (ordered) relation of Eq. (6), that α and β are equal. We also observe that $\gamma \neq \delta$ despite γ and δ just being refinements of α and β respectively. We now consider the epimorphism of groupoid coloured shuffle cooperads $B(P^{f\vee}) \twoheadrightarrow B(P)$ of Proposition 4.2.4. We observe that not only do we have $[\alpha] = [\beta]$, but we also have $[\gamma] = [\delta]$, i.e. as P is a groupoid coloured module, we can push and pull on internal edges of $B(-)$ through the action of \mathbb{V} on P . So, it is straightforward to see in this particular example that $\Delta(\alpha) \in \Delta([\alpha])$ (as needed by Proposition 4.2.4).

Remark 4.2.15. We note it seems very likely that Groebner bases for dioperads could be extended to groupoid coloured dioperads by similar techniques to this section. In addition, it seems likely that the argument of this section could be adapted to prove that a (discrete) coloured operad is Koszul if its corresponding (one coloured discrete or) uncoloured operad is Koszul (see Proposition 1.15 of [25]). In particular, suppose we have a coloured operad P , and the forgetful functor $-^u$ from coloured operads to uncoloured operads, which forgets the underlying colouring. Then there seems to be an epimorphism of the bar complexes $B(P^u) \twoheadrightarrow B(P)^u$. However, whilst this moderately interesting, it is not computationally useful, as the Koszulness of coloured operads is already well understood.

4.3. Rewriting systems and Groebner bases

We close this section by showing how a basis G of an ideal of a discrete coloured shuffle operad defines a terminating rewriting system (RS), and relate the confluence of this system to G being a Groebner basis (Proposition 4.3.4). This connection is known,

and for instance, can be found for operads in Section 8 of [33], we simply state it concisely here, so we may use these confluence ideas to prove the operads governing props and wheeled props are Koszul. The following definitions are standard, and for instance can be found in [13].

Definition 4.3.1. A **rewriting system (RS)** is a binary relation \rightarrow on a set T . The reflexive transitive closure of this relation is denoted \rightarrow_* . We say a given RS is **terminating**, if there exists no endless chain $t_1 \rightarrow t_2 \rightarrow t_3 \rightarrow \dots$ of elements in the set T . We say that a point $w \in T$ is,

- **confluent**, if for all $x, y \in T$ such that $w \rightarrow_* x$ and $w \rightarrow_* y$, there exists a $z \in T$ such that $x \rightarrow_* z$ and $y \rightarrow_* z$.
- **locally confluent**, if for all $x, y \in T$ such that $w \rightarrow x$ and $w \rightarrow y$, there exists a $z \in T$ such that $x \rightarrow_* z$ and $y \rightarrow_* z$.

If either of these properties are true for all $w \in T$, then we say the RS itself is confluent, or locally confluent.

These properties admit the following renowned equivalence.

Proposition 4.3.2 (Diamond Lemma, [45]). *A terminating RS is confluent if, and only if, it is locally confluent.*

The confluence of the following terminating rewriting system associated to a basis of an ideal of a discrete coloured shuffle operad coincides with the basis being a Groebner basis.

Definition 4.3.3. Let G be a basis for an ideal of a discrete coloured shuffle operad which admits an admissible order on its shuffle tree monomials. We define the RS associated to G , say $RS(G)$, to be the subset of $F_{sh}(E)^2$,

$$RS(G) := \{(f, r_g(f)) : f \in F_{sh}(E), g \in G \text{ and } lt(g) \text{ divides } lt(f)\}$$

Proposition 4.3.4. *The following characterisations are equivalent.*

- (1) $RS(G)$ is confluent.
- (2) $RS(G)$ is confluent on small common multiples of G .
- (3) G is a Groebner basis.

Proof. The first condition clearly implies the second. The second condition implies the third, as if $RS(G)$ is confluent on the small common multiples of G , then for any S -polynomial of G , say $s_\gamma(f, g)$, the confluence forces $s_\gamma(f, g) \equiv 0 \text{ mod } G$. In particular, we have that,

$$\begin{aligned}
s_\gamma(f, g) &= m_{\gamma, lt(f)}(f) - \frac{c_f}{c_g} m_{\gamma, lt(g)}(g) \\
&= \frac{c_f}{c_\gamma} \left(\left(\gamma - \frac{c_\gamma}{c_g} m_{\gamma, lt(g)}(g) \right) - \left(\gamma - \frac{c_\gamma}{c_f} m_{\gamma, lt(f)}(f) \right) \right) \\
&= \frac{c_f}{c_\gamma} (r_g(\gamma) - r_f(\gamma)) \\
&\rightarrow_* \frac{c_f}{c_\gamma} (\gamma' - \gamma') = 0
\end{aligned}$$

where, γ' is given by the confluence of small common multiples. Finally, the third condition implies the first through the unique minimal form given by the Groebner basis. In particular, if G is a Groebner basis, then $RS(G)$ is confluent as $f \rightarrow_* f'$ and $f \rightarrow_* f''$, implies $f', f'' \rightarrow_* \bar{f}$. \square

We note that the small common multiples must be a subset of the shuffle tree monomials, so showing that all shuffle tree monomials are confluent is sufficient to show we have a Groebner basis. We will use this technique to prove that the operads governing props and wheeled props are Koszul. The more common technique for showing you have a Groebner basis (Buchberger's algorithm, see for instance [14]), amounts to checking the local confluence of the small common multiples (through S -polynomials). Here is a closing example that illustrates the link between rewriting systems and Groebner bases.

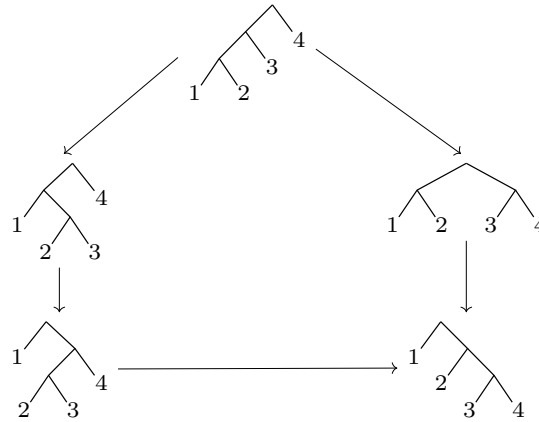
Example 4.3.5 (See Example 10 of [14]). The associative operad admits the presentation,

$$P = F_\Sigma(1 \frown 2) / \langle 1 \frown 2 \text{ } 3 - 1 \text{ } 2 \frown 3 \rangle$$

The shuffle operad P^f is calculated by taking the orbit of the generators and the relation. In particular, if we let $f(1, 2) := 1 \frown 2$ and $f(2, 1) := 2 \frown 1$ then because we are forgetting Σ we need to introduce a new generator to our shuffle operad $h(1, 2) := f(2, 1)$. We then proceed through and orient the $3!$ orbit elements of our sole relation using $h(1, 2)$ to replace $f(2, 1)$.

$$\begin{aligned}
f(f(1, 2), 3) - f(1, f(2, 3)) &\mapsto f(f(1, 2), 3) - f(1, f(2, 3)) \\
f(f(1, 3), 2) - f(1, f(3, 2)) &\mapsto f(f(1, 3), 2) - f(1, h(2, 3)) \\
f(f(2, 1), 3) - f(2, f(1, 3)) &\mapsto f(h(1, 2), 3) - h(f(1, 3), 2) \\
f(f(2, 3), 1) - f(2, f(3, 1)) &\mapsto h(1, f(2, 3)) - h(h(1, 3), 2) \\
f(f(3, 1), 2) - f(3, f(1, 2)) &\mapsto f(h(1, 3), 2) - h(f(1, 2), 3) \\
f(f(3, 2), 1) - f(3, f(2, 1)) &\mapsto h(1, h(2, 3)) - h(h(1, 2), 3)
\end{aligned}$$

Hence, our shuffle operad is $P^f = F_{sh}(f, h)/\langle G \rangle$ where G is the six relations on the right. It turns out that there exists a total admissible order such that G is a (quadratic) Groebner basis. This Groebner basis admits many small common multiples with S -polynomials witnessing their reduction. Here is one small common multiple whose two possible reduction paths generate the associative coherence pentagon.



In this example every single tree monomial except the bottom right corner is divisible by

$$lt(g) := lt\left(\begin{array}{c} 1 \\ \swarrow \quad \searrow \\ 1 \quad 3 \\ \swarrow \quad \searrow \\ 2 \quad 3 \end{array} - \begin{array}{c} 1 \\ \swarrow \quad \searrow \\ 1 \quad 3 \\ \swarrow \quad \searrow \\ 2 \quad 3 \end{array} \right) = \begin{array}{c} 1 \\ \swarrow \quad \searrow \\ 1 \quad 3 \\ \swarrow \quad \searrow \\ 2 \quad 3 \end{array}, \text{ e.g. } \begin{array}{c} 1 \\ \swarrow \quad \searrow \\ 1 \quad 4 \\ \swarrow \quad \searrow \\ 2 \quad 3 \end{array} = \begin{array}{c} 1 \\ \swarrow \quad \searrow \\ 1 \quad 2 \\ \swarrow \quad \searrow \\ 2 \quad 3 \end{array} \circ_{2, id} \begin{array}{c} 1 \\ \swarrow \quad \searrow \\ 1 \quad 3 \\ \swarrow \quad \searrow \\ 2 \quad 3 \end{array}$$

Furthermore, each arrow corresponds to a reduction $f \mapsto r_g(f)$. The top tree monomial γ is a small common multiple as it is divisible by $lt(g)$ in two different ways and the corresponding subtrees of the divisors overlap. We can calculate

$$s_\gamma = \begin{array}{c} 1 \\ \swarrow \quad \searrow \\ 1 \quad 4 \\ \swarrow \quad \searrow \\ 2 \quad 3 \end{array} - \begin{array}{c} 1 \\ \swarrow \quad \searrow \\ 1 \quad 4 \\ \swarrow \quad \searrow \\ 2 \quad 3 \end{array}$$

and the congruence of this S -polynomial to 0 witnesses that the two reductions of γ are (locally) confluent. Note, the unique normal form of all tree monomials in the diagram is the bottom right tree monomial.

5. The operad governing wheeled props

We now seek to define a groupoid coloured operad governing wheeled props, which we can show is Koszul, through use of the preceding theory. The main ingredient needed is a new biased definition of a wheeled prop (Definition 5.1.2), whose axioms, apart from the unital and biequivariance axioms, are all quadratic. By translating the biequivariance axioms into actions of a groupoid, we will define \mathbb{W} to be a quadratic non-unital groupoid coloured operad whose algebras are non-unital wheeled props. We then prove this operad is Koszul, by constructing its shuffle operad, and applying the Groebner basis machinery.

5.1. Wheeled props

We introduce our alternate definition of a wheeled prop, which is precisely Definition 11.33 of [57] with all compositions and axioms extended via actions of the bimodule (see Section 2.1). We then prove its equivalence to the original definition, and define augmented and non-unital versions of these structures. A key property of the new definition is that its equivariance axioms yield the following result.

Proposition 5.1.1. *Every valid composite of operations in Definition 5.1.2 admits a simple canonical form, where all non-identity permutations are pushed to the outermost operation.*

Proof. While we have an inner operation with non-identity permutations, use right compatibility to push the permutations off it and left compatibility to push them back on to the next operation. \square

This not only allows us to simplify the remaining axioms, but also when we translate the equivariance axioms into actions of the groupoid, it will induce a simple canonical representative of every groupoid coloured tree monomial in \mathbb{W} (see Example 5.2.1). We note that all definitions and diagrams referenced in the following definition are sourced from [57].

Definition 5.1.2. Let \mathcal{E} be a symmetric monoidal category, a **wheeled prop** consists of the following.

- (1) A bimodule $P : \mathcal{P}(\mathfrak{C})^{op} \times \mathcal{P}(\mathfrak{C}) \rightarrow \mathcal{E}$.
- (2) An extended horizontal composition,

$$P\left(\frac{\underline{d}}{\underline{c}}\right) \otimes P\left(\frac{\underline{b}}{\underline{a}}\right) \xrightarrow{\otimes_h, \left(\frac{\sigma}{\tau}\right)} P\left(\frac{\sigma(\underline{d}, \underline{b})}{(\underline{c}, \underline{a})\tau}\right),$$

where $(\otimes_h, \left(\frac{\sigma}{\tau}\right))(\alpha, \beta) := \otimes_h(\alpha, \beta) \cdot \left(\frac{\sigma}{\tau}\right)$, with $\otimes_h(-, -)$ being the horizontal composition of 11.33.

- (3) An extended contraction,

$$P\left(\frac{\underline{d}}{\underline{c}}\right) \xrightarrow{(\varepsilon_j^i, \left(\frac{\sigma}{\tau}\right))} P\left(\frac{\sigma(\underline{d} \setminus d_i)}{(\underline{c} \setminus c_j)\tau}\right),$$

where $(\varepsilon_j^i, \left(\frac{\sigma}{\tau}\right))(\alpha) := \varepsilon_j^i(\alpha) \cdot \left(\frac{\sigma}{\tau}\right)$, with $\varepsilon_j^i(-)$ being the contraction of 11.33.

- (4) The same units as 11.33 (or to be consistent, they may be extended with trivial permutations).

In presenting the axioms, we assume all profiles, permutations and contraction indices are such that the diagrams make sense. Before each diagram, we cite the corresponding

diagram in [57]. We will not express the various extended unity diagrams (as we will quickly move to non-unital wheeled props) but the obvious extensions to (11.21 and 11.33) are also present. The extended horizontal composition operation satisfies the following right, left and switch compatibility axioms. The right compatibility axiom is an immediate consequence of being a horizontal composition extended by an action of the bimodule. The left and switch compatibility axioms correspond to diagrams 11.19 and 11.20.

$$\begin{array}{ccc}
 P(\underline{d}) \otimes P(\underline{b}) & & P(\underline{d}) \otimes P(\underline{b}) \\
 (\otimes_h, (\sigma_\tau)) \downarrow & \searrow (\otimes_h, (\sigma'_\tau \sigma)) & (\sigma_1) \otimes (\sigma_2) \downarrow \quad (\otimes_h, (\sigma(\sigma_1 \times \sigma_2)_\tau)) \searrow \\
 P(\sigma(\underline{d}, \underline{b})_{(\underline{c}, \underline{a})\tau}) & \xrightarrow{(\sigma'_\tau)} & P(\sigma'_\tau \sigma(\underline{d}, \underline{b})_{(\underline{c}, \underline{a})\tau\tau'}) & P(\sigma_1 \underline{d}) \otimes P(\sigma_2 \underline{b}) & \xrightarrow{(\otimes_h, (\sigma_\tau))} & P(\sigma(\sigma_1 \underline{d}, \sigma_2 \underline{b})_{(\underline{c}\tau_1, \underline{a}\tau_2)\tau}) \\
 & & & & & \\
 & & P(\underline{b}) \otimes P(\underline{d}) & & & \\
 & & \text{switch} \downarrow \quad (\otimes_h, (\sigma'_\tau)) \searrow & & & \\
 & & P(\underline{d}) \otimes P(\underline{b}) & \xrightarrow{(\otimes_h, (\sigma_\tau))} & P(\sigma(\underline{d}, \underline{b})_{(\underline{c}, \underline{a})\tau}) &
 \end{array}$$

In the switch compatibility diagram, (σ'_τ) is the unique permutation such that $(\sigma(\underline{d}, \underline{b})_{(\underline{c}, \underline{a})\tau}) = (\sigma'(\underline{b}, \underline{d})_{(\underline{a}, \underline{c})\tau'})$. The extended contraction operator satisfies the following left and right compatibility axioms. The right compatibility axiom is an immediate consequence of being a contraction operation extended by an action of the bimodule, and the left compatibility axiom corresponds to (11.34).

$$\begin{array}{ccc}
 P(\underline{d}) & & P(\underline{d}) \\
 (\varepsilon_j^i, (\sigma_\tau)) \downarrow & \searrow (\varepsilon_j^i, (\sigma'_\tau \sigma)) & (\varepsilon_j^i, (\sigma(\sigma'(\tau'(j)))_\tau)) \searrow \\
 P(\sigma(\underline{d} \setminus d_i)_{(\underline{c} \setminus c_j)\tau}) & \xrightarrow{(\sigma'_\tau)} & P(\sigma'_\tau \sigma(\underline{d} \setminus d_i)_{(\underline{c} \setminus c_j)\tau\tau'}) & P(\sigma' \underline{d}) & \xrightarrow{(\varepsilon_{\tau'(j)}^{\sigma' - 1(i)}, (\sigma_\tau))} & P(\sigma(\sigma'(\tau'(j))(\underline{d} \setminus d_i)_{(\underline{c} \setminus c_j)(\tau'(j))\tau}) \\
 & & & & &
 \end{array}$$

In the left compatibility diagram $\sigma'^{(i)}$ and $\tau'^{(j)}$ are the obvious permutations acting on $\underline{d} \setminus d_i$ and $\underline{c} \setminus c_j$ which are induced by the permutations σ' and τ' (acting on \underline{d} , \underline{c}).

The language of Proposition 5.1.1 should now be clear, and we can use it to simplify the remaining diagrams (by pushing all permutations from the top/left arrows to the bottom/right arrows). We note that it is possible to encode the remaining diagrams entirely graphically (see Table 1). We will however write out the remaining axioms in full to make it clear they are precisely the axioms of [57] extended by an action of the bimodule. This helps to clarify that the definitions are indeed equivalent.

The associativity diagram of \otimes_h (11.18)

$$\begin{array}{ccc}
P\left(\frac{f}{\underline{e}}\right) \otimes P\left(\frac{d}{\underline{c}}\right) \otimes P\left(\frac{b}{\underline{a}}\right) & \xrightarrow{(\otimes_h, (id)) \otimes id} & P\left(\frac{f, d}{\underline{e}, \underline{c}}\right) \otimes P\left(\frac{b}{\underline{a}}\right) \\
id \otimes (\otimes_h, (id)) \downarrow & & \downarrow (\otimes_h, (\sigma)) \\
P\left(\frac{f}{\underline{e}}\right) \otimes P\left(\frac{d, b}{\underline{c}, \underline{a}}\right) & \xrightarrow{(\otimes_h, (\sigma))} & P\left(\frac{\sigma(f, d, b)}{(\underline{e}, \underline{c}, \underline{a})\tau}\right)
\end{array}$$

The commutativity diagrams of ε (11.35, 11.36). Suppose that $|d|, |c| \geq 2$, $d_i = c_j$ and $d_{i'} = c_{j'}$ for some $i \neq i' \leq |d|$ and $j \neq j' \leq |c|$. In the left diagram $i < i', j < j'$, and in the right diagram $i > i', j < j'$.

$$\begin{array}{ccc}
P\left(\frac{d}{\underline{c}}\right) & \xrightarrow{(\varepsilon_j^i, (id))} & P\left(\frac{d \setminus d_i}{\underline{c} \setminus c_j}\right) \\
(\varepsilon_{j'}^{i'}, (id)) \downarrow & & \downarrow (\varepsilon_{j'-1}^{i'-1}, (\sigma)) \\
P\left(\frac{d \setminus d_{i'}}{\underline{c} \setminus c_{j'}}\right) & \xrightarrow{(\varepsilon_j^i, (\sigma))} & P\left(\frac{\sigma(d \setminus \{d_i, d_{i'}\})}{(\underline{c} \setminus \{c_j, c_{j'}\})\tau}\right)
\end{array}
\qquad
\begin{array}{ccc}
P\left(\frac{d}{\underline{c}}\right) & \xrightarrow{(\varepsilon_j^i, (id))} & P\left(\frac{d \setminus d_i}{\underline{c} \setminus c_j}\right) \\
(\varepsilon_{j'}^{i'}, (id)) \downarrow & & \downarrow (\varepsilon_{j'-1}^{i'-1}, (\sigma)) \\
P\left(\frac{d \setminus d_{i'}}{\underline{c} \setminus c_{j'}}\right) & \xrightarrow{(\varepsilon_j^{i-1}, (\sigma))} & P\left(\frac{\sigma(d \setminus \{d_i, d_{i'}\})}{(\underline{c} \setminus \{c_j, c_{j'}\})\tau}\right)
\end{array}$$

Note the right diagram has slightly altered indexing from 11.36, which uses $i < i'$ and $j > j'$ instead. This alteration arises from a later choice in Definition 5.4.1 where we choose to prioritise inputs over outputs, and making this (equivalent) alteration here slightly cleans up the relations.

The compatibility diagrams of \otimes_h, ε (11.37, 11.38). In the left diagram $i \leq |d|, j \leq |c|$, and in the right diagram $i \leq |b|, j \leq |a|$

$$\begin{array}{ccc}
P\left(\frac{d}{\underline{c}}\right) \otimes P\left(\frac{b}{\underline{a}}\right) & \xrightarrow{(\otimes_h, (id))} & P\left(\frac{d, b}{\underline{c}, \underline{a}}\right) \\
(\varepsilon_j^i, (id)) \otimes id \downarrow & & \downarrow (\varepsilon_j^i, (\sigma)) \\
P\left(\frac{d \setminus d_i}{\underline{c} \setminus c_j}\right) \otimes P\left(\frac{b}{\underline{a}}\right) & \xrightarrow{(\otimes_h, (\sigma))} & P\left(\frac{\sigma(d \setminus d_i, b)}{(\underline{c} \setminus c_j, \underline{a})\tau}\right)
\end{array}
\qquad
\begin{array}{ccc}
P\left(\frac{d}{\underline{c}}\right) \otimes P\left(\frac{b}{\underline{a}}\right) & \xrightarrow{(\otimes_h, (id))} & P\left(\frac{d, b}{\underline{c}, \underline{a}}\right) \\
id \otimes (\varepsilon_j^i, (id)) \downarrow & & \downarrow (\varepsilon_{|c|+j}^{|d|+i}, (\sigma)) \\
P\left(\frac{d}{\underline{c}}\right) \otimes P\left(\frac{b \setminus b_i}{\underline{a} \setminus a_j}\right) & \xrightarrow{(\otimes_h, (\sigma))} & P\left(\frac{\sigma(d, b \setminus b_i)}{(\underline{c}, \underline{a} \setminus a_j)\tau}\right)
\end{array}$$

Lemma 5.1.3. *Definition 5.1.2, and Definition 11.33 of [57] are equivalent definitions of wheeled props.*

Proof. In presenting the alternate definition, we already established how the extended operations and axioms can be obtained from the original operations and axioms. We can similarly re-obtain the original operations and axioms from the alternate operations and axioms by taking specific cases of them. \square

We will now refer to alternate wheeled props as wheeled props, but will continue to use alternate if we need to emphasise the use of this particular presentation. We now define augmented and non-unital versions of this definition.

Definition 5.1.4. Let \mathcal{K} be the trivial wheeled prop in $Vect_{\mathbb{K}}$ whose only constituents are the horizontal and vertical units, and the contractions of the vertical units (this is a technical requirement for wheeled props).

Definition 5.1.5. An **augmentation** of a wheeled prop P in $dgVect_{\mathbb{K}}$ is a morphism (of wheeled props, see Corollary 11.36 of [57]) $\epsilon : P \rightarrow \mathcal{K}$. Wheeled props with an augmentation are called **augmented wheeled props**.

Definition 5.1.6. A **non-unital wheeled prop** consists of all the data of a wheeled prop, excluding the units and the corresponding axioms.

As one would expect, we have the following isomorphism.

Proposition 5.1.7. *Augmented wheeled props and non-unital wheeled props are isomorphic.*

Proof. This is a clear analogue of the classical result for partial operads, see Proposition 21 of [34]. \square

5.2. A groupoid coloured quadratic operad

We now produce a quadratic non-unital groupoid coloured operad $\mathbb{W} := F_{\Sigma}^{S(\mathfrak{C})}(E)/\langle R \rangle$ whose algebras are non-unital wheeled props. After we have presented the generators of our operad, we will explore in Example 5.2.1 how the groupoid actions enable a simple canonical representative of each groupoid coloured tree monomial of $F_{\Sigma}^{S(\mathfrak{C})}(E)$. Finally, we use this canonical form to provide a diagrammatic representation of the quadratic ideal R .

The underlying groupoid of our operad is $\mathcal{S}(\mathfrak{C}) := \mathcal{P}(\mathfrak{C})^{op} \times \mathcal{P}(\mathfrak{C})$, and the groupoid coloured module E (Definition 2.1.2) is constructed from the compositions of the wheeled prop as follows. Let $\left(\frac{b}{a}\right), \left(\frac{d}{c}\right), \left(\frac{f}{e}\right) \in \mathcal{P}(\mathfrak{C})^{op} \times \mathcal{P}(\mathfrak{C})$, then,

$$\begin{aligned} E\left(\left(\frac{d}{c}\right); \left(\frac{b}{a}\right)\right) &:= \{(\varepsilon_j^i, \left(\frac{\sigma}{\tau}\right))(-) : d_i = c_j, \text{ and } \left(\frac{\sigma(d \setminus \{d_i\})}{(c \setminus \{c_j\})\tau}\right) = \left(\frac{b}{a}\right)\} \\ E\left(\left(\frac{d}{c}\right), \left(\frac{b}{a}\right); \left(\frac{f}{e}\right)\right) &:= \{(\otimes_h, \left(\frac{\sigma}{\tau}\right))(-, -) : \left(\frac{\sigma(d, b)}{(c, a)\tau}\right) = \left(\frac{f}{e}\right)\} \end{aligned}$$

where $i \in \{1, \dots, |d|\}, j \in \{1, \dots, |c|\}$ and the $\left(\frac{\sigma}{\tau}\right)$'s are morphisms in $\mathcal{P}(\mathfrak{C})^{op} \times \mathcal{P}(\mathfrak{C})$. The necessary left, right and Σ_2 actions on \otimes_h are directly given by the left, right and switch biequivariance/compatibility axioms of \otimes_h (Definition 5.1.2). Similarly, the necessary left and right actions on ε are directly given by the left and right compatibility axioms of ε . The necessary Σ_1 action on ε is the trivial action. To clarify by example, we now unpack the right action of \otimes_h . Let $(\otimes_h, \left(\frac{\sigma}{\tau}\right)) \in E\left(\left(\frac{d}{c}\right), \left(\frac{b}{a}\right); \left(\frac{f}{e}\right)\right)$ and $\left(\frac{\sigma'}{\tau'}\right) \in Iso_{\mathcal{S}(\mathfrak{C})}\left(\left(\frac{f}{e}\right), \left(\frac{\sigma' f}{e \tau'}\right)\right)$ then,

$$(\otimes_h, \left(\frac{\sigma}{\tau}\right))\left(\frac{\sigma'}{\tau'}\right) = (\otimes_h, \left(\frac{\sigma' \sigma}{\tau \tau'}\right)) \in E\left(\left(\frac{d}{c}\right), \left(\frac{b}{a}\right); \left(\frac{\sigma' f}{e \tau'}\right)\right)$$

i.e. the bottom-left and diagonal path for the right compatibility diagram of \otimes_h are equal (Definition 5.1.2).

We now provide an example of composition in this operad, and these actions.

Example 5.2.1. Suppose we have the following profiles,

$$p_x = \begin{pmatrix} d_1, d_2 \\ c_1, c_2, c_3 \end{pmatrix}, p_y = \begin{pmatrix} c_3 \\ \emptyset \end{pmatrix}, p = \begin{pmatrix} d_2, d_1, c_3 \\ c_2, c_3, c_1 \end{pmatrix}, p_\gamma = \begin{pmatrix} d_2, d_1 \\ c_2, c_1 \end{pmatrix}$$

then using the inline notation for permutations (here and in the rest of the paper)

$$(\otimes_h, \begin{pmatrix} 213 \\ 231 \end{pmatrix}) \in E \begin{pmatrix} p \\ p_x, p_y \end{pmatrix} \quad \text{and} \quad (\varepsilon_2^3, \begin{pmatrix} id \\ id \end{pmatrix}) \in E \begin{pmatrix} p_\gamma \\ p \end{pmatrix}$$

We can compose these two generators to form a groupoid coloured tree monomial with at least two distinct representatives.

$$\begin{array}{ccc} (\varepsilon_2^3, \begin{pmatrix} id \\ id \end{pmatrix}) & & (\varepsilon_3^3, \begin{pmatrix} 21 \\ 21 \end{pmatrix}) \\ | & & | \\ (\otimes_h, \begin{pmatrix} 213 \\ 231 \end{pmatrix}) & & (\otimes_h, \begin{pmatrix} id \\ id \end{pmatrix}) \\ \wedge & & \wedge \\ p_x & p_y & p_x & p_y \end{array}$$

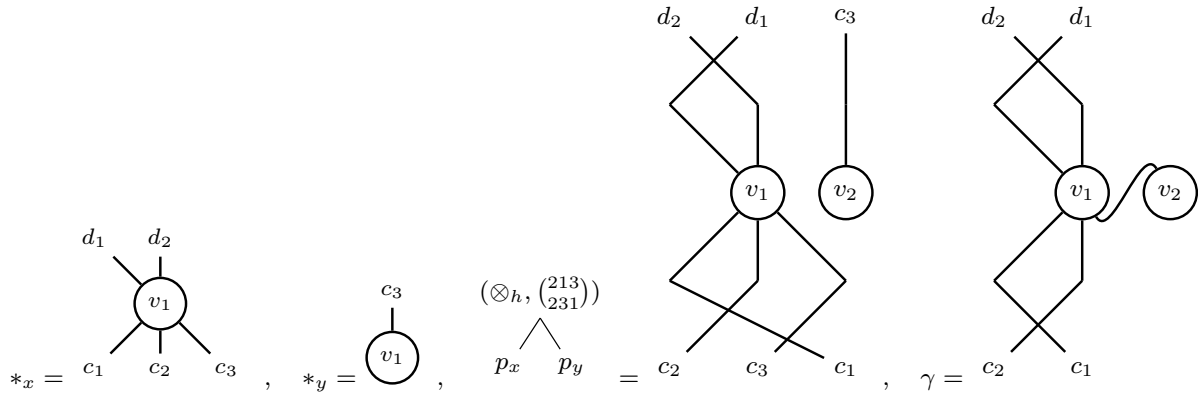
$$(\varepsilon_2^3, \begin{pmatrix} id \\ id \end{pmatrix}) \circ_1 (\otimes_h, \begin{pmatrix} 213 \\ 231 \end{pmatrix}) = [\begin{array}{cc} p_x & p_y \end{array}] = [\begin{array}{cc} p_x & p_y \end{array}] \in E \begin{pmatrix} p_\gamma \\ p_x, p_y \end{pmatrix}$$

We can explicitly compute that these two tree monomials are part of the same equivalence class as follows. The output edge of $(\otimes_h, \begin{pmatrix} 213 \\ 231 \end{pmatrix})$ is coloured by the profile p (in this example). The identity morphism is an automorphism of p and splits as $id = p \xrightarrow{\begin{pmatrix} 213 \\ 231 \end{pmatrix}^{-1}} p' \xrightarrow{\begin{pmatrix} 213 \\ 231 \end{pmatrix}} p \in Aut(p)$ where $p' = \begin{pmatrix} d_1, d_2, c_3 \\ c_1, c_2, c_3 \end{pmatrix}$. Hence by Eq. (3), contraction left action, and horizontal right action we have the following equalities.

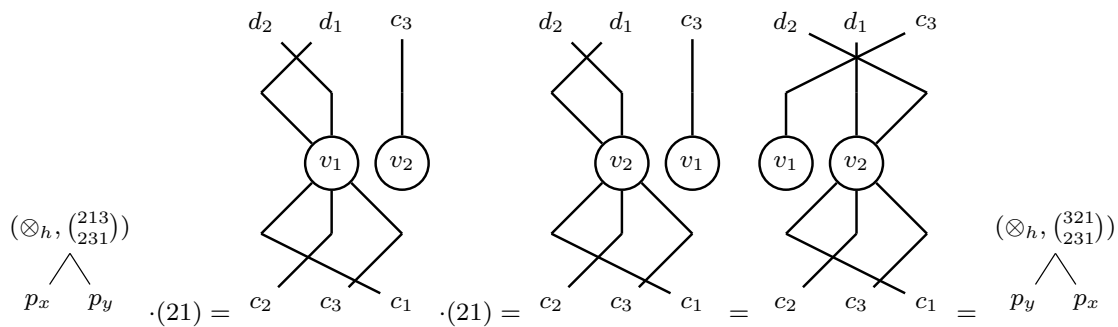
$$\begin{array}{ccc} (\varepsilon_2^3, \begin{pmatrix} id \\ id \end{pmatrix}) & \begin{pmatrix} 213 \\ 231 \end{pmatrix} \cdot (\varepsilon_2^3, \begin{pmatrix} id \\ id \end{pmatrix}) & (\varepsilon_3^3, \begin{pmatrix} 21 \\ 21 \end{pmatrix}) \\ | & | & | \\ (\otimes_h, \begin{pmatrix} 213 \\ 231 \end{pmatrix}) & (\otimes_h, \begin{pmatrix} 213 \\ 231 \end{pmatrix}) \cdot \begin{pmatrix} 213 \\ 231 \end{pmatrix}^{-1} & (\otimes_h, \begin{pmatrix} id \\ id \end{pmatrix}) \\ \wedge & \wedge & \wedge \\ p_x & p_y & p_x & p_y \end{array}$$

$$[\begin{array}{cc} p_x & p_y \end{array}] \stackrel{id}{=} [\begin{array}{cc} p_x & p_y \end{array}] \stackrel{\text{left+right actions}}{=} [\begin{array}{cc} p_x & p_y \end{array}]$$

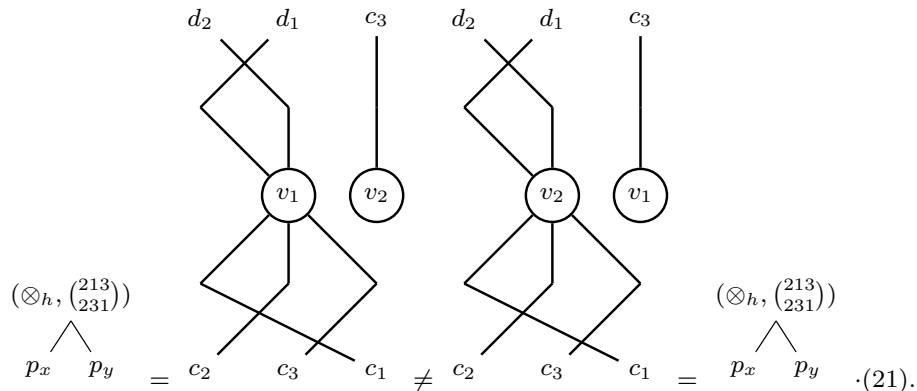
By construction, every shuffle tree monomial of the operad can be seen as providing instructions for forming a wheeled graph via horizontal compositions and contractions. The fact that these two tree monomials are in the same equivalence class can be visually verified by seeing they provide two different ways of forming the following graph γ from two corollas $*_x$ and $*_y$ through different horizontal compositions and contractions. (Recall that all directed graphs in this paper are drawn with inputs on the bottom, and outputs on the top).



We note that the vertex labelling of γ (i.e. v_1, v_2), is encoded by the order of the inputs of the tree monomial, i.e. the corolla $*_x$ is labelled v_1 and the corolla $*_y$ is labelled v_2 because $(\varepsilon_2^3, \binom{id}{id}) \circ_1 (\otimes_h, \binom{213}{231}) \in E_{p_x, p_y}^{p_\gamma}$. Thus, we can also interpret the symmetric action of the operad as switching the labels of the vertices. For example, here is the graphical interpretation of the Σ_2 action on $(\otimes_h, \binom{213}{231}) \in E_{p_x, p_y}^p$.



Here the outermost tree monomials are equal under the definition of the Σ_2 action. The inner equalities provide a graphical interpretation of this result, where the second equality uses the Σ_2 action to switch the vertex labels, and the third equality is an equality of graphs (these graphs are indistinguishable under Definition 2.2.4). This example is also sufficient to illustrate that horizontal composition is not necessarily strictly commutative (see Proposition 7.0.2 for an important case when it is commutative), as



Observe that in the prior example, the action of the groupoid was used to push all permutations to the top (i.e. the only non-identity permutation is that used by the generator at the root). This trick can be exploited to produce a canonical element of

the equivalence class of any groupoid coloured tree monomial, i.e. whilst there is a non-identity permutation on a generator below the root, we use the action of the groupoid via the internal edge above it to push the permutation up the tree. So, the canonical element of any \mathbb{V} -coloured tree monomial can be taken as the $ob(\mathbb{V})$ -coloured tree monomial whose (potentially) only non-identity permutations are those at the root most generator.

The relations R of our operad \mathbb{W} are given by the five remaining quadratic axioms of the alternate definition of a wheeled prop. These can be explicitly written out if desired, but we will use the canonical form to provide a concise graphical representation of the relations in Table 1 (see the souls of [4] for a similar graphical encoding of relations). Note, by construction this table precisely corresponds to the non-unital and non-biequivariance axioms of Definition 5.1.2. The table makes use of a suppressed notation, which we clarify by example. On the second row,

- The diagram (of the graph) represents a graph with two vertices in which one of the output flags of the first vertex is connected to one of the input flags of the first vertex, forming an edge. There are no other edges present in the graph, but there may be other flags (which are suppressed) and these flags may have an arbitrary listing in the graph (i.e. the graph may have any permutations of its inputs and outputs).
- The groupoid coloured tree monomials to the right are then taken under the implicit understanding that they output the graph on the left. Consequently, the profile of the i th input of the tree monomial must correspond to the profile of the i th vertex of the graph, see Example 5.2.1. (We are actually using a slightly abusive notation that we will clarify in Eq. (7)). The unary vertices of the tree monomials correspond to contractions, and the binary vertices correspond to horizontal compositions. There is no need to explicitly include the permutations or the indices used by these compositions. A canonical element of the equivalence class of each groupoid coloured tree monomial can be recovered by pushing all permutations to the top. From here, the necessary indices to contract by to form the edge are uniquely specified by the graph; similarly, the topmost permutations (σ_τ) are uniquely determined by needing to match the listings of the open flags of the graph.

By the construction of this section, the following is immediate.


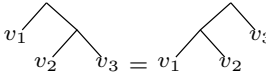
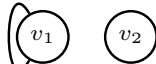
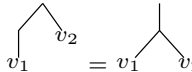
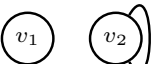
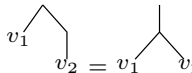

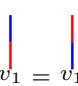
Corollary 5.2.2. *A algebra over \mathbb{W} is a non-unital wheeled prop.*

5.3. The shuffle operad

So having defined a quadratic groupoid coloured operad governing wheeled props \mathbb{W} , we must now prove that it is Koszul. We will do this by showing $(\mathbb{W}^f)_*$ admits a quadratic Groebner basis, but first we must calculate $\mathbb{W}^f = (F_\Sigma^{S(\mathfrak{e})}(E)/\langle R \rangle)^f \cong F_{sh}^{S(\mathfrak{e})}(E^f)/\langle R^f \rangle$. It may be helpful to review the calculation of $-^f$ in the (discrete) coloured case prior to stepping through this section, see for instance Section 2.6 of [25] or Example 4.3.5.

Table 1

The relations of the operad governing wheeled props, and dually, the non-unital and non-biequivariance relations of an alternate wheeled prop.

Graphs	Relations
	
	
	
	

We first observe how $-^f$ acts on the generators. Every unary generator has only a trivial orbit under Σ_1 . The binary generators have non-trivial orbits, however the Σ_2 action on \otimes_h sends every generator to another generator (see Example 5.2.1), so there is no need to introduce further generators to account for the orbits (this is comparable to the shuffle Lie operad only needing a single generator, see Example 9 of [14]). This tells us that $E^f = E$.

We now consider how $-^f$ acts on the relations, we do so by calculating the orbit of each relation of \mathbb{W} then orienting each element of the orbit to use shuffle compositions. Let A be the first relation of Table 1 written down for a particular graph via the following notation, $\otimes_h(\otimes_h(*_{v_1}, *_{v_2}), *_{v_3}) = \otimes_h(*_{v_1}, \otimes_h(*_{v_2}, *_{v_3}))$, where $*_{v_i}$ is the profile of the i th vertex of the graph. We now orient each element of the Σ_3 orbit of A ,

$$\begin{aligned}
 A \cdot (123) &\mapsto \otimes_h(\otimes_h(*_{v_1}, *_{v_2}), *_{v_3}) \cdot (123) = \otimes_h(*_{v_1}, \otimes_h(*_{v_2}, *_{v_3})) \cdot (123) \\
 A \cdot (132) &\mapsto \otimes_h(\otimes_h(*_{v_1}, *_{v_2}), *_{v_3}) \cdot (132) = \otimes_h(*_{v_1}, \otimes_h(*_{v_3}, *_{v_2})) \cdot (123) \\
 A \cdot (213) &\mapsto \otimes_h(\otimes_h(*_{v_2}, *_{v_1}), *_{v_3}) \cdot (123) = \otimes_h(\otimes_h(*_{v_2}, *_{v_2}), *_{v_3}) \cdot (132) \\
 A \cdot (231) &\mapsto \otimes_h(*_{v_3}, \otimes_h(*_{v_1}, *_{v_2})) \cdot (123) = \otimes_h(\otimes_h(*_{v_3}, *_{v_2}), *_{v_1}) \cdot (132) \\
 A \cdot (312) &\mapsto \otimes_h(\otimes_h(*_{v_2}, *_{v_1}), *_{v_3}) \cdot (132) = \otimes_h(\otimes_h(*_{v_2}, *_{v_3}), *_{v_1}) \cdot (123) \\
 A \cdot (321) &\mapsto \otimes_h(*_{v_3}, \otimes_h(*_{v_2}, *_{v_1})) \cdot (123) = \otimes_h(\otimes_h(*_{v_3}, *_{v_2}), *_{v_1}) \cdot (123)
 \end{aligned}$$

One might expect that every time we orient an element of the orbit we would obtain a new relation in the shuffle operad, however observe that the orientation of the orbit $A \cdot (321)$ is precisely $A' = \otimes_h(\otimes_h(*_{v'_1}, *_{v'_2}), *_{v'_3}) = \otimes_h(*_{v'_1}, \otimes_h(*_{v'_2}, *_{v'_3}))$ where $*_{v'_1} = *_{v_3}$, $*_{v'_2} = *_{v_2}$ and $*_{v'_3} = *_{v_1}$, so it is a redundant relation. In fact, it is straightforward to show that each orientation arises as a consequence of the following two families of equations (the families are all graphs of this form with all possible graph and vertex profiles)

Table 2

The relations of the shuffle operad governing wheeled props.

Graphs	Relations

$$\begin{array}{c}
 \begin{array}{c} \text{---} v_1 \\ \text{---} v_2 \end{array} \quad \begin{array}{c} \text{---} v_2 \\ \text{---} v_3 \end{array} \quad \begin{array}{c} \text{---} v_3 \\ \text{---} v_2 \end{array}, \quad \begin{array}{c} v_1 \\ \text{---} v_2 \end{array} = \begin{array}{c} v_1 \\ \text{---} v_3 \end{array}, \quad \begin{array}{c} v_1 \\ \text{---} v_2 \end{array} = \begin{array}{c} v_1 \\ \text{---} v_3 \end{array}
 \end{array}$$

Here we have used the notation,

$$\begin{array}{c} \text{---} v_3 \\ \text{---} v_2 \end{array} := \begin{array}{c} \text{---} *v_3 \\ \text{---} *v_2 \end{array} \cdot (123), \quad \begin{array}{c} \text{---} v_2 \\ \text{---} v_3 \end{array} := \begin{array}{c} \text{---} *v_2 \\ \text{---} *v_3 \end{array} \cdot (132) \quad (7)$$

The permutation (132) is ensuring that the profile of the corolla $*v_3$ (which is just a element of $\mathcal{P}(\mathfrak{C})^{op} \times \mathcal{P}(\mathfrak{C})$ and has no notion of order with other profiles, see the end of Example 5.2.1) is the third input of the shuffle tree monomial. So, this orientation of the orbit has revealed a new way to form this graph with 3 vertices via shuffle tree monomials (given we have broken the symmetry). If we proceed to calculate the orbit of the remaining relations of the operad governing wheeled props (each with arity ≤ 2) then we will find that no new relations are required.

We once again encode the relations of the shuffle operad graphically in Table 2. This table uses the same conventions as Table 1, and the notation regarding shuffle permutations defined in Eq. (7). Furthermore, each equation is now numbered for referencing and directed using a total order given in the next section, the larger element is on the left-hand side of each equation.

5.4. Ordering the object coloured tree monomials

In order to show that $(\mathbb{W}_f)^*$ admits a Groebner basis, we must define a total admissible order on the underlying $ob(\mathcal{S}(\mathfrak{C}))$ -coloured tree monomials of the shuffle operad. In this section we define an order on the $ob(\mathcal{S}(\mathfrak{C}))$ -coloured tree monomials of $F_{sh}(E)$ and show that this order is total and admissible. The order is a variant of a path lexicographic order of Section 3.2 of [14] (for extending path lexicographic orders to discrete coloured operads

see [25]), and although it looks complicated, we will show that it is a composite of simpler admissible orders. The underlying motivation for the order is that it provides a simple unique minimal shuffle tree monomial encoding any wheeled graph (Construction 5.5.2). As such, the key features of the order that the reader should observe are the following, the order prefers

- contractions being above horizontal compositions.
- horizontal compositions being composed to the left, i.e. $\otimes_h(\otimes_h(v_1, v_2), v_3) < \otimes_h(v_1, \otimes_h(v_2, v_3))$.
- tree monomials whose inputs are ordered linearly, i.e. $\otimes_h(\otimes_h(v_1, v_2), v_3) < \otimes_h(\otimes_h(v_1, v_3), v_2)$.
- tree monomials where the only non-identity permutations used by a generator are at the root.
- contractions where larger input indices are used.

Here is the formal definition of our needed order, and we prove it is total and admissible in Lemma 5.4.4.

Definition 5.4.1 (*Total Admissible Order*). Let α, β be two tree monomials of $F_{sh}(E)$, we define $\alpha \leq \beta$ if:

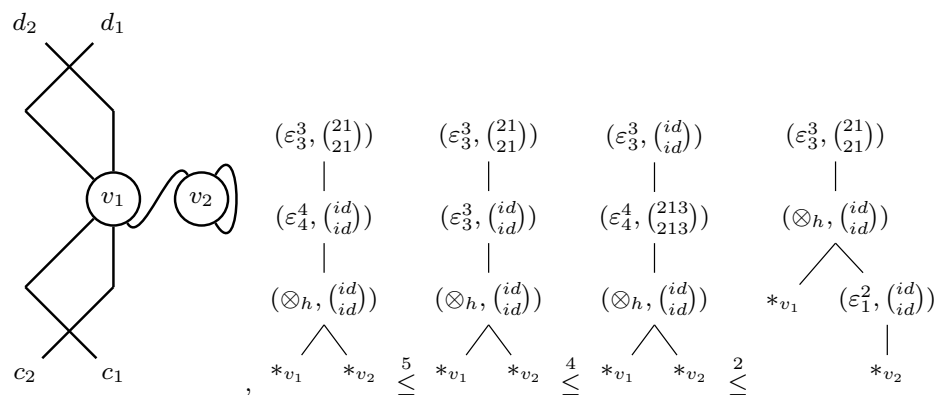
- (1) The arity of $\alpha < \beta$.
- (2) Or, if all the prior are equal, then compare $P^\alpha < P^\beta$ where:
 - if α and β have arity n then $P^\alpha := (P_1^\alpha, \dots, P_n^\alpha)$, where P_i^α is the word formed out of the generators when stepping from the i th input to the root in the tree monomial α .
 - P^α and P^β are compared lexicographically. Two paths from the same input are compared
 - First by degree, the **longer** path is smaller.
 - Next by a partial lexicographic order where two generators are compared using the partial order $\otimes_h < \varepsilon$ (i.e. indices and permutations are ignored).
- (3) Or, if all the prior are equal, then compare the **input permutations** of the shuffle tree monomials (not the permutations of the generators) via lexicographic order.
- (4) Or, if all the prior are equal, then compare the permutations of all the generators as follows
 - For a given generator s (e.g. $(\otimes_h, \binom{\sigma}{\tau})$) let $p(s)$ be its permutations (e.g. $p((\otimes_h, \binom{\sigma}{\tau})) = \binom{\sigma}{\tau}$).
 - For any given tree monomial there is a natural total order of its generators/vertices, where any vertex with k vertices between it and the root is smaller than any vertex with $j < k$ vertices between it and the root, and any two vertices at the same depth are ordered left to right using the planar embedding of the tree monomial.

- We use this order and the map p to write out the permutations of all generators of each tree monomial as a single word (the letters correspond to $\binom{\sigma}{\tau}$).
 - We compare the words lexicographically, where $\binom{\sigma}{\tau} \leq \binom{\sigma'}{\tau'}$ if $\sigma < \sigma'$, or $\sigma = \sigma'$ and $\tau < \tau'$. Here, two individual permutations are compared lexicographically.
- (5) Or, if all the prior are equal, then we again compare $P^\alpha < P^\beta$ lexicographically, this time with a total order on generators.
- $\otimes_h < \varepsilon$
 - $\varepsilon_j^i \leq \varepsilon_{j'}^{i'}$ if $j > j'$, or $j = j'$ and $i > i'$.
 - If the composition type is the same then the permutations are compared with, where we define $\binom{\sigma}{\tau} \leq \binom{\sigma'}{\tau'}$ if $\sigma < \sigma'$, or $\sigma = \sigma'$ and $\tau < \tau'$
 - if s and s' are identical on all prior checks then compare their input colour(s) (left then right input if \otimes_h) then their output colour. Input and output colours are profiles $\binom{d}{c}, \binom{b}{a} \in \mathcal{P}(\mathfrak{C})^{op} \times \mathcal{P}(\mathfrak{C})$, we say $\binom{d}{c} \leq \binom{b}{a}$ if $\underline{d} < \underline{b}$, or $\underline{d} = \underline{b}$ and $\underline{c} \leq \underline{a}$. We compare two sequences of colours using a degree lexicographic order induced by a total order on \mathfrak{C} .

Remark 5.4.2. The assumption of having a total order on the underlying set of colours \mathfrak{C} (which is implied by the axiom of choice) could be relaxed. We can define the order of Definition 5.4.1 as a partial order, where we do not compare generators via their input and output colours. This order will still be total on the equivalence class corresponding to each groupoid coloured tree monomial, and will still enable the confluence of the rewriting system which is equivalent to the Groebner basis to be computed.

We note that several choices were made in the order, such as favouring inputs over outputs or larger indices over smaller indices. Alternate orders exist, and this particular order was constructed as it provides a simple unique minimal form.

Example 5.4.3. The following ordered tree monomials all output the graph depicted on the left.



We have labelled each \leq with the step of Definition 5.4.1 that orders each pair of tree monomials.

Before we prove this order is admissible, we need a simple helper lemma.

Lemma 5.4.4. *If \leq_1, \leq_2 are admissible orders, then the order \leq defined by $\alpha \leq \beta$ if $\alpha <_1 \beta$ or $\alpha =_1 \beta$ and $\alpha \leq_2 \beta$, is also admissible.*

Proof. For all $\alpha, \alpha', \beta, \beta'$ if $\alpha \leq \alpha'$ and $\beta \leq \beta'$ then each of the four possibilities (in terms of \leq_1, \leq_2) lead to $\alpha \circ_\varphi \beta \leq \alpha' \circ_\varphi \beta'$. \square

With this result in hand, we now prove the following.

Lemma 5.4.5. *The order of Definition 5.4.1 is total and admissible.*

Proof. It is straightforward to see the order is total, as eventually the order compares all the data of the two shuffle tree monomials. It suffices to consider its admissibility. The comparisons of the order \leq of steps 1 – 3 is a path lexicographic order of [14] and hence is an admissible (partial) order. We now argue that tacking on step 4 still results in admissible order. It is slightly easier to work with an alternate characterisation of admissibility,

$$\forall \alpha, \alpha', \beta, \beta', \quad (\alpha \leq \alpha' \text{ and } \beta \leq \beta') \implies \alpha \circ_\varphi \beta \leq \alpha' \circ_\varphi \beta'$$

$$\iff$$

$$(\forall \alpha, \alpha', \beta, \alpha \leq \alpha' \implies \alpha \circ_\varphi \beta \leq \alpha' \circ_\varphi \beta) \text{ and } (\forall \alpha, \beta, \beta', \beta \leq \beta' \implies \alpha \circ_\varphi \beta \leq \alpha \circ_\varphi \beta').$$

This variant of the definition allows us to vary one side of the composition at a time. Suppose that $\beta \leq \beta'$, and we wish to show that $\alpha \circ_\varphi \beta \leq \alpha \circ_\varphi \beta'$. Suppose that the first difference between β and β' occurs as a result of step 4. That is to say the tree monomials β and β' have the same underlying ‘shape’ (as unary binary trees) but when comparing the permutations of the generators (bottom to top, left to right), all permutations are equal until we reach some particular vertex pair which satisfies $\binom{\sigma}{\tau} < \binom{\sigma'}{\tau'}$.

As β and β' have the same underlying ‘shape’ (as unary binary trees) this implies that $\alpha \circ_\varphi \beta$ and $\alpha \circ_\varphi \beta'$ have the same underlying shape. As such, we can see that the order on the generators of β, β' (bottom to top, left to right) will naturally inject into the order on the generators of $\alpha \circ_\varphi \beta$ and $\alpha \circ_\varphi \beta'$. This means that the vertex pair of β, β' causing $\binom{\sigma}{\tau} < \binom{\sigma'}{\tau'}$ will also induce $\alpha \circ_\varphi \beta < \alpha \circ_\varphi \beta'$ via step 4 via the same vertex pair. A similar argument yields $\alpha \leq \alpha' \implies \alpha \circ_\varphi \beta \leq \alpha' \circ_\varphi \beta$.

Finally, to add in condition 5 of Definition 5.4.1, we first observe that performing the steps 1, 5, 3 in order is a path lexicographic order of [14], and hence is admissible. We then notice that performing steps 1 – 4 followed by steps 1, 5, 3 is just equivalent to performing steps 1 – 5 (i.e. performing steps 1 and 3 again provides no new order information). As such steps 1 – 5 are the composite of two admissible orders, and hence by Lemma 5.4.4, is also an admissible order. \square

We close this section by noting that, as observed in Section 4.2, we may use this total order on the underlying $ob(\mathcal{S}(\mathfrak{C}))$ -coloured tree monomials to order the relations of the groupoid coloured shuffle operad governing wheeled props. This induced order is precisely what has been used in Table 2.

5.5. The operad governing wheeled props is Koszul

This section is devoted to the proof that the groupoid coloured operad \mathbb{W} is Koszul. In the prior section, we calculated an explicit presentation of the shuffle operad $\mathbb{W}^f = F_{sh}^{\mathcal{S}(\mathfrak{C})}(E)/\langle R^f \rangle$. We now apply Theorem 4.2.13, to show that \mathbb{W} is Koszul, if G is a quadratic Groebner basis for the $ob(\mathcal{S}(\mathfrak{C}))$ -coloured shuffle operad $F_{sh}^{ob(\mathcal{S}(\mathfrak{C}))}(E^{f_{\mathcal{S}(\mathfrak{C})}})/\langle G \rangle$, where $G := E_*^2 \sqcup (R^f)_*$. We note that in our particular case that the relations of $(R^f)_*$ are precisely the pairs of canonical elements of the corresponding relations for the shuffle operad, and we will use i_* to refer to the ‘groupoid minimised’ version of the i th relation in Table 2. We note that the relations of $E_*^2 = \{\alpha \circ_\varphi \beta \rightarrow [\alpha \circ_\varphi \beta]_* : \alpha, \beta \in E^{f_v}\}$ are all by definition directed towards the minimal element. As an explicit example, from Example 5.2.1, we see that $(\varepsilon_2^3, \binom{id}{id}) \circ_1 (\otimes_h, \binom{213}{231}) \rightarrow (\varepsilon_3^3, \binom{21}{21}) \circ_1 (\otimes_h, \binom{id}{id}) \in E_*^2$.

Lemma 5.5.1. *Under the order of Definition 5.4.1, G is a quadratic Groebner basis for $F_{sh}^{ob(\mathcal{S}(\mathfrak{C}))}(E^{f_{\mathcal{S}(\mathfrak{C})}})/\langle G \rangle$.*

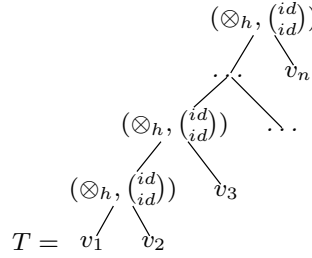
Proof. We prove this lemma as follows.

- In Construction 5.5.2 we describe an algorithm that produces a unique minimal shuffle tree monomial encoding every graph. We show this algorithm is well-defined in Lemma 5.5.4.
- We then prove every shuffle tree monomial which is not the unique minimal shuffle tree monomial of a wheeled graph admits a rewrite using $RS(G)$ (see Section 4.3), establishing the confluence of the rewriting system on all shuffle tree monomials. This is done in Lemma 5.5.5.
- Hence, through Proposition 4.3.4, this proves G is a Groebner basis. \square

The remainder of this section outlines the construction and the two needed lemmas.

Construction 5.5.2. *The following algorithm produces the unique smallest shuffle tree monomial encoding a wheeled graph γ with at least one vertex, we denote the outputted tree $UMF_\circ(\gamma)$.*

- If γ has just one vertex then let $T = v_1$, otherwise if γ has $n > 1$ vertices then let



- Let $\gamma_R = \gamma$.
- While there is an edge in γ_R :
 - Pick the edge $e \in \gamma_R$ that uses the largest input in the graph outputted by T , and identify the necessary contraction indices (i, j) to form this edge (in the graph outputted by T).
 - Update $T = (\varepsilon_j^i, (id_{id}))(T)$.
 - Remove the edge e from γ_R .
- If T is not a vertex, update the permutations of the root-most operation of T so that the corresponding graph outputted by T has the same ordering on its open flags as γ .
- Return T .

Example 5.5.3. For the graph γ in Example 5.4.3, $UMF_{\cup}(\gamma)$ is the smallest tree monomial of that example.

Lemma 5.5.4. The unique minimal form algorithm of Construction 5.5.2 is well-defined.

Proof. It is straightforward to verify that this algorithm produces a (well-formed) shuffle tree monomial that produces the graph γ . We now verify that the algorithm produces the minimal shuffle tree encoding γ by verifying each of the enumerated conditions of Definition 5.4.1.

- (1) Any tree monomial encoding a graph γ with n vertices must have arity n , so there is nothing to minimise here.
- (2) The path from the 1st input to the root is minimal as it is of maximal degree (all generators are above it and there cannot be another tree forming the same graph with a different number of generators) and all contraction generators come after horizontal compositions. Similarly, we can verify that the path from the n th input to the root is minimal, conditional on all paths from smaller inputs being fixed.
- (3) The inputs of the shuffle tree monomials have already been minimised by the prior condition.
- (4) Having all identity permutations except for the final generator is clearly minimal.
- (5) The contractions needed to form the graph γ were greedily added to the tree T by the algorithm by their largest inputs first, and $\varepsilon_j^i < \varepsilon_{j'}^{i'}$, if $j > j'$. \square

Lemma 5.5.5. *Let T be a shuffle tree monomial for a directed graph γ such that $T \neq UMF_{\circlearrowleft}(\gamma)$. Then, T is rewritable by G .*

Proof. Suppose that T is larger than $UMF_{\circlearrowleft}(\gamma)$ as a result of not being normalised with respect to the action of the groupoid. Then there exists an internal edge of T which sits above a non-identity permutation. This internal edge defines a corresponding action of the groupoid which we can translate into an element of E_*^2 . This defines a corresponding rewrite (which will push the permutation up the tree). So given we have access to this rewrite for the remainder of this proof, we suppose that T is normalised with respect to the action of the groupoid.

Suppose that T is larger than $UMF_{\circlearrowleft}(\gamma)$ as a result of having a contraction below a horizontal composition. Then T must have the form of the left-hand side of one of the following equations, and hence must admit the corresponding rewrite.

$$\begin{array}{ccc}
 \begin{array}{c} T_u \\ | \\ (\otimes_h, (\sigma_\tau)) \\ / \quad \backslash \\ (\varepsilon_j^i, (id)) \quad T_2 \\ | \\ T_1 \end{array} & \xrightarrow{3_*} & \begin{array}{c} T_u \\ | \\ (\varepsilon_j^i, (\sigma_\tau)) \\ | \\ (\otimes_h, (id)) \\ / \quad \backslash \\ T_1 \quad T_2 \end{array}
 \end{array}
 \quad \text{or} \quad
 \begin{array}{ccc}
 \begin{array}{c} T_u \\ | \\ (\otimes_h, (\sigma_\tau)) \\ / \quad \backslash \\ T_1 \quad (\varepsilon_j^i, (id)) \\ | \\ T_2 \end{array} & \xrightarrow{4_*} & \begin{array}{c} T_u \\ | \\ (\varepsilon_{j+|c|}^{i+|d|}, (\sigma_\tau)) \\ | \\ (\otimes_h, (id)) \\ / \quad \backslash \\ T_1 \quad T_2 \end{array}
 \end{array}$$

Here T_1 and T_2 are subtrees of T , T_u is the remainder of the tree T (close to root), in the case the second equation we also suppose that T_1 outputs a graph with profile (\underline{d}) . We note that if T_u is not empty, then (σ_τ) must be the identity permutations. Suppose that T is larger than $UMF_{\circlearrowleft}(\gamma)$ as a result of having a horizontal composition appear in the right terminal of another horizontal composition, then T must admit the following form and rewrite.

$$\begin{array}{ccc}
 \begin{array}{c} T_u \\ | \\ (\otimes_h, (\sigma_\tau)) \\ / \quad \backslash \\ T_1 \quad (\otimes_h, (id)) \\ / \quad \backslash \\ T_2 \quad T_3 \end{array} & \xrightarrow{1_*} & \begin{array}{c} T_u \\ | \\ (\otimes_h, (\sigma_\tau)) \\ / \quad \backslash \\ (\otimes_h, (id)) \quad T_3 \\ / \quad \backslash \\ T_1 \quad T_2 \end{array}
 \end{array}$$

Suppose that T has all generators on the path from the minimal vertex to the root, but has a different order of its inputs than $UMF_{\circlearrowleft}(\gamma)$. Then T must admit the following form and rewrite.

$$\begin{array}{ccc}
 \begin{array}{c} T_u \\ | \\ (\otimes_h, (\sigma_\tau)) \\ / \quad \backslash \\ (\otimes_h, (id)) \quad c_i \\ / \quad \backslash \\ T_1 \quad c_j \end{array} & \xrightarrow{2_*} & \begin{array}{c} T_u \\ | \\ (\otimes_h, (\sigma'_{\tau'})) \\ / \quad \backslash \\ (\otimes_h, (id)) \quad c_j \\ / \quad \backslash \\ T_1 \quad c_i \end{array}
 \end{array}$$

Here $i < j$, and the alteration of (σ_τ) to $(\sigma'_{\tau'})$ is needed in general with this interchange of vertices. As T is a shuffle tree monomial, T_1 must contain c_1 . Finally, suppose that

T is larger than $UMF_{\circ}(\gamma)$ as a result of using a different contraction sequence in the ‘topmost’ vertical segment. This implies there must exist two adjacent contractions such that the lower contraction uses input index j , the higher contraction uses input index $j' - 1$ and $j < j'$. Then T must admit either of the following forms and rewrites.

$$\begin{array}{ccc}
 \begin{array}{c} T_u \\ | \\ (\varepsilon_{j'-1}^{i'-1}, (\sigma)) \\ | \\ (\varepsilon_j^i, (id)) \\ | \\ T_1 \end{array} & \xrightarrow{5_*} & \begin{array}{c} T_u \\ | \\ (\varepsilon_j^i, (\sigma)) \\ | \\ (\varepsilon_{j'}^{i'}, (id)) \\ | \\ T_1 \end{array} \\
 \text{If } i < i' & & \text{, if } i > i'
 \end{array}
 \qquad
 \begin{array}{ccc}
 \begin{array}{c} T_u \\ | \\ (\varepsilon_{j'-1}^{i'}, (\sigma)) \\ | \\ (\varepsilon_j^i, (id)) \\ | \\ T_1 \end{array} & \xrightarrow{6_*} & \begin{array}{c} T_u \\ | \\ (\varepsilon_j^{i'-1}, (\sigma)) \\ | \\ (\varepsilon_{j'}^{i'}, (id)) \\ | \\ T_1 \end{array}
 \end{array}$$

We conclude this proof by noting that there are no further ways for T to be greater than $UMF_{\circ}(\gamma)$, hence either $T = UMF_{\circ}(\gamma)$ or T admits a rewrite. \square

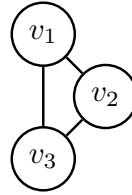
6. The operad governing props

We will now mirror the methodology of the preceding section to define a groupoid coloured operad \mathbb{P} governing props. We then show this operad is Koszul (Section 6.5). We will assume that the reader has read (or is reading in parallel) Section 5, so that we may streamline identical proofs and focus on technical difficulties arising from the nature of props.

6.1. Props

We wish to define an alternate biased prop which will induce a nice definition of a quadratic groupoid coloured operad governing props. Such a definition is not as straightforward to produce as the alternate definition for wheeled props (Definition 5.1.2). As such, we first discuss the necessary features of an ‘alternate biased prop’, before presenting it (Definition 6.1.2) and proving it is equivalent to a standard definition of a prop (Definition 11.30 of [57], through Proposition 6.1.4). Finally, we will discuss non-unital and augmented variants of this definition.

Our alternate definition of a prop should use the same extended horizontal composition as the alternate wheeled prop (Definition 5.1.2), and then have some way to connect flags of graphs without the possibility of forming wheels. The standard vertical composition of props which connects all outputs of one graph to all inputs of another (see for instance Definition 11.30 of [57]) is not a good candidate for at least two reasons. Firstly, a non-unital version of such a prop would not be able to form graphs like the Bow graph.



This is similar to how a non-unital May operad, defined via $\gamma : O(n) \times O(k_1) \times \dots O(k_n) \rightarrow O(k_1 + \dots + k_n)$, is incapable of forming a partial operadic composition $\circ_i : O(n) \times O(k) \rightarrow O(n + k - 1)$ (see [34]). Secondly, props with the standard vertical composition satisfy the interchange axiom (11.26 of [57]) which is a ternary relation, and hence would not induce a quadratic presentation of our operad. As such, instead of seeking to modify vertical composition, we will instead define an extended properadic composition, which we now discuss the motivation for.

In [57] two biased definitions of properads are provided. The first, Definition 11.25, uses a properadic composition of the form

$$P\left(\frac{d}{c}\right) \otimes P\left(\frac{b}{a}\right) \xrightarrow{\boxtimes_{\left(\frac{c'}{b'}\right)}} P\left(\frac{b \circ_{b'} d}{c \circ_{c'} a}\right) \quad (8)$$

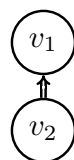
This composition connects two graphs via contiguous k -segments $c' \subset c$ and $b' \subset b$. By c' is a contiguous k -segment of c (Definition 1.5 of [57]), we mean that $c = (c_1, \dots, c_{i-1}, c', c_{i+k+1}, \dots, c_{|c|})$, and $c \circ_{c'} a$ is syntactic sugar denoting $c \circ_{c'} a := (c_1, \dots, c_{i-1}, a, c_{i+k+1}, \dots, c_{|c|})$. The second definition of a properad in [57], Definition 11.27, uses a properadic composition which is an extension of the prior.

$$P\left(\frac{d}{c}\right) \otimes P\left(\frac{b}{a}\right) \xrightarrow{\boxtimes_{\left(\frac{c'}{b'}\right), \left(\sigma\right)}} P\left(\frac{\sigma b \circ_{b'} d}{c\tau \circ_{c'} a}\right),$$

defined by,

$$\alpha \boxtimes_{\left(\frac{c'}{b'}\right), \left(\sigma\right)} \beta := \left(\alpha \cdot \begin{pmatrix} id \\ \tau \end{pmatrix}\right) \boxtimes_{\left(\frac{c'}{b'}\right)} \left(\beta \cdot \begin{pmatrix} \sigma \\ id \end{pmatrix}\right). \quad (9)$$

This composition connects two graphs via the contiguous k -segments $c' \subset c\tau$ and $b' \subset \sigma b$. This in effect allows the composition of two graphs via potentially dis-contiguous segments via first permuting the dis-contiguous segments into contiguous segments. In particular we could form any connected graph with two vertices γ , by first forming the internal edges of γ via Eq. (9), and then producing any listing of the remaining flags via an action of the bimodule. We will use the following diagram to represent the graph γ .



Unfortunately, $\boxtimes_{(\underline{c}', \underline{b}'), (\sigma)}$ satisfies inner biequivariance axioms (see Definition 11.27 of [57]) such as

$$\begin{array}{c} \text{Diagram 1} \end{array} \boxtimes_{(\underline{c}', \underline{b}'), (\sigma)} \begin{array}{c} \text{Diagram 2} \end{array} = \begin{array}{c} \text{Diagram 3} \end{array} \boxtimes_{(\underline{c}', \underline{b}'), (\sigma)} \begin{array}{c} \text{Diagram 4} \end{array}$$

Hence, if we were to take this as our definition of properadic composition, then the operad governing props would satisfy unary relations. Thus, for any connected graph with two vertices γ , we wish to identify a unique way of forming γ from these vertices (with their specific listings, Definition 2.2.4). Or combinatorially, we wish to uniquely identify: an instance of Eq. (9) which forms the k connected edges of γ by connecting the potentially dis-contiguous k -segments $\underline{c}' \subseteq \underline{c}$ and $\underline{b}' \subseteq \underline{b}$, subject to $\underline{c}' = \underline{b}'$; and a pair of permutations which produces the specific listing of the remaining open inputs and outputs of γ .

- We assume $\underline{c}' \subseteq \underline{c}$ admits the reduced order of \underline{c} , i.e. if $c_i, c_j \in \underline{c}'$ and $c_i < c_j$ in \underline{c} , then $c_i < c_j$ in \underline{c}' . If this was not the case, then there exists a permutation σ such that $\underline{c}'\sigma$ admits the reduced order, and we could proceed with this pair instead (clearly $\underline{c}'\sigma = \underline{b}'\sigma$).
- The properadic composition of Eq. (8), is defined whenever both \underline{c}' and \underline{b}' are contiguous, thus we could apply any pair of permutations τ, σ such that $\underline{c}\tau = (\underline{c}_l, \underline{c}', \underline{c}_r)$ and $\sigma\underline{b} = (\underline{b}_l, \underline{b}', \underline{b}_r)$. Of these possibilities, we choose the unique permutations $\tau_{\underline{c}'}^{\underline{c}}, \sigma_{\underline{b}'}^{\underline{b}}$ such that $\underline{c}\tau_{\underline{c}'}^{\underline{c}} = (\underline{c}', \underline{c} \setminus \underline{c}')$ and $\sigma_{\underline{b}'}^{\underline{b}}\underline{b} = (\underline{b}', \underline{b} \setminus \underline{b}')$, i.e. we choose the unique permutations which pull the connecting segments to the left, and conserve the order of the remaining elements.
- Hence by the definition of $\circ_{\underline{c}'}$ below Eq. (8), $\underline{c}\tau_{\underline{c}'}^{\underline{c}} \circ_{\underline{c}'} \underline{a} = (\underline{a}, \underline{c} \setminus \underline{c}')$ and $\sigma_{\underline{b}'}^{\underline{b}} \underline{b} \circ_{\underline{b}'} \underline{d} = (\underline{d}, \underline{b} \setminus \underline{b}')$.
- Finally, there exist unique permutations (σ_{τ}) producing any listing of the remaining inputs+outputs.

That is to say we identify our properadic composition as the composite,

$$\begin{array}{ccc}
 P(\underline{d}) \otimes P(\underline{b}) & \xrightarrow{(\tau_{\underline{c}'}^{\underline{c}}) \otimes (\sigma_{\underline{b}'}^{\underline{b}})} & P(\underline{d}_{\underline{c}', \underline{c} \setminus \underline{c}'}) \otimes P(\underline{b}_{\underline{a}}) \\
 & \searrow \circ_{(\underline{c}', \underline{b}'), (\sigma)} & \downarrow \boxtimes_{(\underline{c}', \underline{b}')} \\
 & & P(\underline{d}_{\underline{a}, \underline{c} \setminus \underline{c}'}) \\
 & & \downarrow (\sigma_{\tau}) \\
 & & P(\sigma(\underline{d}_{\underline{a}, \underline{c} \setminus \underline{c}'}))
 \end{array}$$

Note, in Definition 6.1.2, we do not define our composition to be equal to this composite, but rather alter the underlying biequivariance axioms so it behaves in this fashion (see Remark 6.1.5). We also note that other ways of producing a representative are possible, such as giving \underline{b}' the reduced order of \underline{b} , or pulling the connecting segments to the right. We only care that there is a unique way to form each connected graph with two vertices via our defined composition. We illustrate this with the following example.

Example 6.1.1. Recalling that we use the line permutation notation, we compute

$$\begin{array}{c} d_1 \\ \circlearrowleft v_1 \\ \swarrow \quad \downarrow \quad \searrow \\ c_1 \quad c_2 \quad c_3 \end{array} \circ_{\left(\begin{smallmatrix} c_1, c_3 \\ b_3, b_2 \end{smallmatrix}\right), \left(\begin{smallmatrix} 21 \\ id \end{smallmatrix}\right)} \begin{array}{c} b_1 \quad b_2 \quad b_3 \\ \swarrow \quad \downarrow \quad \searrow \\ \circlearrowleft v_1 \\ a_1 \end{array} = \begin{array}{c} d_1 \\ \circlearrowleft v_1 \\ \swarrow \quad \downarrow \quad \searrow \\ c_1 \quad c_2 \quad c_3 \end{array} \cdot \left(\begin{smallmatrix} id \\ 132 \end{smallmatrix}\right) \boxtimes_{\left(\begin{smallmatrix} c_1, c_3 \\ b_3, b_2 \end{smallmatrix}\right)} \begin{array}{c} b_1 \quad b_2 \quad b_3 \\ \swarrow \quad \downarrow \quad \searrow \\ \circlearrowleft v_1 \\ a_1 \end{array} \cdot \left(\begin{smallmatrix} 321 \\ id \end{smallmatrix}\right) \cdot \left(\begin{smallmatrix} 21 \\ id \end{smallmatrix}\right) = \begin{array}{c} b_1 \quad d_1 \\ \swarrow \quad \searrow \\ \circlearrowleft v_1 \\ \swarrow \quad \downarrow \quad \searrow \\ \circlearrowleft v_2 \\ a_1 \quad c_2 \end{array}$$

We verify that there is a unique composite $\alpha \circ_{\left(\frac{\underline{c}'}{\underline{b}'}, (\sigma_\tau)\right)} \beta$ forming this graph γ . In particular:

- α must be the top vertex and β the lower (i.e inputs of α are connected to outputs of β);
- we identify the subset of flags $\underline{c}' = \{c_1, c_3\} = \{b_3, b_2\} = \underline{b}'$ being connected by the properadic join;
- the listing of $\underline{c}' = (c_1, c_3)$ is then determined by the listing of α , as \underline{c}' admits the reduced order of \underline{c} (recall each vertex has specific listing data, Definition 2.2.4);
- the listing of \underline{c}' determines the listing of $\underline{b}' = (b_3, b_2)$;
- this completely determines $\boxtimes_{\left(\frac{\underline{c}'}{\underline{b}'}, (\sigma_\tau)\right)} = \boxtimes_{\left(\begin{smallmatrix} c_1, c_3 \\ b_3, b_2 \end{smallmatrix}\right), \left(\begin{smallmatrix} 132 \\ 321 \end{smallmatrix}\right)}$; and
- the final permutation $(\sigma_\tau) = \left(\begin{smallmatrix} 21 \\ id \end{smallmatrix}\right)$ is determined by the relative listing of γ to $\alpha \boxtimes_{\left(\begin{smallmatrix} c_1, c_3 \\ b_3, b_2 \end{smallmatrix}\right), \left(\begin{smallmatrix} 132 \\ 321 \end{smallmatrix}\right)} \beta$.

We now present our definition.

Definition 6.1.2. Let \mathcal{E} be a symmetric monoidal category, a **alternate prop** P consists of the following.

- (1) A bimodule $P \in \mathcal{E}^{\mathcal{S}(\mathfrak{C})}$.
- (2) An extended horizontal composition,

$$P\left(\frac{\underline{d}}{\underline{c}}\right) \otimes P\left(\frac{\underline{b}}{\underline{a}}\right) \xrightarrow{\otimes_h, (\sigma_\tau)} P\left(\frac{\sigma(\underline{d}, \underline{b})}{(\underline{c}, \underline{a})\tau}\right).$$

(3) An alternate properadic composition,

$$P\left(\frac{\underline{d}}{\underline{c}}\right) \otimes P\left(\frac{\underline{b}}{\underline{a}}\right) \xrightarrow{\circ_{(\frac{\underline{c}'}{\underline{b}'})}, (\sigma_\tau)} P\left(\frac{\sigma(\underline{d}, \underline{b} \setminus \underline{b}')}{(\underline{a}, \underline{c} \setminus \underline{c}')\tau}\right),$$

where $\underline{c}' \subseteq \underline{c}$, $\underline{b}' \subseteq \underline{b}$, $\underline{c}' = \underline{b}'$ and \underline{c}' admits the reduction of the order of \underline{c} .

(4) An opposing alternate properadic composition defined by

$$\hat{\circ}_{(\frac{\underline{c}'}{\underline{b}'})}, (\sigma_\tau)(\alpha, \beta) := \circ_{(\frac{\underline{c}'}{\underline{b}'})}, (\sigma_\tau)(\beta, \alpha)$$

(5) Units for properadic and horizontal composition.

In situations where the permutations and indices are either arbitrary or clear, we will use \otimes_h , \circ_v and $\hat{\circ}_v$ to refer to these compositions. The opposing extended properadic composition $\hat{\circ}_v$ does not increase the expressive power of this definition of a prop, but rather exists to be paired off with \circ_v under a Σ_2 -action in our latter definition of the operad governing props.

We now present the axioms satisfied by these compositions. We will not express the various unity diagrams (as we will quickly move to using a non-unital definition) but the obvious extensions to (Definitions 11.21 and 11.9 of [57]) are also present. We have the same biequivariance and associativity axioms of \otimes_h as for wheeled props (Definition 5.1.2). The other compositions are right, left and switch biequivariant as follows, (the axioms for $\hat{\circ}_v$ are obvious variants of \circ_v)

$$\begin{array}{ccc} P\left(\frac{\underline{d}}{\underline{c}}\right) \otimes P\left(\frac{\underline{b}}{\underline{a}}\right) & & P\left(\frac{\underline{d}}{\underline{c}}\right) \otimes P\left(\frac{\underline{b}}{\underline{a}}\right) \\ \circ_{(\frac{\underline{c}'}{\underline{b}'})}, (\sigma_\tau) \downarrow & \searrow \circ_{(\frac{\underline{c}'}{\underline{b}'})}, (\sigma'_\tau \sigma) & (\sigma_1) \otimes (\sigma_2) \downarrow \searrow \circ_{(\frac{\underline{c}''}{\underline{b}''})}, (\sigma'_\tau) \\ P\left(\frac{\sigma(\underline{d}, \underline{b})}{(\underline{c}, \underline{a})\tau}\right) & \xrightarrow{(\sigma'_\tau)} & P\left(\frac{\sigma' \sigma(\underline{d}, \underline{b})}{(\underline{c}, \underline{a})\tau \tau'}\right) & P\left(\frac{\sigma_1 \underline{d}}{\underline{c} \tau_1}\right) \otimes P\left(\frac{\sigma_2 \underline{b}}{\underline{a} \tau_2}\right) & \xrightarrow{\circ_{(\frac{\underline{c}'}{\underline{b}'})}, (\sigma_\tau)} & P\left(\frac{\sigma(\sigma_1 \underline{d}, \sigma_2 \underline{b} \setminus \underline{b}')}{(\underline{a} \tau_2, \underline{c} \tau_1 \setminus \underline{c}')\tau}\right) \\ & & & & & \\ & & & & & \\ P\left(\frac{\underline{d}}{\underline{c}}\right) \otimes P\left(\frac{\underline{b}}{\underline{a}}\right) & & & & & \\ \text{switch} \downarrow & \searrow \circ_{(\frac{\underline{c}'}{\underline{b}'})}, (\sigma_\tau) & & & & \\ P\left(\frac{\underline{b}}{\underline{a}}\right) \otimes P\left(\frac{\underline{d}}{\underline{c}}\right) & \xrightarrow{\hat{\circ}_{(\frac{\underline{c}'}{\underline{b}'})}, (\sigma_\tau)} & & & & P\left(\frac{\sigma(\underline{d}, \underline{b} \setminus \underline{b}')}{(\underline{a}, \underline{c} \setminus \underline{c}')\tau}\right) \end{array}$$

In the second diagram, if $\sigma_{\underline{c}}$ is the unique permutation that gives $\underline{c}'(\tau^{-1}|_{\underline{c}'})$ the same reduced order as \underline{c} , then $\underline{c}'' := \underline{c}'(\tau^{-1}|_{\underline{c}'})\sigma_{\underline{c}}$, which by construction has the same reduced order as \underline{c} . Then (in order to connect the exact same wires), we define $\underline{b}'' := \underline{b}'(\tau^{-1}|_{\underline{c}'})\sigma_{\underline{c}}$. Notice that in general \underline{b}'' will be a dis-contiguous subset of \underline{b} . Finally, in order to match permutations, we define σ', τ' such that $\left(\frac{\sigma(\sigma_1 \underline{d}, \sigma_2 \underline{b} \setminus \underline{b}')}{(\underline{a} \tau_2, \underline{c} \tau_1 \setminus \underline{c}')\tau}\right) = \left(\frac{\sigma'(\underline{d}, \underline{b} \setminus \underline{b}'')}{(\underline{a}, \underline{c} \setminus \underline{c}'')\tau'}\right)$. To place the diagrams in context, the left and right compatibility diagram encode similar information to the biequivariance diagram of Definition 11.27 of [57], and the switch diagram is the definition of $\hat{\circ}_v$ restated in diagram form.

With these axioms we can prove Proposition 6.1.3, and use it to simplify the remaining axioms. These include the four associativity diagrams of properadic composition, extended in the obvious way (see Definition 11.25 of [57]). We shall refer to these diagrams as the Caterpillar, Lighthouse, Fireworks and Bow diagrams following the conventions of [57] (sometimes abbreviated using the capitalised first letter where obvious). Finally, a new axiom regarding compatibility of \otimes_h and \circ_v is required, which we refer to as the Third-wheel.

These relations are encoded graphically in Table 3, however the interested reader may also find them explicitly written out in Section 8. This table uses the same notation as introduced in Table 1. In other words, each composite of operations is given under the implicit understanding that it is forming the graph on the left. As we may use the biequivariance axioms to push all permutations to the top (Proposition 6.1.3), this indicates that the permutations of the operations and the sub-profiles of any properadic joins are uniquely specified by the graph. As such, we may use a suppressed notation where we omit the permutations and the specific indices used by each binary operation.

As was the case for wheeled props (Proposition 5.1.1), the equivariance axioms yield the following.

Proposition 6.1.3. *Every valid composite of operations in Definition 6.1.2 admits a simple canonical form, where all non-identity permutations are pushed to the outermost operation.*

This result not only lets us simplify the other axioms of Definition 6.1.2, but it will also induce a simple canonical form for every groupoid coloured tree monomial in \mathbb{P} (Section 6.2). We now prove our definition is indeed a prop, by establishing equivalence with a known definition.

Proposition 6.1.4. *Definition 6.1.2 and Definition 11.30 of [57] are equivalent definitions of props.*

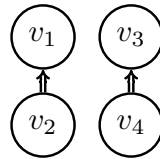
Proof. The equivalence of the underlying operations is easy to establish. The vertical composition (which we denote) \circ_v , and the horizontal composition \otimes_h of Definition 11.30 of [57], are particular instances of the extended compositions, i.e. $\circ_v : P(\frac{c}{b}) \otimes P(\frac{b}{a}) \rightarrow P(\frac{c}{a})$ is equal to $\circ_{(\frac{b}{b}), (id)}$, and $\otimes_h = (\otimes_h, \binom{id}{id})$. In the other direction, the extended horizontal composition $(\otimes_h, \binom{\sigma}{\tau})$ can be obtained by \otimes_h followed by an action of the bimodule (Section 2.1). The extended properadic composition can be obtained through the following commutative diagram,

$$\begin{array}{ccc}
P(\underline{d}) \otimes P(\underline{b}) & \xrightarrow{\text{pad with units}} & P(\underline{d}, \underline{b} \setminus \underline{b}') \otimes P(\underline{b}, \underline{c} \setminus \underline{c}') \\
& \searrow \circ(\underline{c'}, \underline{b'}) & \downarrow (i_d) \otimes (\tau'_{id}) \\
& & P(\underline{c'}, \underline{c} \setminus \underline{c'}, \underline{b} \setminus \underline{b}') \otimes P(\underline{b'}, \underline{c} \setminus \underline{c'}, \underline{b} \setminus \underline{b}') \\
& & \downarrow \circ_V \\
& & P(\underline{d}, \underline{b} \setminus \underline{b}') \\
& & \downarrow \text{remove dangling units} \\
& & P(\underline{d}, \underline{b} \setminus \underline{b}') \\
& & \downarrow (\sigma) \\
& & P(\underline{\sigma(d, b \setminus b')}) \\
& & \downarrow (\sigma) \\
& & P(\underline{\sigma(d, b \setminus b')})
\end{array}$$

where σ', τ' are the unique permutations (outputting the target profiles) which move the connecting segments $\underline{c'}, \underline{b'}$ to the left (recall that $\underline{c'}$ is ordered by \underline{c} , and $\underline{b'}$ by $\underline{c'}$), and align the remaining flags with an identity.

The axioms of Definition 11.30 of [57] arise from the axioms of the alternate definition as follows

- The axioms regarding the extended horizontal composition can be restricted to the standard horizontal composition (associativity, biequivariance and unity).
- The axioms regarding the extended properadic composition can be restricted down to the vertical compositions (associativity, biequivariance and unity).
- The interchange axiom (11.26) is obtained as follows. As vertical composition is an instance of extended properadic composition, the interchange axiom corresponds to the following graph.



With this diagram as a guide we then apply a chain of axioms of our alternate definition to reproduce the interchange axiom $\otimes_h(\circ_V(v_1, v_2), \circ_V(v_3, v_4)) = \circ_V(\otimes_h(v_1, v_3), \otimes_h(v_2, v_4))$. To aid readability, an underline is used to group anything that is treated as a ‘single variable’ by an equation.

$$\circ_V(\otimes_h(\underline{v_1, v_3}), \otimes_h(v_2, v_4)) = \circ_V(\circ_V(\otimes_h(v_1, v_3), v_2), v_4), \quad (L)$$

$$= \circ_V(\otimes_h(\underline{\circ_V(v_1, v_2)}, v_3), v_4), \quad (T)$$

$$= \circ_V(\otimes_h(v_3, \underline{\circ_V(v_1, v_2)}), v_4), \quad (\text{Bi-eq } \otimes_h)$$

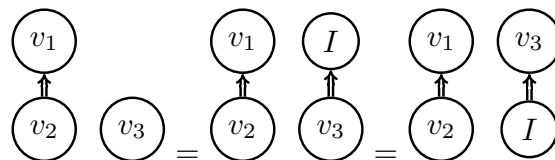
$$= \otimes_h (\underline{\circ_V(v_3, v_4)}, \underline{\circ_V(v_1, v_2)}), \quad (T)$$

$$= \otimes_h (\circ_V(v_1, v_2), \circ_V(v_3, v_4)), \quad (\text{Bi-eq } \otimes_h)$$

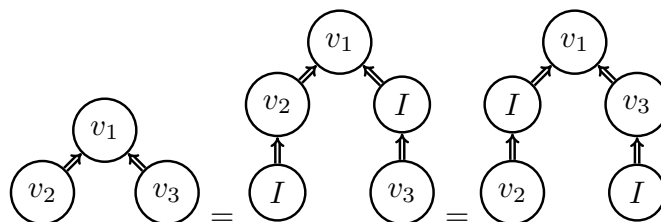
We have suppressed the permutations above, but there are non-identity permutations in the second to fourth line that for instance force the output flags of v_1 to appear before the output flags of v_3 and similar. The needed permutations are reverted to identities by the final biequivariance of \otimes_h .

The axioms of our alternate definition of a prop arise from the axioms of Definition 11.30 [57] as follows.

- The axioms which just involve horizontal composition arise as described in wheeled props (Definition 5.1.2).
- The biequivariance axioms of $\circ_v, \hat{\circ}_v$ arise from the biequivariance diagram of \circ_V (Diagram 11.23 [57]). This is a straightforward but tedious exercise. Start with one side of the biequivariance diagram, and blow up \circ_v using its \circ_V commutative diagram description, then manipulate it into the other side through unit axioms, biequivariance axioms (of \circ_V), and actions of the bimodule.
- The caterpillar diagram arises from the associativity relation of vertical composition, as the extended properadic composition is defined from vertical composition (with appropriate padding with units).
- The third-wheel axiom arises from the interchange axiom and the vertical unit. The corresponding diagram illustrating this result is



- The caterpillar axiom, the interchange axiom and vertical units can collectively be used to construct the lighthouse, fireworks and bow diagrams. Here is an outline of how the lighthouse axiom arises, and the others are similar. In the diagram below, the vertices labelled I denote any appropriate block of units.



Then the first equality of diagrams corresponds to,

$$\begin{aligned}
 \circ_v(v_1, \otimes_h(v_2, v_3)) &= \circ_v(v_1, \otimes_h(\circ_v(v_2, I), \circ_v(I, v_3))) && \text{(Units)} \\
 &= \circ_v(v_1, \circ_v(\otimes_h(v_2, I), \otimes_h(I, v_3))) && \text{(Interchange)} \\
 &= \circ_v(\circ_v(v_1, \otimes_h(v_2, I)), \otimes_h(I, v_3)) && \text{(Caterpillar)} \\
 &= \circ_v(\circ_v(v_1, v_2), v_3) && \text{(unit)}
 \end{aligned}$$

and the third diagram can be interpreted similarly. \square

Remark 6.1.5. The restriction of Definition 6.1.2 to just include the properadic composition and the connected axioms, also provides an equivalent definition of a coloured properad (Definition 11.7.2 of [57] is the closest analogue). This is a straightforward but tedious proof, so we only sketch the idea here. The connection between the properadic composition of Definition 6.1.2 and Definition 11.7.2 of [57] is given in the preamble of Section 6.1. By the “connected axioms” of Definition 6.1.2, we mean the Bow+Caterpillar axioms, and the two relations of the Lighthouse+Fireworks axioms that only use the properadic compositions. Each of these axioms have their analogue in Definition 11.7.2 of [57].

We now define augmented and non-unital versions of this definition, mirroring the corresponding section for wheeled props.

Definition 6.1.6. Let \mathcal{K} be the trivial prop in $Vect_{\mathbb{K}}$ whose only constituents are the vertical and horizontal units.

Definition 6.1.7. An **augmentation** of a prop P in $dgVect_{\mathbb{K}}$ is a morphism (of props, see Corollary 11.32 of [57]) $\epsilon : P \rightarrow \mathcal{K}$. Props with an augmentation are called **augmented props**.

Definition 6.1.8. A **non-unital alternate prop** consists of all the data of an alternate prop, excluding the units and the corresponding axioms.

Proposition 6.1.9. *Augmented alternate props and non-unital alternate props are isomorphic.*

Proof. This is a clear analogue of the classical result for partial operads see Proposition 21 of [34]. \square

The last definition and isomorphism have only been presented for alternate props, and not Definition 11.30 of [57]. The non-unital version of Definition 11.30 of [57], is not isomorphic to an augmented prop. This follows from the bow graph counter example given in the preamble Section 6.1. More explicitly, we can observe that because the

standard vertical composition must connect all inputs of one graph with all outputs of another graph, the corresponding graphs of the non-unital version of Definition 11.30 of [57] will satisfy an additional convexity condition. This being, if two vertices u and v are connected by an edge then there can be no other vertex w on a path between them. Thus, for the rest of the paper when we speak of a non-unital prop we mean a non-unital alternate prop.

6.2. A groupoid coloured quadratic presentation

We now produce a quadratic non-unital groupoid coloured operad $\mathbb{P} = F_{\Sigma}^{\mathcal{S}(\mathfrak{C})}(E)/\langle R \rangle$, whose algebras are non-unital props (mirroring Section 5.2). The underlying groupoid of our operad is $\mathcal{S}(\mathfrak{C}) := \mathcal{P}(\mathfrak{C})^{op} \times \mathcal{P}(\mathfrak{C})$. The generators E correspond to the compositions as follows, let $(\frac{b}{a}), (\frac{d}{c}), (\frac{f}{e}) \in \mathcal{P}(\mathfrak{C})^{op} \times \mathcal{P}(\mathfrak{C})$ then

$$\begin{aligned} E\left(\left(\frac{d}{c}\right), \left(\frac{b}{a}\right); \left(\frac{f}{e}\right)\right) &:= \{(\otimes_h, \left(\frac{\sigma}{\tau}\right))(-, -) : \left(\frac{\sigma(\underline{d}, \underline{b})}{(\underline{c}, \underline{a})\tau}\right) = \left(\frac{f}{e}\right)\} \sqcup \\ &\quad \{\circ_{(\frac{c'}{b'}), (\frac{\sigma}{\tau})}(-, -) : \left(\frac{\sigma(\underline{d}, \underline{b} \setminus \underline{b}')}{(\underline{a}, \underline{c} \setminus \underline{c}')\tau}\right) = \left(\frac{f}{e}\right)\} \sqcup \\ &\quad \{\hat{\circ}_{(\frac{a'}{d'}), (\frac{\sigma}{\tau})}(-, -) : \left(\frac{\sigma(\underline{b}, \underline{d} \setminus \underline{d}')}{(\underline{c}, \underline{a} \setminus \underline{a}')\tau}\right) = \left(\frac{f}{e}\right)\} \end{aligned}$$

The necessary left, right and Σ actions are then given by the biequivariance axioms of Definition 6.1.2 (note the biequivariance axioms for \otimes_h are found in Definition 5.1.2). These groupoid actions once again provide a simple canonical form of every groupoid coloured tree monomial (where all permutations are pushed to the top) which enables us to encode the quadratic relations R graphically in Table 3. By construction, it follows that,

Corollary 6.2.1. *Algebras over \mathbb{P} are non-unital props.*


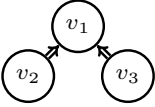
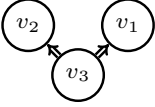
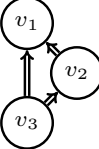
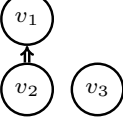

6.3. The shuffle operad

In this section, we explicitly describe $\mathbb{P}^f = (F_{\Sigma}^{\mathcal{S}(\mathfrak{C})}(E)/R)^f \cong F_{sh}^{\mathcal{S}(\mathfrak{C})}(E^f)/R^f$ (mirroring Section 5.3). We first observe how $-^f$ acts on the binary generators and their orbits. The generator \otimes_h is handled as in Section 5.3, and as the other Σ_2 actions map generators to generators, i.e. $\circ_{(\frac{c'}{b'}), (\frac{\sigma}{\tau})}(\alpha, \beta) \mapsto \hat{\circ}_{(\frac{c'}{b'}), (\frac{\sigma}{\tau})}(\beta, \alpha)$ and $\hat{\circ}_{(\frac{c'}{b'}), (\frac{\sigma}{\tau})}(\alpha, \beta) \mapsto \circ_{(\frac{c'}{b'}), (\frac{\sigma}{\tau})}(\beta, \alpha)$, we have no need to introduce further generators in our shuffle operad.

We now observe how $-^f$ acts on the relations by orienting each element of the orbit, of each relation of \mathbb{P} , to use shuffle compositions. As each of our families of relations corresponds to a given graph, we take the orbit of the relations corresponding to each graph. In the table below, the line $\gamma \cdot p, e_1 \leftarrow e_2, e_3$ means: we take the relations corresponding to

Table 3

The relations of the operad governing props, and dually, the non-unital and non-biequivariance relations of an alternate prop.

Names	Graphs	Relations
Caterpillar		$\circ_v(\circ_v(v_1, v_2), v_3) = \circ_v(v_1, \circ_v(v_2, v_3))$
Lighthouse		$\circ_v(\circ_v(v_1, v_2), v_3) = \circ_v(\circ_v(v_1, v_3), v_2) = \circ_v(v_1, \otimes_h(v_2, v_3))$
Fireworks		$\circ_v(\otimes_h(v_1, v_2), v_3) = \circ_v(v_1, \circ_v(v_2, v_3)) = \circ_v(v_2, \circ_v(v_1, v_3))$
Bow		$\circ_v(\circ_v(v_1, v_2), v_3) = \circ_v(v_1, \circ_v(v_2, v_3))$
Third-wheel		$\otimes_h(\circ_v(v_1, v_2), v_3) = \circ_v(v_1, \otimes_h(v_2, v_3)) = \circ_v(\otimes_h(v_1, v_3), v_2)$
Associativity \otimes_h		$\otimes_h(\otimes_h(v_1, v_2), v_3) = \otimes_h(v_1, \otimes_h(v_2, v_3))$

the graph γ and act on them via p (graphically this corresponds to switching the vertex labels of the graph) after we orient these relations as shuffle tree monomials we are left with $e_1 = e_2 = e_3$, and e_1 is the smallest shuffle tree monomial under an order introduced in the next section. However, as was the case in Section 5.3, we find that many orbit elements admit the same orientation. We will use the notation $\gamma \cdot p_1, \gamma \cdot p_2, e_1 \leftarrow e_2, e_3$ to denote the orbit elements $\gamma \cdot p_1$ and $\gamma \cdot p_2$ being oriented into the same relations. We now list all 38 resulting directed relations of the shuffle operad.

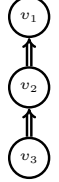
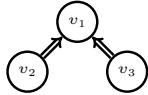
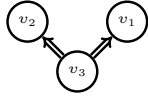
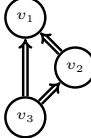
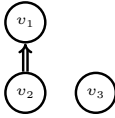

This completes the presentation of the relations of the shuffle operad \mathbb{P}^f , these relations encode all the equivalent ways to form directed wheel-free graphs with 3 vertices via shuffle tree monomials.

6.4. Ordering the object coloured tree monomials

We now define a total admissible order on the underlying $ob(\mathcal{S}(\mathfrak{C}))$ -coloured tree monomials of $F_{sh}(E)$. The motivation of this order as in Section 5.4 is to provide a

Table 4

The relations of the shuffle operad governing props.

Caterpillar:		$C \cdot (123)$	$\circ_v(\circ_v(v_1, v_2), v_3) \leftarrow \circ_v(v_1, \circ_v(v_2, v_3))$
		$C \cdot (132)$	$\circ_v(\circ_v(v_1, v_3), v_2) \leftarrow \circ_v(v_1, \hat{\circ}_v(v_2, v_3))$
		$C \cdot (213)$	$\circ_v(\hat{\circ}_v(v_1, v_2), v_3) \leftarrow \hat{\circ}_v(\circ_v(v_1, v_3), v_2)$
		$C \cdot (231)$	$\hat{\circ}_v(\hat{\circ}_v(v_1, v_3), v_2) \leftarrow \hat{\circ}_v(v_1, \circ_v(v_2, v_3))$
		$C \cdot (312)$	$\hat{\circ}_v(\circ_v(v_1, v_2), v_3) \leftarrow \circ_v(\hat{\circ}_v(v_1, v_3), v_2)$
		$C \cdot (321)$	$\hat{\circ}_v(\hat{\circ}_v(v_1, v_2), v_3) \leftarrow \hat{\circ}_v(v_1, \hat{\circ}_v(v_2, v_3))$
Lighthouse:		$L \cdot (123), L \cdot (132)$	$\circ_v(\circ_v(v_1, v_2), v_3) \leftarrow \circ_v(\circ_v(v_1, v_3), v_2), \circ_v(v_1, \otimes_h(v_2, v_3))$
		$L \cdot (213), L \cdot (231)$	$\circ_v(\hat{\circ}_v(v_1, v_2), v_3) \leftarrow \hat{\circ}_v(\otimes_h(v_1, v_3), v_2), \hat{\circ}_v(v_1, \circ_v(v_2, v_3))$
		$L \cdot (312), L \cdot (321)$	$\hat{\circ}_v(\otimes_h(v_1, v_2), v_3) \leftarrow \hat{\circ}_v(\hat{\circ}_v(v_1, v_3), v_2), \hat{\circ}_v(v_1, \hat{\circ}_v(v_2, v_3))$
Fireworks:		$F \cdot (123), F \cdot (213)$	$\circ_v(\otimes_h(v_1, v_2), v_3) \leftarrow \hat{\circ}_v(\circ_v(v_1, v_3), v_2), \circ_v(v_1, \circ_v(v_2, v_3))$
		$F \cdot (132), F \cdot (312)$	$\hat{\circ}_v(\circ_v(v_1, v_2), v_3) \leftarrow \hat{\circ}_v(\otimes_h(v_1, v_3), v_2), \circ_v(v_1, \hat{\circ}_v(v_2, v_3))$
		$F \cdot (231), F \cdot (321)$	$\hat{\circ}_v(\hat{\circ}_v(v_1, v_2), v_3) \leftarrow \hat{\circ}_v(\hat{\circ}_v(v_1, v_3), v_2), \hat{\circ}_v(v_1, \otimes_h(v_2, v_3))$
Bow:		$B \cdot (123)$	$\circ_v(\circ_v(v_1, v_2), v_3) \leftarrow \circ_v(v_1, \circ_v(v_2, v_3))$
		$B \cdot (132)$	$\circ_v(\circ_v(v_1, v_3), v_2) \leftarrow \circ_v(v_1, \hat{\circ}_v(v_2, v_3))$
		$B \cdot (213)$	$\circ_v(\hat{\circ}_v(v_1, v_2), v_3) \leftarrow \hat{\circ}_v(\circ_v(v_1, v_3), v_2)$
		$B \cdot (231)$	$\hat{\circ}_v(\hat{\circ}_v(v_1, v_3), v_2) \leftarrow \hat{\circ}_v(v_1, \circ_v(v_2, v_3))$
		$B \cdot (312)$	$\hat{\circ}_v(\circ_v(v_1, v_2), v_3) \leftarrow \circ_v(\hat{\circ}_v(v_1, v_3), v_2)$
		$B \cdot (321)$	$\hat{\circ}_v(\hat{\circ}_v(v_1, v_2), v_3) \leftarrow \hat{\circ}_v(v_1, \hat{\circ}_v(v_2, v_3))$
Third-wheel:		$T \cdot (123)$	$\otimes_h(\circ_v(v_1, v_2), v_3) \leftarrow \circ_v(v_1, \otimes_h(v_2, v_3)), \circ_v(\otimes_h(v_1, v_3), v_2)$
		$T \cdot (132)$	$\circ_v(\otimes_h(v_1, v_2), v_3) \leftarrow \otimes_h(\circ_v(v_1, v_3), v_2), \circ_v(v_1, \otimes_h(v_2, v_3))$
		$T \cdot (213)$	$\otimes_h(\hat{\circ}_v(v_1, v_2), v_3) \leftarrow \hat{\circ}_v(v_1, \otimes_h(v_2, v_3)), \hat{\circ}_v(\otimes_h(v_1, v_3), v_2)$
		$T \cdot (231)$	$\circ_v(\otimes_h(v_1, v_2), v_3) \leftarrow \otimes_h(v_1, \circ_v(v_2, v_3)), \hat{\circ}_v(\otimes_h(v_1, v_3), v_2)$
		$T \cdot (312)$	$\hat{\circ}_v(\otimes_h(v_1, v_2), v_3) \leftarrow \otimes_h(\hat{\circ}_v(v_1, v_3), v_2), \hat{\circ}_v(v_1, \otimes_h(v_2, v_3))$
		$T \cdot (321)$	$\hat{\circ}_v(\otimes_h(v_1, v_2), v_3) \leftarrow \otimes_h(v_1, \hat{\circ}_v(v_2, v_3)), \circ_v(\otimes_h(v_1, v_3), v_2)$
Ass. of \otimes_h :		$A \cdot (123), \dots, A \cdot (321)$	$\otimes_h(\otimes_h(v_1, v_2), v_3) \leftarrow \otimes_h(\otimes_h(v_1, v_3), v_2), \otimes_h(v_1, \otimes_h(v_2, v_3))$

simple unique minimal shuffle tree monomial encoding any wheel-free graph (Construction 6.5.2).

Definition 6.4.1. Let α, β be two tree monomials of $F_{sh}(E)$, we define $\alpha \leq \beta$ if:

- (1) The arity of $\alpha < \beta$
- (2) Or, if all the prior are equal, then compare $P^\alpha < P^\beta$ where
 - if α and β have arity n then $P^\alpha := (P_1^\alpha, \dots, P_n^\alpha)$, where P_i^α is the word formed out of the generators when stepping from the i th input to the root in the tree monomial α .
 - P^α and P^β are compared lexicographically, and two paths are compared only by degree (symbols ignored).
- (3) Or, if all the prior are equal, then compare the **input permutations** (not the permutations of the generators) of the shuffle tree monomials via lexicographic order.
- (4) Or, if all the prior are equal, then compare the permutations of the generators with condition 4 of Definition 5.4.1.

(5) Or, if all the prior are equal, then we again compare $P^\alpha < P^\beta$ lexicographically, this time with a total order on generators.

- $\otimes_h < \circ_v < \hat{\circ}_v$
- if the composition type is the same then the permutations are compared with, $\binom{\sigma}{\tau} \leq \binom{\sigma'}{\tau'}$ if $\sigma < \sigma'$, or $\sigma = \sigma'$ and $\tau < \tau'$
- if s and s' are identical generators symbol wise then first compare their input colours left to right, then their output colour. Input and output colours are profiles $\binom{d}{c}, \binom{b}{a} \in \mathcal{P}(\mathfrak{C})^{op} \times \mathcal{P}(\mathfrak{C})$, we say $\binom{d}{c} \leq \binom{b}{a}$ if $\underline{d} < \underline{b}$, or $\underline{d} = \underline{b}$ and $\underline{c} \leq \underline{a}$. We compare two sequences of colours using a degree lexicographic order induced by a total order on \mathfrak{C} .

Lemma 6.4.2. *The order of Definition 6.4.1 is total and admissible.*

Proof. A similar argument to Lemma 5.4.5. \square

We close this section by noting that we may use this total order on the underlying $ob(\mathcal{S}(\mathfrak{C}))$ -coloured tree monomials to order the relations of \mathbb{P}^f by the minimal element in each groupoid coloured tree monomial, and this is precisely the order used in the prior section.

6.5. The operad governing props is Koszul

This section proves that the groupoid coloured operad governing props \mathbb{P} is Koszul, before outlining how this construction can be modified to yield Koszul operads governing other similar operadic families. We shall use the same proof method as used for \mathbb{W} (in Section 5.5) with some minor combinatorial complications thrown in by the nature of props. In the prior section, we calculated an explicit presentation of the groupoid coloured shuffle operad $\mathbb{P}^f = F_{sh}^{S(\mathfrak{C})}(E)/\langle R^f \rangle$. We now apply Theorem 4.2.13, to show that \mathbb{P} is Koszul, if G is a quadratic Groebner basis for the $ob(\mathcal{S}(\mathfrak{C}))$ -coloured shuffle operad $F_{sh}^{ob(\mathcal{S}(\mathfrak{C}))}(E^{f_{\mathcal{S}(\mathfrak{C})}})/\langle G \rangle$, where $G := E_*^2 \sqcup (R^f)_*$.

Lemma 6.5.1. *Under the order of Definition 6.4.1, G is a quadratic Groebner basis for $F_{sh}^{ob(\mathcal{S}(\mathfrak{C}))}(E^{f_{\mathcal{S}(\mathfrak{C})}})/\langle G \rangle$.*

Proof. We prove this lemma as follows.

- In Construction 6.5.2, we describe an algorithm that produces a unique minimal shuffle tree monomial encoding every wheel-free graph. We then show this algorithm is well-defined in Lemma 6.5.4.
- We then prove every shuffle tree monomial which is not the unique minimal shuffle tree monomial admits a rewrite using $RS(G)$ (see Section 4.3), establishing the confluence of the rewriting system on all shuffle tree monomials. This will be accomplished by Lemma 6.5.5.

- Hence, through Proposition 4.3.4, this proves G is a Groebner basis. \square

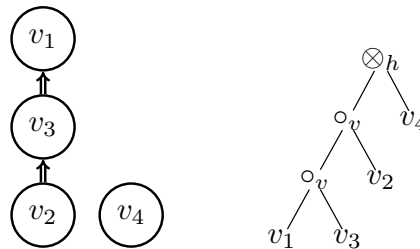
The main complication in this proof compared to wheeled props is the more complicated unique minimal form, which we now detail, before giving an illustrative example (Example 6.5.3).

Construction 6.5.2. *The following algorithm produces the unique smallest shuffle tree monomial encoding a directed cycle free graph γ with at least one vertex, we denote the outputted tree $UMF_{\uparrow}(\gamma)$.*

- Initiate $T = *_v, V = \{v\}$ and $V_R = Vertices(\gamma) \setminus \{v\}$ where v is the smallest vertex in γ .
- While there is a vertex in V_R :
 - Let v be the smallest vertex in V_R such that there does not exist a directed path (in either direction) in γ between v and a vertex in V which passes through another vertex in V_R . This can be partitioned into three cases,
 - (1) the vertex v is disconnected from V , so update $T = (\otimes_h, \binom{id}{id})(T, *_v)$
 - (2) the input flags of a vertex in V are connected to the output flags of v , so $T = (\circ_v, \binom{id}{id})(T, *_v)$
 - (3) the output flags of a vertex in V are connected to the input flags of v , so $T = (\hat{\circ}_v, \binom{id}{id})(T, *_v)$

The necessary segments of \circ_v and $\hat{\circ}_v$ may be identified from the graph γ and the graph outputted by T .
 - Update $V = V \cup \{v\}$ and $V_R = V_R \setminus \{v\}$.
- Update the permutations of the root-most operation of T (if T is not a vertex) so that the corresponding graph outputted by T has the same ordering on its open flags as γ .
- Return T .

Example 6.5.3. The algorithm applied to the following graph γ yields,



We note that there does not exist a shuffle tree monomial forming γ which contains $\otimes_h(v_1, v_2)$ as a subtree (as we would need access to a composition $\circ'(\otimes_h(v_1, v_2), v_3)$ which connects both inputs and outputs of both of its arguments). This illustrates why the restriction of the main loop of the algorithm is needed.

Lemma 6.5.4. *The unique minimal form algorithm of Construction 6.5.2 is well-defined.*

Proof. It is straightforward to verify that this algorithm produces a shuffle tree monomial that produces the graph γ (note that T_* is given the smallest vertex of the graph at initialisation, so all compositions used in the construction of T_* are valid shuffle operadic compositions). It remains to verify that the algorithm produces the minimal shuffle tree encoding γ .

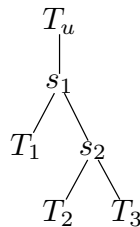
Firstly, we observe that the algorithm constructs a maximal length path from the minimal vertex to the root, i.e. our shuffle tree is ‘left aligned’. So given our shuffle tree monomial has this shape, we observe that maximising the length of the path from the next smallest vertex (and so on) is equivalent to minimising the shuffle tree monomial permutation (ordering of the vertices of the graph). Our algorithm does this by greedily picking the smallest ‘valid’ vertex. If the algorithm at any stage picked a smaller vertex by ignoring the restriction, then it would be impossible to form the graph γ from this subgraph γ_* , as illustrated in Example 6.5.3.

Finally, given our algorithm produces a left aligned shuffle tree monomial with a minimal shuffle tree permutation, this information uniquely determines the contents of each of the generators. Indeed, every generator of the shuffle tree monomial must perform a specific horizontal composition or properadic join over particular segments, and any permutations can be passed up and down the tree via the action of the groupoid. \square

Lemma 6.5.5. *Let T be a shuffle tree monomial for a direct cycle free graph γ such that $T \neq UMF_{\uparrow}(\gamma)$, then T is rewritable by G .*

Proof. Suppose that T is larger than $UMF_{\uparrow}(\gamma)$ as a result of not being normalised with respect to the action of the groupoid. Then there exists an internal edge of T which sits above a non-identity permutation. This internal edge defines a corresponding action of the groupoid which we can translate into an element of E_*^2 . This defines a corresponding rewrite (which will push the permutation up the tree). So given we have access to this rewrite for the remainder of this proof, we suppose that T is normalised with respect to the action of the groupoid.

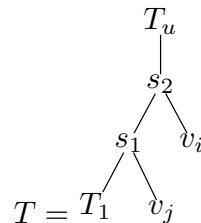
Suppose that T is larger than $UMF_{\uparrow}(\gamma)$ as a result of not having all generators on the path from the minimal vertex to the root (not being left aligned). Then T must have the following form



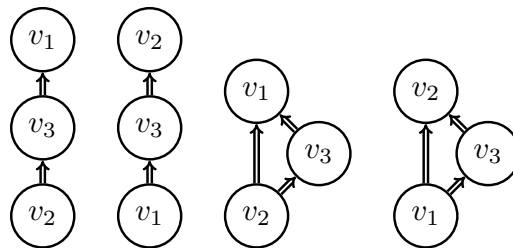
where T_1, T_2, T_3 are subtrees of T , T_u is the remainder of the tree T (close to the root), s_1, s_2 are arbitrary generators, and due to T being a shuffle tree monomial, the minimal

vertices of $T_1 < T_2 < T_3$. Let $T' = s_1(T_1, s_2(T_2, T_3))$ then the corresponding shuffle tree monomial of T' is $s_1(v_1, s_2(v_2, v_3))$. This shuffle tree monomial describes how to form a graph with 3 vertices, and as T is normalised $s_1(v_1, s_2(v_2, v_3))$ must be normalised. Observe that in the relations of \mathbb{P}^f whenever we have a shuffle tree monomial of the form $s_1(v_1, s_2(v_2, v_3))$ forming a particular graph with 3 vertices, that it appears as the leading term of a directed equation. So let g be the corresponding directed equation with $lt(g) = s_1(v_1, s_2(v_2, v_3))$, then T will admit a rewrite through the subtree T' to $r_g(T)$.

Suppose that T has all generators on the path from the minimal vertex to the root, but has a different shuffle permutation to $UMF_{\uparrow}(\gamma)$. It must be the case that T admits a decomposition of the form



where $i < j$ and there does not exist a directed path from a vertex of T_1 to v_i that passes through v_j , or a directed path from v_i to a vertex of T_1 that passes through v_j (if such a decomposition didn't exist then $T = UMF_{\uparrow}(\gamma)$). Here s_1, s_2 are arbitrary generators and T_1 and T_u are the rest of the tree T . Let $T' = s_2(s_1(T_1, v_j), v_i)$ then the corresponding shuffle tree monomial of T' is $s_2(s_1(v_1, v_3), v_2)$. This (normalised) shuffle tree monomial describes how to form a graph with three vertices subject to the condition above. The only graphs with 3 vertices that do not meet the required condition are



which correspond to $C \cdot (132), C \cdot (231), B \cdot (132)$ and $B \cdot (231)$ in Table 4. Manually inspecting the other relations of \mathbb{P}^f , we observe that for every other graph with 3 vertices, that $s_2(s_1(v_1, v_3), v_2)$ only appears as the leading term of directed equations. So for the corresponding g with leading term $s_2(s_1(v_1, v_3), v_2)$, the tree T will admit a rewrite through the subtree T' to $r_g(T)$. \square

6.6. Applying these techniques to other operadic structures

The construction of this section can be easily specialised to provide Koszul operads governing di-ops (dioperadic composition + horizontal composition) or ops (operadic composition + horizontal composition). This follows from observing that dioperadic composition is an obvious restriction of properadic composition, and hence we can restrict

the alternate biased definition of a prop Definition 6.1.2 into alternate biased definitions of these structures (with the axioms restricted in the obvious ways). These new biased definitions then induce quadratic presentations of their operads. The restriction of the total order of Definition 6.4.1 then provides the exact same unique minimal shuffle tree monomials governing these (restricted) directed cycle free graphs as that provided by Construction 6.5.2. Then as non-minimal trees admit rewrites (Lemma 6.5.5) this proves the restricted operads are Koszul.

A less straightforward specialisation is the construction of a Koszul operad governing properads, here is a brief outline. The alternate biased definition of a prop with its horizontal composition removed provides an alternate definition of a properad and hence a quadratic presentation of the operad governing properads (Remark 6.1.5). The corresponding shuffle operad is an obvious restriction of the shuffle operad for props, with no third wheel, no associativity of \otimes_h and no ways to form fireworks/lighthouse with \otimes_h . If we apply the restriction of the total order of Definition 6.4.1, then we obtain a new unique minimal (properadic) shuffle tree monomial forming any connected directed cycle free graph. Then, proving that any non-minimal shuffle tree monomial admits a rewrite reproves (see Section 1) that the operad governing properads is Koszul. Dioperads and operads can then be obtained as a further specialisation of this construction.

We note that there is no easy way to specialise the construction of a Koszul operad governing wheeled props into Koszul operads governing connected wheeled operadic structures, e.g. wheeled properads. This is because wheeled props form dioperadic joins by horizontal composition then contractions. The overall methodology of this paper however can still be applied starting from an alternate biased definition of a wheeled properad that uses extended dioperadic compositions and extended contractions. We don't repeat this construction, as it is a known result (see Section 1). Other potential targets for the methods of this paper include disconnected/Schwarz modular operads [28], and multi-oriented props [36]. We note that [28] subsequently developed distributive rewriting techniques for groupoid coloured operads to prove the operad governing disconnected modular operads is Koszul. This distributive specialisation can also be used to study the operad governing wheeled props, but not the operad governing props, as \circ_v and \otimes_h are non-distributive (see for instance the lighthouse relation of Table 3).

7. Homotopy (wheeled) props

Given the operads \mathbb{W} and \mathbb{P} are Koszul (Definition 3.6.7), we immediately obtain the following corollary.

Corollary 7.0.1.

- (1) $\mathbb{W}_\infty := \Omega(\mathbb{W}^i)$ is a (quadratic) minimal model for \mathbb{W} .
- (2) $\mathbb{P}_\infty := \Omega(\mathbb{P}^i)$ is a (quadratic) minimal model for \mathbb{P} .

As such, we define a **homotopy (wheeled) prop** to be an algebra over \mathbb{P}_∞ (respectively, \mathbb{W}_∞). This includes non-trivial examples such as,

- The homology of (wheeled) props, as shown in Section 7.2.
- The weakly vertically associative (wheeled) props of [56].
- The completions of virtual and welded tangles are examples of homotopy wheeled props ([11], [12]). These structures permit a topological characterisation of the Kashiwara-Vergne groups.

In this section, we unpack what it means to be a homotopy (wheeled) prop. We also show in Section 7.1, that we cannot use polytopes to describe these homotopy (wheeled) props, in a clear departure from the theory of connected operadic structures. Finally, we close this paper by exploring consequences of homotopy transfer theory on these structures (Section 7.2).

We first seek to understand the minimal models. The cobar construction (Definition 3.6.5) yields,

$$\Omega(\mathbb{W}^i) = (F(s^{-1}\mathbb{W}^i), d), \quad \Omega(\mathbb{P}^i) = (F(s^{-1}\mathbb{P}^i), d)$$

where the differentials are given by the cooperadic expansion of the Koszul dual cooperads \mathbb{W}^i and \mathbb{P}^i . We now unpack what this entails for \mathbb{W}_∞ , and similar reasoning works for \mathbb{P}_∞ . The differential d of $\Omega(\mathbb{W}^i)$ will be induced by understanding how the cooperadic expansion into two pieces $\Delta_{(1)} : \mathbb{W}^i \rightarrow \mathbb{W}^i \otimes \mathbb{W}^i$, also known as the **infinitesimal decomposition**, acts on the basis elements of \mathbb{W}^i . If $\mu \in \mathbb{W}^i$, then we will denote the image of μ under the infinitesimal decomposition map by $\Delta_{(1)}(\mu) = \sum (\mu_{(1)} \circ_i \mu_{(2)})\sigma$. Recall from Definition 3.6.3, that the Koszul dual cooperad \mathbb{W}^i is universal amongst the sub-cooperads C of $F^c(sE)$ such that following composite is 0.

$$C \hookrightarrow F^c(sE) = F(sE) \twoheadrightarrow F(sE)^{(2)}/s^2R$$

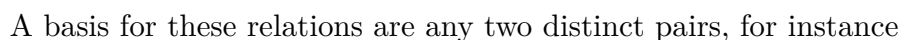
That is to say, $\mathbb{W}^{i(1)} = E$, $\mathbb{W}^{i(2)} = R$ and higher degree elements of \mathbb{W}^i are all in the ideal of R . An algebra over \mathbb{W}_∞ is a morphism of groupoid coloured operads $\varphi : W_\infty \rightarrow \text{End}_A$. As such, a homotopy wheeled prop will be a family of graded vector spaces $A\left(\frac{d}{\underline{c}}\right)_{(\frac{d}{\underline{c}}) \in \mathcal{P}(\mathfrak{C})^{op} \times \mathcal{P}(\mathfrak{C})}$ together with operations,

$$m_\gamma : A\left(\frac{d_1}{\underline{c}_1}\right) \otimes \dots \otimes A\left(\frac{d_k}{\underline{c}_k}\right) \rightarrow A\left(\frac{d}{\underline{c}}\right)$$

where $m_\gamma = \varphi(\mu_\gamma)$, and μ_γ is a basis element of \mathbb{W}^i . This tells us, each operation will be compatible with the groupoid $\mathcal{P}(\mathfrak{C})^{op} \times \mathcal{P}(\mathfrak{C})$, i.e. they will admit left, right and Σ_k actions by translating across the actions of \mathbb{W} . The decomposition $\Delta_{(1)}(\mu_\gamma) = \sum (\mu_{\gamma_1} \circ_i \mu_{\gamma_2})\sigma$, will induce relations of the form

In particular, we know that the following operations and relations will be present,

- There will be differentials, i.e. degree -1 operations $d_1 : A(\underline{d}) \rightarrow A(\underline{c})$ such that $d_1^2 = 0$.
- There will be degree 0 operations for each generator of the operad \mathbb{W} that satisfy $\partial_A(m_\gamma) = 0$.
- There will be operations of degree 1 , witnessing that each relation holds up to homotopy. Here is an example that illustrates a potential subtlety. For the operad \mathbb{P} , this particular lighthouse graph witnesses the following relations.



Under this choice of basis, the relations yield operators $m_{r_1}, m_{r_2} : A\left(\frac{d_1}{c_1}\right) \otimes A\left(\frac{d_2}{c_2}\right) \otimes A\left(\frac{d_3}{c_3}\right) \rightarrow A\left(\frac{d}{c}\right)$. In this example,

where e_2 is the generator that performs $\circ_v(v_1, v_2)$ in the context of γ , and e_1 is the generator that takes the output of e_2 together with v_3 and forms γ . Note that individually each m_{r_i} witness a homotopy between two terms, but together they witness homotopies between three terms.

$$Com = F(\begin{array}{c} \diagup \\ 1 \end{array} \begin{array}{c} \diagdown \\ 2 \end{array} = \begin{array}{c} \diagdown \\ 2 \end{array} \begin{array}{c} \diagup \\ 1 \end{array}) / \langle \begin{array}{c} \diagup \\ 1 \end{array} \begin{array}{c} \diagdown \\ 2 \end{array} \begin{array}{c} \diagup \\ 3 \end{array} - \begin{array}{c} \diagdown \\ 1 \end{array} \begin{array}{c} \diagup \\ 2 \end{array} \begin{array}{c} \diagdown \\ 3 \end{array} \rangle.$$

Proposition 7.0.2. *The commutative operad is isomorphic to suboperads of both \mathbb{W} and \mathbb{P} .*

Proof. Observe that $\mathbb{W}((\emptyset), (\emptyset); (\emptyset))$ and $\mathbb{P}((\emptyset), (\emptyset); (\emptyset))$ only contain a single basis element $(\otimes_h, (id_\emptyset))$. We can graphically interpret this basis element as the graph with two vertices, neither of which has any inputs or outputs, and consequently the graph has no inputs or outputs. Furthermore, we can observe either directly from the biequivariance axiom of horizontal composition (Definition 5.1.2), or from the following graphical argument, that the Σ_2 action on $(\otimes_h, (id_\emptyset))$ is trivial.

$$(\otimes_h, (id_\emptyset)) \cdot (21) = \begin{array}{c} \bigcirc \\ v_1 \end{array} \begin{array}{c} \bigcirc \\ v_2 \end{array} \cdot (21) = \begin{array}{c} \bigcirc \\ v_2 \end{array} \begin{array}{c} \bigcirc \\ v_1 \end{array} = \begin{array}{c} \bigcirc \\ v_1 \end{array} \begin{array}{c} \bigcirc \\ v_2 \end{array} = (\otimes_h, (id_\emptyset)).$$

Equality two follows as the action of the symmetric group on the graph switches the label of the two vertices, and equality three follows from the definition of a graph (Definition 2.2.1), see also Example 5.2.1.

Let \mathbb{H} be the suboperad of both \mathbb{W} and \mathbb{P} generated by $(\otimes_h, (id_\emptyset))$. We observe that \mathbb{H} will satisfy the horizontal associativity relation (Row 1 of Table 1, or equivalently the horizontal associativity axiom of Definition 5.1.2), and will satisfy no further relations, as all other relations of \mathbb{W} and \mathbb{P} involve either contractions or properadic compositions. In addition, we observe that we no longer need to use the full groupoid $\mathcal{S}(\mathfrak{C}) := \mathcal{P}(\mathfrak{C})^{op} \times \mathcal{P}(\mathfrak{C})$ to describe \mathbb{H} but rather only $\emptyset^{op} \times \emptyset$ which is a single object discrete category, and hence isomorphic to $\mathbf{1}$. Thus, the generating groupoid coloured modules of Com and \mathbb{H} are isomorphic (Definition 2.1.4), through the isomorphism of groupoids $f_0 : \mathbf{1} \rightarrow \emptyset^{op} \times \emptyset$, and the compatible bijective map of generators $f_1(\wedge) := (\otimes_h, (id_\emptyset))$. Hence, Com and \mathbb{H} are isomorphic as groupoid coloured operads.

We note that the graphical interpretation of the sole basis element in each $\mathbb{H}((\emptyset)^n; (\emptyset))$ is the graph with n vertices, none of which have any inputs or outputs. This basis element has a trivial Σ_n action, as permuting the labels of these vertices will not produce a new graph (Definition 2.2.1). \square

It is a classical result that the commutative operad is Koszul, and that its Koszul dual is Lie, i.e. Com^i is the co-Lie cooperad. When we construct the minimal model of Com using the (un coloured) Koszul machine $C_\infty := \Omega(Com^i)$, the associativity relation is relaxed up to homotopy, and commutativity continues to hold strictly. As such, a C_∞ algebra can be regarded as an A_∞ algebra with the additional property that the operations are trivial on skew-symmetric shuffle products (see Proposition 13.1.6 of [33], and Example 3.134 of [41]). Explicitly, they satisfy relations such as:

$$\begin{aligned} m_2(\alpha, \beta) - (-1)^{|\alpha||\beta|} m_2(\beta, \alpha) &= 0 \\ m_3(\alpha, \beta, \gamma) - (-1)^{|\alpha||\beta|} m_3(\beta, \alpha, \gamma) + (-1)^{|\alpha|(|\beta|+|\gamma|)} m_3(\beta, \gamma, \alpha) &= 0 \\ m_3(\alpha, \beta, \gamma) - (-1)^{|\beta||\gamma|} m_3(\alpha, \gamma, \beta) + (-1)^{(|\alpha|+|\beta|)|\gamma|} m_3(\gamma, \alpha, \beta) &= 0. \end{aligned}$$

Analogous relations hold in higher degree. The inclusion of Com into both \mathbb{W} and \mathbb{P} tells us these relations will hold (up to inclusion) in algebras over \mathbb{W}_∞ and \mathbb{P}_∞ . Consequently,

these structure will satisfy appropriately generalised versions of the prior relations, once one accounts for the presence of the contraction operators for \mathbb{W} , and the properadic compositions for \mathbb{P} .

A ‘simple combinatorial model’ for homotopy (wheeled) props is beyond the scope of this paper. However, it is straightforward to perform low dimensional computations, as the following examples show. These calculations will also act as counter examples in the next section.

Example 7.0.3. Recall from Table 1, that in the operad \mathbb{W} , the followings graphs encode relations in $R = \mathbb{W}^{i(2)}$, and thus the corresponding infinitesimal decompositions.

Graph	Encodes Relation r	$\Delta_{(1)}(r)$

We use the graph $\gamma = \text{graph with } v_1 \text{ and } v_2 \text{ connected by a blue edge, and } v_1 \text{ has a red self-loop}$, to encode $\alpha - \beta \in \mathbb{W}^i$, where α, β are any two elements of

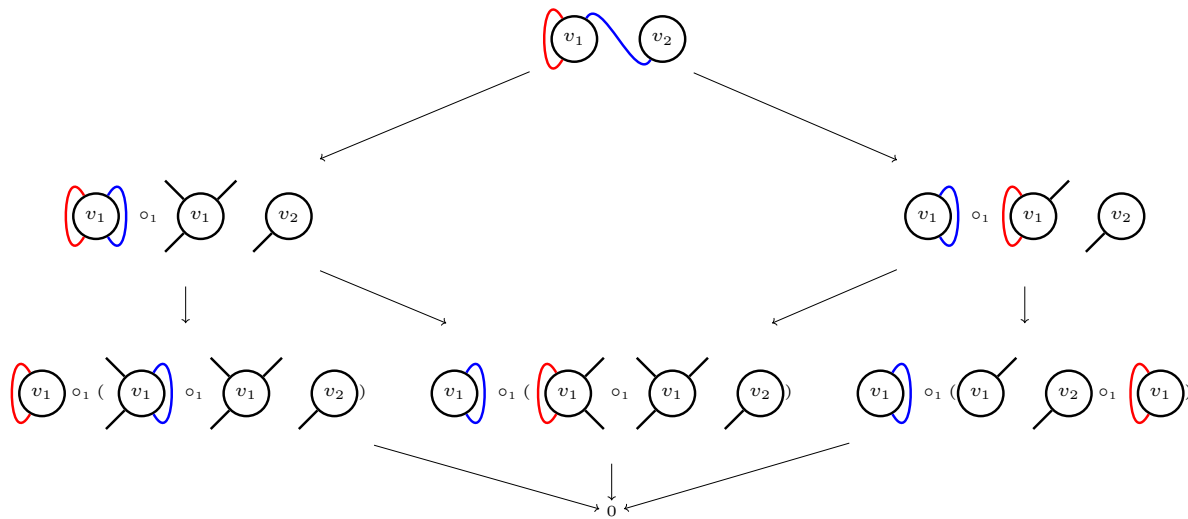
$$\text{tree monomial with root } v_1 \text{ and child } v_2 = \text{tree monomial with root } v_1 \text{ and child } v_2 = \text{tree monomial with root } v_1 \text{ and child } v_2$$

We calculate,

$$\Delta_{(1)}(\text{graph } \gamma) = \pm \text{graph with } v_1 \text{ and } v_2 \text{ connected by a blue edge, and } v_1 \text{ has a red self-loop} \circ_1 \text{graph with } v_1 \text{ and } v_2 \text{ connected by a blue edge, and } v_1 \text{ has a red self-loop} \pm \text{graph with } v_1 \text{ and } v_2 \text{ connected by a blue edge, and } v_1 \text{ has a red self-loop} \circ_1 \text{graph with } v_1 \text{ and } v_2 \text{ connected by a blue edge, and } v_1 \text{ has a red self-loop}$$

The first term arises from cutting the first two tree monomials under the blue¹ unary contraction, the second term arises from cutting the last two terms under the contractions/(above the binary fork). Encoding successive calculations via diagram, we compute the subcomplex generated by $\alpha - \beta$,

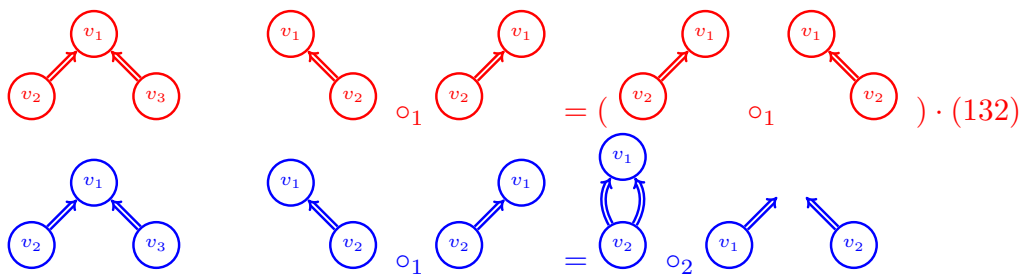
¹ For interpretation of the references to color please refer to the web version of this article.



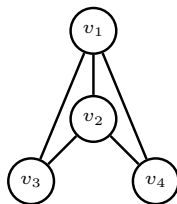
Where the image of the infinitesimal decomposition of a particular term (up to signs), is given by the target of all arrows whose source is that term. Note the bracketing on the third line can be rearranged using the associativity of operadic composition. We emphasise:

The bargraph $\begin{array}{c} \textcircled{v_1} \\ \textcircled{v_2} \end{array}$ never appears in the diagram, as it encodes no relation in \mathbb{W}^i .

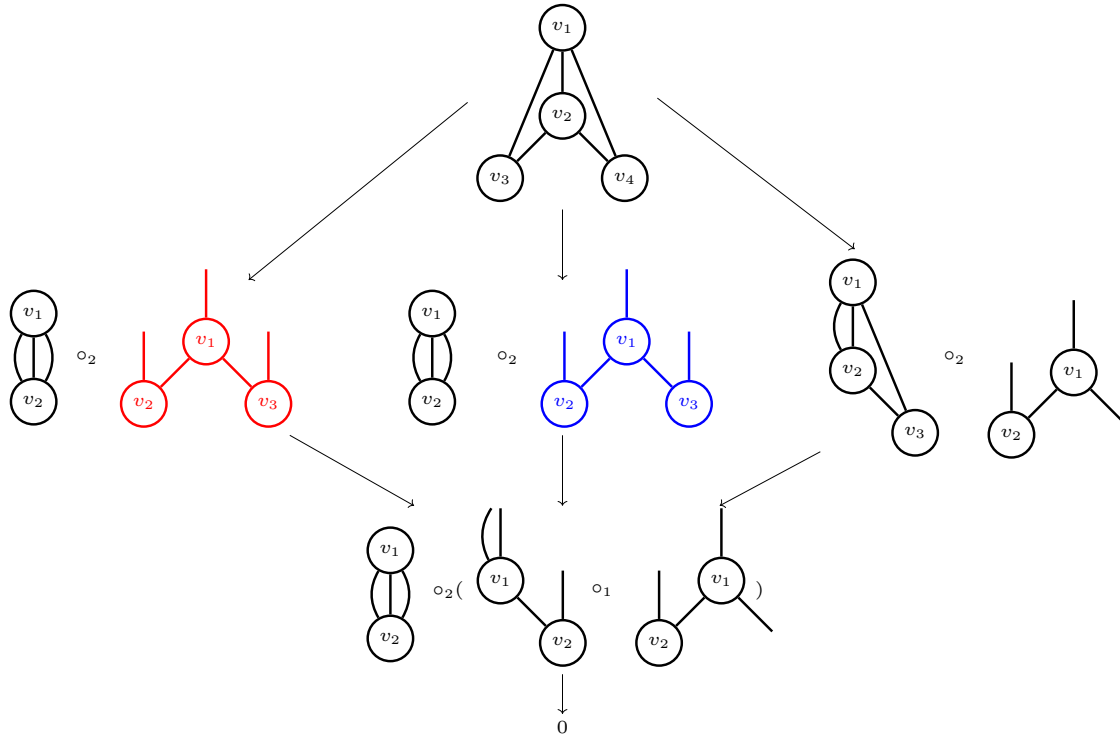
Example 7.0.4. Let red and blue lighthouse graphs, provide a graphical encoding of our choice of basis for the lighthouse relations,



In terms of Eq. (10), the red relation is r_1 , and the blue relation is r_2 . Then, let $\alpha - \beta \in \mathbb{P}^{i(3)}$, be any two terms of \mathbb{P} which generate the following graph.



We partially compute a portion of the subcomplex generated by $\alpha - \beta$, using the notation of the prior example. We have omitted many elements of the subcomplex for brevity.



7.1. Nesting models and polytope based techniques

The minimal models of the Koszul operads governing connected operadic structures all have polytope based interpretations ([4], [27], [29], [55]), however this no longer holds true for (wheeled) props.

Theorem 7.1.1. *There exist subcomplexes of \mathbb{W}_∞ and \mathbb{P}_∞ which are **not** isomorphic as lattices, to the face poset of convex polytopes.*

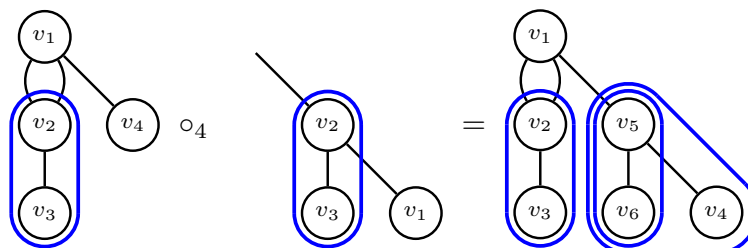
Proof. A necessary condition for a lattice to be the face poset of a convex polytope is that it meets the diamond condition (Theorem 2.7 [58]). That is to say, every interval of length two has precisely four elements, and thus looks like a diamond. Consequently, the diagrams of Examples 7.0.3 and 7.0.4, cannot be isomorphic as lattices, to the face posets of convex polytopes. This follows for \mathbb{W}_∞ , as Example 7.0.3 has an interval of length two which contain only three elements. For \mathbb{P}_∞ , we observe that Example 7.0.4 contains an interval of length 2 which has at least five elements. If another of the $\binom{3}{2,1}$ bases for the lighthouse relation is chosen (instead of Eq. (10)), then a similar counter example will be obtained. This is because every possible basis pair contains an overlapping term. \square

As \mathbb{W}_∞ and \mathbb{P}_∞ are the minimal models for \mathbb{W} and \mathbb{P} , these obstructions in homology will be present in all models for these operads. Consequently, there does not exist a polytope based nesting model for the operads governing (wheeled) props (see Section 4 of [29], for what this means for the operad governing operads).

Remark 7.1.2. The fact that these nesting complexes are not isomorphic to the face poset of convex polytopes can be interpreted as obstructions to using the techniques of [4] and [27] to prove that the operads governing (wheeled) props are Koszul. These papers use polytopes to prove these results, explicitly though the hypergraph polytopes of [5] in the first case, and implicitly through cubical Feynman categories in the second case.

Another way to see how this obstruction manifests, specifically for cubical Feynman categories, is as follows. By Definition 7.4 of [26], given the definition of \mathbb{W} , the bar graph should have degree 2, and as such, should admit a free Σ_2 action on all the ways to form the graph. However, there is only one way to form the bar graph, a horizontal composition followed by a contraction, so no such action can exist. Similarly, given the definition of \mathbb{P} , the lighthouse graph should have degree 2 for this operad, and have exactly two ways to form it, when we know there are three. The lighthouse graph was previously identified as an impediment to the existence of a cubical Feynman category for props in Figure 10. of [26].

Remark 7.1.3. Properads may be seen as props restricted to connected graphs. As outlined in Remark 6.1.5 and Section 6.6, the Koszul groupoid coloured quadratic operad governing properads \mathbb{P}^c (c for connected), consists of just the properadic generators of \mathbb{P} and its associated connected axioms. Given the work of [4], [5] and [27], it is known that \mathbb{P}^c has a polytope based nesting model, as a result of more general theory. However, it is possible to show that the specific polytope based nesting model for properads corresponds to the poset associahedra of Galashin [18]. This is a useful observation, as given the recent realisations of poset associahedra as convex polytopes, performed in [39] and [49], it is now possible to carry out the program of [29], at the level of properads. That is to say, one can define a minimal model for the operad governing properads whose groupoid coloured module consists of connected wheel-free graphs with an acyclic tubing, and whose operadic composition is given by substitution of nested/tubed graphs, e.g.



Then, by mirroring Section 4 of [29], it is possible to use this minimal model, and the realisation of the polytopes, to provide an explicit functorial tensor product of homotopy properads. This is a subject for future research.

7.2. Homotopy transfer theory

One of the main motivations for constructing Koszul operads governing (wheeled) props is to extend homotopy transfer theory (HTT) to these structures. We recall the necessary theory developed by Ward [55] in the groupoid coloured case, before deriving consequences in formality theory, and recovering a theorem of Mac Lane [37] as an instance of HTT.

Definition 7.2.1 (*Definition 2.56 [55]*). Let A, B be \mathbb{V} -modules (in $dgVect$). We say B is a **homotopy (deformation) retract** of A , if there are a family of homotopy (deformation) retracts indexed by $ob(\mathbb{V})$ such that h_v, i_v, p_v are $Aut(v)$ -equivariant.

$$h_v \hookrightarrow A(v) \begin{array}{c} \xrightarrow{p_v} \\ \xleftarrow{i_v} \end{array} B(v)$$

See for instance [33] Section 1.5.5, for the definition of a homotopy/deformation retract.

As we are operating over a field of characteristic 0, a fundamental example is

Proposition 7.2.2 (*Lemma 2.57 [55]*). For a given \mathbb{V} -module A , the homology $H(A)$ is a deformation retract of A .

From here Ward specialises HTT to this particular deformation retract, but as he points out in his proof of Theorem 2.58, the only new requirement of his extension over the uncoloured case of [33] is the equivariance of the retract.

Proposition 7.2.3 (*Generalising Theorem 2.58 [55], and Theorem 10.3.1 of [33]*). Let P be a Koszul groupoid coloured operad and A, B be \mathbb{V} -modules such that B is a homotopy retract of A . Then any P_∞ -algebra structure on A can be transferred into a P_∞ -algebra structure on B such that i extends into a ∞ -quasi-isomorphism.

Proof. Ward's specialised proof works with these slightly more general assumptions. The structure maps are then obvious alterations of those in the uncoloured case see Section 10.3 of [33], i.e. the formulae work for groupoid coloured trees given the equivariance of the retract. \square

Ward's specialisation to homology is then summarised in the following corollary.

Corollary 7.2.4 (*Theorem 2.58 [55]*). Let P be a Koszul groupoid coloured operad, and A a dg algebra over P . The homology $H(A)$ admits the structure of a P_∞ algebra, and the inclusion $i : A \rightarrow H(A)$ extends to a ∞ -quasi-isomorphism.

The higher P_∞ operations on the homology are known as **Massey products**. The existence of Massey products has applications in formality.

Definition 7.2.5 (Section 11.4.6 [33]). A dg-algebra A over a Koszul groupoid coloured operad P is said to be formal if there exists a ∞ -quasi-isomorphism of dg- P -algebras between it and its homology $H(A)$.

From this definition, it follows that a necessary condition for a dg-algebra to be formal, is for its Massey products to vanish uniformly ([10]). (If the Massey products do not vanish uniformly, then the best we could hope for would be a ∞ -quasi-isomorphism of dg- P_∞ -algebras.) In addition, given our assumptions, we also have the following result.

Proposition 7.2.6 (Proposition 11.4.10 [33]). Let P be a Koszul groupoid coloured operad and A a dg- P -algebra. If the Massey products on $H(A)$ vanish, then A is formal.

Proof. Using the extensions of Ward, the proof of [33] applies verbatim to the groupoid coloured case. \square

So, as a consequence of these results and the constructions of this paper, we have the following two results for dg (wheeled) props over a field of characteristic 0.

Corollary 7.2.7. *The homology of a (wheeled) prop admits Massey products.*

Corollary 7.2.8. *Thus, if P is a dg (wheeled) prop and A a dg- P -algebra, then*

- *if the Massey products on $H(A)$ vanish then A is formal, and*
- *if A is formal, then the Massey products on $H(A)$ vanish uniformly.*

Thus we have a new tool in the study of the formality of (wheeled) props. One wheeled prop, which is likely formal, is the category of arrow diagrams ([12]). However, in this case, it might be easier to demonstrate formality by constructing an explicit GT action (see [47] and [1]). Alternatively, it would be interesting if the non-formality of a particular (wheeled) prop could be demonstrated using these Massey products, perhaps using a similar approach to [31].

It also turns out that one of the first theorems regarding (homotopy) props can be seen as a consequence of HTT. In [37], Mac Lane defines both PROPs and PACTs (an early form of a homotopy prop). He then expounds the existence of higher homotopies for the following particular prop. Let $K(H_{fc})$ be the prop governing dg-Hopf algebras with commutative products. Let $K(H_{fcc})$ be the prop governing dg-Hopf algebras with commutative products and co-commutative co-products.

Theorem (25.1 of [37]). *If U is a $K(H_{fcc})$ algebra, then there is a PACT $P \supset K(H_{fc})$, which acts on the bar construction $B^*(U)$ and on the reduced bar construction $\overline{B}^*(U)$, and a map $\theta : P \rightarrow K(H_{fcc})$ of PACTs such that the induced homology map*

$$\theta_* : H(P) \cong H(K(H_{fcc}))$$

is an isomorphism.

He described this result as “a covert statement on the existence of higher homotopies”, then used an action of $K(H_{fcc})$ on U to induce an action on $\overline{B'}(U)$, which then induced an explicit example of a higher homotopy. However, by the constructions of this section we know that the homology of $K(H_{fcc})$ is a homotopy prop, with higher homotopies corresponding to the Massey products. Furthermore, the higher homotopies identified by Mac Lane must at least be ∞ -isomorphic to the Massey products (see Theorem 10.3.10 of [33]).

Remark 7.2.9. Having access to homotopy transfer theory for (wheeled) props provides an alternate pathway to the deformation theory of these structures (for instance, for props see [42], [43], and for wheeled props see [1], [38], [35]). In particular, given that \mathbb{W} and \mathbb{P} are now known to be Koszul, the HTT techniques of Section 12.2 of [33] can also be applied. We note that this potential approach to defining homotopy props, and studying their deformations, was already suggested in a remark in Section 4.1 of [42]. We note that some care should be taken when comparing the results of this paper to theirs, as their graphical definition of a homotopy prop, introduced in Section 4.3, strictifies to a different notion of a prop than the one employed in this paper. This can be seen as their notion of an admissible subgraph of a connected graph provides no means of forming a connected graph via disconnected subgraphs (i.e. through use of horizontal composition).

8. Appendix: axioms of an alternate prop

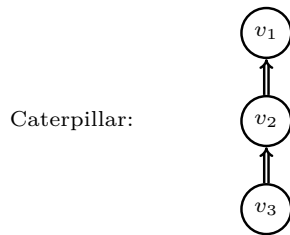
In presenting Definition 6.1.2, we chose to encode the non-unital and non-biequivariance axioms of the definition graphically in Table 3. We now formally write out these axioms for the interested reader. We will first introduce some simplifying terminology.

Let $\underline{c}', \underline{c}''$ be two disjoint subsequences of \underline{c} , which both admit the reduction of the order of \underline{c} . Then there exists a unique way to merge them into a subsequence of \underline{c} (which also admits the reduction of the order of \underline{c}), which we denote $m(\underline{c}', \underline{c}'')$. In other words, there exists a unique permutation σ_m such that $m(\underline{c}', \underline{c}'') = (\underline{c}', \underline{c}'')\sigma_m$. Then, if in addition we have disjoint subsequences of \underline{b} say $\underline{b}', \underline{b}''$ such that $(\underline{c}', \underline{c}'') = (\underline{b}', \underline{b}'')$ then we also reorder these sequences by the **same** permutation σ_m , and in an abuse of notation, denote this reordering

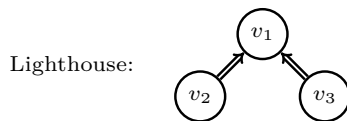
$$\begin{pmatrix} m(\underline{c}', \underline{c}'') \\ m(\underline{b}', \underline{b}'') \end{pmatrix} := \begin{pmatrix} (\underline{c}', \underline{c}'')\sigma_m \\ (\underline{b}', \underline{b}'')\sigma_m \end{pmatrix}$$

To ease readability, we make use of the following conventions. For each commutative diagram, we shall include the corresponding graph behind the axiom. These graphs each have 3 vertices v_1, v_2, v_3 with respective profiles $\begin{pmatrix} f \\ e \end{pmatrix}$, $\begin{pmatrix} d \\ c \end{pmatrix}$ and $\begin{pmatrix} b \\ a \end{pmatrix}$. We shall use primes to indicate dis-contiguous sub-profiles, if a profile \underline{e} has multiple sub-profiles then we

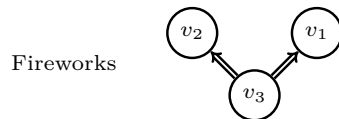
will use \underline{e}' to refer to the sub-profile associated to the join to the smallest neighbouring vertex, and \underline{e}'' for the other sub-profile. Any equalities satisfied by these sub-profiles are informed by the diagrams. We will also suppose that all input sub-profiles have the same respective order as their enveloping profile. For instance, the caterpillar diagram has sub-profiles $\underline{b}', \underline{c}', \underline{d}', \underline{e}'$, they satisfy $\underline{c}' = \underline{b}'$, and $\underline{e}' = \underline{d}'$, and the orders on $\underline{c}', \underline{e}'$ are the restriction of the orders on $\underline{c}, \underline{e}$ respectively. Any permutations present on the commutative diagram are assumed to be such that the concrete assignments of the final profile $\left(\frac{g}{h}\right)$ (as defined by the arrows) are all equal.



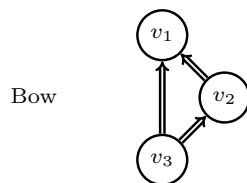
$$\begin{array}{ccc} P(\underline{f}_{\underline{e}}) \otimes P(\underline{d}_{\underline{c}}) \otimes P(\underline{b}_{\underline{a}}) & \xrightarrow{\circ(\underline{e}'), (id) \otimes id} & P(\underline{f}_{\underline{e}}) \otimes P(\underline{d}_{\underline{a}, \underline{c} \setminus \underline{e}'}) \\ \downarrow \circ(\underline{e}'), (id) \otimes id & & \downarrow \circ(\underline{e}'), (\sigma_1) \otimes id \\ P(\underline{f}_{\underline{c}, \underline{e} \setminus \underline{e}'} \setminus \underline{d}') \otimes P(\underline{b}_{\underline{a}}) & \xrightarrow{\circ(\underline{e}'), (\sigma_2)} & P(\underline{g}_{\underline{h}}) \end{array}$$



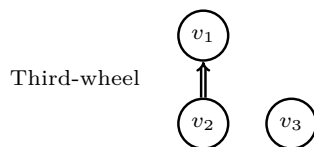
$$\begin{array}{ccc} P(\underline{f}_{\underline{e}}) \otimes P(\underline{d}_{\underline{c}}) \otimes P(\underline{b}_{\underline{a}}) & \xrightarrow{id \otimes (\otimes_h, (id))} & P(\underline{f}_{\underline{e}}) \otimes P(\underline{d}_{\underline{c}, \underline{a}}) \\ \downarrow \circ(\underline{e}'), (id) \otimes id & & \downarrow \circ(\underline{e}'), (\sigma_1) \otimes id \\ P(\underline{f}_{\underline{c}, \underline{e} \setminus \underline{e}'} \setminus \underline{d}') \otimes P(\underline{b}_{\underline{a}}) & \xrightarrow{\circ(\underline{e}'), (\sigma_2)} & P(\underline{g}_{\underline{h}}) \end{array}$$



$$\begin{array}{ccc} P(\underline{f}_{\underline{e}}) \otimes P(\underline{d}_{\underline{c}}) \otimes P(\underline{b}_{\underline{a}}) & \xrightarrow{id \otimes (\otimes_h, (id)) \otimes id} & P(\underline{f}_{\underline{e}}) \otimes P(\underline{d}_{\underline{c}, \underline{a}}) \\ \downarrow id \otimes \circ(\underline{e}'), (id) \otimes id & & \downarrow \circ(\underline{e}'), (\sigma_1) \otimes id \\ P(\underline{f}_{\underline{e}}) \otimes P(\underline{d}_{\underline{a}, \underline{c} \setminus \underline{e}'} \setminus \underline{b}') & \xrightarrow{\circ(\underline{e}'), (\sigma_2)} & P(\underline{g}_{\underline{h}}) \end{array}$$



$$\begin{array}{ccc} P(\underline{f}_{\underline{e}}) \otimes P(\underline{d}_{\underline{c}}) \otimes P(\underline{b}_{\underline{a}}) & \xrightarrow{\circ(\underline{e}'), (id) \otimes id} & P(\underline{f}_{\underline{e}}) \otimes P(\underline{d}_{\underline{a}, \underline{c} \setminus \underline{e}'}) \\ \downarrow \circ(\underline{e}'), (id) \otimes id & & \downarrow \circ(\underline{e}'), (\sigma_1) \otimes id \\ P(\underline{f}_{\underline{c}, \underline{e} \setminus \underline{e}'} \setminus \underline{d}') \otimes P(\underline{b}_{\underline{a}}) & \xrightarrow{\circ(\underline{e}'), (\sigma_2)} & P(\underline{g}_{\underline{h}}) \end{array}$$



$$\begin{array}{ccc} P(\underline{f}_{\underline{e}}) \otimes P(\underline{d}_{\underline{c}}) \otimes P(\underline{b}_{\underline{a}}) & \xrightarrow{id \otimes (\otimes_h, (id))} & P(\underline{f}_{\underline{e}}) \otimes P(\underline{d}_{\underline{c}, \underline{a}}) \\ \downarrow \circ(\underline{e}'), (id) \otimes id & & \downarrow \circ(\underline{e}'), (\sigma_1) \otimes id \\ P(\underline{f}_{\underline{c}, \underline{e} \setminus \underline{e}'} \setminus \underline{d}') \otimes P(\underline{b}_{\underline{a}}) & \xrightarrow{(\otimes_h, (\sigma_2))} & P(\underline{g}_{\underline{h}}) \end{array}$$

References

- [1] A. Andersson, S. Merkulov, From deformation theory of wheeled props to classification of Kontsevich formality maps, *Int. Math. Res. Not.* 2022 (12) (2022) 9275–9307, arXiv:1911.09089.
- [2] M.R. Bremner, V. Dotsenko, *Algebraic Operads: an Algorithmic Companion*, CRC Press, 2016.

- [3] M. Batanin, J. Kock, M. Weber, Regular patterns, substitutes, Feynman categories and operads, *Theory Appl. Categ.* 33 (7) (2018) 148–192, arXiv:1510.08934.
- [4] M. Batanin, M. Markl, Koszul duality for operadic categories, *Compositionality* 5 (4) (2023) 56, arXiv:2105.05198.
- [5] M. Batanin, M. Markl, J. Obradović, Minimal models for graph-related (hyper) operads, *J. Pure Appl. Algebra* (2023) 107329, arXiv:2002.06640.
- [6] S. Barkan, J. Steinebrunner, The equifibered approach to infinity-properads, arXiv preprint arXiv:2211.02576, 2022.
- [7] J.M. Boardman, R.M. Vogt, *Homotopy Invariant Algebraic Structures on Topological Spaces*, vol. 347, Springer, 2006.
- [8] G. Caviglia, The Dwyer-Kan model structure for enriched coloured PROPs, arXiv preprint arXiv:1510.01289, 2015.
- [9] D.-C. Cisinski, I. Moerdijk, Dendroidal sets and simplicial operads, *J. Topol.* 6 (3) (2013) 705–756, arXiv:1109.1004.
- [10] P. Deligne, P. Griffiths, J. Morgan, D. Sullivan, Real homotopy theory of Kähler manifolds, *Invent. Math.* 29 (1975) 245–274.
- [11] Z. Dancso, I. Halacheva, M. Robertson, Circuit algebras are wheeled props, *J. Pure Appl. Algebra* 225 (12) (2021) 106767, arXiv:2009.09738.
- [12] Z. Dancso, I. Halacheva, M. Robertson, A topological characterisation of the Kashiwara–Vergne groups, *Trans. Amer. Math. Soc.* (2023), arXiv:2106.02373.
- [13] N. Dershowitz, J.-P. Jouannaud, Rewrite systems, in: *Formal Models and Semantics*, Elsevier, 1990, pp. 243–320.
- [14] V. Dotsenko, A. Khoroshkin, Gröbner bases for operads, *Duke Math. J.* 153 (2) (2010) 363–396, arXiv:0812.4069.
- [15] V. Dotsenko, A. Khoroshkin, Quillen homology for operads via Gröbner bases, *Doc. Math.* 18 (2013) 707–747, arXiv:1203.5053.
- [16] H. Derksen, V. Makam, Invariant theory and wheeled props, *J. Pure Appl. Algebra* (2023) 107302, arXiv:1909.00443.
- [17] B. Day, R. Street, Abstract substitution in enriched categories, *J. Pure Appl. Algebra* 179 (1–2) (2003) 49–63.
- [18] P. Galashin, P-associahedra, arXiv preprint arXiv:2110.07257, 2021.
- [19] E. Getzler, Operads revisited, in: *Algebra, Arithmetic, and Geometry: Volume I: In Honor of Yu. I.*, 2009, pp. 675–698, arXiv:math/0701767.
- [20] J. Granåker, Strong homotopy properads, *Int. Math. Res. Not.* 2007 (9) (2007) rnm044, arXiv:math/0611066.
- [21] R. Haugseng, J. Kock, Infinity operads as symmetric monoidal infinity categories, *Publ. Mat.* 68 (1) (2024) 111–137, arXiv:2106.12975.
- [22] E. Hoffbeck, A Poincaré–Birkhoff–Witt criterion for Koszul operads, *Manuscripta Math.* 131 (1) (2010) 87–110, arXiv:0709.2286.
- [23] P. Hackney, M. Robertson, The homotopy theory of simplicial props, *Israel J. Math.* 219 (2) (2017) 835–902, arXiv:1209.1087.
- [24] P. Hackney, M. Robertson, D. Yau, *Infinity Properads and Infinity Wheeled Properads*, vol. 2147, Springer, 2015.
- [25] V. Kharitonov, A. Khoroshkin, Gröbner bases for coloured operads, *Ann. Mat. Pura Appl.* (4) 201 (1) (2022) 203–241, arXiv:2008.05295.
- [26] R. Kaufmann, B. Ward, *Feynman Categories*, Asterisque Series, Société mathématique de France, 2017, arXiv:1312.1269.
- [27] R. Kaufmann, B. Ward, Koszul Feynman categories, *Proc. Amer. Math. Soc.* 151 (8) (2023) 3253–3267, arXiv:2108.09251.
- [28] R. Kaufmann, B. Ward, Schwarz modular operads revisited. arXiv preprint, arXiv:2404.17540, 2024.
- [29] G. Laplante-Anfossi, The diagonal of the operahedra, *Adv. Math.* 405 (2022) 108494, arXiv:2110.14062.
- [30] B. Le Grignou, From homotopy operads to infinity-operads, *J. Noncommut. Geom.* 11 (1) (2017) 309–365.
- [31] M. Livernet, Non-formality of the Swiss-Cheese operad, *J. Topol.* 8 (4) (2015) 1156–1166, arXiv:1404.2484.
- [32] J. Lurie, *Higher Algebra*, 2017, Preprint, available at <https://www.math.ias.edu/~lurie/>, 2016.
- [33] J.-L. Loday, B. Vallette, *Algebraic Operads*, vol. 346, Springer Science & Business Media, 2012.
- [34] M. Markl, Operads and props, *Handb. Algebr.* 5 (2008) 87–140, arXiv:math/0601129.

- [35] S. Merkulov, Wheeled props in algebra, geometry and quantization, in: European Congress of Mathematics, Eur. Math. Soc., Zürich, 2010, pp. 83–114, arXiv:0911.3321.
- [36] S. Merkulov, Multi-oriented props and homotopy algebras with branes, *Lett. Math. Phys.* 110 (6) (2020) 1425–1475, arXiv:1712.09268.
- [37] S. Mac Lane, Categorical algebra, *Bull. Amer. Math. Soc.* 71 (1) (1965) 40–106.
- [38] M. Markl, S. Merkulov, S. Shadrin, Wheeled props, graph complexes and the master equation, *J. Pure Appl. Algebra* 213 (4) (2009) 496–535, arXiv:math/0610683.
- [39] M. Chiara, A. Padrol, V. Pilaud, Acyclonestohedra: when oriented matroids meet nestohedra, 2023, in preparation.
- [40] P. Malbos, I. Ren, Shuffle polygraphic resolutions for operads, *J. Lond. Math. Soc.* 107 (1) (2023) 61–122, arXiv:2012.15718.
- [41] M. Markl, S. Shnider, J. Stasheff, *Operads in Algebra, Topology and Physics*, vol. 96, American Mathematical Society, Providence, RI, 2002.
- [42] S. Merkulov, B. Vallette, Deformation theory of representation of prop(erad)s I, *J. Reine Angew. Math.* 634 (2009) 51–106, arXiv:0707.0889.
- [43] S. Merkulov, B. Vallette, Deformation theory of representation of prop(erad)s ii, *J. Reine Angew. Math.* 636 (2009) 123–174, arXiv:0707.0889.
- [44] I. Moerdijk, I. Weiss, On inner Kan complexes in the category of dendroidal sets, *Adv. Math.* 221 (2) (2009) 343–389, arXiv:math/0701295.
- [45] M. Herman, A. Newman, On theories with a combinatorial definition of “equivalence”, *Ann. Math.* (1942) 223–243.
- [46] D. Petersen, The operad structure of admissible g-covers, *Algebra Number Theory* 7 (8) (2013) 1953–1975, arXiv:1205.0420.
- [47] D. Petersen, Minimal models, gt-action and formality of the little disk operad, *Selecta Math. (N.S.)* 20 (3) (2014) 817–822, arXiv:1303.1448.
- [48] S. Raynor, Brauer diagrams, modular operads, and a graphical nerve theorem for circuit algebras, arXiv preprint arXiv:2108.04557, 2021.
- [49] A. Sack, A realization of poset associahedra, arXiv preprint arXiv:2301.11449, 2023.
- [50] D.E. Santander, Comparing fat graph models of moduli space, arXiv preprint arXiv:1508.03433, 2015.
- [51] D. Sinha, A pairing between graphs and trees, arXiv preprint arXiv:math/0502547, 2005.
- [52] V. Tourtchine, On the other side of the bialgebra of chord diagrams, *J. Knot Theory Ramifications* 16 (05) (2007) 575–629, arXiv:math/0411436.
- [53] D. Trnka, Category-colored operads, internal operads, and Markl o-operads, *Theory Appl. Categ.* 39 (39) (2023) 874–915, arXiv:2304.02446.
- [54] P. Van der Laan, Coloured Koszul duality and strongly homotopy operads, arXiv preprint arXiv:math/0312147, 2003.
- [55] B. Ward, Massey products for graph homology, *Int. Math. Res. Not.* 2022 (11) (2022) 8086–8161, arXiv:1903.12055.
- [56] N. Wahl, C. Westerland, Hochschild homology of structured algebras, *Adv. Math.* 288 (2016) 240–307, arXiv:1110.0651.
- [57] D. Yau, M.W. Johnson, *A Foundation for PROPs, Algebras, and Modules*, vol. 203, American Mathematical Soc., 2015.
- [58] G.M. Ziegler, *Lectures on Polytopes*, vol. 152, Springer Science & Business Media, 2012.

CELLULAR DIAGONALS OF PERMUTAHEDRA

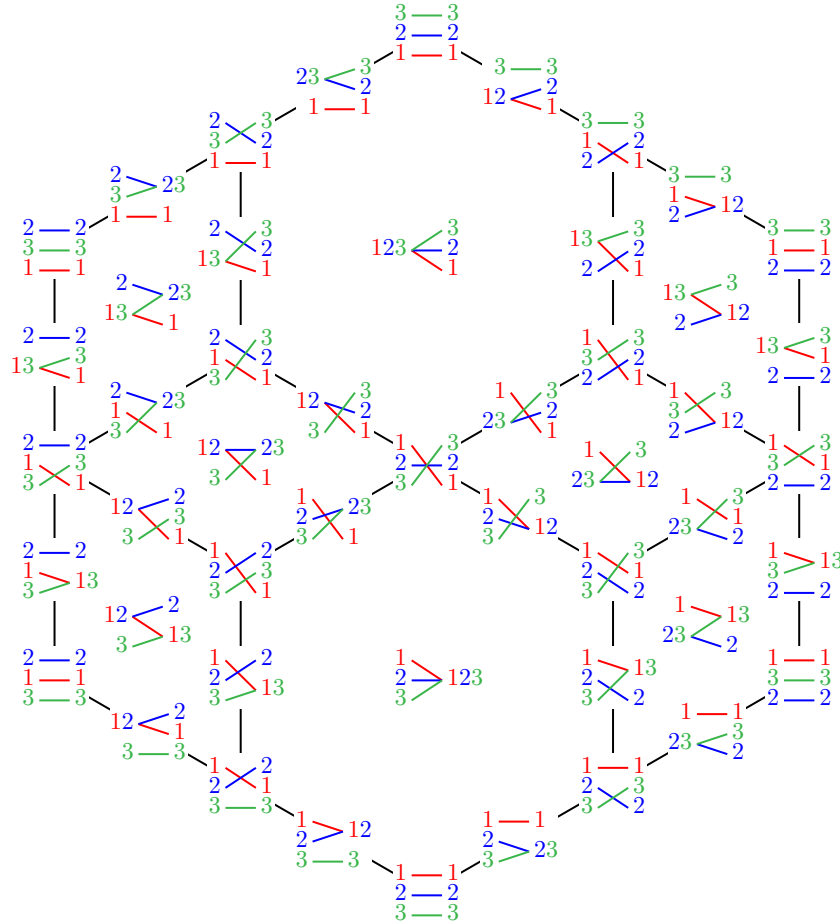
BÉRÉNICE DELCROIX-OGER, GUILLAUME LAPLANTE-ANFOSSI, VINCENT PILAUD,
AND KURT STOECKL

ABSTRACT. We provide a systematic enumerative and combinatorial study of geometric cellular diagonals on the permutahedra.

In the first part of the paper, we study the combinatorics of certain hyperplane arrangements obtained as the union of ℓ generically translated copies of the classical braid arrangement. Based on Zaslavsky's theory, we derive enumerative results on the faces of these arrangements involving combinatorial objects named partition forests and rainbow forests. This yields in particular nice formulas for the number of regions and bounded regions in terms of exponentials of generating functions of Fuss-Catalan numbers. By duality, the specialization of these results to the case $\ell = 2$ gives the enumeration of any geometric diagonal of the permutahedron.

In the second part of the paper, we study diagonals which respect the operadic structure on the family of permutahedra. We show that there are exactly two such diagonals, which are moreover isomorphic. We describe their facets by a simple rule on paths in partition trees, and their vertices as pattern-avoiding pairs of permutations. We show that one of these diagonals is a topological enhancement of the Sanbeblidze–Umble diagonal, and unravel a natural lattice structure on their sets of facets.

In the third part of the paper, we use the preceding results to show that there are precisely two isomorphic topological cellular operadic structures on the families of operahedra and multipihedra, and exactly two infinity-isomorphic geometric universal tensor products of homotopy operads and A-infinity morphisms.



BDO was partially supported by the French ANR grants ALCOHOL (ANR-19-CE40-0006), CARPLO (ANR-20-CE40-0007), HighAGT (ANR-20-CE40-0016) and S3 (ANR-20-CE48-0010). GLA and KS were supported by the Australian Research Council Future Fellowship FT210100256. KS was supported by an Australian Government Research Training Program (RTP) Scholarship. VP was partially supported by the French ANR grant CHARMS (ANR-19-CE40-0017) and by the French–Austrian project PAGCAP (ANR-21-CE48-0020 & FWF I 5788).

CONTENTS

Introduction	3
Part I. Combinatorics of multiple braid arrangements	4
Part II. Diagonals of permutahedra	5
Part III. Higher algebraic structures	7
Acknowledgements	7
PART I. COMBINATORICS OF MULTIPLE BRAID ARRANGEMENTS	8
1. Recollection on hyperplane arrangements and braid arrangements	8
1.1. Hyperplane arrangements	8
1.2. The braid arrangement	9
1.3. The (ℓ, n) -braid arrangement	12
2. Flat poset and enumeration of \mathcal{B}_n^ℓ	14
2.1. Partition forests	14
2.2. Möbius polynomial	15
2.3. Rainbow forests	18
2.4. Enumeration of vertices of \mathcal{B}_n^ℓ	21
2.5. Enumeration of regions and bounded regions of \mathcal{B}_n^ℓ	22
3. Face poset and combinatorial description of $\mathcal{B}_n^\ell(a)$	24
3.1. Ordered partition forests	24
3.2. From partition forests to ordered partition forests	25
3.3. A criterion for ordered partition forests	27
PART II. DIAGONALS OF PERMUTAHEDRA	29
4. Cellular diagonals	29
4.1. Cellular diagonals for polytopes	29
4.2. Cellular diagonals for the permutahedra	32
4.3. Enumerative results on cellular diagonals of the permutahedra	34
5. Operadic diagonals	36
5.1. The LA and SU diagonals	36
5.2. The operadic property	36
5.3. Isomorphisms between operadic diagonals	39
5.4. Facets of operadic diagonals	40
5.5. Vertices of operadic diagonals	41
5.6. Relation to the facial weak order	43
6. Shift lattices	44
6.1. Topological enhancement of the original SU diagonal	44
6.2. Shifts under the face poset isomorphism	51
6.3. Shift lattices	52
6.4. Cubical description	55
6.5. Matrix description	60
PART III. HIGHER ALGEBRAIC STRUCTURES	62
7. Higher tensor products	62
7.1. Topological operadic structures	62
7.2. Relating operadic structures	65
7.3. Tensor products	67
References	70

INTRODUCTION

The purpose of this article is to study *cellular diagonals* on the *permutahedra*, which are cellular maps homotopic to the usual *thin diagonal* $\Delta : P \rightarrow P \times P$, $x \mapsto (x, x)$ (Definitions 4.1 and 4.2). Such diagonals, and in particular coherent families that we call *operadic diagonals* (Definition 5.5), are of interest in algebraic geometry and topology: via the theory of Fulton–Sturmfels [FS97], they give explicit formulas for the cup product on Losev–Manin toric varieties [LM00]; they define universal tensor products of permutadic A_∞ -algebras [LR13, Mar20]; they define a coproduct on permutahedral sets, which are models of two-fold loop spaces [SU04], and their study is needed to pursue the work of H. J. Baues aiming at defining explicit combinatorial models for higher iterated loop spaces [Bau80]; using the canonical projections to the operahedra, associahedra and multiplihedra, they define universal tensor products of homotopy operads, A_∞ -algebras and A_∞ -morphisms, respectively [LA22, LAM23].

Cellular diagonals for face-coherent families of polytopes are a fundamental object in algebraic topology. The Alexander–Whitney diagonal for simplices [EM54], and the Serre map for cubes [Ser51], allow one to define the cup product in singular simplicial and cubical cohomology. These two diagonals are also needed in the study of iterated loop spaces [Bau80], while other diagonals are needed in the study of the homology of fibered spaces [San09, RS18, Pro11]. In another direction, cellular diagonals allow one to define universal tensor products in homotopical algebra. The seminal case of the *associahedra* has a rich history: the first algebraic diagonal was found by S. Saneblidze and R. Umble [SU04], followed by a second one by M. Markl and S. Shnider [MS06], which was conjectured to coincide with the first one. This has recently been shown to hold [SU22], while a topological enhancement of the *magical formula* of [MS06] was provided by N. Masuda, H. Thomas, A. Tonks and B. Vallette [MTTV21].

In [MTTV21], the authors re-introduced the powerful technique of Fulton–Sturmfels [FS97], which came from the theory of fiber polytopes of [BS92], to define a topological cellular diagonal of the associahedra. We shall call such a diagonal a *geometric diagonal* (Definition 4.5). There are two remarkable features of this diagonal (or more precisely this family of diagonals, one for the Loday associahedron in each dimension). First, it respects the operadic structure of the associahedra (in fact, forces a unique topological cellular operad structure on them!), that is, the fact that each face of an associahedron is isomorphic to a product of lower-dimensional associahedra. Second, it satisfies the *magical formula* of J.-L. Loday: the faces in the image of the diagonal are given by the pairs of faces which are comparable in the Tamari order (see Section 4 and Remark 4.9 for a precise statement). This magical formula for the associahedra recently lead to new enumerative results for Tamari intervals [BCP23].

Building on [MTTV21], a general theory of geometric diagonals was developed in [LA22]. In particular, a combinatorial formula describing the image of the diagonal of any polytope was given [LA22, Thm. 1.26]. The topological operad structure of [MTTV21] on the associahedra was generalized to the family of *operahedra*, which comprise the family of permutahedra, and encodes the notion of homotopy operad. Cellular diagonals of the operahedra do *not* satisfy the magical formula, and the combinatorial difficulty of describing their image is what prompted the development of the theory in [LA22]. In fact, there is an interesting dichotomy between the families of polytopes which satisfy the magical formula (simplices, cubes, freehedra, associahedra) and those who do not (permutahedra, multiplihedra, operahedra).

Since the operahedra are *generalized permutahedra* [Pos09], their operadic diagonals are completely determined by the operadic diagonals of permutahedra (see [LA22, Sect. 1.6]), which is the purpose of study of the present paper.

The first cellular diagonal of the permutahedra was obtained at the algebraic level by S. Saneblidze and R. Umble [SU04]. We shall call this diagonal the *original SU diagonal*. The first topological cellular diagonal of the permutahedra was defined in [LA22], we shall call it the *geometric LA diagonal*. Both of these families of diagonals are *operadic*, *i.e.* they respect the product structure on the faces of permutahedra (this property is called “comultiplicativity” in [SU04]). More precisely, the algebraic structure encoded by the permutahedra is that of permutadic A_∞ -algebra [LR13, Mar20].

The toric varieties associated with the permutahedra are called Losev–Manin varieties, introduced in [LM00]. At this level, the operadic structure is that of a reconnectad [DKL22]. The cohomology ring structure was studied by A. Losev and Y. Manin, and quite extensively since then, see for instance [BM14, Lin16]. Our current work brings a completely combinatorially explicit description of the cup product; it would be interesting to know if this new description can lead to new results, or how it can be used to recover existing ones.

The first part of the paper derives enumerative results for the iterations of any geometric diagonal of the permutahedra. According to the Fulton–Sturmfels formula [FS97] (see Proposition 4.7 and Remark 4.10), this amounts to the study of hyperplane arrangements made of generically translated copies of the braid arrangement. The second part studies in depth the combinatorics of operadic diagonals of the permutahedra, providing in particular a topological enhancement of the original SU diagonal, while the third part derives consequences of this combinatorial study in the field of homotopical algebra. We now proceed to introduce separately each part in more detail.

Part I. Combinatorics of multiple braid arrangements. As the dual of the permutahedron $\text{Perm}(n)$ is the classical braid arrangement \mathcal{B}_n , the dual of a diagonal of the permutahedron $\text{Perm}(n)$ is a hyperplane arrangement \mathcal{B}_n^2 made of 2 generically translated copies of the braid arrangement \mathcal{B}_n . In the first part of the paper, we therefore study the combinatorics of the (ℓ, n) -braid arrangement \mathcal{B}_n^ℓ , defined as the union of ℓ generically translated copies of the braid arrangement \mathcal{B}_n (Definition 1.14). We are mainly interested in the $\ell = 2$ case for the enumeration of the faces of the diagonals of the permutahedron $\text{Perm}(n)$, but the general ℓ case is not much harder and corresponds algebraically to the enumeration of the faces of cellular ℓ -gonals of the permutahedron $\text{Perm}(n)$.

Section 2 is dedicated to the combinatorial description of the flat poset of \mathcal{B}_n^ℓ and its enumerative consequences. We first observe that the flats of \mathcal{B}_n^ℓ are in bijection with (ℓ, n) -partition forests, defined as ℓ -tuples of (unordered) partitions of $[n]$ whose intersection hypergraph is a hyperforest (Definition 2.2). As this description is independent of the translations of the different copies (as long as these translations are generic), we obtain by T. Zaslavsky’s theory that the number of k -dimensional faces and of bounded faces of \mathcal{B}_n^ℓ only depends on k , ℓ , and n . In fact, we obtain the following formula for the Möbius polynomial of the (ℓ, n) -braid arrangement \mathcal{B}_n^ℓ in terms of pairs of (ℓ, n) -partition forests.

Theorem (Theorem 2.4). *The Möbius polynomial of the (ℓ, n) -braid arrangement \mathcal{B}_n^ℓ is given by*

$$\mu_{\mathcal{B}_n^\ell}(x, y) = x^{n-1-\ell n} y^{n-1-\ell n} \sum_{\mathbf{F} \leq \mathbf{G}} \prod_{i \in [\ell]} x^{\#F_i} y^{\#G_i} \prod_{p \in G_i} (-1)^{\#F_i[p]-1} (\#F_i[p] - 1)!,$$

where $\mathbf{F} \leq \mathbf{G}$ ranges over all intervals of the (ℓ, n) -partition forest poset, and $F_i[p]$ denotes the restriction of the partition F_i to the part p of G_i .

This formula is not particularly easy to handle, but it turns out to simplify to very elegant formulas for the number of vertices, regions, and bounded regions of the (ℓ, n) -braid arrangement \mathcal{B}_n^ℓ . Namely, using an alternative combinatorial description of the (ℓ, n) -partition forests in terms of (ℓ, n) -rainbow forests and a colored analogue of the classical Prüfer code for permutations, we first obtain the number of vertices of the (ℓ, n) -braid arrangement \mathcal{B}_n^ℓ .

Theorem (Theorem 2.18). *The number of vertices of the (ℓ, n) -braid arrangement \mathcal{B}_n^ℓ is*

$$f_0(\mathcal{B}_n^\ell) = \ell((\ell - 1)n + 1)^{n-2}.$$

This result can even be refined according to the dimension of the flats of the different copies intersected to obtain the vertices of the (ℓ, n) -braid arrangement \mathcal{B}_n^ℓ .

Theorem (Theorem 2.19). *For any k_1, \dots, k_ℓ such that $0 \leq k_i \leq n-1$ for $i \in [\ell]$ and $\sum_{i \in [\ell]} k_i = n-1$, the number of vertices v of the (ℓ, n) -braid arrangement \mathcal{B}_n^ℓ such that the smallest flat of the i^{th} copy of \mathcal{B}_n containing v has dimension $n - k_i - 1$ is given by*

$$n^{\ell-1} \binom{n-1}{k_1, \dots, k_\ell} \prod_{i \in [\ell]} (n - k_i)^{k_i-1}.$$

We then consider the regions of the (ℓ, n) -braid arrangement \mathcal{B}_n^ℓ . We first obtain a very simple exponential formula for its characteristic polynomial.

Theorem (Theorem 2.20). *The characteristic polynomial $\chi_{\mathcal{B}_n^\ell}(y)$ of the (ℓ, n) -braid arrangement \mathcal{B}_n^ℓ is given by*

$$\chi_{\mathcal{B}_n^\ell}(y) = \frac{(-1)^n n!}{y} [z^n] \exp \left(- \sum_{m \geq 1} \frac{F_{\ell, m} y z^m}{m} \right),$$

where $F_{\ell, m} := \frac{1}{(\ell-1)m+1} \binom{\ell m}{m}$ is the Fuss-Catalan number.

Evaluating the characteristic polynomial at $y = -1$ and $y = 1$ respectively, we obtain by T. Zaslavsky's theory the numbers of regions and bounded regions of the (ℓ, n) -braid arrangement \mathcal{B}_n^ℓ .

Theorem (Theorem 2.21). *The numbers of regions and of bounded regions of the (ℓ, n) -braid arrangement \mathcal{B}_n^ℓ are given by*

$$\begin{aligned} f_{n-1}(\mathcal{B}_n^\ell) &= n! [z^n] \exp \left(\sum_{m \geq 1} \frac{F_{\ell, m} z^m}{m} \right) \\ \text{and} \quad b_{n-1}(\mathcal{B}_n^\ell) &= (n-1)! [z^{n-1}] \exp \left((\ell-1) \sum_{m \geq 1} F_{\ell, m} z^m \right), \end{aligned}$$

where $F_{\ell, m} := \frac{1}{(\ell-1)m+1} \binom{\ell m}{m}$ is the Fuss-Catalan number.

Finally, Section 3 is dedicated to the combinatorial description of the face poset of \mathcal{B}_n^ℓ . We observe that the faces of \mathcal{B}_n^ℓ are in bijection with certain *ordered* (ℓ, n) -partition forests, defined as ℓ -tuples of ordered partitions of $[n]$ whose underlying unordered partitions form an (unordered) (ℓ, n) -partition forest (Definition 3.1). Here, which ordered (ℓ, n) -partition forests actually appear as faces of \mathcal{B}_n^ℓ depends on the choice of the translations of the different copies. We provide a combinatorial description of the possible orderings of a (ℓ, n) -partition forest compatible with some given translations in terms of certain paths in the forest (Propositions 3.3 and 3.5), and a combinatorial characterization of the ordered partition forests which appear for some given translations in terms of the circuits of a certain oriented graph (Proposition 3.7).

Part II. Diagonals of permutahedra. We present cellular diagonals, the Fulton–Sturmfels method, the magical formula and specialize the results of Part I to the permutahedra in Section 4. Then, we initiate in Section 5 the study of operadic diagonals (Definition 5.5). These are families of diagonals of the permutahedra which are compatible with the property that faces of permutahedra are product of lower-dimensional permutahedra.

Theorem (Theorems 5.13 and 5.15). *There are exactly four operadic geometric diagonals of the permutahedra, the geometric LA and SU diagonals and their opposites, and only the first two respect the weak order on permutations. Moreover, their cellular images are isomorphic as posets.*

It turns out that the facets and vertices of operadic diagonals admit elegant combinatorial descriptions. The following is a consequence of a general geometrical result, that holds for any diagonal (Proposition 3.3).

Theorem (Theorem 5.17). *A pair of ordered partitions (σ, τ) forming a partition tree is a facet of the LA (resp. SU) geometric diagonal if and only if the minimum (resp. maximum) of every directed path between two consecutive blocks of σ or τ is oriented from σ to τ (resp. from τ to σ).*

Vertices of operadic diagonals are pairs of permutations, and form a strict subset of intervals of the weak order. They admit an analogous description in terms of pattern-avoidance.

Theorem (Theorem 5.24). *A pair of permutations of $[n]$ is a vertex of the LA (resp. SU) diagonal if and only if for any $k \geq 1$ and for any $I = \{i_1, \dots, i_k\}, J = \{j_1, \dots, j_k\} \subset [k]$ such that $i_1 = 1$ (resp. $j_k = 2k$) it avoids the patterns*

$$(LA) \quad (j_1 i_1 j_2 i_2 \cdots j_k i_k, i_2 j_1 i_3 j_2 \cdots i_k j_{k-1} i_1 j_k),$$

$$(SU) \quad \text{resp. } (j_1 i_1 j_2 i_2 \cdots j_k i_k, i_1 j_k i_2 j_1 \cdots i_{k-1} j_{k-2} i_k j_{k-1}),$$

For each $k \geq 1$, there are $\binom{2k-1}{k-1,k}(k-1)!k!$ such patterns, which are $(21, 12)$ for $k = 1$, and the following for $k = 2$

- LA avoids $(3142, 2314), (4132, 2413), (2143, 3214), (4123, 3412), (2134, 4213), (3124, 4312),$
- SU avoids $(1243, 2431), (1342, 3421), (2143, 1432), (2341, 3412), (3142, 1423), (3241, 2413).$

In Section 6, we introduce *shifts* that can be performed on the facets of operadic diagonals. These allow us to show that the geometric SU diagonal is a topological enhancement of the original SU diagonal.

Theorem (Theorem 6.24). *The original and geometric SU diagonals coincide.*

The proof of this result, quite technical, proceeds by showing the equivalence between 4 different descriptions of the diagonal: the original, 1-shift, m -shift and geometric SU diagonals (Section 6.1). This brings a positive answer to [LA22, Rem. 2.19], showing that the original SU diagonal can be recovered from a choice of chambers in the fundamental hyperplane arrangement of the permutahedron. Our formulas for the number of facets also agrees with the experimental count made in [Vej07]. Moreover, it provides a new proof that all known diagonals on the associahedra coincide [SU22]. Indeed, since the family of vectors inducing the geometric SU diagonal all have strictly decreasing coordinates, the diagonal induced on the associahedron is given by the magical formula [MTTV21, Thm. 2], see also [LA22, Prop. 3.8].

The above theorem also allows us to translate the different combinatorial descriptions of the facets of operadic diagonals from one to the other, compiled in the following table.

Description	SU diagonal	LA diagonal
Original	[SU04]	Definition 6.26
Geometric	Theorem 5.4	[LA22]
Path extrema	Theorem 5.17	Theorem 5.17
1-shifts	Definition 6.10	Definition 6.26
m -shifts	Definition 6.10	Definition 6.26
Lattice	Proposition 6.37	Proposition 6.37
Cubical	[SU04]	Theorem 6.51
Matrix	[SU04]	Section 6.5

In Section 6.3, we show that the facets of operadic diagonals are disjoint unions of lattices, that we call the *shift lattices*. These lattices are isomorphic to a product of chains, and are indexed by the permutations of $[n]$. Moreover, while the pairs of facets of operadic diagonals are intervals of the facial weak order (Section 5.6), the shift lattices are not sub-lattices of this order's product (see Figure 20).

Finally, we present the alternative cubical (Section 6.4) and matrix (Section 6.5) descriptions of the SU diagonal from [SU04, SU22], providing proofs of their equivalence with the other descriptions, and giving their LA counterparts. The existence of this cubical description, based on a subdivision of the cube combinatorially isomorphic to the permutahedron, finds its conceptual root in the bar-cobar resolution of the associative permutad. Indeed, this resolution is encoded by the dual subdivision of the permutahedron, which is cubical since $\text{Perm}(n)$ is a simple polytope, and a diagonal can be obtained from the classical Serre diagonal via retraction, in the same fashion as for the associahedra, see [MS06, Lod11] and [LAM23, Sec. 5.1].

Part III. Higher algebraic structures. In this shorter third part of the paper, we derive some higher algebraic consequences of the preceding results, which were the original motivation for the present study. They concern the *operahedra*, a family of polytopes indexed by planar trees, which encode (non-symmetric non-unital) homotopy operads [LA22], and the *multiplihedra*, a family of polytopes indexed by 2-colored nested linear trees, which encode A_∞ -morphisms [LAM23]. Both of these admit realizations “à la Loday”, which generalize the Loday realizations of the associahedra. The faces of an operahedron are in bijection with *nestings*, or parenthesization, of the corresponding planar tree, while the faces of a multiplihedron are in bijection with 2-colored nestings of the corresponding linear tree. The main results concerning the operahedra are summarized as follows.

Theorem (Theorems 7.3, 7.12 and 7.18). *There are exactly*

- (1) *two geometric operadic diagonals of the Loday operahedra, the LA and SU diagonals,*
- (2) *two geometric topological cellular colored operad structures on the Loday operahedra,*
- (3) *two geometric universal tensor products of homotopy operads,*

which agree with the generalized Tamari order on fully nested trees. Moreover, the two topological operad structures are isomorphic, and the two tensor products are not strictly isomorphic, but are related by an ∞ -isotopy.

As the associahedra and the permutahedra are part of the family of operahedra, we get analogous results for A_∞ -algebras and permutadic A_∞ -algebras. The main results concerning the multiplihedra are summarized as follows.

Theorem (Theorems 7.8, 7.16 and 7.22). *There are exactly*

- (1) *two geometric operadic diagonals of the Forcey multiplihedra, the LA and SU diagonals,*
- (2) *two geometric topological cellular operadic bimodule structures (over the Loday associahedra) on the Forcey multiplihedra,*
- (3) *two compatible geometric universal tensor products of A_∞ -algebras and A_∞ -morphisms,*

which agree with the Tamari-type order on atomic 2-colored nested linear trees. Moreover, the two topological operadic bimodule structures are isomorphic, and the two tensor products are not strictly isomorphic, but are related by an ∞ -isotopy.

Here, by the adjective “geometric”, we mean diagonal, operadic structure and tensor product which are obtained geometrically on the polytopes via the Fulton–Sturmfelds method. By “universal”, we mean formulas for the tensor products which apply to *any* pair of homotopy operads or A_∞ -morphisms.

However, the isomorphisms of topological operads (resp. operadic bimodules) takes place in a category of polytopes Poly for which the morphisms are *not* affine maps [LA22, Def. 4.13], and it does *not* commute with the diagonal maps (Examples 7.14 and 7.17). Moreover, the pairs of faces in the image of the two operadic diagonals are in general not in bijection (see Examples 7.20 and 7.24), yielding different (but ∞ -isomorphic) tensor products of homotopy operads (resp. A_∞ -morphisms).

ACKNOWLEDGEMENTS

We are indebted to Matthieu Josuat-Vergès for taking part in the premises of this paper, in particular for conjecturing the case $\ell = 2$ of Theorem 2.19, for working on the proof of Theorem 5.24, and for implementing some sage code used during the project. GLA is grateful to Hugh Thomas for raising the question to count the facets of the LA diagonal and for preliminary discussions during a visit at the LACIM in the summer of 2021 where the project started, and to the Max Planck Institute for Mathematics in Bonn where part of this work was carried out. We are grateful to Sylvie Corteel for pointing out the relevance of the dual perspective for the purpose of counting. VP is grateful to the organizers (Karim Adiprasito, Alexey Glazyrin, Isabella Novic, and Igor Pak) of the workshop “Combinatorics and Geometry of Convex Polyhedra” held at the Simons Center for Geometry and Physics in March 2023 for the opportunity to present a preliminary version of our enumerative results, and to Pavel Galashin for asking about the characteristic polynomial of the multiple braid arrangement during this presentation. We thank Samson Sanedidze and Ron Umble for useful correspondence.

Part I. Combinatorics of multiple braid arrangements

In this first part, we study the combinatorics of hyperplane arrangements obtained as unions of generically translated copies of the braid arrangement. In Section 1, we first recall some classical facts on the enumeration of hyperplane arrangements (Section 1.1), present the classical braid arrangement (Section 1.2), and define our multiple braid arrangements (Section 1.3). Then in Section 2, we describe their flat posets in terms of partition forests (Section 2.1) and rainbow forests (Section 2.3), from which we derive their Möbius polynomials (Section 2.2), and some surprising formulas for their numbers of vertices (Section 2.4) and regions (Section 2.5). Finally, in Section 3, we describe their face posets in terms of ordered partition forests (Section 3.1), and explore some combinatorial criteria to describe the ordered partition forests that appear as faces of a given multiple braid arrangement (Sections 3.2 and 3.3).

1. RECOLLECTION ON HYPERPLANE ARRANGEMENTS AND BRAID ARRANGEMENTS

1.1. Hyperplane arrangements. We first briefly recall classical results on the combinatorics of affine hyperplane arrangements, in particular the enumerative connection between their intersection posets and their face lattices due to T. Zaslavsky [Zas75].

Definition 1.1. A finite affine real *hyperplane arrangement* is a finite set \mathcal{A} of affine hyperplanes in \mathbb{R}^d .

Definition 1.2. A *region* of \mathcal{A} is a connected component of $\mathbb{R}^d \setminus \bigcup_{H \in \mathcal{A}} H$. The *faces* of \mathcal{A} are the closures of the regions of \mathcal{A} and all their intersections with a hyperplane of \mathcal{A} . The *face poset* of \mathcal{A} is the poset $\text{Fa}(\mathcal{A})$ of faces of \mathcal{A} ordered by inclusion. The *f-polynomial* $f_{\mathcal{A}}(x)$ and *b-polynomial* $b_{\mathcal{A}}(x)$ of \mathcal{A} are the polynomials

$$f_{\mathcal{A}}(x) := \sum_{k=0}^d f_k(\mathcal{A}) x^k \quad \text{and} \quad b_{\mathcal{A}}(x) := \sum_{k=0}^d b_k(\mathcal{A}) x^k,$$

where $f_k(\mathcal{A})$ denotes the number of k -dimensional faces of \mathcal{A} , while $b_k(\mathcal{A})$ denotes the number of bounded k -dimensional faces of \mathcal{A} .

Definition 1.3. A *flat* of \mathcal{A} is a non-empty affine subspace of \mathbb{R}^d that can be obtained as the intersection of some hyperplanes of \mathcal{A} . The *flat poset* of \mathcal{A} is the poset $\text{Fl}(\mathcal{A})$ of flats of \mathcal{A} ordered by reverse inclusion.

Definition 1.4. The *Möbius polynomial* $\mu_{\mathcal{A}}(x, y)$ of \mathcal{A} is the polynomial defined by

$$\mu_{\mathcal{A}}(x, y) := \sum_{F \leq G} \mu_{\text{Fl}(\mathcal{A})}(F, G) x^{\dim(F)} y^{\dim(G)},$$

where $F \leq G$ ranges over all intervals of the flat poset $\text{Fl}(\mathcal{A})$, and $\mu_{\text{Fl}(\mathcal{A})}(F, G)$ denotes the *Möbius function* on the flat poset $\text{Fl}(\mathcal{A})$ defined as usual by

$$\mu_{\text{Fl}(\mathcal{A})}(F, F) = 1 \quad \text{and} \quad \sum_{F \leq G \leq H} \mu_{\text{Fl}(\mathcal{A})}(F, G) = 0$$

for all $F < H$ in $\text{Fl}(\mathcal{A})$.

Remark 1.5. Our definition of the Möbius polynomial slightly differs from that of [Zas75] as we use the dimension of F instead of its codimension, in order to simplify slightly the following statement.

Theorem 1.6 ([Zas75, Thm. A]). *The f-polynomial, the b-polynomial, and the Möbius polynomial of the hyperplane arrangement \mathcal{A} are related by*

$$f_{\mathcal{A}}(x) = \mu_{\mathcal{A}}(-x, -1) \quad \text{and} \quad b_{\mathcal{A}}(x) = \mu_{\mathcal{A}}(-x, 1).$$

Example 1.7. For the arrangement \mathcal{A} of 5 hyperplanes of Figure 1, we have

$$\mu_{\mathcal{A}}(x, y) = x^2 y^2 - 5x^2 y + 6x^2 + 5xy - 10x + 4,$$

so that

$$f_{\mathcal{A}}(x) = \mu_{\mathcal{A}}(-x, -1) = 12x^2 + 15x + 4 \quad \text{and} \quad b_{\mathcal{A}}(x) = \mu_{\mathcal{A}}(-x, 1) = 2x^2 + 5x + 4.$$

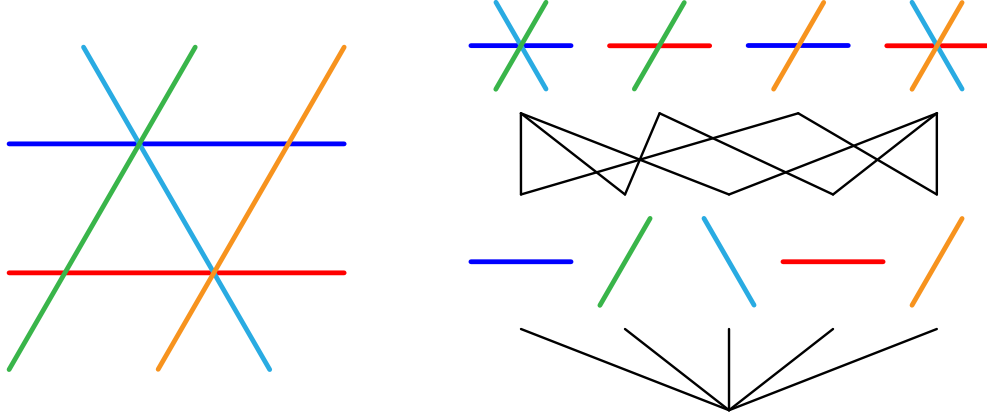


FIGURE 1. A hyperplane arrangement (left) and its intersection poset (right).

Remark 1.8. The coefficient of x^d in the Möbius polynomial $\mu_{\mathcal{A}}(x, y)$ gives the more classical *characteristic polynomial*

$$\chi_{\mathcal{A}}(y) := [x^d] \mu_{\mathcal{A}}(x, y) = \sum_F \mu_{\text{Fl}(\mathcal{A})}(\mathbb{R}^d, F) y^{\dim(F)}.$$

By Theorem 1.6, we thus have

$$f_d(\mathcal{A}) = (-1)^d \chi_{\mathcal{A}}(-1) \quad \text{and} \quad b_d(\mathcal{A}) = (-1)^d \chi_{\mathcal{A}}(1).$$

1.2. The braid arrangement. We now briefly recall the classical combinatorics of the braid arrangement. See Figures 2 to 4 for illustrations when $n = 3$ and $n = 4$.

Definition 1.9. Fix $n \geq 1$ and denote by \mathbb{H} the hyperplane of \mathbb{R}^n defined by $\sum_{s \in [n]} x_s = 0$. The *braid arrangement* \mathcal{B}_n is the arrangement of the hyperplanes $\{\mathbf{x} \in \mathbb{H} \mid x_s = x_t\}$ for all $1 \leq s < t \leq n$.

Remark 1.10. Note that we have decided to work in the space \mathbb{H} rather than in the space \mathbb{R}^n . The advantage is that the braid arrangement \mathcal{B}_n in \mathbb{H} is essential, so that we can speak of its rays. Working in \mathbb{R}^n would change rays to walls, and would multiply all Möbius polynomials by a factor xy .

The combinatorics of the braid arrangement \mathcal{B}_n is well-known. The descriptions of its face and flat posets involve both ordered and unordered set partitions. To avoid confusions, we will always mark with an arrow the ordered structures (ordered set partitions, ordered partition forests, etc.). Hence, the letter π denotes an unordered set partition (the order is irrelevant, neither inside each part, nor between two distinct parts), while $\vec{\pi}$ denotes an ordered set partition (the order inside each part is irrelevant, but the order between distinct parts is relevant).

The braid arrangement \mathcal{B}_n has a k -dimensional face

$$\Phi(\vec{\pi}) := \{\mathbf{x} \in \mathbb{R}^n \mid x_s \leq x_t \text{ for all } s, t \text{ such that the part of } s \text{ is weakly before the part of } t \text{ in } \vec{\pi}\}$$

for each ordered set partition $\vec{\pi}$ of $[n]$ into $k+1$ parts, or equivalently, for each surjection from $[n]$ to $[k+1]$. The face poset $\text{Fa}(\mathcal{B}_n)$ is thus isomorphic to the refinement poset $\vec{\Pi}_n$ on ordered set partitions, where an ordered partition $\vec{\pi}$ is smaller than an ordered partition $\vec{\omega}$ if each part of $\vec{\pi}$ is the union of an interval of consecutive parts in $\vec{\omega}$. In particular, it has a single vertex corresponding to the ordered partition $[n]$, $2^n - 2$ rays corresponding to the proper nonempty subsets of $[n]$ (ordered partitions of $[n]$ into 2 parts), and $n!$ regions corresponding to the permutations of $[n]$ (ordered partitions of $[n]$ into n parts). As an example, Figure 2 illustrates the face poset of the braid arrangement \mathcal{B}_3 .

The braid arrangement \mathcal{B}_n has a k -dimensional flat

$$\Psi(\pi) := \{\mathbf{x} \in \mathbb{R}^n \mid x_s = x_t \text{ for all } s, t \text{ which belong to the same part of } \pi\}$$

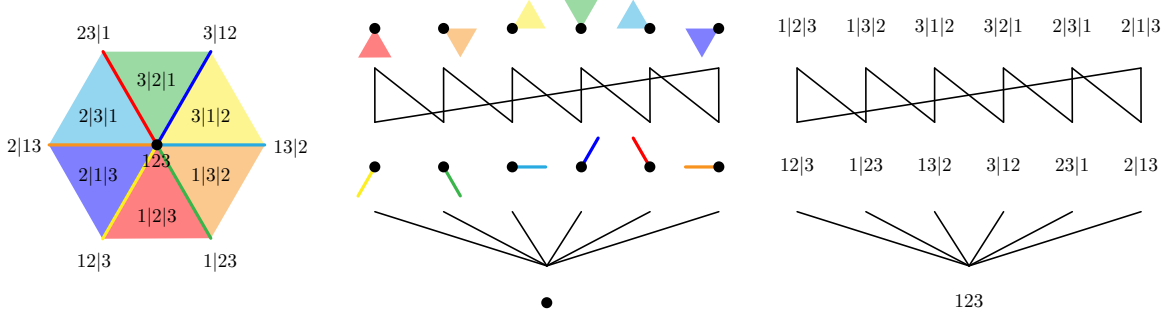


FIGURE 2. The face poset $\text{Fa}(\mathcal{B}_3)$ of the braid arrangement \mathcal{B}_3 (left), where faces are represented as cones (middle) or as ordered set partitions of $[3]$ (right).

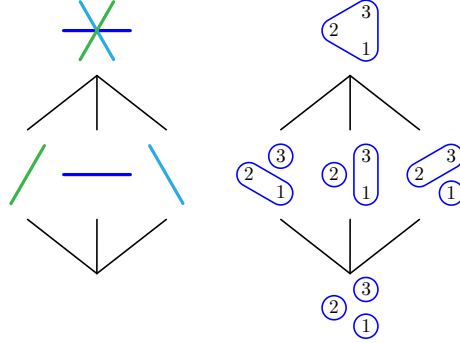


FIGURE 3. The flat poset $\text{Fl}(\mathcal{B}_3)$ of the braid arrangement \mathcal{B}_3 , where flats are represented as intersections of hyperplanes (left) or as set partitions of $[3]$ (right).

for each unordered set partition π of $[n]$ into $k+1$ parts. The flat poset $\text{Fl}(\mathcal{B}_n)$ is thus isomorphic to the refinement poset Π_n on set partitions of $[n]$, where a partition π is smaller than a partition ω if each part of π is contained in a part of ω . For instance, Figures 3 and 4 illustrate the flat posets of the braid arrangements \mathcal{B}_3 and \mathcal{B}_4 . Note that the refinement in $\overline{\Pi}_n$ and in Π_n are in opposite direction.

The Möbius function of the set partitions poset Π_n is given by

$$\mu_{\Pi_n}(\pi, \omega) = \prod_{p \in \omega} (-1)^{\#\pi[p]-1} (\#\pi[p] - 1)!,$$

where $\pi[p]$ denotes the restriction of the partition π to the part p of the partition ω , and $\#\pi[p]$ denotes its number of parts. See for instance [Bir95, Rot64]. The Möbius polynomial of the braid arrangement \mathcal{B}_n is given by

$$\mu_{\mathcal{B}_n}(x, y) = \sum_{k \in [n]} x^{k-1} S(n, k) \prod_{i \in [k-1]} (y - i),$$

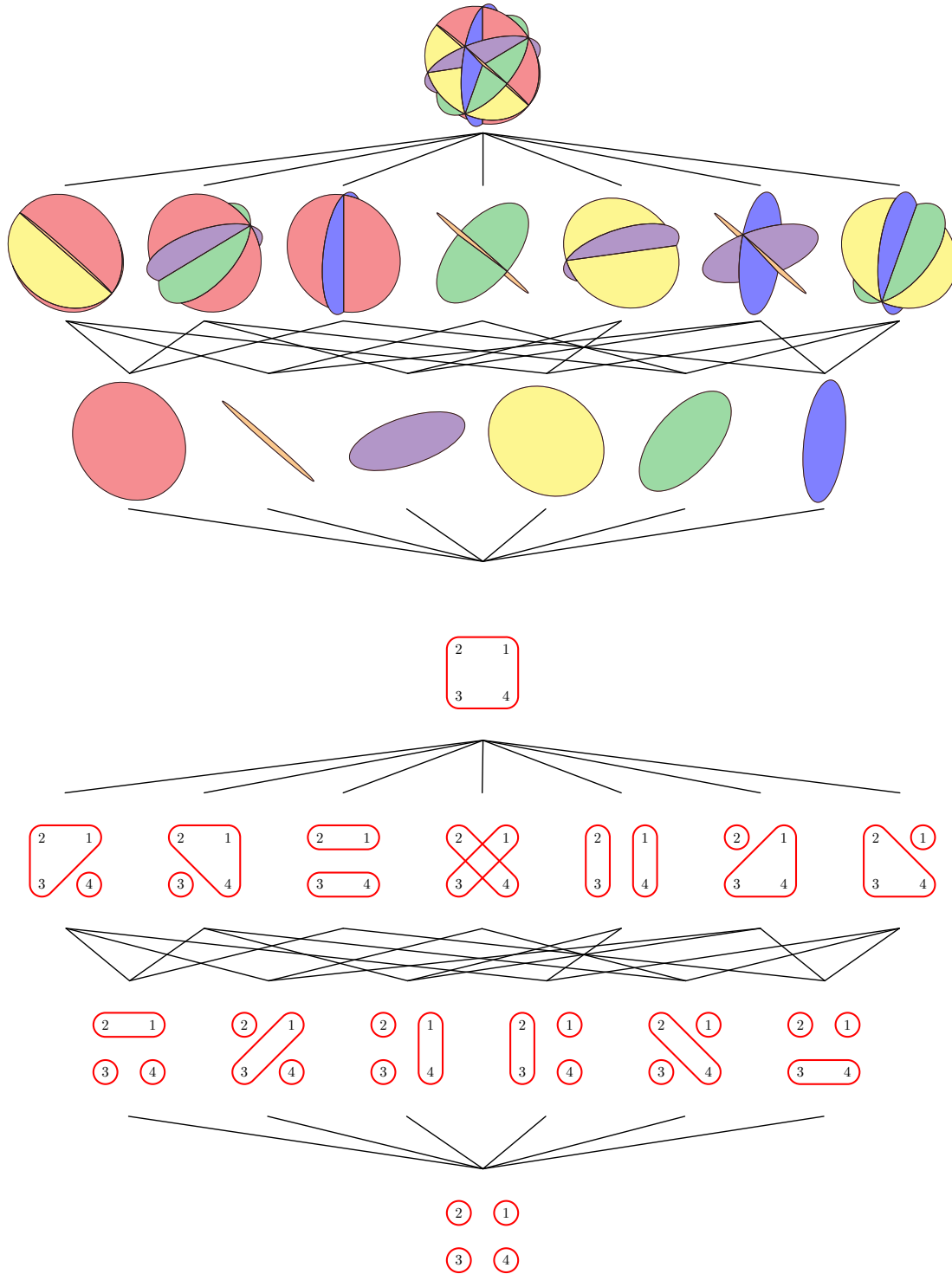


FIGURE 4. The flat poset $\text{Fl}(\mathcal{B}_4)$ of the braid arrangement \mathcal{B}_4 , where flats are represented as intersections of hyperplanes (top) or as set partitions of $[4]$ (bottom).

where $S(n, k)$ denotes the Stirling number of the second kind [OEI10, A008277], *i.e.* the number of set partitions of $[n]$ into k parts. For instance

$$\begin{aligned}\mu_{\mathcal{B}_1}(x, y) &= 1 \\ \mu_{\mathcal{B}_2}(x, y) &= xy - x + 1 = x(y - 1) + 1 \\ \mu_{\mathcal{B}_3}(x, y) &= x^2y^2 - 3x^2y + 2x^2 + 3xy - 3x + 1 = x^2(y - 1)(y - 2) + 3x(y - 1) + 1 \\ \mu_{\mathcal{B}_4}(x, y) &= x^3y^3 - 6x^3y^2 + 11x^3y - 6x^3 + 6x^2y^2 - 18x^2y + 12x^2 + 7xy - 7x + 1 \\ &= x^3(y - 1)(y - 2)(y - 3) + 6x^2(y - 1)(y - 2) + 7x(y - 1) + 1.\end{aligned}$$

In particular, the characteristic polynomial of the braid arrangement \mathcal{B}_n is given by

$$\chi_{\mathcal{B}_n}(y) = (y - 1)(y - 2) \dots (y - n - 1).$$

Working in \mathbb{R}^n rather than in \mathbb{H} would lead to an additional y factor in this formula, which might be more familiar to the reader. See Remark 1.10.

Finally, we will consider the evaluation of the Möbius polynomial $\mu_{\mathcal{B}_n}(x, y)$ at $y = 0$:

$$\pi_n(x) := \mu_{\mathcal{B}_n}(x, 0) = \sum_{k \in [n]} (-1)^{k-1} (k-1)! S(n, k) x^{k-1}.$$

The coefficients of this polynomial are given by the sequence [OEI10, A028246]. We just observe here that it is connected to the \mathbf{f} -polynomial of \mathcal{B}_n .

Lemma 1.11. *We have $\pi_n(x) = (1 - x) \mathbf{f}_{\mathcal{B}_n}(x)$.*

Proof. This lemma is equivalent to the equality

$$\sum_{k=1}^n (-1)^{k-1} (k-1)! S(n, k) x^{k-1} = (1 - x) \sum_{k=1}^{n-1} (-1)^{k-1} k! S(n-1, k) x^{k-1}.$$

Distributing $(1 - x)$ in the right hand side gives:

$$\begin{aligned}& (1 - x) \sum_{k=1}^{n-1} (-1)^{k-1} k! S(n-1, k) x^{k-1} \\ &= \sum_{k=1}^{n-1} k! S(n-1, k) (-x)^{k-1} + \sum_{k=1}^{n-1} k! S(n-1, k) (-x)^k \\ &= \sum_{k=1}^{n-1} k! S(n-1, k) (-x)^{k-1} + \sum_{k=2}^n (k-1)! S(n-1, k-1) (-x)^{k-1} + (n-1)! S(n-1, n-1) (-x)^{n-1} \\ &= S(n-1, 1) (-x)^0 + \sum_{k=2}^{n-1} (k-1)! (S(n-1, k-1) + k S(n-1, k)) (-x)^{k-1}.\end{aligned}$$

The result thus follows from the inductive formula on Stirling numbers of the second kind

$$S(n+1, k) = k S(n, k) + S(n, k-1)$$

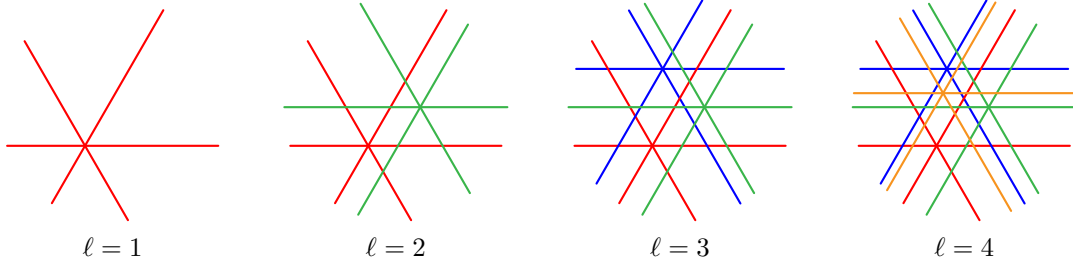
for $0 < k < n$. □

1.3. The (ℓ, n) -braid arrangement. We now focus on the following specific hyperplane arrangements, illustrated in Figure 5. We still denote by \mathbb{H} the hyperplane of \mathbb{R}^n defined by $\sum_{s \in [n]} x_s = 0$.

Definition 1.12. For any integers $\ell, n \geq 1$, and any matrix $\mathbf{a} := (a_{i,j}) \in M_{\ell, n-1}(\mathbb{R})$, the **\mathbf{a} -braid arrangement $\mathcal{B}_n^\ell(\mathbf{a})$** is the arrangement of hyperplanes $\{\mathbf{x} \in \mathbb{H} \mid x_s - x_t = A_{i,s,t}\}$ for all $1 \leq s < t \leq n$ and $i \in [\ell]$, where $A_{i,s,t} := \sum_{s \leq j < t} a_{i,j}$.

In other words, the \mathbf{a} -braid arrangement $\mathcal{B}_n^\ell(\mathbf{a})$ is the union of ℓ copies of the braid arrangement \mathcal{B}_n translated according to the matrix \mathbf{a} . Of course, the \mathbf{a} -braid arrangement $\mathcal{B}_n^\ell(\mathbf{a})$ highly depends on \mathbf{a} . In this paper, we are interested in the case where \mathbf{a} is generic in the following sense.

Definition 1.13. A matrix $\mathbf{a} := (a_{i,j}) \in M_{\ell, n-1}(\mathbb{R})$ is **generic** if for any $i_1, \dots, i_k \in [\ell]$ and distinct $r_1, \dots, r_k \in [n]$, the equality $\sum_{j \in [k]} A_{i_j, r_{j-1}, r_j} = 0$ implies $i_1 = \dots = i_k$ (with the notation $A_{i,s,t} := \sum_{s \leq j < t} a_{i,j}$ and the convention $r_0 = r_k$).

FIGURE 5. The $(\ell, 3)$ -braid arrangements for $\ell \in [4]$.

We will see that many combinatorial aspects of $\mathcal{B}_n^\ell(\mathbf{a})$, in particular its flat poset and thus its Möbius, f - and b -polynomials, are in fact independent of the matrix \mathbf{a} as long as it is generic. We therefore consider the following definition.

Definition 1.14. The (ℓ, n) -braid arrangement \mathcal{B}_n^ℓ is the arrangement in \mathbb{H} obtained as the union of ℓ generically translated copies of the braid arrangement \mathcal{B}_n (that is, any \mathbf{a} -braid arrangement for some generic matrix $\mathbf{a} \in M_{\ell, n-1}(\mathbb{R})$).

The objective of Part I is to explore the combinatorics of these multiple braid arrangements. We have split our presentation into two sections:

- In Section 2, we describe the flat poset $\text{Fl}(\mathcal{B}_n^\ell)$ of the (ℓ, n) -braid arrangement \mathcal{B}_n^ℓ in terms of (ℓ, n) -partition forests (Section 2.1) and labeled (ℓ, n) -rainbow forests (Section 2.3), which enables us to derive its Möbius, f - and b -polynomials (Section 2.2), from which we extract interesting formulas for the number of vertices (Section 2.4) and regions (Section 2.5). Note that all these results are independent of the translation matrix.
- In Section 3, we describe the face poset $\text{Fa}(\mathcal{B}_n^\ell(\mathbf{a}))$ of the \mathbf{a} -braid arrangement $\mathcal{B}_n^\ell(\mathbf{a})$ in terms of ordered (ℓ, n) -partition forests (Section 3.1). In contrast to the flat poset, this description of the face poset depends on the translation matrix \mathbf{a} . For a given choice of \mathbf{a} , we describe in particular the ordered (ℓ, n) -partition forests with a given underlying (unordered) (ℓ, n) -partition forest (Section 3.2). We then give a criterion to decide whether a given ordered (ℓ, n) -partition forest corresponds to a face of $\mathcal{B}_n^\ell(\mathbf{a})$ (Section 3.3).

Remark 1.15. Note that each hyperplane of the (ℓ, n) -braid arrangement \mathcal{B}_n^ℓ is orthogonal to a root $\mathbf{e}_i - \mathbf{e}_j$ of the type A root system. Many such arrangements have been studied previously, for instance, the *Shi arrangement* [Shi86, Shi87], the *Catalan arrangement* [PS00, Sect. 7], the *Linial arrangement* [PS00, Sect. 8], the *generic arrangement* of [PS00, Sect. 5], or the *discriminantal arrangements* of [MS89, BB97]. We refer to the work of A. Postnikov and R. Stanley [PS00] and of O. Bernardi [Ber18] for much more references. However, in all these examples, either the copies of the braid arrangement are perturbed, or they are translated non-generically. We have not been able to find the (ℓ, n) -braid arrangement \mathcal{B}_n^ℓ properly treated in the literature.

Remark 1.16. Part of our discussion on the (ℓ, n) -braid arrangement \mathcal{B}_n^ℓ could actually be developed for a hyperplane arrangement \mathcal{A}^ℓ obtained as the union of ℓ generically translated copies of an arbitrary linear hyperplane arrangement \mathcal{A} . Similarly to Proposition 2.3, the flat poset $\text{Fl}(\mathcal{A}^\ell)$ is isomorphic to the lower set of the ℓ^{th} Cartesian power of the flat poset $\text{Fl}(\mathcal{A})$ induced by the ℓ -tuples whose meet in the flat poset $\text{Fl}(\mathcal{A})$ is the bottom element $\mathbf{0}$ (these are sometimes called strong antichains) and which are minimal for this property. Similar to Theorem 2.4, this yields a general formula for the Möbius polynomial of \mathcal{A}^ℓ in terms of the Möbius function of the flat poset $\text{Fl}(\mathcal{A})$. Here, we additionally benefit from the nice properties of the Möbius polynomial of the braid arrangement \mathcal{B}_n to obtain appealing formulas for the vertices, regions and bounded regions of the (ℓ, n) -braid arrangement \mathcal{B}_n^ℓ (see Theorems 2.18 to 2.21). We have therefore decided to restrict our attention to the (ℓ, n) -braid arrangement \mathcal{B}_n^ℓ .

2. FLAT POSET AND ENUMERATION OF \mathcal{B}_n^ℓ

In this section, we describe the flat poset of the (ℓ, n) -braid arrangement \mathcal{B}_n^ℓ in terms of (ℓ, n) -partition forests and derive explicit formulas for its f -vector. Remarkably, the flat poset (and thus the Möbius, f - and b -polynomials) of \mathcal{B}_n^ℓ is independent of the translation vectors as long as they are generic.

2.1. Partition forests. We first introduce the main characters of this section, which will describe the combinatorics of the flat poset of the (ℓ, n) -braid arrangement \mathcal{B}_n^ℓ of Definition 1.14.

Definition 2.1. The *intersection hypergraph* of a ℓ -tuple $\mathbf{F} := (F_1, \dots, F_\ell)$ of set partitions of $[n]$ is the ℓ -regular ℓ -partite hypergraph on all parts of all the partitions F_i for $i \in [\ell]$, with a hyperedge connecting the parts containing j for each $j \in [n]$.

Definition 2.2. An (ℓ, n) -*partition forest* (resp. (ℓ, n) -*partition tree*) is a ℓ -tuple $\mathbf{F} := (F_1, \dots, F_\ell)$ of set partitions of $[n]$ whose intersection hypergraph is a hyperforest (resp. hypertree). See Figure 6. The *dimension* of \mathbf{F} is $\dim(\mathbf{F}) := n - 1 - \ell n + \sum_{i \in [\ell]} \#F_i$. The (ℓ, n) -*partition forest poset* is the poset Φ_n^ℓ on (ℓ, n) -partition forests ordered by componentwise refinement.

In other words, Φ_n^ℓ is the lower set of the ℓ^{th} Cartesian power of the partition poset Π_n induced by (ℓ, n) -partition forests. Note that the maximal elements of Φ_n^ℓ are the (ℓ, n) -partition trees.

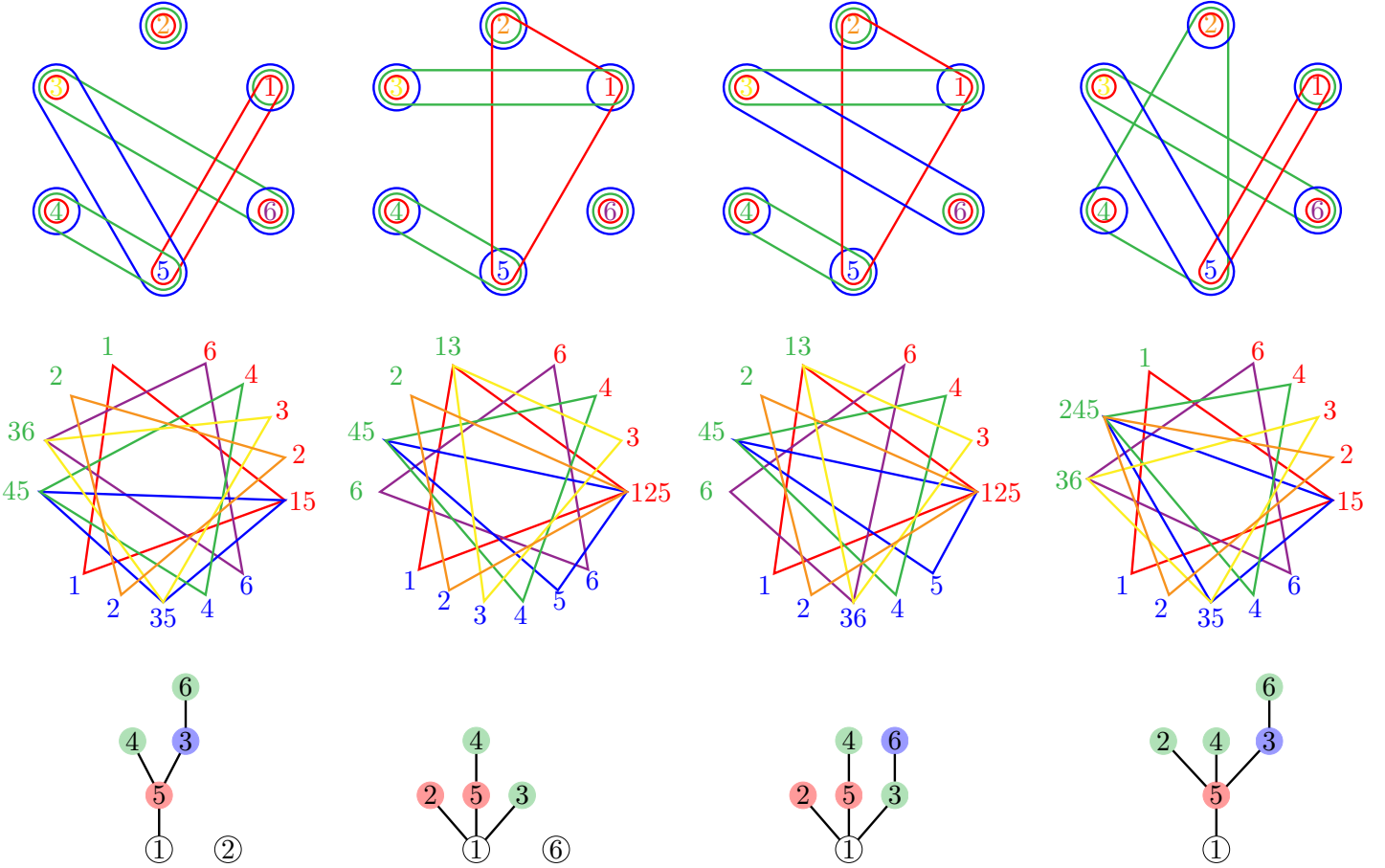


FIGURE 6. Some $(3, 6)$ -partition forests (top) with their intersection hypergraphs (middle) and the corresponding labeled $(3, 6)$ -rainbow forests (bottom). The last two are trees. The order of the colors in the bottom pictures is red, green, blue.

The following statement is illustrated in Figure 7.

Proposition 2.3. *The flat poset $\text{Fl}(\mathcal{B}_n^\ell)$ of the (ℓ, n) -braid arrangement \mathcal{B}_n^ℓ is isomorphic to the (ℓ, n) -partition forest poset.*

Proof. Consider that \mathcal{B}_n^ℓ is the \mathbf{a} -braid arrangement $\mathcal{B}_n^\ell(\mathbf{a})$ for some generic matrix \mathbf{a} . In view of our discussion in Section 1.2, observe that, for each $i \in [\ell]$, each set partition π of $[n]$ corresponds to a $(\#\pi)$ -dimensional flat

$$\Psi_i(\pi) := \{\mathbf{x} \in \mathbb{H} \mid x_s - x_t = A_{i,s,t} \text{ for all } s, t \text{ in the same part of } \pi\}$$

of the i^{th} copy of the braid arrangement \mathcal{B}_n . The flats of the (ℓ, n) -braid arrangement \mathcal{B}_n^ℓ are thus all of the form

$$\Psi(\mathbf{F}) := \bigcap_{i \in [\ell]} \Psi_i(F_i)$$

for certain ℓ -tuples $\mathbf{F} := (F_1, \dots, F_\ell)$ of set partitions of $[n]$. Since the matrix \mathbf{a} is generic, $\Psi(\mathbf{F})$ is non-empty if and only if the intersection hypergraph of \mathbf{F} is acyclic. Moreover, $\Psi(\mathbf{F})$ is included in $\Psi(\mathbf{G})$ if and only if \mathbf{F} refines \mathbf{G} componentwise. Hence, the flat poset of \mathcal{B}_n^ℓ is isomorphic to the (ℓ, n) -partition forest poset. Finally, notice that the codimension of the flat $\Psi(\mathbf{F})$ is the sum of the codimensions of the flats $\Psi_i(F_i)$ for $i \in [\ell]$, so that $\dim(\mathbf{F}) := n - 1 - \ell n + \sum_{i \in [\ell]} \#F_i$ is indeed the dimension of the flat $\Psi(\mathbf{F})$. \square

2.2. Möbius polynomial. We now derive from Definition 1.4 and Proposition 2.3 the Möbius polynomial of the (ℓ, n) -braid arrangement \mathcal{B}_n^ℓ .

Theorem 2.4. *The Möbius polynomial of the (ℓ, n) -braid arrangement \mathcal{B}_n^ℓ is given by*

$$\mu_{\mathcal{B}_n^\ell}(x, y) = x^{n-1-\ell n} y^{n-1-\ell n} \sum_{\mathbf{F} \leq \mathbf{G}} \prod_{i \in [\ell]} x^{\#F_i} y^{\#G_i} \prod_{p \in G_i} (-1)^{\#F_i[p]-1} (\#F_i[p] - 1)!,$$

where $\mathbf{F} \leq \mathbf{G}$ ranges over all intervals of the (ℓ, n) -partition forest poset Φ_n^ℓ , and $F_i[p]$ denotes the restriction of the partition F_i to the part p of G_i .

Proof. Observe that for $\mathbf{F} := (F_1, \dots, F_\ell)$ and $\mathbf{G} := (G_1, \dots, G_\ell)$ in Φ_n^ℓ , we have

$$[\mathbf{F}, \mathbf{G}] = \prod_{i \in [\ell]} [F_i, G_i] \simeq \prod_{i \in [\ell]} \prod_{p \in G_i} \Pi_{\#F_i[p]}.$$

Recall that the Möbius function is multiplicative: $\mu_{P \times Q}((p, q), (p', q')) = \mu_P(p, p') \cdot \mu_Q(q, q')$, for all $p, p' \in P$ and $q, q' \in Q$. Hence, we obtain that

$$\mu_{\Phi_n^\ell}(\mathbf{F}, \mathbf{G}) = \prod_{i \in [\ell]} \prod_{p \in G_i} (-1)^{\#F_i[p]-1} (\#F_i[p] - 1)!.$$

Hence, we derive from Definition 1.4 and Proposition 2.3 that

$$\begin{aligned} \mu_{\mathcal{B}_n^\ell}(x, y) &= \sum_{\mathbf{F} \leq \mathbf{G}} \mu_{\Phi_n^\ell}(\mathbf{F}, \mathbf{G}) x^{\dim(\mathbf{F})} y^{\dim(\mathbf{G})} \\ &= x^{n-1-\ell n} y^{n-1-\ell n} \sum_{\mathbf{F} \leq \mathbf{G}} \prod_{i \in [\ell]} x^{\#F_i} y^{\#G_i} \prod_{p \in G_i} (-1)^{\#F_i[p]-1} (\#F_i[p] - 1)!. \end{aligned} \quad \square$$

By using the polynomial

$$\pi_n(x) := \mu_{\mathcal{B}_n}(x, 0) = \sum_{k \in [n]} (-1)^{k-1} (k-1)! S(n, k) x^{k-1}$$

introduced at the end of Section 1.2, the Möbius polynomial $\mu_{\mathcal{B}_n^\ell}(x, y)$ can also be expressed as follows.

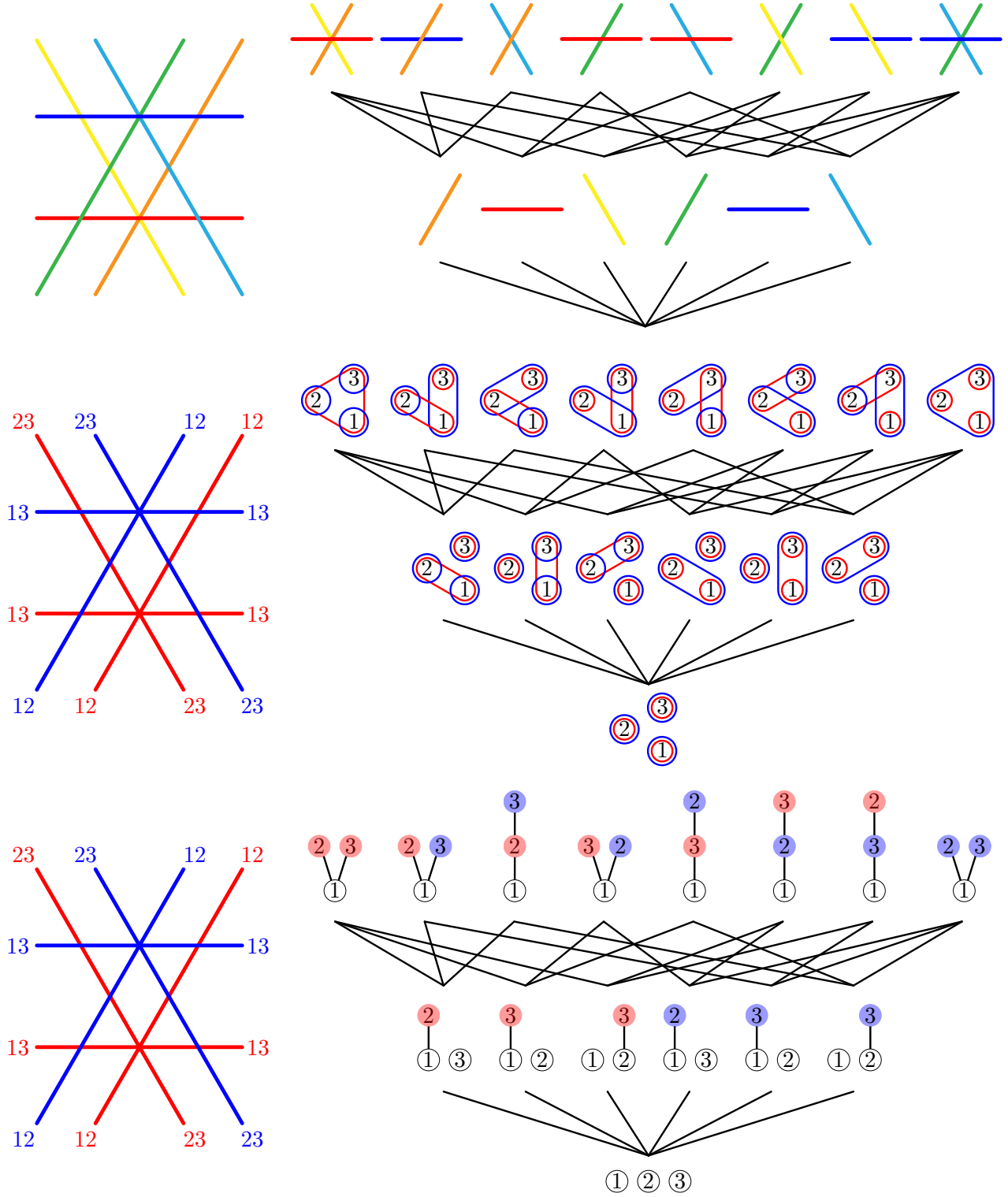


FIGURE 7. The $(2,3)$ -braid arrangement \mathcal{B}_3^2 (left), and its flat poset (right), where flats are represented as intersections of hyperplanes (top), as $(2,3)$ -partitions forests (middle), and as labeled $(2,3)$ -rainbow forests (bottom).

$\ell = 1$						$\ell = 2$						$\ell = 3$						$\ell = 4$					
$n \setminus k$	0	1	2	3	Σ	$n \setminus k$	0	1	2	3	Σ	$n \setminus k$	0	1	2	3	Σ	$n \setminus k$	0	1	2	3	Σ
1	1				1	1	1				1	1	1				1	1	1				1
2	2	1			3	2	3	2			5	2	4	3			7	2	5	4			9
3	6	6	1		13	3	17	24	8		49	3	34	54	21		109	3	57	96	40		193
4	24	36	14	1	75	4	149	324	226	50	749	4	472	1152	924	243	2791	4	1089	2808	2396	676	6969
$n \setminus k$	0	1	2	3	Σ	$n \setminus k$	0	1	2	3	Σ	$n \setminus k$	0	1	2	3	Σ	$n \setminus k$	0	1	2	3	Σ
1	1				1	1	1				1	1	1				1	1	1				1
2	0	1			1	2	1	2			3	2	2	3			5	2	3	4			7
3	0	0	1		1	3	5	12	8		25	3	16	36	21		73	3	33	72	40		145
4	0	0	0	1	1	4	43	132	138	50	363	4	224	684	702	243	1853	4	639	1944	1980	676	5239

TABLE 1. The face numbers (top) and the bounded face numbers (bottom) of the (ℓ, n) -braid arrangements for $\ell, n \in [4]$.

Proposition 2.5. *The Möbius polynomial of the (ℓ, n) -braid arrangement \mathcal{B}_n^ℓ is given by*

$$\mu_{\mathcal{B}_n^\ell}(x, y) = x^{(n-1)(1-\ell)} \sum_{G \in \Phi_n^\ell} y^{n-1-\ell n + \sum_{i \in [\ell]} \#G_i} \prod_{i \in [\ell]} \pi_{\#G_i}(x).$$

Proof. As already mentioned, the (ℓ, n) -partition forest poset Φ_n^ℓ is a lower set of the ℓ^{th} Cartesian power of the partition poset Π_n . In other words, given a (ℓ, n) -partition forest $\mathbf{G} := (G_1, \dots, G_\ell)$, any ℓ -tuple $\mathbf{F} := (F_1, \dots, F_\ell)$ of partitions satisfying $F_i \leq_{\Pi_n} G_i$ for all $i \in [\ell]$ is a (ℓ, n) -partition forest. Hence, we obtain from Definition 1.4 and Proposition 2.3 that

$$\begin{aligned} \mu_{\mathcal{B}_n^\ell}(x, y) &= \sum_{G \in \Phi_n^\ell} y^{n-\ell n-1+\sum_{i \in [\ell]} \#G_i} \prod_{i \in [\ell]} \sum_{F_i \leq_{\Pi_n} G_i} \mu_{\Pi_n}(F_i, G_i) x^{n-\ell n-1+\sum_{i \in [\ell]} \#F_i}, \\ &= \sum_{G \in \Phi_n^\ell} y^{n-\ell n-1+\sum_{i \in [\ell]} \#G_i} x^{(n-1)(1-\ell)} \prod_{i \in [\ell]} \sum_{\pi_i \in \Pi_{\#G_i}} \mu_{\Pi_{\#G_i}}(\pi_i, \hat{1}) x^{\#\pi_i-1}, \end{aligned}$$

where $\hat{1}$ denotes the maximal element in $\Pi_{\#G_i}$ and π_i is obtained from F_i by merging elements in the same part of G_i . The result follows since $\pi_{\#G_i}(x) = \sum_{\pi_i \in \Pi_{\#G_i}} \mu_{\Pi_{\#G_i}}(\pi_i, \hat{1}) x^{\#\pi_i-1}$. \square

From Theorems 1.6 and 2.4, we thus obtain the face numbers and bounded face numbers of \mathcal{B}_n^ℓ , whose first few values are gathered in Table 1.

Corollary 2.6. *The f - and b -polynomials of the (ℓ, n) -braid arrangement \mathcal{B}_n^ℓ are given by*

$$\begin{aligned} f_{\mathcal{B}_n^\ell}(x) &= x^{n-1-\ell n} \sum_{\mathbf{F} \leq \mathbf{G}} \prod_{i \in [\ell]} x^{\#F_i} \prod_{p \in G_i} (\#F_i[p] - 1)!, \\ \text{and} \quad b_{\mathcal{B}_n^\ell}(x) &= (-1)^\ell x^{n-1-\ell n} \sum_{\mathbf{F} \leq \mathbf{G}} \prod_{i \in [\ell]} x^{\#F_i} \prod_{p \in G_i} -(\#F_i[p] - 1)!, \end{aligned}$$

where $\mathbf{F} \leq \mathbf{G}$ ranges over all intervals of the (ℓ, n) -partition forest poset Φ_n^ℓ , and $F_i[p]$ denotes the restriction of the partition F_i to the part p of G_i .

Example 2.7. For $n = 1$, we have

$$\mu_{\mathcal{B}_1^\ell}(x, y) = f_{\mathcal{B}_1^\ell}(x) = b_{\mathcal{B}_1^\ell}(x) = 1.$$

For $n = 2$, we have

$$\mu_{\mathcal{B}_2^\ell}(x, y) = xy - \ell x + \ell, \quad f_{\mathcal{B}_2^\ell}(x) = (\ell + 1)x + \ell \quad \text{and} \quad b_{\mathcal{B}_2^\ell}(x) = (\ell - 1)x + \ell.$$

The case $n = 3$ is already more interesting. Consider the set partitions $P := \{\{1\}, \{2\}, \{3\}\}$, $Q_i := \{\{i\}, [3] \setminus \{i\}\}$ for $i \in [3]$, and $R := \{[3]\}$. Observe that the $(\ell, 3)$ -partition forests are all of the form

$$\mathbf{F} := P^\ell, \quad \mathbf{G}_i^p := P^p Q_i P^{\ell-p-1}, \quad \mathbf{H}_{i,j}^{p,q} := P^p Q_i P^{\ell-p-q-2} Q_j P^q \quad (i \neq j) \quad \text{or} \quad \mathbf{K}^p := P^p R P^{\ell-p-1}.$$

(where we write a tuple of partitions of $[3]$ as a word on $\{P, Q_1, Q_2, Q_3, R\}$). Moreover, the cover relations in the $(\ell, 3)$ -partition forest poset are precisely the relations

$$\begin{array}{c} \swarrow \mathbf{H}_{i,j}^{p,q} \\ \mathbf{F} \leq \mathbf{G}_i^p \leq \mathbf{K}^p \\ \searrow \mathbf{H}_{j,i}^{\ell-q-1, \ell-p-1} \end{array}$$

for $i \neq j$ and p, q such that $p + q \leq \ell - 2$. Hence, we have

$$\begin{aligned} \mu_{\mathcal{B}_3^\ell}(x, y) &= x^2 y^2 - 3\ell x^2 y + \ell(3\ell - 1)x^2 + 3\ell xy - 3\ell(2\ell - 1)x + \ell(3\ell - 2), \\ \mathbf{f}_{\mathcal{B}_3^\ell}(x) &= (3\ell^2 + 2\ell + 1)x^2 + 6\ell^2 x + \ell(3\ell - 2), \\ \text{and } \mathbf{b}_{\mathcal{B}_3^\ell}(x) &= (3\ell^2 - 4\ell + 1)x^2 + 6\ell(\ell - 1)x + \ell(3\ell - 2). \end{aligned}$$

Observe that $3\ell^2 + 2\ell + 1$ is [OEI10, A056109], that $\ell(3\ell - 2)$ is [OEI10, A000567], and that $3\ell^2 - 4\ell + 1$ is [OEI10, A045944].

2.3. Rainbow forests. In order to obtain more explicit formulas for the number of vertices and regions of the (ℓ, n) -braid arrangement \mathcal{B}_n^ℓ in Sections 2.4 and 2.5, we now introduce another combinatorial model for (ℓ, n) -partition forests which is more adapted to their enumeration.

Definition 2.8. An ℓ -rainbow coloring of a rooted plane forest F is an assignment of colors of $[\ell]$ to the non-root nodes of F such that

- (i) there is no monochromatic edge,
- (ii) the colors of siblings are increasing from left to right.

We denote by $\|F\|$ the number of nodes of F and by $\#F$ the number of trees of the forest F (i.e. its number of connected components). An (ℓ, n) -rainbow forest (resp. tree) is a ℓ -rainbow colored forest (resp. tree) with $\|F\| = n$ nodes. We denote by Ψ_n^ℓ (resp. \mathbf{T}_n^ℓ) the set of (ℓ, n) -rainbow forests (resp. trees), and set $\Psi^\ell := \bigsqcup_n \Psi_n^\ell$ (resp. $\mathbf{T}^\ell := \bigsqcup_n \mathbf{T}_n^\ell$).

For instance, we have listed the 14 $(2, 4)$ -rainbow trees in Figure 8 (top). This figure actually illustrates the following statement.

Lemma 2.9. The (ℓ, m) -rainbow trees are counted by the Fuss-Catalan number

$$\#\mathbf{T}_m^\ell = F_{\ell, m} := \frac{1}{(\ell - 1)m + 1} \binom{\ell m}{m} \quad [\text{OEI10, A062993}].$$

Proof. We can transform a ℓ -rainbow tree R to an ℓ -ary tree T as illustrated in Figure 8. Namely, the parent of a node N in T is the previous sibling colored as N in R if it exists, and the parent of N in R otherwise. This classical map is a bijection from ℓ -rainbow trees to ℓ -ary trees, which are counted by the Fuss-Catalan numbers [Kla70, HP91]. \square

Remark 2.10. Recall that the corresponding generating function $F_\ell(z) := \sum_{m \geq 0} F_{\ell, m} z^m$ satisfies the functional equation

$$F_\ell(z) = 1 + z F_\ell(z)^\ell.$$

Definition 2.11. For a (ℓ, n) -rainbow forest F , we define

$$\omega(F) := \prod_{i \in [\ell]} \prod_{N \in F} \#C_i(N)!,$$

where N ranges over all nodes of F and $C_i(N)$ denotes the children of N colored by i .

Definition 2.12. A labeling of a (ℓ, n) -rainbow forest F is a bijective map from the nodes of F to $[n]$ such that

- (i) the label of each root is minimal in its tree,
- (ii) the labels of siblings with the same color are increasing from left to right.

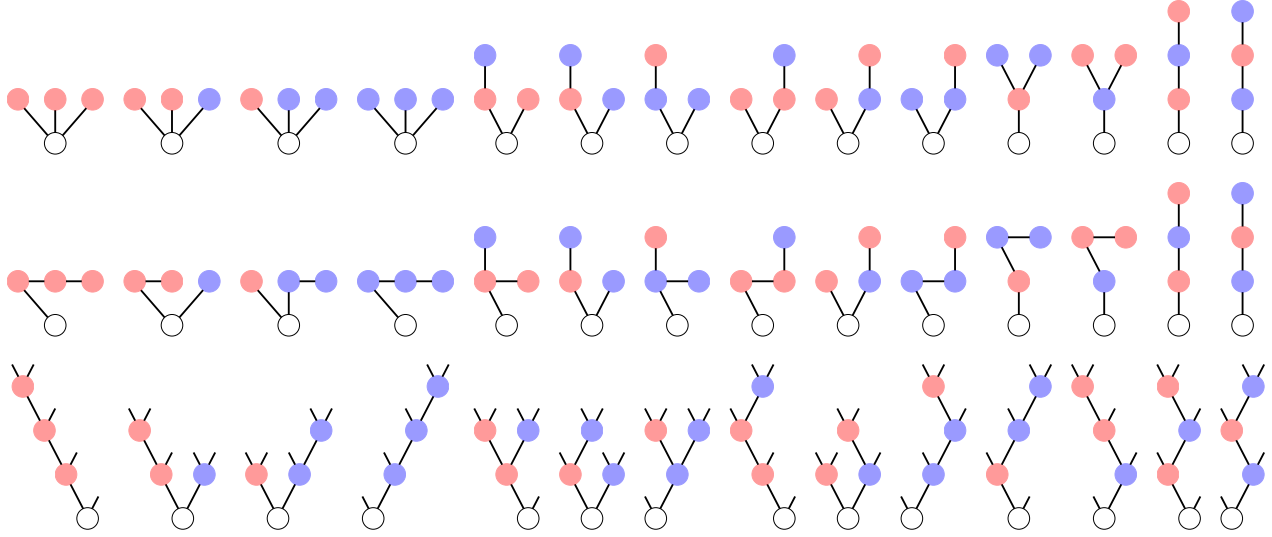


FIGURE 8. The 14 $(2, 4)$ -rainbow trees (top) and 14 binary trees (bottom), and the simple bijection between them (middle). The order of the colors is red, blue.

$m \setminus \ell$	1	2	3	4	5	6	7	8	9
1	1	1	1	1	1	1	1	1	1
2	1	2	3	4	5	6	7	8	9
3	1	5	12	22	35	51	70	92	117
4	1	14	55	140	285	506	819	1240	1785
5	1	42	273	969	2530	5481	10472	18278	29799
6	1	132	1428	7084	23751	62832	141778	285384	527085
7	1	429	7752	53820	231880	749398	1997688	4638348	9706503
8	1	1430	43263	420732	2330445	9203634	28989675	77652024	184138713
9	1	4862	246675	3362260	23950355	115607310	430321633	1329890705	3573805950

TABLE 2. The Fuss-Catalan numbers $F_{\ell, m} = \frac{1}{(\ell-1)m+1} \binom{\ell m}{m}$ for $\ell, m \in [9]$. See [OEI10, A062993].

Lemma 2.13. *The number $\lambda(F)$ of labelings of a (ℓ, n) -rainbow forest F is given by*

$$\lambda(F) = \frac{n!}{\omega(F) \prod_{T \in F} \|T\|}.$$

Proof. Out of all $n!$ bijective maps from the nodes of F to $[n]$, only $1/\prod_{T \in F} \|T\|$ satisfy Condition (i) of Definition 2.12, and only $1/\prod_{i \in [\ell]} \prod_{N \in F} \#C_i(N)! = 1/\omega(F)$ satisfy Condition (ii) of Definition 2.12. \square

The following statement is illustrated in Figure 6.

Proposition 2.14. *There is a bijection from (ℓ, n) -partition forests to labeled (ℓ, n) -rainbow forests, such that if the partition forest \mathbf{F} is sent to the labeled rainbow forest F , then*

$$\dim(\mathbf{F}) = \#F - 1 \quad \text{and} \quad \mu_{\Phi_n^\ell}(\mathbb{H}, \mathbf{F}) = (-1)^{n-\#F} \omega(F).$$

Proof. From a labeled (ℓ, n) -rainbow forest F , we construct a (ℓ, n) -partition forest $\mathbf{F} := (F_1, \dots, F_\ell)$ whose i^{th} partition F_i has a part $\{N\} \cup C_i(N)$ for each node N of F not colored i . Condition (i) of Definition 2.8 ensures that each F_i is indeed a partition.

Conversely, start from a (ℓ, n) -partition forest $\mathbf{F} := (F_1, \dots, F_\ell)$. Consider the colored clique graph $K_{\mathbf{F}}$ on $[n]$ obtained by replacing each part in F_i by a clique of edges colored by i . For each $1 < j \leq n$, there is a unique shortest path in $K_{\mathbf{F}}$ from the vertex j to the smallest vertex in

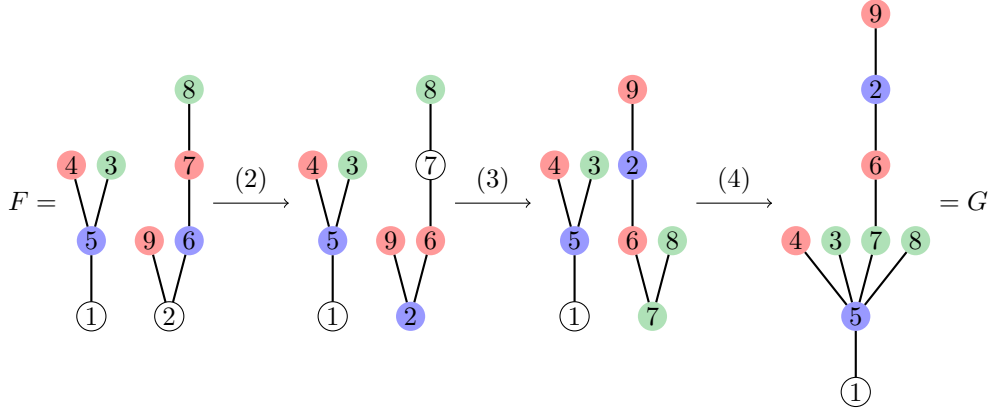


FIGURE 9. A covering relation described in Proposition 2.15, choosing c to be green, a to be 5 and b to be 7.

the connected component of j . Define the parent p of j to be the next vertex along this path, and color the node j by the color of the edge between j and p . This defines a labeled (ℓ, n) -rainbow forest F .

Finally, observe that

$$\dim(\mathbf{F}) = n - 1 - \ell n + \sum_{i \in [\ell]} \#F_i = \#F - 1, \quad \text{and}$$

$$\mu_{\Phi_n^\ell}(\mathbb{H}, \mathbf{F}) = \prod_{i \in [\ell]} \prod_{p \in F_i} (-1)^{\#p-1} (\#p - 1) = \prod_{i \in [\ell]} \prod_{N \in F} (-1)^{\#C_i(N)} \#C_i(N)! = (-1)^{n-\#F} \omega(\mathbf{F}). \square$$

We now transport via this bijection the partial order of the flat lattice on rainbow forests. For a node a of a forest F , we denote by $\text{Root}(a)$ the root of the tree of F containing a . The following statement is illustrated in Figure 9, choosing c to be green, a to be 5 and b to be 7.

Proposition 2.15. *In the flat poset $\text{Fl}(\mathcal{B}_n^\ell)$ labeled by rainbow forests using Propositions 2.3 and 2.14, a rainbow forest F is covered by a rainbow forest G if and only if G can be obtained from F by:*

- (1) *choosing a color c , and two vertices a and b not colored with c and with $\text{Root}(a) < \text{Root}(b)$,*
- (2) *shifting the colors along the path from $\text{Root}(b)$ to b , so that each node along this path is now colored by the former color of its child and b is not colored anymore,*
- (3) *rerooting at b the tree containing b at b , and coloring b with c ,*
- (4) *adding an edge (a, b) and replacing the edge (b, e) by an edge (a, e) for each child e of b colored with c .*

Proof. Let us first remark that the graph obtained by these operations is indeed a rainbow forest. First, we add an edge between two distinct connected components, so that the result is indeed acyclic. Moreover, the condition on the color of a and on the deletion of edges between b and vertices of color c ensures that we do not add an edge between two vertices of the same color. Note that the parent of b inherits the color of b which is not c .

Let us recall that the cover relations in the flat poset $\text{Fl}(\mathcal{B}_n^\ell)$ are given in terms of (ℓ, n) -partition forests by choosing a partition π of the partition tuple (which corresponds directly to choosing a color), choosing two parts π_a and π_b in the partition π , and merging them, without creating a loop in the intersection hypergraph.

By choosing two vertices in different connected components of the rainbow forest, we are sure that the intersection hypergraph obtained by adding an edge is still acyclic.

The last point that has to be explained is the link between the condition on the color of a and merging two parts in the same partition. If one of the two nodes, say a for instance is of color c , then it belongs to the same part of π as its parent z . The merging is the same if we choose z

$n \setminus \ell$	1	2	3	4	5	6	7	8
1	1	1	1	1	1	1	1	1
2	1	2	3	4	5	6	7	8
3	1	8	21	40	65	96	133	176
4	1	50	243	676	1445	2646	4375	6728
5	1	432	3993	16384	46305	105456	208537	373248
6	1	4802	85683	521284	1953125	5541126	13119127	27350408
7	1	65536	2278125	20614528	102555745	362797056	1029059101	2500000000
8	1	1062882	72412707	976562500	6457339845	28500625446	96889010407	274371577992

TABLE 3. The numbers $f_0(\mathcal{B}_n^\ell) = \ell((\ell - 1)n + 1)^{n-2}$ of vertices of \mathcal{B}_n^ℓ for $\ell, n \in [8]$.

which is not colored c . Moreover, as b is in a different connected component, the corresponding two parts are distinct in π . Finally, a part is just a corolla so the merging corresponds to building a corolla with a , b and their children of color c . \square

We finally recast Proposition 2.5 in terms of rainbow forests.

Proposition 2.16. *The Möbius polynomial of the (ℓ, n) -braid arrangement \mathcal{B}_n^ℓ is given by*

$$\mu_{\mathcal{B}_n^\ell}(x, y) = x^{(n-1)(1-\ell)} \sum_{G \in \Psi_n^\ell} y^{n-1+\#E(G)} \prod_{i \in [\ell]} \pi_{n-\#E(G,i)}(x).$$

Remark 2.17. To further simplify this expression, we would need to count the number of rainbow forests with a prescribed number of colored edges. However, this number does not admit a known multiplicative formula, up to our knowledge. When there is only one color, the corresponding sequence (counting non-colored forests on n nodes and k edges, rooted in the minimal label of each connected component) is [OEI10, A138464].

2.4. Enumeration of vertices of \mathcal{B}_n^ℓ . We now use the labeled (ℓ, n) -rainbow forests of Section 2.3 to derive more explicit formulas for the number of vertices of the (ℓ, n) -braid arrangement \mathcal{B}_n^ℓ . The first few values are gathered in Table 3.

Theorem 2.18. *The number of vertices of the (ℓ, n) -braid arrangement \mathcal{B}_n^ℓ is*

$$f_0(\mathcal{B}_n^\ell) = \ell((\ell - 1)n + 1)^{n-2}.$$

Proof. By Propositions 2.3 and 2.14, we just need to count the labeled (ℓ, n) -rainbow trees. A common reasoning for counting Cayley trees is the use of its Prüfer code defined by recursively pruning the smallest leaf while writing down the label of its parent. This bijection can be adapted to colored Cayley trees by writing down the label of the parent colored by the color of the pruned leaf. This leads to a bijection with certain colored words of length $n - 1$. Namely, there are two possibilities:

- either the pruned leaf is attached to the node 1 and it can have all ℓ colors,
- or it is attached to one of the $n - 1$ other nodes and it can only have $\ell - 1$ colors.

Note that the last letter in the Prüfer code (obtained by removing the last edge) is necessarily the root 1, with ℓ possible different colors. Hence, there are

$$(\ell + (n - 1)(\ell - 1))^{n-2} \ell = \ell((\ell - 1)n + 1)^{n-2}$$

such words. Similar ideas were used in [Lew99]. \square

We can refine the formula of Theorem 2.18 according to the dimension of the flats of the different copies intersected to obtain the vertices of the (ℓ, n) -braid arrangement \mathcal{B}_n^ℓ .

Theorem 2.19. *For any k_1, \dots, k_ℓ such that $0 \leq k_i \leq n - 1$ for $i \in [\ell]$ and $\sum_{i \in [\ell]} k_i = n - 1$, the number of vertices v of the (ℓ, n) -braid arrangement \mathcal{B}_n^ℓ such that the smallest flat of the i^{th} copy of \mathcal{B}_n containing v has dimension $n - k_i - 1$ is given by*

$$n^{\ell-1} \binom{n-1}{k_1, \dots, k_\ell} \prod_{i \in [\ell]} (n - k_i)^{k_i-1}.$$

Proof. By Propositions 2.3 and 2.14, we just need to count the labeled (ℓ, n) -rainbow trees with k_i nodes colored by i . Forgetting the labels, the (ℓ, n) -rainbow trees with k_i nodes colored by i are precisely the spanning trees of the complete multipartite graph $K_{k_1, \dots, k_\ell, 1}$ (where the last 1 stands for the uncolored root). Using a Prüfer code similar to that of the proof of Theorem 2.18, R. Lewis proved in [Lew99] that the latter are counted by $n^{\ell-1} \prod_{i \in [\ell]} (n - k_i)^{k_i-1}$. Finally, the possible labelings are counted by the multinomial coefficient $\binom{n-1}{k_1, \dots, k_\ell}$. \square

2.5. Enumeration of regions and bounded regions of \mathcal{B}_n^ℓ . We finally use the labeled (ℓ, n) -rainbow forests of Section 2.3 to derive more explicit formulas for the number of regions and bounded regions of the (ℓ, n) -braid arrangement \mathcal{B}_n^ℓ . The first few values are gathered in Tables 4 and 5. We first compute the characteristic polynomial of \mathcal{B}_n^ℓ .

Theorem 2.20. *The characteristic polynomial $\chi_{\mathcal{B}_n^\ell}(y)$ of the (ℓ, n) -braid arrangement \mathcal{B}_n^ℓ is given by*

$$\chi_{\mathcal{B}_n^\ell}(y) = \frac{(-1)^n n!}{y} [z^n] \exp \left(- \sum_{m \geq 1} \frac{F_{\ell, m} y z^m}{m} \right),$$

where $F_{\ell, m} := \frac{1}{(\ell-1)m+1} \binom{\ell m}{m}$ is the Fuss-Catalan number.

Proof. By Theorem 2.4 and Proposition 2.14, the characteristic polynomial $\chi_{\mathcal{B}_n^\ell}(y)$ is

$$\chi_{\mathcal{B}_n^\ell}(y) = \sum_{F \in \Phi_n^\ell} \mu_{\Phi_n^\ell}(\mathbb{H}, F) y^{\dim(F)} = \sum_{F \in \Psi_n^\ell} \lambda(F) (-1)^{n-\#F} \omega(F) y^{\#F-1}.$$

From Lemma 2.13, we observe that

$$\frac{\lambda(F) \omega(F) (-y)^{\#F} z^{\|F\|}}{\|F\|!} = \prod_{T \in F} \frac{-y z^{\|T\|}}{\|T\|},$$

where T ranges over the trees of F . Now using that rainbow forests are exactly sets of rainbow trees, we obtain that

$$\sum_{F \in \Psi_n^\ell} \frac{\lambda(F) \omega(F) (-y)^{\#F} z^{\|F\|}}{\|F\|!} = \sum_{F \in \Psi_n^\ell} \prod_{T \in F} \frac{-y z^{\|T\|}}{\|T\|} = \exp \left(\sum_{T \in \mathbf{T}^\ell} \frac{-y z^{\|T\|}}{\|T\|} \right).$$

From Lemma 2.9, we obtain that

$$\exp \left(\sum_{T \in \mathbf{T}^\ell} \frac{-y z^{\|T\|}}{\|T\|} \right) = \exp \left(- \sum_{m \geq 1} \frac{F_{\ell, m} y z^m}{m} \right).$$

We conclude that

$$\begin{aligned} \chi_{\mathcal{B}_n^\ell}(y) &= \sum_{F \in \Psi_n^\ell} \lambda(F) (-1)^{n-\#F} \omega(F) y^{\#F-1} \\ &= \frac{(-1)^n n!}{y} [z^n] \sum_{F \in \Psi_n^\ell} \frac{\lambda(F) \omega(F) (-y)^{\#F} z^{\|F\|}}{\|F\|!} \\ &= \frac{(-1)^n n!}{y} [z^n] \exp \left(- \sum_{m \geq 1} \frac{F_{\ell, m} y z^m}{m} \right). \end{aligned} \quad \square$$

From the characteristic polynomial of \mathcal{B}_n^ℓ and Remark 1.8, we obtain its numbers of regions and bounded regions.

$n \setminus \ell$	1	2	3	4	5	6	7	8
1	1	1	1	1	1	1	1	1
2	2	3	4	5	6	7	8	9
3	6	17	34	57	86	121	162	209
4	24	149	472	1089	2096	3589	5664	8417
5	120	1809	9328	29937	73896	154465	287904	493473
6	720	28399	241888	1085157	3442816	8795635	19376064	38323753
7	5040	550297	7806832	49075065	200320816	625812385	1629858672	3720648337
8	40320	12732873	302346112	2666534049	14010892416	53536186825	164859458688	434390214657

TABLE 4. The numbers $f_{n-1}(\mathcal{B}_n^\ell)$ of regions of \mathcal{B}_n^ℓ for $\ell, n \in [8]$.

$n \setminus \ell$	1	2	3	4	5	6	7	8
1	1	1	1	1	1	1	1	1
2	0	1	2	3	4	5	6	7
3	0	5	16	33	56	85	120	161
4	0	43	224	639	1384	2555	4248	6559
5	0	529	4528	17937	49696	111745	219024	389473
6	0	8501	120272	663363	2354624	6455225	14926176	30583847
7	0	169021	3968704	30533409	138995776	464913325	1268796096	2996735329
8	0	4010455	156745472	1684352799	9841053184	40179437975	129465630720	352560518527

TABLE 5. The numbers $b_{n-1}(\mathcal{B}_n^\ell)$ of bounded regions of \mathcal{B}_n^ℓ for $\ell, n \in [8]$.

Theorem 2.21. *The numbers of regions and of bounded regions of the (ℓ, n) -braid arrangement \mathcal{B}_n^ℓ are given by*

$$f_{n-1}(\mathcal{B}_n^\ell) = n! [z^n] \exp \left(\sum_{m \geq 1} \frac{F_{\ell, m} z^m}{m} \right)$$

$$\text{and} \quad b_{n-1}(\mathcal{B}_n^\ell) = (n-1)! [z^{n-1}] \exp \left((\ell-1) \sum_{m \geq 1} F_{\ell, m} z^m \right),$$

where $F_{\ell, m} := \frac{1}{(\ell-1)m+1} \binom{\ell m}{m}$ is the Fuss-Catalan number.

Proof. By Remark 1.8, we obtain from Theorem 2.20 that

$$f_{n-1}(\mathcal{B}_n^\ell) = (-1)^{n-1} \chi_{\mathcal{B}_n^\ell}(-1) = n! [z^n] \exp \left(\sum_{m \geq 1} \frac{F_{\ell, m} z^m}{m} \right),$$

$$b_{n-1}(\mathcal{B}_n^\ell) = (-1)^{n-1} \chi_{\mathcal{B}_n^\ell}(1) = -n! [z^n] \exp \left(- \sum_{m \geq 1} \frac{F_{\ell, m} z^m}{m} \right).$$

To conclude, we thus just need to observe that $U_\ell(z) = \frac{\partial}{\partial z} V_\ell(z)$ where

$$U_\ell(z) := \exp \left((\ell-1) \sum_{m \geq 1} F_{\ell, m} z^m \right) \quad \text{and} \quad V_\ell(z) := - \exp \left(- \sum_{m \geq 1} \frac{F_{\ell, m} z^m}{m} \right).$$

For this, consider the generating functions

$$F_\ell(z) := \sum_{m \geq 0} F_{\ell, m} z^m \quad \text{and} \quad G_\ell(z) := \sum_{m \geq 1} \frac{F_{\ell, m} z^m}{m}.$$

Recall from Remark 2.10 that $F_\ell(z)$ satisfies the functional equation

$$F_\ell(z) = 1 + z F_\ell(z)^\ell.$$

We thus obtain that

$$F'_\ell(z)(1 - \ell z F_\ell(z)^{\ell-1}) = F_\ell(z)^\ell \quad \text{and} \quad F_\ell(z)(1 - \ell z F_\ell(z)^{\ell-1}) = 1 - (\ell-1) z F_\ell(z)^\ell.$$

Combining these two equations, we get

$$(1) \quad F_\ell(z)^{\ell+1} = F'_\ell(z)(1 - (\ell - 1)z F_\ell(z)^\ell).$$

Observe now that

$$(2) \quad z G'_\ell(z) = F_\ell(z) - 1 = z F_\ell(z)^\ell \quad \text{and} \quad G''_\ell(z) = \ell F_\ell(z)^{\ell-1} F'_\ell(z).$$

Hence

$$U_\ell(z) = \exp((\ell - 1)(F_\ell(z) - 1)) = \exp((\ell - 1)z G'_\ell(z))$$

and

$$V'_\ell(z) = \frac{\partial}{\partial z} - \exp(-G_\ell(z)) = G'_\ell(z) \exp(-G_\ell(z)).$$

Consider now the function

$$W_\ell(z) = V'_\ell(z)/U_\ell(z) = G'_\ell(z) \exp(-G_\ell(z) - (\ell - 1)z G'_\ell(z)).$$

Clearly, $W_\ell(0) = 1$. Moreover, using (2), we obtain that its derivative is

$$\begin{aligned} W'_\ell(z) &= \left(G''_\ell(z)(1 - (\ell - 1)z G'_\ell(z)) - \ell G'_\ell(z)^2 \right) \exp(-G_\ell(z) - (\ell - 1)z G'_\ell(z)) \\ &= \ell F_\ell(z)^{\ell-1} \left(F'_\ell(z)(1 - (\ell - 1)z F_\ell(z)^\ell) - F_\ell(z)^{\ell+1} \right) \exp(-G_\ell(z) - (\ell - 1)z G'_\ell(z)), \end{aligned}$$

which vanishes by (1). \square

3. FACE POSET AND COMBINATORIAL DESCRIPTION OF $\mathcal{B}_n^\ell(\mathbf{a})$

In this section, we describe the face poset of the \mathbf{a} -braid arrangement $\mathcal{B}_n^\ell(\mathbf{a})$ in terms of ordered (ℓ, n) -partition forests. This section highly depends on the choice of the translation matrix \mathbf{a} .

3.1. Ordered partition forests. We now introduce the combinatorial objects that will be used to encode the faces of the \mathbf{a} -braid arrangement $\mathcal{B}_n^\ell(\mathbf{a})$ of Definition 1.12.

Definition 3.1. An *ordered (ℓ, n) -partition forest* (resp. *tree*) is an ℓ -tuple $\vec{\mathbf{F}} := (\vec{F}_1, \dots, \vec{F}_\ell)$ of ordered set partitions of $[n]$ such that the corresponding ℓ -tuple $\mathbf{F} := (F_1, \dots, F_\ell)$ of unordered set partitions of $[n]$ forms an (ℓ, n) -partition forest (resp. tree). The *ordered (ℓ, n) -partition forest poset* is the poset Φ_n^ℓ on ordered (ℓ, n) -partition forests ordered by componentwise refinement. In other words, Φ_n^ℓ is the subposet of the ℓ^{th} Cartesian power of the ordered partition poset Π_n induced by ordered (ℓ, n) -partition forests. Note that the maximal elements of Φ_n^ℓ are the ordered (ℓ, n) -partition trees.

The following statement is the analogue of Proposition 2.3, and is illustrated in Figures 10 and 11.

Proposition 3.2. *The face poset $\text{Fa}(\mathcal{B}_n^\ell(\mathbf{a}))$ of the \mathbf{a} -braid arrangement $\mathcal{B}_n^\ell(\mathbf{a})$ is isomorphic to an upper set $\bar{\Phi}_n^\ell(\mathbf{a})$ of the ordered (ℓ, n) -partition forest poset Φ_n^ℓ .*

Proof. The proof is based on that of Proposition 2.3. A face of $\mathcal{B}_n^\ell(\mathbf{a})$ is an intersection of faces of the ℓ copies of \mathcal{B}_n^ℓ , hence corresponds to an ℓ -tuple of ordered partitions of $[n]$. Moreover, the flats supporting these faces intersect, so that the corresponding unordered partitions must form an (ℓ, n) -partition forest. Hence, each face of $\mathcal{B}_n^\ell(\mathbf{a})$ corresponds to a certain ordered (ℓ, n) -partition forest. Moreover, the inclusion of faces of $\mathcal{B}_n^\ell(\mathbf{a})$ translates to the componentwise refinement on ordered partitions. Finally, by genericity, it is immediate that we obtain an upper set of this componentwise refinement order. \square

We now fix a generic translation matrix $\mathbf{a} := (a_{i,j})$ and still denote by $A_{i,s,t} := \sum_{s \leq j < t} a_{i,j}$ for all $1 \leq s < t \leq n$ and $i \in [\ell]$ (and often write $A_{i,t,s}$ for $-A_{i,s,t}$). The objective of this section is to describe

- the ordered (ℓ, n) -partitions forests of the upper set $\bar{\Phi}_n^\ell(\mathbf{a})$ with a given underlying (unordered) (ℓ, n) -partition forest (Section 3.2),
- a criterion to decide whether a given ordered (ℓ, n) -partition forest belongs to the upper set $\bar{\Phi}_n^\ell(\mathbf{a})$, i.e. corresponds to a face of $\mathcal{B}_n^\ell(\mathbf{a})$ (Section 3.3).

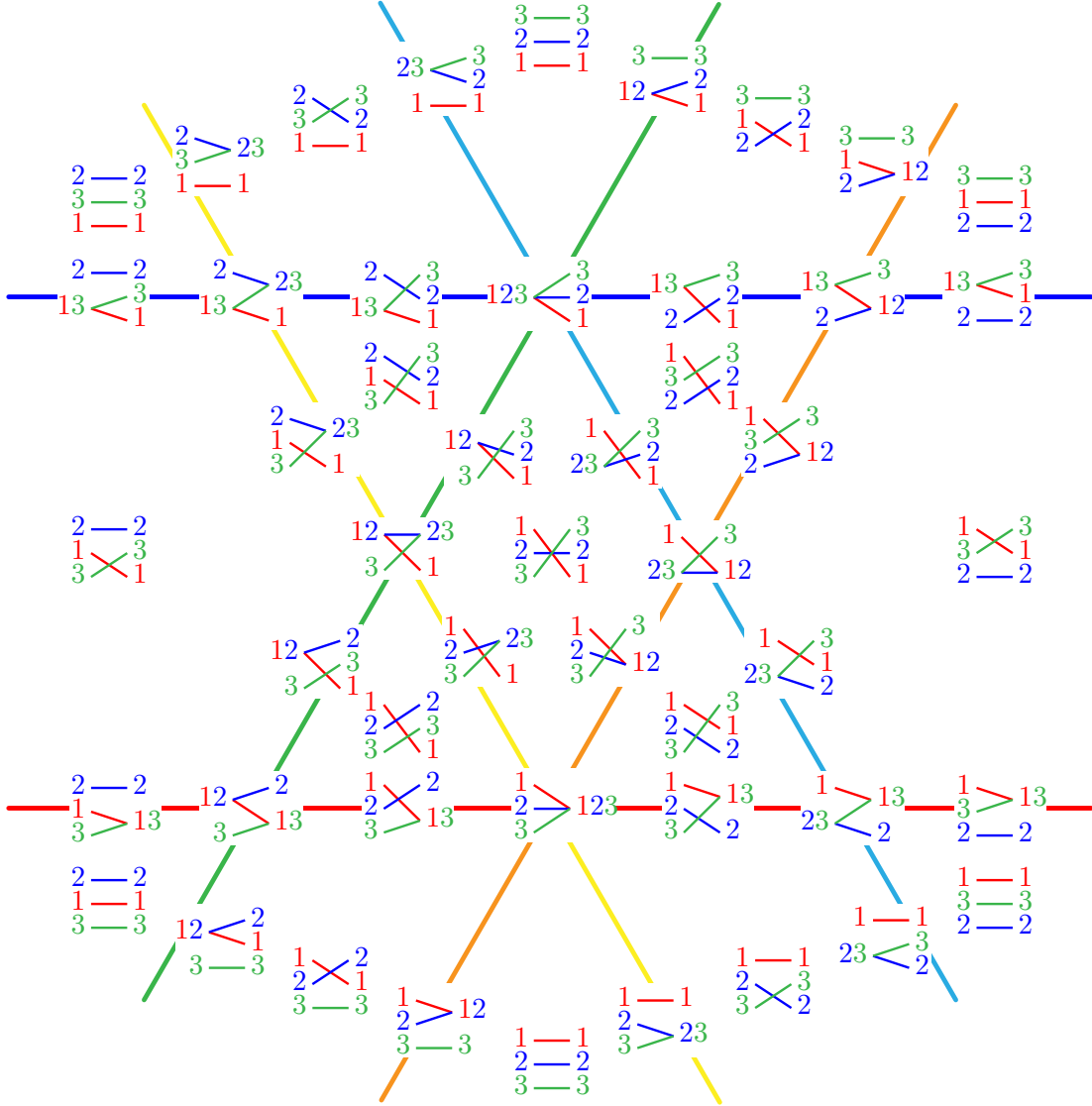


FIGURE 10. Labelings of the faces of the arrangement $\mathcal{B}_3^2(\mathbf{a})$ for $\mathbf{a} = \begin{bmatrix} 0 & 0 \\ -1 & -1 \end{bmatrix}$.

3.2. From partition forests to ordered partition forests. In this section, we describe the ordered (ℓ, n) -partitions forests $\overline{\mathbf{F}}$ of the upper set $\overline{\Phi}_n^\ell(\mathbf{a})$ with a given underlying (ℓ, n) -partition forest \mathbf{F} . We denote by $cc(\mathbf{F})$ the connected components of \mathbf{F} , meaning the partition of $[n]$ given by the hyperedge labels of the connected components of the intersection hypergraph of \mathbf{F} . We first observe that the choice of \mathbf{a} fixes the order of the parts in a common connected component of \mathbf{F} .

Proposition 3.3. *Consider a (ℓ, n) -partition forest $\mathbf{F} := (F_1, \dots, F_\ell)$, and two integers $s, t \in [n]$ labeling two hyperedges in the same connected component of the intersection hypergraph of \mathbf{F} . Assume that the unique path from s to t in the hypergraph of \mathbf{F} passes through the hyperedges labeled by $s = r_0, \dots, r_q = t$ and through parts of the partitions F_{i_1}, \dots, F_{i_q} . Then for any ordered (ℓ, n) -partition forest $\overline{\mathbf{F}} := (\overline{F}_1, \dots, \overline{F}_\ell)$ of the upper set $\overline{\Phi}_n^\ell(\mathbf{a})$ with underlying (ℓ, n) -partition forest \mathbf{F} and any $i \in [\ell]$, the order of s and t in \overline{F}_i is given by the sign of $A_{i,s,t} - \sum_{p \in [q]} A_{i_p, r_p-1, r_p}$.*

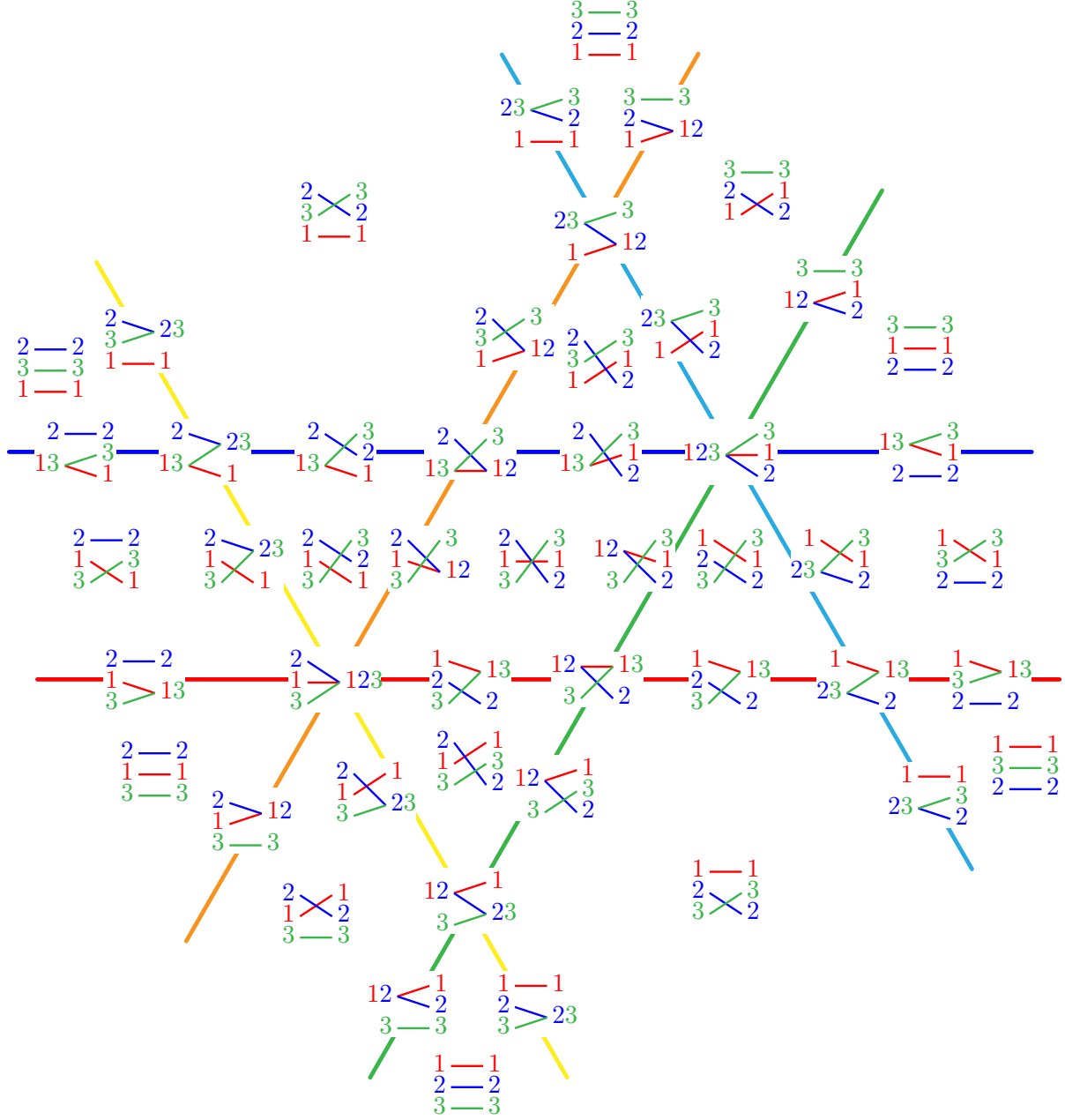


FIGURE 11. Labelings of the faces of the arrangement $\mathcal{B}_3^2(\mathbf{a})$ for $\mathbf{a} = \begin{bmatrix} 0 & 0 \\ 1 & -2 \end{bmatrix}$.

Proof. Consider any point \mathbf{x} in the face of $\mathcal{B}_n^\ell(\mathbf{a})$ corresponding to \vec{F} . Along the path from s to t , we have $x_{r_{p-1}} - x_{r_p} = A_{i_p, r_{p-1}, r_p}$ for each $p \in [q]$. Hence, we obtain that

$$x_s - x_t = \sum_{p \in [q]} (x_{r_{p-1}} - x_{r_p}) = \sum_{p \in [q]} A_{i_p, r_{p-1}, r_p}.$$

The order of s, t in \vec{F}_i is given by the sign of $A_{i, s, t} - (x_s - x_t)$, hence of $A_{i, s, t} - \sum_{p \in [q]} A_{i_p, r_{p-1}, r_p}$. \square

We now describe the different ways to order the parts in distinct connected components of \mathbf{F} . For this, we need the following posets.

Definition 3.4. Consider a (ℓ, n) -partition forest \mathbf{F} and denote by $cc(\mathbf{F})$ the connected components of \mathbf{F} . For each pair $s, t \in [n]$ in distinct connected components of $cc(\mathbf{F})$, we define the chain $<_{s,t}$ on the ℓ triples (i, s, t) for $i \in [\ell]$ given by the order of the values $A_{i,s,t}$. The *inversion poset* $\text{Inv}(\mathbf{F}, \mathbf{a})$ is then the poset obtained by quotienting the disjoint union of the chains $<_{s,t}$ (for all $s, t \in [n]$ in distinct connected components of $cc(\mathbf{F})$) by the equivalence relation $(i, s, t) \equiv (i, s', t')$ if s and s' belong to the same part of F_i and t and t' belong to the same part of F_i . We say that a subset X of $\text{Inv}(\mathbf{F}, \mathbf{a})$ is antisymmetric if $(i, s, t) \in X \iff (i, t, s) \notin X$.

Proposition 3.5. *The ordered (ℓ, n) -partition forests of the upper set $\vec{\Phi}_n^\ell(\mathbf{a})$ with a given underlying (ℓ, n) -partition forest \mathbf{F} are in bijection with the antisymmetric lower sets of the inversion poset $\text{Inv}(\mathbf{F}, \mathbf{a})$.*

Proof. Consider an ordered (ℓ, n) -partition forest \vec{F} of the upper set $\vec{\Phi}_n^\ell(\mathbf{a})$. Let \mathbf{x} be any point of the face of $\mathcal{B}_n^\ell(\mathbf{a})$ corresponding to \vec{F} . For each pair $s, t \in [n]$ in distinct connected components of $cc(\mathbf{F})$, let $I_{s,t}(\mathbf{F})$ be the set of indices $i \in [\ell]$ such that $x_s - x_t < A_{i,s,t}$. Note that $I_{s,t}$ is by definition a lower set of the chain $<_{s,t}$ of $\text{Inv}(\mathbf{F}, \mathbf{a})$. Hence, $I(\vec{F}) := \bigcup_{s,t} I_{s,t} / \equiv$ is a lower set of $\text{Inv}(\mathbf{F}, \mathbf{a})$. Moreover, it is clearly antisymmetric since

$$(i, s, t) \in I(\vec{F}) \iff x_s - x_t < A_{i,s,t} \iff x_t - x_s > A_{i,t,s} \iff (i, t, s) \notin I(\vec{F}).$$

Conversely, given an antisymmetric lower set I of $\text{Inv}(\mathbf{F}, \mathbf{a})$, we can reconstruct an ordered (ℓ, n) -partition forest \vec{F} by ordering each pair $s, t \in [n]$ in F_i

- according to Proposition 3.3 (hence independently of I) if s and t belong to the same connected component of \mathbf{F} ,
- according to I if s and t belong to distinct connected components of \mathbf{F} . Namely, we place the block of \vec{F}_i containing s before the block of \vec{F}_i containing t if and only if $(i, s, t) \in I$.

It is then straightforward to check that the resulting ordered (ℓ, n) -partition forest belongs to the upper set $\vec{\Phi}_n^\ell(\mathbf{a})$, by exhibiting a point \mathbf{x} in of the corresponding face of $\mathcal{B}_n^\ell(\mathbf{a})$. \square

3.3. A criterion for ordered partition forests. We now consider a given ordered (ℓ, n) -partition forest \vec{F} and provide a criterion to decide if it belongs to the upper set $\vec{\Phi}_n^\ell(\mathbf{a})$ corresponding to the faces of $\mathcal{B}_n^\ell(\mathbf{a})$. For this, we need the following directed graph associated to \vec{F} .

Definition 3.6. For an ordered partition $\vec{\pi} := \vec{\pi}_1 | \dots | \vec{\pi}_k$ of $[n]$, we denote by $D_{\vec{\pi}}$ the directed graph on $[n]$ with an arc $\max(\vec{\pi}_j) \rightarrow \min(\vec{\pi}_{j+1})$ for each $j \in [k-1]$ and a cycle $x_1 \rightarrow \dots \rightarrow x_p \rightarrow x_1$ for each part $\vec{\pi}_j = \{x_1 < \dots < x_p\}$. Note that $D_{\vec{\pi}}$ has n vertices and $n + k$ arcs. For an ordered (ℓ, n) -partition forest $\vec{F} := (\vec{F}_1, \dots, \vec{F}_\ell)$, we denote by $D_{\vec{F}}$ the superposition of the directed graphs $D_{\vec{F}_i}$ for $i \in [\ell]$, where the arcs of $D_{\vec{F}_i}$ are labeled by i .

Proposition 3.7. *An ordered (ℓ, n) -partition forest \vec{F} belongs to the upper set $\vec{\Phi}_n^\ell(\mathbf{a})$ if and only if $\sum_{\alpha \in \gamma} A_{i(\alpha), s(\alpha), t(\alpha)} \geq 0$ for any (simple) oriented cycle γ in $D_{\vec{F}}$, where each arc $\alpha \in \gamma$ has label $i(\alpha)$, source $s(\alpha)$, and target $t(\alpha)$.*

Proof. Consider an ordered (ℓ, n) -partition forest $\vec{F} := (\vec{F}_1, \dots, \vec{F}_\ell)$. For each $i \in [\ell]$, denote by

- m_i the number of arcs of $D_{\vec{F}_i}$
- M_i the incidence matrix of $D_{\vec{F}_i}$, with m_i rows and n columns, with a row for each arc α of $D_{\vec{F}_i}$ containing a -1 in column $s(\alpha)$, a 1 in column $t(\alpha)$, and 0 elsewhere,
- \mathbf{z}_i the column vector in \mathbb{R}^{m_i} with a row for each arc α of $D_{\vec{F}_i}$ containing the value $A_{i(\alpha), s(\alpha), t(\alpha)}$.

Then a point $\mathbf{x} \in \mathbb{R}^n$ belongs to the face of the i^{th} braid arrangement corresponding to \vec{F}_i if and only if it satisfies $M_i \mathbf{x} \leq \mathbf{z}_i$. Hence, \vec{F} appears as a face of the \mathbf{a} -braid arrangement if and only if there exists $\mathbf{x} \in \mathbb{R}^n$ such that $M \mathbf{x} \leq \mathbf{z}$, where M is the $(m \times n)$ -matrix (where $m := \sum_{i \in [\ell]} m_i$), obtained by piling the matrices M_i for $i \in [\ell]$ and similarly, \mathbf{z} is the column vector obtained by piling the vectors \mathbf{z}_i . A direct application of the Farkas lemma (see e.g. [Zie98, Prop. 1.7]), there exists $\mathbf{x} \in \mathbb{R}^n$ such that $M \mathbf{x} \leq \mathbf{z}$ if and only if $\mathbf{c} \mathbf{z} \geq 0$ for any $\mathbf{c} \in (\mathbb{R}^m)^*$ with $\mathbf{c} \geq \mathbf{0}$ and $\mathbf{c} M = \mathbf{0}$. Now it is classical that the left kernel of the incidence matrix of a directed graph is generated

by its circuits (non-necessarily oriented cycles), and that the positive cone in this left kernel is generated by its oriented cycles. \square

Remark 3.8. Note that we made some arbitrary choices here by choosing the arc from $\max(\vec{\pi}_j)$ to $\min(\vec{\pi}_{j+1})$ between two consecutive parts $\vec{\pi}_j$ and $\vec{\pi}_{j+1}$ and a cycle inside each part $\vec{\pi}_j$ (while we said that the order in each part is irrelevant). We could instead have considered all arcs connecting two elements of two consecutive parts, or two elements inside the same part. Our choices just limit the amount of oriented cycles in $D_{\vec{\pi}}$.

Part II. Diagonals of permutahedra

In this second part, we study the combinatorics of the diagonals of the permutahedra. In Section 4, we first recall the definition and some known facts about cellular diagonals of polytopes (Section 4.1), which we immediately specialize to the classical permutahedron (Section 4.2), and connect to Part I to derive enumerative statements on the diagonals of permutahedra (Section 4.3). In Section 5, we consider two particular diagonals, the LA and SU diagonals (Section 5.1), we show that these are the only two operadic diagonals which induce the weak order (Section 5.2), and that they are isomorphic (Section 5.3). Using results from Sections 3 and 4, we then characterize their facets in terms of paths in $(2, n)$ -partition trees (Section 5.4), and their vertices as pattern-avoiding pairs of permutations (Section 5.5). Finally, in Section 6, we show that the geometric SU diagonal Δ^{SU} is a topological enhancement of the original Saneblidze-Umble diagonal [SU04] (Section 6.1). In order to prove this result, we define different types of shifts that can be performed on the facets of the SU diagonal, and give several new equivalent definitions of it. These descriptions are directly translated to the LA diagonal via isomorphism (Section 6.2). Moreover, we observe that the shifts define a natural lattice structure on the set of facets of operadic diagonals, that we call the *shift lattice* (Section 6.3). Finally, we present the alternative matrix (Section 6.5) and cubical (Section 6.4) descriptions of the SU diagonal from [SU04, SU22], provide proofs of their equivalence with the other descriptions, and give their LA counterparts.

4. CELLULAR DIAGONALS

4.1. Cellular diagonals for polytopes. As discussed in the introduction, cellular approximations of the thin diagonal for families of polytopes are of fundamental importance in algebraic topology and geometry. They allow one to define the cup product and thus define the ring structure on the cohomology groups of a topological space, and combinatorially on the Chow groups of a toric variety. We now proceed to define thin, cellular, and geometric diagonals.

Definition 4.1. The *thin diagonal* of a set X is the map $\delta : X \rightarrow X \times X$ defined by $\delta(x) := (x, x)$ for all $x \in X$. See Figure 13 (left).

Definition 4.2. A *cellular diagonal* of a d -dimensional polytope P is a continuous map $\Delta : P \rightarrow P \times P$ such that

- (1) its image is a union of d -dimensional faces of $P \times P$ (i.e. it is *cellular*),
- (2) it agrees with the thin diagonal of P on the vertices of P , and
- (3) it is homotopic to the thin diagonal of P , relative to the image of the vertices of P .

See Figure 13 (middle left). A cellular diagonal is said to be *face coherent* if its restriction to a face of P is itself a cellular diagonal for that face.

A powerful geometric technique to define face coherent cellular diagonals on polytopes first appeared in [FS97], was presented in [MTTV21], and was fully developed in [LA22]. We provide in Theorem 4.4 the precise (but slightly technical) definition of these diagonals, even though we will only use the characterization of the faces in their image provided in Theorem 4.6.

The key idea is that any vector \mathbf{v} in generic position with respect to P defines a cellular diagonal of P . For \mathbf{z} a point of P , we denote by $\rho_{\mathbf{z}}P := 2\mathbf{z} - P$ the reflection of P with respect to the point \mathbf{z} .

Definition 4.3. The *fundamental hyperplane arrangement* \mathcal{H}_P of a polytope $P \subset \mathbb{R}^d$ is the set of all linear hyperplanes of \mathbb{R}^d orthogonal to the edges of $P \cap \rho_{\mathbf{z}}P$ for all $\mathbf{z} \in P$. See Figure 12.

A vector is *generic with respect to P* if it does not belong to the union of the hyperplanes of the fundamental hyperplane arrangement \mathcal{H}_P . In particular, such a vector is not perpendicular to any edge of P , and we denote by $\min_{\mathbf{v}}(P)$ (resp. $\max_{\mathbf{v}}(P)$) the unique vertex of P which minimizes (resp. maximizes) the scalar product with \mathbf{v} . Note that the datum of a polytope P together with a vector \mathbf{v} generic with respect to P was called *positively oriented polytope* in [MTTV21, LA22, LAM23].

Theorem 4.4. *For any vector $\mathbf{v} \in \mathbb{R}^d$ generic with respect to P , the tight coherent section $\Delta_{(P,\mathbf{v})}$ of the projection $P \times P \rightarrow P$, $(\mathbf{x}, \mathbf{y}) \mapsto (\mathbf{x} + \mathbf{y})/2$ selected by the vector $(-\mathbf{v}, \mathbf{v})$ defines a cellular diagonal of P . More precisely, $\Delta_{(P,\mathbf{v})}$ is given by the formula*

$$\begin{aligned} \Delta_{(P,\mathbf{v})} : P &\rightarrow P \times P \\ \mathbf{z} &\mapsto (\min_{\mathbf{v}}(P \cap \rho_{\mathbf{z}}P), \max_{\mathbf{v}}(P \cap \rho_{\mathbf{z}}P)). \end{aligned}$$

Definition 4.5. A *geometric diagonal* of a polytope P is a diagonal of the form $\Delta_{(P,\mathbf{v})}$ for some vector $\mathbf{v} \in \mathbb{R}^d$ generic with respect to P .

Note that the geometric diagonal $\Delta_{(P,\mathbf{v})}$ only depends on the region of \mathcal{H}_P containing \mathbf{v} , see [LA22, Prop. 1.23].

Now the following *universal formula* [LA22, Thm. 1.26] expresses combinatorially the faces in the image of the geometric diagonal $\Delta_{(P,\mathbf{v})}$. Recall that the *normal cone* of a face F of a polytope P in \mathbb{R}^d is the cone of directions $\mathbf{c} \in \mathbb{R}^d$ such that the maximum of the scalar product $\langle \mathbf{c} | \mathbf{x} \rangle$ over P is attained for some \mathbf{x} in F .

Theorem 4.6 ([LA22, Thm. 1.26]). *Fix a vector $\mathbf{v} \in \mathbb{R}^d$ generic with respect to P . For each hyperplane H of the fundamental hyperplane arrangement \mathcal{H}_P , denote by $H^{\mathbf{v}}$ the open half space defined by H and containing \mathbf{v} . The faces of $P \times P$ in the image of the geometric diagonal $\Delta_{(P,\mathbf{v})}$ are the faces $F \times G$ where F and G are faces of P such that either the normal cone of F intersects $H^{-\mathbf{v}}$ or the normal cone of G intersects $H^{\mathbf{v}}$, for each $H \in \mathcal{H}_P$.*

The image of $\Delta_{(P,\mathbf{v})}$ is a union of pairs of faces $F \times G$ of the Cartesian product $P \times P$. By drawing the polytopes $(F + G)/2$ for all pairs of faces $(F, G) \in \text{Im } \Delta_{(P,\mathbf{v})}$, we can visualize $\Delta_{(P,\mathbf{v})}$ as a polytopal subdivision of P . See Figure 13 (middle right) and Figure 14.

It turns out that the dual of this complex is just the common refinement of two translated copies of the normal fan of P . See Figure 13 (right). Recall that the *normal fan* of P is the fan formed by the normal cones of all faces of P . We thus obtain the following statement.

Proposition 4.7 ([LA22, Coro. 1.4]). *The inclusion poset on the faces in the image of the diagonal $\Delta_{(P,\mathbf{v})}$ is isomorphic to the reverse inclusion poset on the faces of the common refinement of two copies of the normal fan of P , translated from each other by the vector \mathbf{v} .*

Finally, the following statement relates the image of the diagonal $\Delta_{(P,\mathbf{v})}$ to the intervals of the poset obtained by orienting the skeleton of P in direction \mathbf{v} .

Proposition 4.8 ([LA22, Prop. 1.17]). *For any polytope P and any generic vector \mathbf{v} , we have*

$$(3) \quad \text{Im } \Delta_{(P,\mathbf{v})} \subseteq \bigcup_{\substack{F,G \text{ faces of } P \\ \max_{\mathbf{v}}(F) \leq \min_{\mathbf{v}}(G)}} F \times G.$$

Remark 4.9. For some polytopes such as the simplices [EM54], the cubes [Ser51], the freehedra [San09], and the associahedra [MTTV21], the reverse inclusion also holds (in the case of the simplices and the cubes, the diagonals are known as the *Alexander–Whitney* map [EM54] and *Serre* map [Ser51]). According to [MTTV21], the resulting equality enhancing (3) was called *magical formula* by J.-L. Loday. This equality simplifies the computation of the f -vectors of the diagonals. For instance, the number of k -dimensional faces in the diagonal of the $(n-1)$ -dimensional simplex, cube, and associahedron are respectively given by

$$f_k(\Delta_{\text{Simplex}(n)}) = (k+1) \binom{n+1}{k+2} \quad [\text{OEI10, A127717}],$$

$$f_k(\Delta_{\text{Cube}(n)}) = \binom{n-1}{k} 2^k 3^{n-1-k} \quad [\text{OEI10, A038220}],$$

$$f_k(\Delta_{\text{Asso}(n)}) = \frac{2}{(3n+1)(3n+2)} \binom{n-1}{k} \binom{4n+1-k}{n+1} \quad [\text{BCP23}].$$

Polytopes of greater complexity such as the multiplihedra [LAM23] or the operahedra [LA22], which include the permutahedra, do not possess this exceptional property, and the f -vectors of their diagonals are harder to compute.

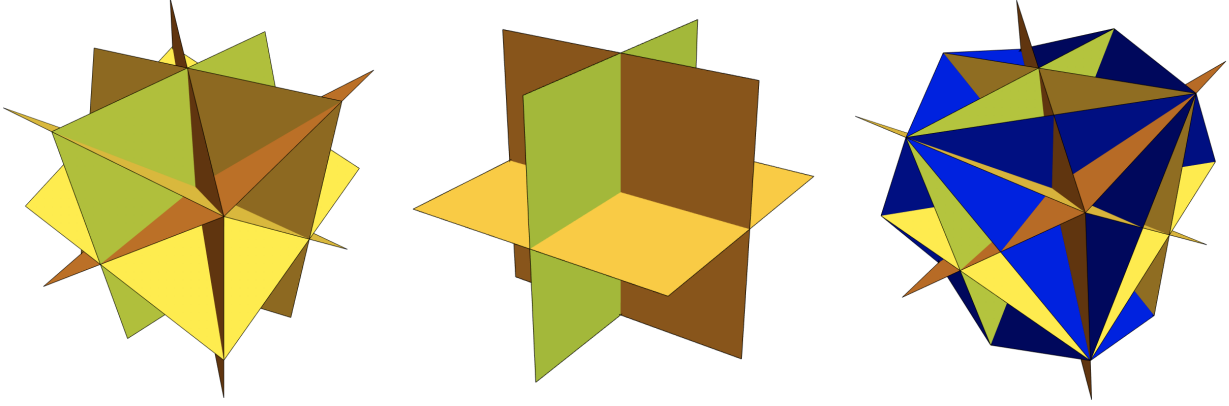


FIGURE 12. The fundamental hyperplane arrangements of the 3-dimensional simplex (left), cube (middle), and permutahedron (right). The hyperplanes perpendicular to edges of some intersection $P \cap \rho_z P$, which are *not* edges of the polytope P , are colored in blue. Left and rightmost illustrations from [LA22, Fig. 12].

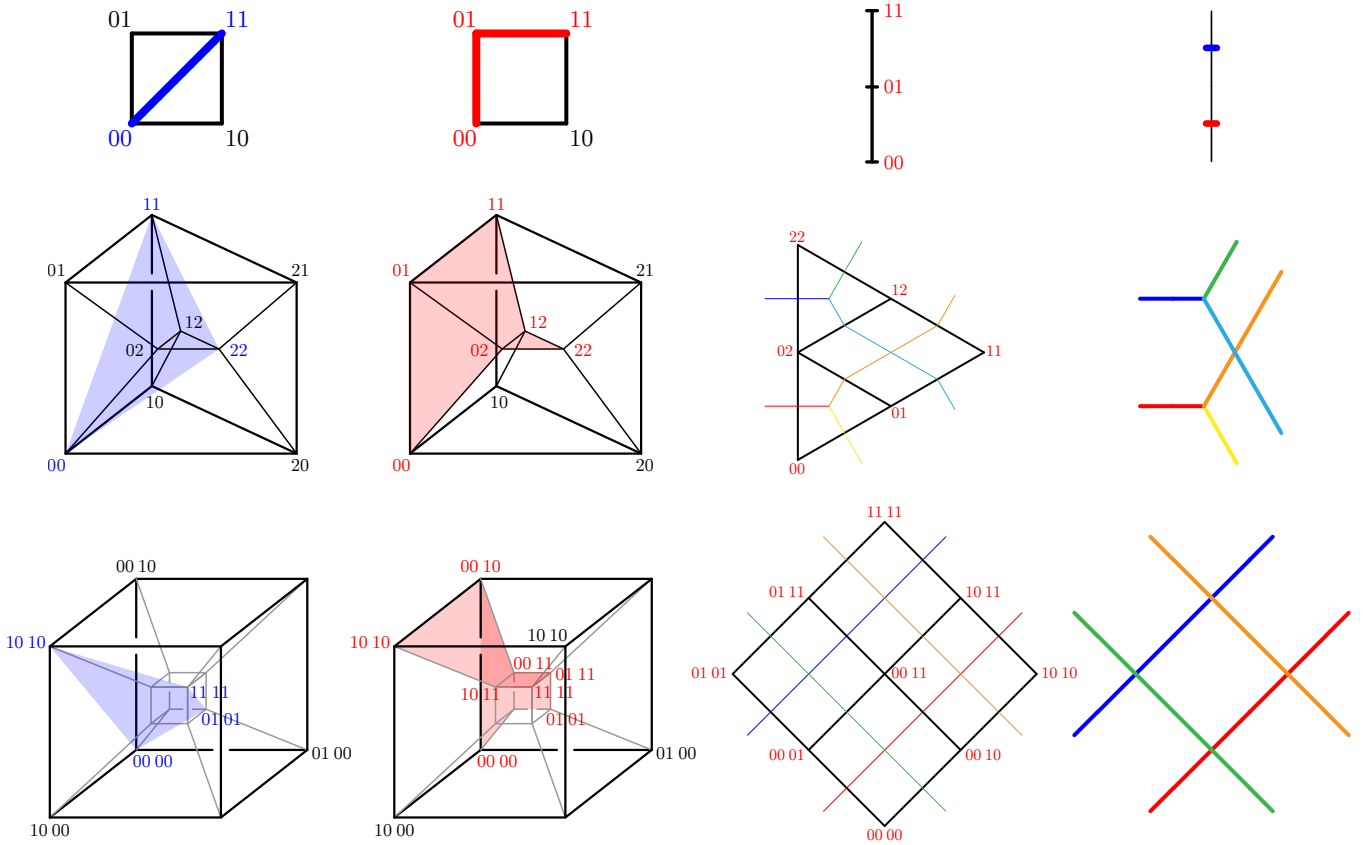


FIGURE 13. Cellular diagonals of the segment (top), the triangle (middle) and the square (bottom). For each of them, we have represented the thin diagonal of P (left, in blue), a cellular diagonal of P (middle left, in red) both in $P \times P$, the associated polytopal subdivision of P (middle right) and the common refinement of the two copies of the normal fan of P (right) both in P .

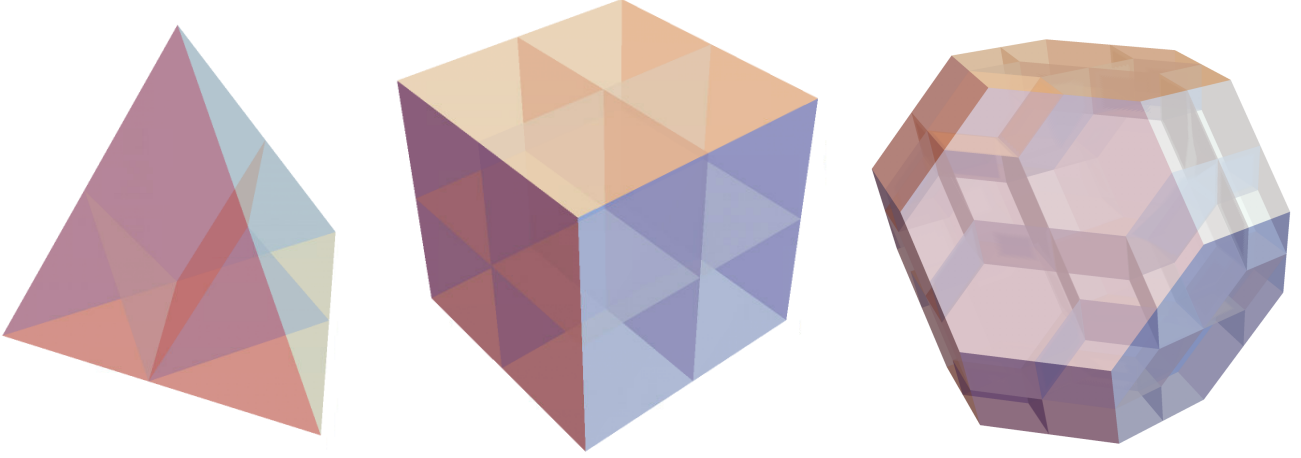


FIGURE 14. The subdivisions induced by cellular diagonals of the 3-dimensional simplex (left), cube (middle), and permutahedron (right). Right illustration from [LA22, Fig. 13].

Remark 4.10. This is in fact precisely the content of the *Fulton–Sturmfels formula* for the intersection product on toric varieties [FS97, Thm. 4.2], where the definition of cellular diagonals as tight coherent sections first appeared.

To conclude, we define the opposite of a geometric diagonal.

Definition 4.11. The *opposite* of the geometric diagonal $\Delta := \Delta_{(P,v)}$ for a vector $v \in \mathbb{R}^d$ generic with respect to P is the geometric diagonal $\Delta^{\text{op}} := \Delta_{(P,-v)}$ for the vector $-v$. Observe that

$$F \times G \in \text{Im } \Delta \iff G \times F \in \text{Im } \Delta^{\text{op}}.$$

4.2. Cellular diagonals for the permutahedra. We now specialize the statements of Section 4.1 to the standard permutahedron. We first recall its definition.

Definition 4.12. The *permutahedron* $\text{Perm}(n)$ is the polytope in \mathbb{R}^n defined equivalently as

- the convex hull of the points $\sum_{i \in [n]} i e_{\sigma(i)}$ for all permutations σ of $[n]$, see [Sch11],
- the intersection of the hyperplane $\{\mathbf{x} \in \mathbb{R}^n \mid \sum_{i \in I} x_i = \binom{n+1}{2}\}$ with the affine halfspaces $\{\mathbf{x} \in \mathbb{R}^n \mid \sum_{i \in I} x_i \geq \binom{\#I+1}{2}\}$ for all $\emptyset \neq I \subsetneq [n]$, see [Rad52].

The normal fan of the permutahedron $\text{Perm}(n)$ is the fan defined by the braid arrangement \mathcal{B}_n . In particular, the faces of $\text{Perm}(n)$ correspond to the ordered partitions of $[n]$. Moreover, when oriented in a generic direction, the skeleton of the permutahedron $\text{Perm}(n)$ is isomorphic to the Hasse diagram of the classical weak order on permutations of $[n]$. See Figure 15.

The fundamental hyperplane arrangement of the permutahedron $\text{Perm}(n)$ was described in [LA22, Sect. 3.1]. As we will use the following set throughout the paper, we embed it in a definition.

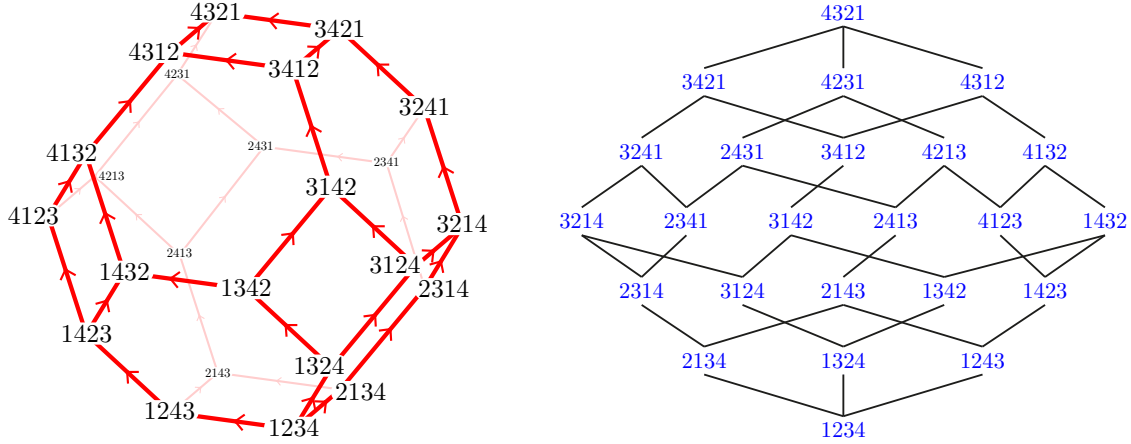
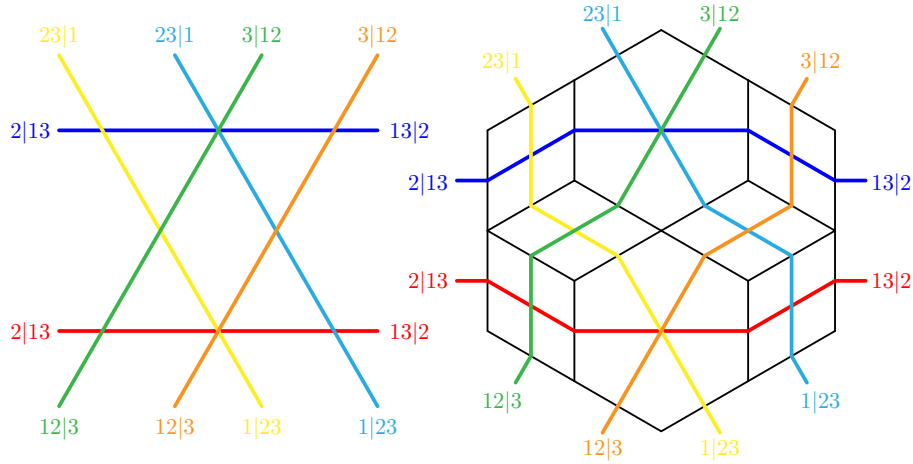
Definition 4.13. For $n \in \mathbb{N}$, we define

$$U(n) := \{\{I, J\} \mid I, J \subset [n] \text{ with } \#I = \#J \text{ and } I \cap J = \emptyset\}.$$

An *ordering* of $U(n)$ is a set containing exactly one of the two ordered pairs (I, J) or (J, I) for each $\{I, J\} \in U(n)$.

Proposition 4.14 ([LA22, Sect. 3.1]). *The fundamental hyperplane arrangement of the permutahedron $\text{Perm}(n)$ is given by the hyperplanes $\{\mathbf{x} \in \mathbb{R}^n \mid \sum_{i \in I} x_i = \sum_{j \in J} x_j\}$ for all $\{I, J\} \in U(n)$.*

For a vector v generic with respect to $\text{Perm}(n)$, we denote by $O(v)$ the ordering of $U(n)$ such that $\sum_{i \in I} v_i > \sum_{j \in J} v_j$ for all $(I, J) \in O(v)$. Applying Theorem 4.6, we next describe the faces in the image of the geometric diagonal $\Delta_{(\text{Perm}(n), v)}$. For this, the following definition will be convenient.

FIGURE 15. The permutahedron $\text{Perm}(4)$ (left) and the weak order on permutations of $[4]$ (right).FIGURE 16. The duality between the $(2,3)$ -braid arrangement \mathcal{B}_3^2 (left) and the diagonal of the permutahedron $\text{Perm}(3)$ (right).

Definition 4.15. For $I, J \subseteq [n]$ and an ordered partition σ of $[n]$ into k blocks, we say that I *dominates* J in σ if for all $\ell \in [k]$, the first ℓ blocks of σ contain at least as many elements of I than of J .

Theorem 4.16 ([LA22, Thm. 3.16]). A pair (σ, τ) of ordered partitions of $[n]$ corresponds to a face in the image of the geometric diagonal $\Delta_{(\text{Perm}(n), \mathbf{v})}$ if and only if, for all $(I, J) \in \mathcal{O}(\mathbf{v})$, J does not dominate I in σ or I does not dominate J in τ .

As the normal fan of the permutahedron $\text{Perm}(n)$ is the fan defined by the braid arrangement \mathcal{B}_n , we obtain by Proposition 4.7 the following connection between the diagonal of $\text{Perm}(n)$ and the $(2, n)$ -braid arrangement \mathcal{B}_2^n studied in Part I. This connection is illustrated in Figure 16.

Proposition 4.17. The inclusion poset on the faces in the image of the diagonal $\Delta_{(\text{Perm}(n), \mathbf{v})}$ is isomorphic to the reverse inclusion poset on the faces of the $(2, n)$ -braid arrangement \mathcal{B}_2^n .

Remark 4.18. To be more precise, the diagonal $\Delta_{(\text{Perm}(n), \mathbf{v})}$ is dual to the \mathbf{a} -braid arrangement $\mathcal{B}_2^n(\mathbf{a})$ where the translation matrix \mathbf{a} has two rows, with first row $\mathbf{a}_{1,j} = 0$ and second

row $\mathbf{a}_{2,j} = v_j - v_{j+1}$ for all $j \in [n-1]$. Since \mathbf{v} is generic with respect to $\text{Perm}(n)$, we have $\sum_{i \in I} v_i \neq \sum_{j \in J} v_j$ for all $(I, J) \in \mathcal{U}(n)$, so that \mathbf{a} is indeed generic.

Remark 4.19. Similarly, the combinatorics of the $(\ell-1)^{\text{st}}$ iteration of a diagonal of the permutahedron $\text{Perm}(n)$ is given by the combinatorics of the (ℓ, n) -braid arrangement.

Finally, the permutahedron $\text{Perm}(n)$ is not magical in the sense of Proposition 4.8. See also Example 5.25.

Proposition 4.20 ([LA22, Sect. 3]). *For any $n > 3$ and any generic vector \mathbf{v} , the diagonal $\Delta_{(\text{Perm}(n), \mathbf{v})}$ of the permutahedron $\text{Perm}(n)$ does not satisfy the magical formula. Namely, we have the strict inclusion*

$$\text{Im } \Delta_{(\text{Perm}(n), \mathbf{v})} \subsetneq \bigcup_{\substack{F, G \text{ faces of } \text{Perm}(n) \\ \max_{\mathbf{v}}(F) \leq \min_{\mathbf{v}}(G)}} F \times G.$$

Remark 4.21. Note that opposite diagonals have opposite orderings. Namely, $\mathcal{O}(-\mathbf{v}) = \mathcal{O}(\mathbf{v})^{\text{op}}$ where $\mathcal{O}^{\text{op}} := \{(J, I) \mid (I, J) \in \mathcal{O}\}$.

4.3. Enumerative results on cellular diagonals of the permutahedra. Relying on Proposition 4.17, we now specialize the results of Part I to the case $\ell = 2$ to derive enumerative results on the diagonals of the permutahedra.

Observe that one can easily compute the full Möbius polynomials of the $(2, n)$ -braid arrangements \mathcal{B}_n^2 from Theorem 2.4:

$$\begin{aligned} \mu_{\mathcal{B}_1^2}(x, y) &= 1, \\ \mu_{\mathcal{B}_2^2}(x, y) &= xy - 2x + 2, \\ \mu_{\mathcal{B}_3^2}(x, y) &= x^2y^2 - 6x^2y + 10x^2 + 6xy - 18x + 8, \\ \mu_{\mathcal{B}_4^2}(x, y) &= x^3y^3 - 12x^3y^2 + 52x^3y - 84x^3 + 12x^2y^2 - 96x^2y + 216x^2 + 44xy - 182x + 50, \\ \mu_{\mathcal{B}_5^2}(x, y) &= x^4y^4 - 20x^4y^3 + 160x^4y^2 - 620x^4y + 1008x^4 \\ &\quad + 20x^3y^3 - 300x^3y^2 + 1640x^3y - 3360x^3 \\ &\quad + 140x^2y^2 - 1430x^2y + 4130x^2 + 410xy - 2210x + 432. \end{aligned}$$

We now focus on the number of vertices, regions, and bounded regions of the $(2, n)$ -braid arrangement \mathcal{B}_n^2 , to obtain the number of facets, vertices, and internal vertices of the diagonal of the permutahedron $\text{Perm}(n)$. The first few values are gathered in Tables 6 and 7.

Corollary 4.22. *The diagonal of the permutahedron $\text{Perm}(n)$ has*

- $2(n+1)^{n-2}$ facets,
- $n \binom{n-1}{k_1} (n-k_1)^{k_1-1} (n-k_2)^{k_2-1}$ facets corresponding to pairs (F_1, F_2) of faces of the permutahedron $\text{Perm}(n)$ with $\dim(F_1) = k_1$ and $\dim(F_2) = k_2$ (thus $k_1 + k_2 = n-1$),
- $n! [z^n] \exp \left(\sum_{m \geq 1} \frac{C_m z^m}{m} \right)$ vertices,
- $(n-1)! [z^{n-1}] \exp \left(\sum_{m \geq 1} C_m z^m \right)$ internal vertices,

where $C_m := \frac{1}{m+1} \binom{2m}{m}$ denotes the m^{th} Catalan number.

Proof. Use the duality between the $(2, n)$ -braid arrangement \mathcal{B}_n^2 and the diagonal of the permutahedron $\text{Perm}(n)$ (see Proposition 4.17 and Figure 16), and specialize Theorems 2.18, 2.19 and 2.21 to the case $\ell = 2$. \square

Remark 4.23. For completeness, we provide an alternative simpler proof of the first point of Corollary 4.22. By Proposition 2.3, we just need to count the $(2, n)$ -partition trees. Consider a $(2, n)$ -partition tree $\mathbf{F} := (F_1, F_2)$ (hence $\#F_1 + \#F_2 = n+1$). Consider the intersection tree T

n	1	2	3	4	5	6	7	8	9	...	OEIS
facets	1	2	8	50	432	4802	65536	1062882	20000000	...	[OEI10, A007334]
vertices	1	3	17	149	1809	28399	550297	12732873	343231361	...	[OEI10, A213507]
int. verts.	1	1	5	43	529	8501	169021	4010455	110676833	...	[OEI10, A251568]

TABLE 6. The numbers of facets, vertices, and internal vertices of the diagonal of the permutahedron $\text{Perm}(n)$ for $n \in [9]$.

$n = 1$		$n = 2$			$n = 3$				$n = 4$				
dim	0	dim	0	1	dim	0	1	2	dim	0	1	2	3
0	1	0	3	1	0	17	12	1	0	149	162	38	1
		1	1		1	12	6		1	162	150	24	
					2	1			2	38	24		
									3	1			

$n = 5$						$n = 6$						
dim	0	1	2	3	4	dim	0	1	2	3	4	5
0	1809	2660	1080	110	1	0	28399	52635	30820	6165	302	1
1	2660	3540	1200	80		1	52635	90870	67580	7785	240	
2	1080	1200	270			2	30820	47580	20480	2160		
3	110	80				3	6165	7785	2160			
4	1					4	302	240				
						5	1					

TABLE 7. Number of pairs of faces in the cellular image of the diagonal of the permutahedron $\text{Perm}(n)$ for $n \in [6]$.

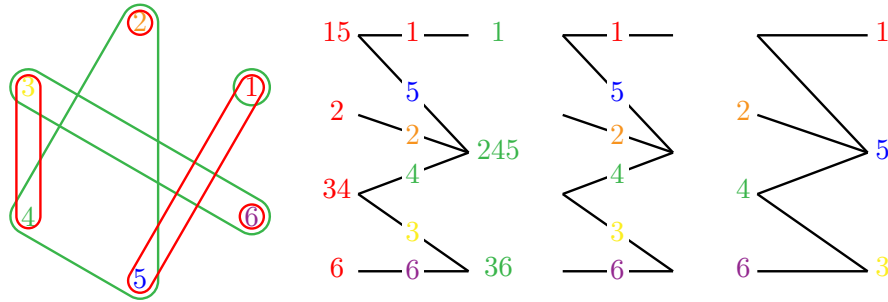


FIGURE 17. The bijection from rooted (ℓ, n) -partition trees (left) to spanning trees of K_{n+1} containing the edge $(0, 1)$ (right).

of \mathbf{F} with vertices labeled by the parts of F_1 and of F_2 and edges labeled by $[n]$, root T at the part of F_1 containing vertex 1, forget the vertex labels of T , and send each edge label of T to the next vertex away from the root, and label the root by 0. See Figure 17. The result is a spanning tree of the complete graph K_{n+1} on $\{0, \dots, n\}$ which must contain the edge $(0, 1)$ (because we have chosen the root to be the part of F_1 containing 1). Finally, by double counting the pairs (T, e) where T is a spanning tree of K_{n+1} and e is an edge of T , we see that n times the number of spanning trees of K_{n+1} equals $\binom{n+1}{2}$ times the number of spanning trees of K_{n+1} containing $(0, 1)$. Hence, by Cayley's formula for spanning trees of K_{n+1} , we obtain that the number of $(2, n)$ -partition trees is

$$\frac{2n}{n(n+1)}(n+1)^{n-1} = 2(n+1)^{n-2}.$$

5. OPERADIC DIAGONALS

This section is devoted to the combinatorics of two specific diagonals of the permutahedra, the LA and SU diagonals, which are shown to be the only operadic geometric diagonals of the permutahedra.

5.1. The LA and SU diagonals. Recall from Section 4.2 that a geometric diagonal of the permutahedron $\text{Perm}(n)$ gives a choice of ordering of the sets $U(n)$ (see Definition 4.13). As we consider in this section diagonals for all permutahedra, we now consider families of orderings.

Definition 5.1. An *ordering* of $U := \{U(n)\}_{n \geq 1}$ is a family $O := \{O(n)\}_{n \geq 1}$ where $O(n)$ is an ordering of $U(n)$ for each $n \geq 1$.

We will be focusing on the following two orderings and their corresponding diagonals.

Definition 5.2. The *LA* and *SU orderings* are defined by

- $\text{LA}(n) := \{(I, J) \mid \{I, J\} \in U(n) \text{ and } \min(I \cup J) = \min I\} \text{ and}$
- $\text{SU}(n) := \{(I, J) \mid \{I, J\} \in U(n) \text{ and } \max(I \cup J) = \max J\}.$

Definition 5.3. The *LA diagonal* Δ^{LA} (resp. *SU diagonal* Δ^{SU}) of the permutahedron $\text{Perm}(n)$ is the geometric diagonal $\Delta_{(\text{Perm}(n), \mathbf{v})}$ given by any vector $\mathbf{v} \in \mathbb{R}^n$ satisfying

$$\sum_{i \in I} v_i > \sum_{j \in J} v_j,$$

for all $(I, J) \in \text{LA}(n)$ (resp. $(I, J) \in \text{SU}(n)$).

First note that this definition makes sense, since vectors $\mathbf{v} = (v_1, \dots, v_n)$ such that $O(\mathbf{v})$ is the LA or SU order do exist: take for instance $v_i := 2^{-i+1}$ for Δ^{LA} and $v_i := 2^n - 2^{i-1}$ for Δ^{SU} . Second, note that the LA and SU diagonals coincide up to dimension 2, but differ in dimension ≥ 3 . The former is illustrated in Figure 18, with the faces labeled by ordered $(2, 3)$ -partition forests.

We will prove in Theorem 6.24 that Δ^{SU} is a topological enhancement of the Sanedblidze–Umble diagonal from [SU04]. The faces of the LA and SU diagonals are described by the following specialization of Theorem 4.16.

Theorem 5.4. *A pair (σ, τ) of ordered partitions of $[n]$ is not a face of the LA diagonal Δ^{LA} if and only if there exists $(I, J) \in \text{LA}(n)$ such that J dominates I in σ and I dominates J in τ . The same holds for the SU diagonal by replacing Δ^{LA} by Δ^{SU} and $\text{LA}(n)$ by $\text{SU}(n)$.*

5.2. The operadic property. The goal of this section is to prove that the LA and SU diagonals are the only two operadic diagonals which induce the weak order on the vertices of the permutahedra (Theorem 5.13). We start by properly defining operadic diagonals.

Let $A \sqcup B = [n]$ be a partition of $[n]$ where $A := \{a_1, \dots, a_p\}$ and $B := \{b_1, \dots, b_q\}$. Recall that the ordered partition $B|A$ corresponds to a facet of the permutahedron $\text{Perm}(n)$ defined by the inequality $\sum_{b \in B} x_b \geq \binom{\#B+1}{2}$. This facet is isomorphic to the Cartesian product

$$(\text{Perm}(p) + q\mathbf{1}_{[p]}) \times \text{Perm}(q)$$

of lower dimensional permutahedra, where the first factor is translated by $q\mathbf{1}_{[p]} := q \sum_{i \in [p]} \mathbf{e}_i$, via the permutation of coordinates

$$\Theta : \begin{array}{ccc} \mathbb{R}^p \times \mathbb{R}^q & \xrightarrow{\cong} & \mathbb{R}^n \\ (x_1, \dots, x_p) \times (x_{p+1}, \dots, x_n) & \longmapsto & (x_{\sigma^{-1}(1)}, \dots, x_{\sigma^{-1}(n)}) \end{array},$$

where σ is the (p, q) -shuffle defined by $\sigma(i) := a_i$ for $i \in [p]$, and $\sigma(p+j) := b_j$ for $j \in [q]$. Note that this map is a particular instance of the eponym map introduced in Point (5) of [LA22, Prop. 2.3].

Definition 5.5. A family of geometric diagonals $\Delta := \{\Delta_n : \text{Perm}(n) \rightarrow \text{Perm}(n) \times \text{Perm}(n)\}_{n \geq 1}$ of the permutahedra is *operadic* if for every face $A_1 | \dots | A_k$ of the permutahedron $\text{Perm}(\#A_1 + \dots + \#A_k)$, the map Θ induces a topological cellular isomorphism

$$\Delta_{\#A_1} \times \dots \times \Delta_{\#A_k} \cong \Delta_{\#A_1 + \dots + \#A_k}.$$

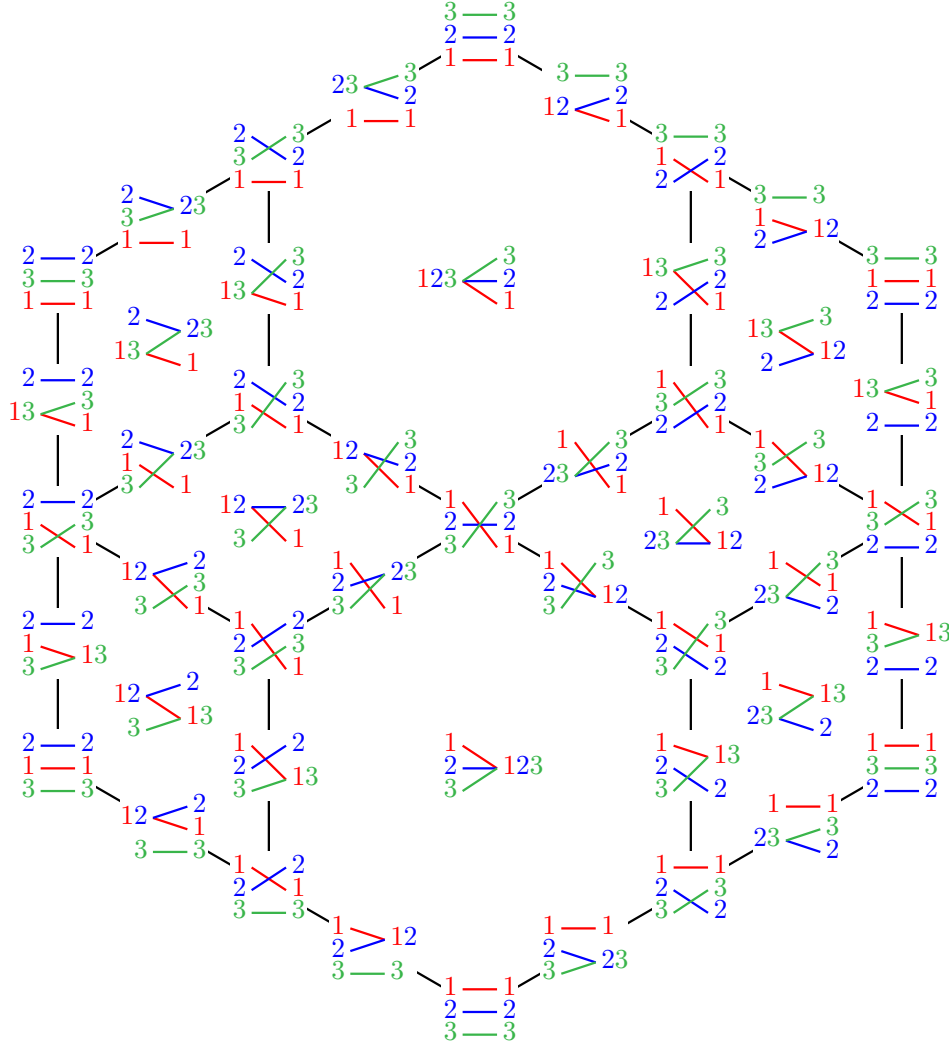


FIGURE 18. The LA (and SU) diagonal of $\text{Perm}(3)$ with faces labeled by ordered $(2, 3)$ -partition forests. (See also Figure 10 for the dual hyperplane arrangement.)

In other words, we require that the diagonal Δ commutes with the map Θ , see [LA22, Sect. 4.2]. At the algebraic level, this property is called “comultiplicativity” in [SU04]. Note that in particular, such an isomorphism respects the poset structures.

We will now translate this operadic property for geometric diagonals to the corresponding orderings O of U . We need the following standardization map (this map is classical for permutations or words, but we use it here for pairs of sets).

Definition 5.6. The *standardization* of a pair (I, J) of disjoint subsets of $[n]$ is the only partition $\text{std}(I, J)$ of $[\#I + \#J]$ where the relative order of the elements is the same as in (I, J) . More precisely, it is defined recursively by

- $\text{std}(\emptyset, \emptyset) := (\emptyset, \emptyset)$, and
- if $k := \#I + \#J$ and $\ell := \max(I \cup J)$ belongs to I (resp. J), then $\text{std}(I, J) = (U \cup \{k\}, V)$ (resp. $\text{std}(I, J) = (U, V \cup \{k\})$) where $(U, V) = \text{std}(I \setminus \{\ell\}, J)$ (resp. $(U, V) = \text{std}(I, J \setminus \{\ell\})$).

For example, $\text{std}(\{5, 9, 10\}, \{6, 8, 12\}) = (\{1, 4, 5\}, \{2, 3, 6\})$.

Definition 5.7. An ordering O of U is *operadic* if every $\{I, J\} \in U$ satisfies the following two conditions

- (1) $\text{std}(I, J) \in O$ implies $(I, J) \in O$,
- (2) if there exist $I' \subset I, J' \subset J$ such that $(I', J') \in O$ and $(I \setminus I', J \setminus J') \in O$, then $(I, J) \in O$.

We call *indecomposables* of O the pairs $(I, J) \in O$ for which the only subpair (I', J') satisfying Condition (2) above is the pair (I, J) itself.

Proposition 5.8. *A geometric diagonal $\Delta := (\Delta_{(\text{Perm}(n), \mathbf{v}_n)})_{n \in \mathbb{N}}$ of the permutahedra is operadic if and only if its associated ordering $O := (O(\mathbf{v}_n))_{n \in \mathbb{N}}$ is operadic.*

Proof. Every operadic diagonal satisfies [LA22, Prop. 4.14], which amounts precisely to an operadic ordering of U in the sense of Definition 5.7. \square

We now turn to the study of the LA and SU orderings.

Lemma 5.9. *The LA and SU orderings are operadic, and their indecomposables are the pairs whose standardization are $(\{1\}, \{2\})$ and*

$$(LA) \quad (\{1, k+2, k+3, \dots, 2k-1, 2k\}, \{2, 3, \dots, k+1\})$$

$$(SU) \quad (\{k, k+1, \dots, 2k-1\}, \{1, 2, 3, \dots, k-1, 2k\})$$

for all $k \geq 1$. The opposite orderings LA^{op} and SU^{op} are also operadic, and generated by the opposite pairs.

Proof. We present the proof for the LA ordering, the proofs for the SU and opposite orders are similar. First, we verify that LA is operadic. Condition (1) follows from the fact that standardizing a pair preserves its minimal element. Condition (2) also holds, since whenever (I', J') and its complement are in LA, we have $\min(I) = \min\{\min(I'), \min(I \setminus I')\}$, and thus (I, J) itself is in LA.

Second, we compute the indecomposables. Let (I, J) be a pair with standardization (LA). If we try to decompose (I, J) as a non-trivial union, there is always one pair (I', J') in this union for which $\min(I \cup J) \notin I'$, so we have $\min(I' \cup J') = \min J'$, which implies that $(I', J') \notin LA$. Thus, the pair (I, J) is indecomposable.

It remains to show that any pair (I, J) in LA whose standardization is not of the form (LA) can be decomposed as a union of such pairs. Let us denote by (I_k, J_k) the standard form (LA) and let $(I, J) \in LA$ be such that $\text{std}(I, J) \neq (I_k, J_k)$. Then there exists $i_2 \in I \setminus \min I$ such that $i_2 < \max J$. This means that (I, J) can be decomposed as a union: if we write it as $(\{i_1, \dots, i_k\}, \{j_1, \dots, j_k\})$, where each set ordered smallest to largest, then we must have $\min(I \cup J) = i_1 < i_2 < j_k$, in which case $(\{i_2\}, \{j_k\})$ and $(\{i_1, i_3, \dots, i_k\}, \{j_1, \dots, j_{k-1}\})$ are both smaller LA pairs. Then it must be the case that $\text{std}((\{i_2\}, \{j_k\})) = (\{1\}, \{2\})$, and $\text{std}((\{i_1, i_3, \dots, i_k\}, \{j_1, \dots, j_{k-1}\}))$ is either (I_{k-1}, J_{k-1}) , or we can repeat this decomposition. \square

Remark 5.10. We note that the decomposition in Lemma 5.9 is one of potentially many different decompositions of the pair (I, J) . However, by definition of the LA order, for any decomposition $(I, J) = (\bigsqcup_{a \in A} I_a, \bigsqcup_{a \in A} J_a)$, we have $\text{std}(I_a, J_a) \in LA$ for all $a \in A$. As such, all decompositions of a pair (I, J) , order it the same way.

Proposition 5.11. *The only operadic orderings of $U = \{U(n)\}_{n \geq 1}$ are the LA, SU, LA^{op} and SU^{op} orderings.*

Proof. We build operadic orderings inductively, showing that the choices for $U(n)$, $n \leq 4$ determine higher ones. We prove the statement for the LA order, the SU and opposite orders are similar. First, we decide to order the unique pair of $U(2)$ as $(\{1\}, \{2\})$. The operadic property then determines the orders of all the pairs of $U(3)$ and $U(4)$, except the pair $\{\{1, 4\}, \{2, 3\}\}$, for which we choose the order $(\{1, 4\}, \{2, 3\})$. Now, we claim that all the higher choices are forced by the operadic property, and lead to the LA diagonal. Starting instead with the orders $(\{1\}, \{2\})$ and $(\{2, 3\}, \{1, 4\})$ would give the SU diagonal, and reversing the pairs would give the opposite orders.

Let $\ell \geq 2$ and suppose that for all $k \leq \ell$, we have given the pair

$$\{I_k, J_k\} := \{\{1, k+2, k+3, \dots, 2k-1, 2k\}, \{2, 3, \dots, k+1\}\}$$

the LA ordering (I_k, J_k) . Then from Lemma 5.9, we know that the only $\{I, J\}$ pair of order $\ell + 1$ that will not decompose, and hence be specified by the already chosen conditions, is $\{I_{\ell+1}, J_{\ell+1}\}$. As such, the only way we can vary from LA is to order this element in the opposite direction $(J_{\ell+1}, I_{\ell+1})$. We now consider a particular decomposable pair $\{I'_m, J'_m\}$ where $I'_m := I_m \sqcup \{3\} \setminus \{m+2\}$ and $J'_m := J_m \sqcup \{m+2\} \setminus \{3\}$, of order $m := \ell + 2$, that will lead to a contradiction (see Example 5.12). On the one side, we can decompose $\{I'_m, J'_m\} = \{I_a \cup I_b, J_a \cup J_b\}$ with $I_a := \{1, m+3, \dots, 2m\}$, $J_a := \{4, 5, \dots, m+2\}$, $I_b := \{3\}$ and $J_b := \{2\}$. By hypothesis, we have the orders (J_a, I_a) and (J_b, I_b) which imply the order (J'_m, I'_m) since our ordering is operadic. On the other side, we can decompose $\{I'_m, J'_m\} = \{I_c \cup I_d, J_c \cup J_d\}$, where $I_c := \{1, m+3, \dots, 2m-1\}$, $J_c := \{2, 5, \dots, m+1\}$, $I_d := \{3, 2m\}$ and $J_d := \{4, m+2\}$. By hypothesis, we have the orders (I_c, J_c) and (I_d, J_d) , which imply that (I'_m, J'_m) since our ordering is operadic. We arrived at a contradiction. Thus, the only possible operadic choice of ordering for $\{I_{\ell+1}, J_{\ell+1}\}$ is the LA ordering, which finishes the proof. \square

Example 5.12. To illustrate our proof of Proposition 5.11, consider an operadic ordering O for which the LA ordering holds for pairs of order 1 and 2, but is reversed for pairs of order 3, *i.e.*

$$(\{1\}, \{2\}) \in O, \quad (\{1, 4\}, \{2, 3\}) \in O, \text{ and } (\{2, 3, 4\}, \{1, 5, 6\}) \in O.$$

Then, the pair $\{I'_4, J'_4\} = \{\{1, 3, 7, 8\}, \{2, 4, 5, 6\}\}$ admits two different orientations. In particular,

$$\begin{aligned} (\{4, 5, 6\}, \{1, 7, 8\}) \in O \text{ and } (\{2\}, \{3\}) \in O &\implies (\{2, 4, 5, 6\}, \{1, 3, 7, 8\}) \in O \text{ and} \\ (\{1, 7\}, \{2, 5\}) \in O \text{ and } (\{3, 8\}, \{4, 6\}) \in O &\implies (\{1, 3, 7, 8\}, \{2, 4, 5, 6\}) \in O. \end{aligned}$$

Combining Proposition 5.8 with Proposition 5.11, we get the main result of this section. Recall that a vector induces the weak order on the vertices of the standard permutahedron if and only if it has strictly decreasing coordinates (see Definition 4.12).

Theorem 5.13. *There are exactly four operadic geometric diagonals of the permutahedra, given by the LA and SU diagonals, and their opposites LA^{op} and SU^{op} . The LA and SU diagonals are the only operadic geometric diagonals which induce the weak order on the vertices of the permutahedron.*

Remark 5.14. This answers by the negative a conjecture regarding unicity of diagonals on the permutahedra, raised at the beginning of [SU04, Sect. 3], and could be seen as an alternative statement. See Section 6 where we prove that the geometric SU diagonal is a topological enhancement of the SU diagonal from [SU04].

5.3. Isomorphisms between operadic diagonals. Let P be a centrally symmetric polytope, and let $s : P \rightarrow P$ be its involution, given by taking a point $p \in P$ to its reflection $s(p)$ with respect to the center of symmetry of P . Note that this map is cellular, and induces an involution on the face lattice of P . For the permutahedron $\text{Perm}(n)$, this face poset involution is given in terms of ordered partitions of $[n]$ by the map $A_1 | \dots | A_k \mapsto A_k | \dots | A_1$.

The permutahedron $\text{Perm}(n)$ possesses another interesting symmetry, namely, the cellular involution $r : \text{Perm}(n) \rightarrow \text{Perm}(n)$ which sends a point $p \in \text{Perm}(n)$ to its reflection with respect to the hyperplane of equation

$$\sum_{i=1}^{\lfloor n/2 \rfloor} x_i = \sum_{i=1}^{\lfloor n/2 \rfloor} x_{n-i+1}.$$

This involution also respects the face poset structure. In terms of ordered partitions, it replaces each block A_j in $A_1 | \dots | A_k$ by the block $r(A_j) := \{r(i) \mid i \in A_j\}$ where $r(i) := n - i + 1$.

The involution $t : P \times P \rightarrow P \times P$, sending (x, y) to (y, x) , takes a cellular diagonal to another cellular diagonal. As we have already remarked in Definition 4.11, this involution sends a geometric diagonal Δ to its opposite Δ^{op} .

Theorem 5.15. *For the permutahedron $\text{Perm}(n)$, the involutions t and $rs \times rs$ are cellular isomorphisms between the four operadic diagonals, through the following commutative diagram*

$$\begin{array}{ccc} \Delta^{\text{LA}} & \xrightarrow{t} & (\Delta^{\text{LA}})^{\text{op}} \\ rs \times rs \downarrow & & \downarrow rs \times rs \\ \Delta^{\text{SU}} & \xrightarrow{t} & (\Delta^{\text{SU}})^{\text{op}} \end{array}$$

Moreover, they induce poset isomorphisms at the level of the face lattices.

Proof. The result for the transpositions t and the commutativity of the diagram are straightforward, so we prove that $rs \times rs$ is a cellular isomorphism respecting the poset structure. First, since $r(\min(I \cup J)) = \max(r(I) \cup r(J))$, we observe that the map $(I, J) \mapsto (r(J), r(I))$ defines a bijection between $\text{LA}(n)$ and $\text{SU}(n)$. Then, if σ is an ordered partition such that I dominates J in σ (Definition 4.15), it must be the case that J dominates I in $s\sigma$, and consequently rJ dominates rI in $rs\sigma$. As such, the domination characterization of the diagonals (Theorem 5.4), tells us $(\sigma, \tau) \in \Delta^{\text{LA}}$ if and only if $(rs(\sigma), rs(\tau)) \in \Delta^{\text{SU}}$. Finally, since both t, r and s preserve the poset structures, so does their composition, which finishes the proof. \square

Remark 5.16. There is a second, distinct isomorphism given by $t(r \times r)$. This follows from the fact that $s \times s : \Delta^{\text{LA}} \rightarrow (\Delta^{\text{LA}})^{\text{op}}$ is an isomorphism (and also for $s \times s : \Delta^{\text{SU}} \rightarrow (\Delta^{\text{SU}})^{\text{op}}$), as such the composite

$$t(r \times r) : \Delta^{\text{LA}} \xrightarrow{s \times s} (\Delta^{\text{LA}})^{\text{op}} \xrightarrow{rs \times rs} (\Delta^{\text{SU}})^{\text{op}} \xrightarrow{t} \Delta^{\text{SU}}$$

is also an isomorphism. This second isomorphism has the conceptual benefit of sending left shift operators to left shift operators (and right to right), see Proposition 6.27.

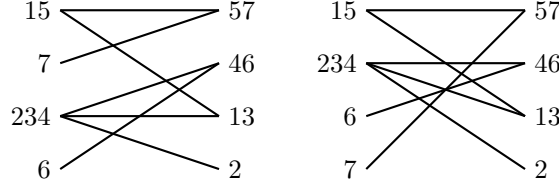
5.4. Facets of operadic diagonals. We now aim at describing the facets of the LA and SU diagonals. We have seen in Section 1.3 that facets of any diagonal of the permutahedron $\text{Perm}(n)$ are in bijection with $(2, n)$ -partition trees, that is, pairs of unordered partitions of $[n]$ whose intersection graph is a tree. These pairs of partitions were first studied and called *essential complementary partitions* in [Che69, CG71, KUC82]. Specializing Proposition 3.3, we now explain how to order these pairs of partitions to get the facets of Δ^{LA} and Δ^{SU} .

Theorem 5.17. *Let (σ, τ) be a pair of ordered partitions of $[n]$ whose underlying intersection graph is a $(2, n)$ -partition tree. The pair (σ, τ) is a facet of the LA (resp. SU) diagonal if and only if the minimum (resp. maximum) of every directed path between two consecutive blocks of σ or τ is oriented from σ to τ (resp. from τ to σ).*

Proof. We specialize Proposition 3.3 to the LA diagonal, the proof for the SU diagonal is similar. Let \mathbf{v} be a vector inducing the LA diagonal as in Definition 5.3. Without loss of generality, we place the first copy of the braid arrangement centered at 0, and the second copy centered at \mathbf{v} . From Definition 1.12 and Remark 4.18, we get that $A_{1,s,t} = 0$ and $A_{2,s,t} = v_s - v_t$ for any edges s, t . We treat the case of two consecutive blocks A and B of σ , the analysis for τ is similar. The directed path between A and B is a sequence of edges r_0, r_1, \dots, r_q . Let us denote by $I := \{r_0, r_2, \dots\}$ the set of edges directed from σ to τ , and by $J := \{r_1, r_3, \dots\}$ its complement. According to Proposition 3.3, the order between A and B is determined by the sign of $A_{1,r_0,r_q} - \sum_{p \in [q]} A_{i_p, r_{p-1}, r_p}$, where i_p is the copy of the block adjacent to both edges r_{p-1} and r_p . Thus, the order between A and B is determined by the sign of $\sum_{i \in I} v_i - \sum_{j \in J} v_j$, which according to the definition of Δ^{LA} is positive whenever $\min(I \cup J) \in I$. Thus, the pair $(\sigma, \tau) \in \Delta^{\text{LA}}$ if and only if the minimum of every directed path between two consecutive blocks of σ or τ is oriented from σ to τ . \square

In the rest of the paper, we shall represent ordered $(2, n)$ -partition trees (σ, τ) of facets by drawing σ on the left, and τ on the right, with their blocks from top to bottom. The conditions “oriented from σ to τ ” in the preceding Theorem then reads as “oriented from left to right”, an expression we shall adopt from now on.

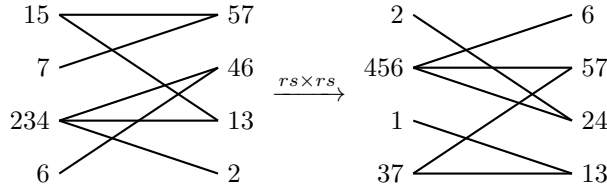
Example 5.18. Below are the two orderings of the $(2, 7)$ -partition tree $\{15, 234, 6, 7\} \times \{13, 2, 46, 57\}$ giving facets of the LA (left) and SU (right) diagonals, obtained via Theorem 5.17. Note that ordered partitions should be read from top to bottom.



In the LA facet (left), we have $7 < 234$, since in the path between the two vertices $7 \xrightarrow{7} 57 \xrightarrow{5} 15 \xrightarrow{1} 13 \xrightarrow{3} 234$, the minimum 1 is oriented from left to right. In this case, we have $(I, J) = (\{1, 7\}, \{3, 5\})$. Similarly, the path $57 \xrightarrow{5} 15 \xrightarrow{1} 13 \xrightarrow{3} 234 \xrightarrow{4} 46$ imposes that $57 < 46$, for $(I, J) = (\{1, 4\}, \{3, 5\})$.

Remark 5.19. Note that forgetting the order in a facet of Δ^{LA} , and then ordering again the $(2, n)$ -partition tree to obtain a facet of Δ^{SU} , provides a bijection between facets that was not considered in Section 5.3. However, this map is not defined on the other faces.

Example 5.20. The isomorphism $rs \times rs$ from Theorem 5.15 sends the LA facet from Example 5.18 (left) to the following SU facet (right).



Moreover, it sends the path $57 \xrightarrow{5} 15 \xrightarrow{1} 13 \xrightarrow{3} 234 \xrightarrow{4} 46$ to the path $24 \xrightarrow{4} 456 \xrightarrow{5} 57 \xrightarrow{7} 37 \xrightarrow{3} 13$, where the maximum 7 is oriented from right to left, witnessing the fact that $24 < 13$. The associated $(I, J) = (\{1, 4\}, \{3, 5\})$ becomes $(r(J), r(I)) = (\{3, 5\}, \{4, 7\})$.

5.5. Vertices of operadic diagonals. We are now interested in characterizing the vertices that occur in an operadic diagonal as pattern-avoiding pairs of partitions of $[n]$. These pairs form a strict subset of the weak order intervals. We first need the following Lemma, which follows directly from the definition of domination (Definition 4.15).

Lemma 5.21. *Let σ be an ordered partition of $[n]$ and let $I, J \subseteq [n]$ be such that I dominates J in σ . For an element i in I or J , we denote by $\sigma^{-1}(i)$ the index of the block containing it in σ . Then, for any $i \in I, j \in J$, we have $I \setminus i$ dominates $J \setminus j$ in σ if and only if*

- (1) *either $\sigma^{-1}(j) < \sigma^{-1}(i)$ (meaning that j comes strictly before i in σ),*
- (2) *or for all k between $\sigma^{-1}(i)$ and $\sigma^{-1}(j)$, the first k blocks of σ contain strictly more elements of I than of J .*

Definition 5.22. For $k \leq n$, a permutation τ of $[k]$ is a **pattern** of a permutation σ of $[n]$ if there exists a subset $I := \{i_1 < \dots < i_k\} \subset [n]$ so that the permutation τ gives the relative order of the entries of σ at positions in I , i.e. $\tau_u < \tau_v := \sigma_{i_u} < \sigma_{i_v}$. We say that σ **avoids** τ if τ is not a pattern of σ .

Example 5.23. The pairs of permutations (σ, τ) avoiding the patterns $(21, 12)$ are precisely the intervals of the weak order.

Theorem 5.24. *A pair of permutations of $[n]$ is a vertex of the LA (resp. SU) diagonal if and only if for any $k \geq 1$ and for any $(I, J) \in \text{LA}(k)$ (resp. $\text{SU}(k)$) of size $\#I = \#J = k$ it avoids the patterns*

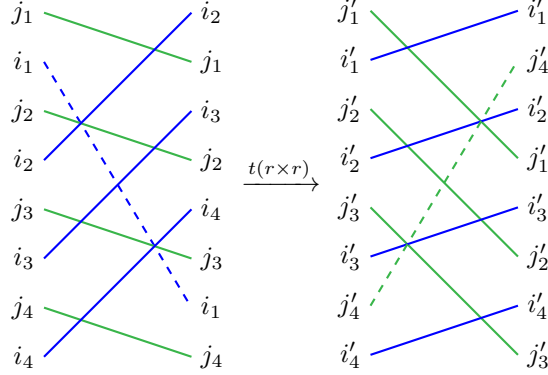
$$\begin{aligned} (\text{LA}) \quad & (j_1 i_1 j_2 i_2 \dots j_k i_k, i_2 j_1 i_3 j_2 \dots i_k j_{k-1} i_1 j_k), \\ (\text{SU}) \quad & \text{resp. } (j_1 i_1 j_2 i_2 \dots j_k i_k, i_1 j_k i_2 j_1 \dots i_{k-1} j_{k-2} i_k j_{k-1}), \end{aligned}$$

where $I = \{i_1, \dots, i_k\}$, $J = \{j_1, \dots, j_k\}$ and $i_1 = 1$ (resp. $j_k = 2k$).

Example 5.25. For each $k \geq 1$, there are $\binom{2k-1}{k-1}(k-1)!k!$ avoided standardized patterns. For $k = 1$, both diagonals avoid $(21, 12)$, so the vertices are intervals of the weak order. For $k = 2$,

- LA avoids $(3142, 2314), (4132, 2413), (2143, 3214), (4123, 3412), (2134, 4213), (3124, 4312)$.
- SU avoids $(1243, 2431), (1342, 3421), (2143, 1432), (2341, 3412), (3142, 1423), (3241, 2413)$.

As such, the vertices of LA and SU are a strict subset of all intervals of the weak order. Here is an illustration of the patterns avoided for $k = 4$. The LA pattern is drawn on the left, the SU pattern is drawn on the right, and they are in bijection under the isomorphism $t(r \times r)$ (Section 5.3), where the bijection between elements is $(i_1, i_2, i_3, i_4) \mapsto (j'_4, j'_1, j'_2, j'_3)$ and $(j_1, j_2, j_3, j_4) \mapsto (i'_1, i'_2, i'_3, i'_4)$.



The alternate isomorphism $t(s \times s)$, provides an alternate way to establish a bijection between these two patterns. The avoided patterns for higher k extend this crisscrossing shape.

Proof of Theorem 5.24. We give the proof for the LA diagonal, the one for the SU diagonal is similar, and can be obtained by applying either of the two isomorphisms of Section 5.3. According to Theorem 4.16, we have $(\sigma, \tau) \notin \Delta^{\text{LA}}$ if and only if there is an (I, J) such that J dominates I in σ and I dominates J in τ . It is clear that if a pair of permutations (σ, τ) contains a pattern of the form (LA), then the associated (I, J) satisfies the domination condition. Thus, we just need to show the reverse implication. We proceed by induction on the cardinality $\#I = \#J$. The case of cardinality 1 is clear. Now suppose that for all (I, J) of size $\#I = \#J \leq m - 1$, we have if J dominates I in σ and I dominates J in τ , then (σ, τ) contains a pattern of the form (LA).

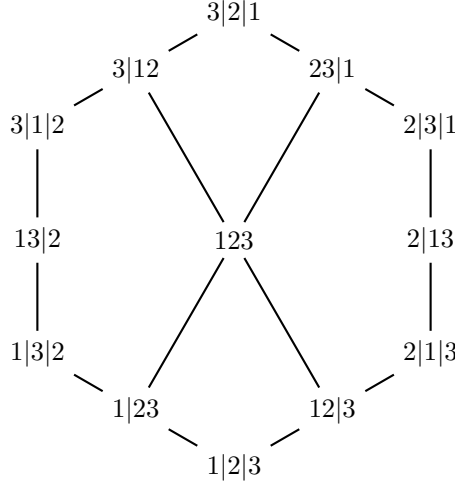
We need to show that this is still true for the pairs (I, J) of size $\#I = \#J = m$. Firstly, we need only consider standardized I, J conditions, and pairs of permutations of $[2m]$. Indeed, if we define $(\sigma', \tau') := \text{std}(\sigma \cap (I \cup J), \tau \cap (I \cup J))$, and $(I', J') := \text{std}(I', J')$, then if (σ, τ) satisfies the (I, J) domination condition, this implies (σ', τ') satisfies (I', J') . Conversely, if (σ', τ') has a pattern, then this implies (σ, τ) has the same pattern, which yields the indicated simplification.

Let (σ, τ) be such a pair of permutations. Suppose the leftmost element i_1 of I in σ is not 1, and let us write j_1 for the leftmost element of J in τ . Consider the pair $(I', J') := (I \setminus \{i_1\}, J \setminus \{j_1\})$. Using both cases of Lemma 5.21, we have J' dominates I' in σ , and I' dominates J' in τ , and we can thus conclude by induction that (σ, τ) contains a smaller pattern.

So, we assume the leftmost element of I in σ is $i_1 = 1$, and for $n \geq 1$ we prove that,

- If $(\sigma, \tau) = (j_1 i_1 j_2 i_2 \dots j_{n-1} i_{n-1} w i_n w', i_2 j_1 i_3 j_2 \dots i_n j_{n-1} w'')$, and j_n is the leftmost element of $J \setminus \{j_1, \dots, j_{n-1}\}$ in τ , then either $w = j_n$, or it matches a smaller pattern.
- If $(\sigma, \tau) = (j_1 i_1 j_2 i_2 \dots j_{n-1} i_{n-1} w'', i_2 j_1 i_3 j_2 \dots i_{n-1} j_{n-2} w j_{n-1} w'')$, and i_n is the leftmost element of $I \setminus \{i_1, \dots, i_{n-1}\}$ in σ , then either $w = i_n$, or it matches a smaller pattern.

We prove (a), the proof of (b) proceeds similarly. Let j_n be the leftmost element of $J \setminus \{j_1, \dots, j_{n-1}\}$ in τ . If $w \neq j_n$, then either (i) w consists of multiple elements of J including j_n , or (ii) j_n comes after i_n in σ . Now consider the pair $(I', J') := (I \setminus \{i_n\}, J \setminus \{j_n\})$. As was the case for the proof that $i_1 = 1$, we have I' dominates J' in τ . To prove that J' dominates I' in σ , we split by the cases. In case (i), we may apply condition (2) of Lemma 5.21. In case (ii), either i_n comes before j_n , in which case we meet condition (1) of Lemma 5.21, or j_n comes before i_n . In this last situation, we have condition (2) of Lemma 5.21 holds as i_n is the leftmost element of $I \setminus \{i_1, \dots, i_{n-1}\}$ in σ . Thus, if $w \neq j_n$, by the inductive hypothesis, we match a smaller pattern.

FIGURE 19. The Hasse diagram of the facial weak order for $\text{Perm}(3)$.

Finally, using statements (a) and (b) above, we can inductively generate (σ, τ) , determining j_1 via (a), then i_2 via (b), then j_2 via (a), and so on. This inductive process fully generates σ , and places all elements of τ except i_1 , yielding $\tau = i_2 j_1 i_3 j_2 \cdots i_k j_{k-1} w j_k w''$. However, as j_k must be dominated by an element of I , this forces $w = i_1$ and $w'' = \emptyset$, completing the proof. \square

5.6. Relation to the facial weak order. There is a natural lattice structure on all ordered partitions of $[n]$ which extends the weak order on permutations of $[n]$. This lattice was introduced in [KLN⁺01], where it is called *pseudo-permutahedron* and defined on packed words rather than ordered partitions. It was later generalized to arbitrary finite Coxeter groups in [PR06, DHP18], where it is called *facial weak order* and expressed in more geometric terms. We now recall a definition of the facial weak order on ordered partitions, and use the vertex characterization of the preceding section to show all faces of the LA and SU diagonal are intervals of this order.

Definition 5.26 ([KLN⁺01, PR06, DHP18]). The *facial weak order* on ordered partitions is the transitive closure of the relations

$$(4) \quad \sigma_1 | \dots | \sigma_k < \sigma_1 | \dots | \sigma_i \sqcup \sigma_{i+1} | \dots | \sigma_k \quad \text{for any } \sigma_1 | \dots | \sigma_k \text{ with } \max \sigma_i < \min \sigma_{i+1},$$

$$(5) \quad \sigma_1 | \dots | \sigma_i \sqcup \sigma_{i+1} | \dots | \sigma_k < \sigma_1 | \dots | \sigma_k \quad \text{for any } \sigma_1 | \dots | \sigma_k \text{ with } \min \sigma_i > \max \sigma_{i+1}.$$

The facial weak order recovers the weak order on permutations as illustrated in Figure 19.

Proposition 5.27. *If $(\sigma, \tau) \in \Delta^{\text{LA}}$, or $(\sigma, \tau) \in \Delta^{\text{SU}}$, then $\sigma \leq \tau$ under the facial weak order.*

Proof. By Proposition 4.8, the faces (σ, τ) satisfy $\max_{\mathbf{v}} \sigma \leq \min_{\mathbf{v}} \tau$ under the weak order. Thus, if we can show that $\sigma \leq \max_{\mathbf{v}} \sigma$ and $\min_{\mathbf{v}} \tau \leq \tau$ under the facial weak order, then the result immediately follows. If σ is a face of the permutahedra, then under both the LA, and SU orientation vectors, the vertex $\max_{\mathbf{v}} \sigma$ is given by writing out each block of σ in decreasing order, and the vertex $\min_{\mathbf{v}} \sigma$ is given by writing out each block of σ in increasing order. Then under the facial weak order $\sigma \leq \max_{\mathbf{v}} \sigma$, as repeated applications of Equation (5) shows that a block of elements is smaller than those same elements arranged in decreasing order. Similarly $\min_{\mathbf{v}} \sigma \leq \sigma$, as repeated applications of Equation (4) shows that a sequence of increasing elements is smaller than those same elements in a block. \square

Example 5.28. The facet $13|24|57|6 \times 3|17|456|2 \in \Delta^{\text{SU}}$, satisfies the inequality through the vertices

$$13|24|57|6 < 3|1|4|2|7|5|6 < 3|1|7|4|5|6|2 < 3|17|456|2.$$

6. SHIFT LATTICES

In this section, we prove that the geometric SU diagonal Δ^{SU} agrees at the cellular level with the original Saneblidze-Umble diagonal defined in [SU04]. This involves some shift operations on facets of the diagonal, which are interesting on their own right, and lead to lattice and cubic structures. The proof is technical and proceeds in several steps: we introduce two additional combinatorial descriptions of the diagonal, that we call the 1-shift and m -shift SU diagonals, and show the sequence of equivalences

$$\text{original } \Delta^{\text{SU}} \xleftrightarrow{6.15} \text{1-shift } \Delta^{\text{SU}} \xleftrightarrow{6.14} \text{m-shift } \Delta^{\text{SU}} \xleftrightarrow{6.23} \text{geometric } \Delta^{\text{SU}}.$$

Throughout this section, we borrow notation from [SU22].

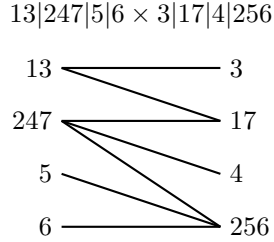
6.1. Topological enhancement of the original SU diagonal. We proceed to introduce different versions of the SU diagonal, and to prove that all these notions coincide.

6.1.1. Strong complementary pairs. We start by the following definition.

Definition 6.1. A *strong complementary pair*, or **SCP** for short, is a pair (σ, τ) of ordered partitions of $[n]$ where σ is obtained from a permutation of $[n]$ by merging the adjacent elements which are decreasing, and τ is obtained from the same permutation by merging the adjacent elements which are increasing.

We denote by $\text{SCP}(n)$ the set of SCPs of $[n]$, which is in bijection with the set of permutations of $[n]$. As is clear from the definition, the intersection graph of a SCP is a $(2, n)$ -partition tree.

Example 6.2. The SCP associated to the permutation $3|1|7|4|2|5|6$ is



Observe that the permutation can be read off the intersection graph of the SCP by a vertical down slice through the edges.

Notation 6.3. For a $(2, n)$ -partition tree (σ, τ) , we denote by $\sigma_{i,j}$ (resp. $\tau_{i,j}$) the unique oriented path between blocks σ_i and σ_j (resp. τ_i and τ_j). Note that we make a slight abuse in notation, as the path $\sigma_{i,j}$ also depends on τ .

We can immediately characterize the paths between adjacent blocks in SCPs.

Proposition 6.4. For any SCP (σ, τ) , we have

- (1) $\sigma_{i,i+1} = (\min \sigma_i, \max \sigma_{i+1})$ and $\min \sigma_i < \max \sigma_{i+1}$, and
- (2) $\tau_{i,i+1} = (\max \tau_i, \min \tau_{i+1})$ and $\min \tau_{i+1} < \max \tau_i$.

As a consequence, all SCPs are in both Δ^{LA} and Δ^{SU} , and constitute precisely the set of facets (σ, τ) of these diagonals such that $\max_{\mathbf{v}}(\sigma) = \min_{\mathbf{v}}(\tau)$.

Proof. First, the path description of (σ, τ) is a straightforward observation. Second, since the minima of these paths are traversed from left to right, and the maxima from right to left, Theorem 5.17 implies that SCPs are in both geometric operadic diagonals Δ^{LA} and Δ^{SU} . Third, the fact that these constitute the facets $(\sigma, \tau) \in \Delta^{\text{LA}}$ or Δ^{SU} satisfying $\max_{\mathbf{v}}(\sigma) = \min_{\mathbf{v}}(\tau)$ can be seen as follows. The maximal (resp. minimal) vertex of a face σ of the permutahedron with respect to the weak order, is obtained by ordering the elements of each block of σ in decreasing (resp. increasing) order. Thus, it is clear that the original permutation giving rise to a SCP (σ, τ) is the permutation $\max_{\mathbf{v}}(\sigma) = \min_{\mathbf{v}}(\tau)$, for any vector \mathbf{v} inducing the weak order. Since both diagonals agree with this order on the vertices, we have that SCPs are indeed facets of Δ^{LA} and

Δ^{SU} with the desired property. The fact that these are *all* the facets with this property follows from the bijection between $\text{SCP}(n)$ and the permutations of $[n]$. \square

6.1.2. *Shifts and the SU diagonals.* We recall the definition of the original SU diagonal of [SU04], based on the exposition given in [SU22]. We then introduce two variants of this definition, the 1-shift and m -shift SU diagonals, which will be shown to be equivalent to the original one.

Definition 6.5. Let $\sigma = \sigma_1 | \cdots | \sigma_k$ be an ordered partition, and let $M \subsetneq \sigma_i$ be a non-empty subset of the block σ_i . For $m \geq 1$, the *right m -shift* R_M , moves the subset M , m blocks to the right, *i.e.*

$$R_M(\sigma) := \sigma_1 | \cdots | \sigma_i \setminus M | \cdots | \sigma_{i+m} \cup M | \cdots | \sigma_k$$

while the *left m -shift* L_M , moves the subset M , m blocks to the left, *i.e.*

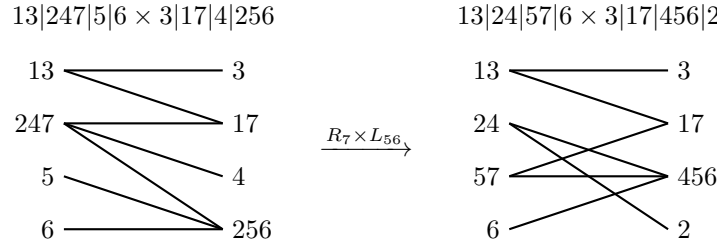
$$L_M(\sigma) := \sigma_1 | \cdots | \sigma_{i-m} \cup M | \cdots | \sigma_i \setminus M | \cdots | \sigma_k.$$

Definition 6.6. Let σ denote either one of the two ordered partitions of $[n]$ in an ordered $(2, n)$ -partition tree, and let $M \subsetneq \sigma_i$. The right m -shift R_M (resp. the left m -shift L_M) is

- (1) *block-admissible* if $\min \sigma_i \notin M$ and $\min M > \max \sigma_{i+m}$ (resp. $\min M > \max \sigma_{i-m}$),
- (2) *path-admissible* if $\min M > \max \sigma_{i,i+m}$ (resp. $\min M > \max \sigma_{i,i-m}$).

Remark 6.7. Observe that for a given subset M , an inverse to the right m -shift R_M (resp. left m -shift L_M) is given by the left m -shift L_M (resp. right m -shift R_M). Moreover, one m -shift is path-admissible if and only if its inverse is.

Example 6.8. Performing the 1-shifts R_7 and L_{56} (they are both block and path admissible) of the SCP (σ, τ) of Example 6.2, one obtains the pair $R_7(\sigma) \times L_{56}(\tau)$, as illustrated below.



We shall concentrate on three families of shifts: block-admissible 1-shifts of subsets of various sizes, path-admissible 1-shifts of singletons, and path-admissible m -shifts of singletons, for various $m \geq 1$, and show that specific sequences generate the same diagonal.

Definition 6.9. Let σ denote either one of the two ordered partitions of $[n]$ in an ordered $(2, n)$ -partition tree, and let $\mathbf{M} = (M_1, \dots, M_p)$ with $M_1 \subsetneq \sigma_{i_1}, \dots, M_p \subsetneq \sigma_{i_p}$ for some $p \geq 1$. Then the sequence of right shifts $R_{\mathbf{M}}(\sigma) := R_{M_p} \dots R_{M_1}(\sigma)$ is

- (1) *block-admissible* if we have $1 \leq i_1 < i_2 < \dots < i_p \leq k-1$, and each R_{M_j} is a block-admissible 1-shift,
- (2) *path-admissible* if each R_{M_j} is a path-admissible m_j -shift, for some $m_j \geq 1$.

Admissible sequences of left shifts are defined similarly and are denoted by $L_{\mathbf{M}}(\tau)$.

By convention, we declare the empty sequence of shift operators to be admissible, and to act by the identity, *i.e.* we have $R_{\emptyset}(\sigma) := \sigma$ and $L_{\emptyset}(\tau) := \tau$.

Definition 6.10. The facets of the *original SU diagonal*, the *1-shift SU diagonal* and the *m -shift SU diagonal* are defined by the formula

$$\Delta^{\text{SU}}([n]) = \bigcup_{(\sigma, \tau)} \bigcup_{\mathbf{M}, \mathbf{N}} R_{\mathbf{M}}(\sigma) \times L_{\mathbf{N}}(\tau)$$

where the unions are taken over all SCPs (σ, τ) of $[n]$, and respectively over all block-admissible sequences of subset 1-shifts \mathbf{M}, \mathbf{N} , over all path-admissible sequences of singleton 1-shifts, and over all path-admissible sequences of singleton m_j -shifts, for various $m_j \geq 1$.

Remark 6.11. Observe that the left (resp. right) shifts acts on the right (resp. left) ordered partition. In the analogous description for the LA diagonal Δ^{LA} obtained at in Section 6.2, left and right shifts act on the left and right ordered partitions, respectively.

6.1.3. *First isomorphism between SU diagonals.* We start by analyzing the original SU diagonal.

Proposition 6.12. *Block-admissible sequences of subset 1-shifts, defining the original SU diagonal, conserve*

- (1) *the maximal element of any path between two blocks of the same ordered partition,*
- (2) *the direction in which this element is traversed.*

In particular, for a pair of ordered partitions $(R_{\mathbf{M}}(\sigma), L_{\mathbf{N}}(\tau))$ obtained via a block-admissible sequence of 1-shifts from a SCP (σ, τ) , we have

$$(P) \quad \max R_{\mathbf{M}}(\sigma)_{i,j} = \max \sigma_{i,j} \quad \text{and} \quad \max L_{\mathbf{N}}(\tau)_{i,j} = \max \tau_{i,j}$$

and consequently

$$(B) \quad \max R_{\mathbf{M}}(\sigma)_{i,i+1} = \max \sigma_{i+1} \quad \text{and} \quad \max L_{\mathbf{N}}(\tau)_{i,i+1} = \max \tau_i.$$

Note that in Equation (P), the maxima $\max \sigma_{i,j}$ and $\max \tau_{i,j}$ are maxima of *paths*, while in Equation (B) the maxima $\max \sigma_{i+1}$ and $\max \tau_i$ are maxima of *blocks*.

Proof. We consider the right shift operator; the left shift operator proceeds similarly. Let us start with Point (1). As SCPs trivially meet the above conditions, we will prove the result inductively by assuming that the result holds for $(R_{\mathbf{M}}(\sigma), L_{\mathbf{N}}(\tau))$, and then showing that applying a block-admissible operator R_{M_k} , for $M_k \subsetneq \sigma_k$, conserves the maximal elements of paths. By the inductive hypothesis, we know that $\max R_{\mathbf{M}}(\sigma)_{k,k+1} = \max \sigma_{k+1}$. As R_{M_k} is an admissible operator, we know two things: firstly that $\min M_k > \max R_{\mathbf{M}}(\sigma)_{k+1}$, and secondly that $\max \sigma_{k+1} = \max R_{\mathbf{M}}(\sigma)_{k+1}$, as k is greater than the maximal index used by \mathbf{M} . So combining these, we know that

$$(W) \quad \min M_k > \max R_{\mathbf{M}}(\sigma)_{k+1} = \max \sigma_{k+1} = \max R_{\mathbf{M}}(\sigma)_{k,k+1}.$$

A key consequence of this inequality is that the intersection graph of $(R_{M_k} R_{\mathbf{M}}(\sigma), L_{\mathbf{N}}(\tau))$ is a bipartite tree conditional on $(R_{\mathbf{M}}(\sigma), L_{\mathbf{N}}(\tau))$ being a bipartite tree: the shift will not disconnect the graph as none of the shifted elements are in the path $R_{\mathbf{M}}(\sigma)_{k,k+1}$. So, it is legitimate to speak of unique paths between blocks.

We now explicitly explore how the shift operator R_{M_k} alters paths. Throughout the rest of this proof, we use the following shorthand: we denote by $\delta_{k,k+1} := R_{\mathbf{M}}(\sigma)_{k,k+1}$ the path between the k^{th} and $(k+1)^{\text{st}}$ blocks in $(R_{\mathbf{M}}(\sigma), L_{\mathbf{N}}(\tau))$, and by $\delta_{k+1,k}$ the same path reversed. Let γ be any path between two blocks of $(R_{\mathbf{M}}(\sigma), L_{\mathbf{N}}(\tau))$, and let γ' be the path between the same blocks, by indices, in $(R_{M_k} R_{\mathbf{M}}(\sigma), L_{\mathbf{N}}(\tau))$. There are four cases to consider.

- i) the path γ does not contain an element of M_k . In this case, it is unaffected by the shift, so $\gamma' = \gamma$. We note that in light of Equation (W), the path $\delta_{k,k+1}$ meets this case.
- ii) the path γ contains one element $m \in M_k$, *i.e.* it is of the form $\gamma = \alpha m \beta$, with α or β possibly empty. We assume that m is incoming to $R_{\mathbf{M}}(\sigma)_k$, the case when it is outgoing is similar. We must have $\alpha \cap \delta_{k,k+1} = \emptyset$, since otherwise there would be an oriented loop from $R_{\mathbf{M}}(\sigma)_k$ to itself. For the same reason, $\beta \cap \delta_{k,k+1}$ must be connected and starting at $R_{\mathbf{M}}(\sigma)_k$. Then there are two cases to consider:
 - (a) the path β does not use any steps of $\delta_{k,k+1}$, in which case $\gamma' = \alpha m \delta_{k+1,k} \beta$. This is a path in the tree of $(R_{M_k} R_{\mathbf{M}}(\sigma), L_{\mathbf{N}}(\tau))$ with no repeated steps, as such it must be the unique minimal path.
 - (b) the path β uses steps of $\delta_{k,k+1}$, in which case $\gamma' = \alpha m (\delta_{k+1,k} \setminus \beta) (\beta \setminus \delta_{k+1,k})$. This follows, as we know that β must follow the path $\delta_{k,k+1}$ for some time before diverging (β could also be a subset of $\delta_{k,k+1}$, in which case it will never diverge). As such, the path $(\delta_{k+1,k} \setminus \beta)$ reaches the point of divergence from $R_{\mathbf{M}}(\sigma)_{k+1}$ instead of $R_{\mathbf{M}}(\sigma)_k$, and the path $(\beta \setminus \delta_{k+1,k})$ completes the rest of the route unchanged.

- iii) the path γ contains two elements of M_k . In this case we still have $\gamma' = \gamma$ (in path elements) but γ' will step through the $(k+1)^{\text{st}}$ block instead of γ stepping through the k^{th} block.
- iv) the path γ contains more than two elements of M_k . This is impossible, as γ would not be a minimal path on a tree.

Observe that all (non-trivial or non-contradictory) paths γ' contain $m \geq \min M_k$ and either some addition or deletion by $\delta_{k,k+1}$. It thus follows from Equation (W) that $\max \gamma' = \max \gamma$, since in each case, the maximal element will either be m , or in α , or in β . This finishes the proof of Point (1).

For Point (2), we need to see that the maximal element $\max \gamma = \max \gamma'$ is traversed in the same direction. It is immediate for cases (i), (ii.a) and (iii); the condition is empty in the case (iv). For the case (ii.b) it follows from the observation that the number of steps of $\beta \cap \delta_{k,k+1}$ and $\delta_{k,k+1} \setminus \beta$ have the same parity: since $\delta_{k,k+1}$ has an even number of steps, either they both have an even number of steps, or an odd number, which completes the proof. \square

Corollary 6.13. *Path-admissible sequences of singleton 1-shifts, defining the 1-shift SU diagonal, conserve*

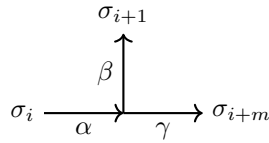
- (1) *the maximal element of any path between two blocks of the same ordered partition,*
- (2) *the direction in which this element is traversed.*

Proof. By the definition of path-admissible 1-shifts (Definition 6.9), the outer inequality of Equation (W) holds by assumption. As such, can run the proof of Proposition 6.12 *mutatis mutandis*. \square

We are now in position to show that the 1-shift and m -shift descriptions are equivalent.

Proposition 6.14. *The 1-shift and m -shift SU diagonals coincide.*

Proof. It is clear that any path-admissible sequence of 1-shifts is a path-admissible sequence of m -shifts, and thus that the facets of the 1-shift SU diagonal are facets of the m -shift SU diagonal. For the reverse inclusion, we need to show that any m -shift can be re-expressed as a path-admissible sequence of 1-shifts. We proceed by induction, and consider only the case of right shifts, the case of left shifts is similar. For right 1-shifts, there is nothing to prove. Let (σ, τ) be a pair of ordered partitions which has been generated only by k -shifts, for $k < m$. We wish to show that any path-admissible right m -shift R_ρ^m on σ can be decomposed as a path-admissible 1-shift R_ρ^1 followed by a path-admissible $(m-1)$ -shift R_ρ^{m-1} , which yields the result by induction. As R_ρ^m is path-admissible, we know that $\rho > \max \sigma_{i,i+m}$, and we want to show that $\rho > \max \sigma_{i,i+m} \geq \max \sigma_{i,i+1}, \max R_\rho^1(\sigma)_{i+1,i+m}$.



We define the oriented paths $\alpha := \sigma_{i,i+1} \setminus \sigma_{i+1,i+m}$, $\beta := \sigma_{i,i+1} \setminus \sigma_{i,i+m}$ and $\gamma := \sigma_{i,i+m} \setminus \sigma_{i,i+1}$, as illustrated above. Suppose that β is not empty, and moreover that $\max \sigma_{i+1,i+m} > \max \sigma_{i,i+m}$ or $\max \sigma_{i,i+1} > \max \sigma_{i,i+m}$. Then we must have that $\max \beta > \max \alpha, \max \gamma$. However, $\max \beta$ cannot be the maximum of both $\sigma_{i,i+1}$ and $\sigma_{i+1,i+m}$. Indeed, in this case, it would be traversed in two opposite directions, which is impossible since by the induction hypothesis (σ, τ) can be generated by 1-shifts, and by Corollary 6.13 these conserve the maximal elements of paths and their direction. We thus have $\max \sigma_{i,i+m} \geq \max \sigma_{i,i+1}, \max \sigma_{i+1,i+m}$, and applying Corollary 6.13 again yields $\max \sigma_{i,i+m} \geq \max R_\rho^1(\sigma)_{i+1,i+m}$ as required. \square

We stress that Equation (W) holds for m -shifts without us needing to perform shifts in increasing order, or requiring $\min M_k > \max R_M(\sigma)_{k+1}$. We are now ready to prove that the m -shift description is equivalent to the original one.

Theorem 6.15. *The original and m -shift SU diagonals coincide.*

Proof. Since m -shift and 1-shift diagonals are equivalent (Proposition 6.14), it suffices to show that the 1-shift and original SU diagonals coincide. We analyze the right shift operator, the case of the left shift is similar. First, we observe that any block-admissible right shift $R_M(\sigma)$, for $M \subsetneq \sigma_k$, can be decomposed into a series of singleton right 1-shifts; since $\min M > \max \sigma_{k,k+1}$ by the proof of Proposition 6.12, we can shift the elements of M to the right, one after the other (in any order!). This shows that any facet of the original SU diagonal is also a facet in the 1-shift SU diagonal.

For the reverse inclusion, we proceed by induction. We are required to show that if we apply a right 1-shift to $(R_M(\sigma), L_N(\tau))$, say $(R_\rho R_M(\sigma), L_N(\tau))$, then this can be re-expressed as a well-defined subset shift operation $(R_{M'}(\sigma), L_N(\tau))$. Suppose that prior to the 1-shift, the element ρ lives in block ℓ , then we must have

$$1 \leq i_1 < \dots < i_j \leq \ell < i_{j+1} < \dots < i_p \leq k-1$$

for some j . If $i_j < \ell$, then we have $R_\rho R_M(\sigma) = R_{M_p} \dots R_{\{\rho\}} R_{M_j} \dots R_{M_1}(\sigma)$, and we are done. Otherwise, if $i_j = \ell$, we set $M'_j := M_j \cup \{\rho\}$. It is clear that $R_\rho R_M(\sigma) = R_{M_p} \dots R_{M'_j} \dots R_{M_1}(\sigma)$, however, we need to check that $R_{M'_j}$ is block-admissible, *i.e.* that $\min M'_j > \max(R_{M_{j-1}} \dots R_{M_1}(\sigma))_{i_j+1}$. If we have $\rho > \min M_j$, then we are done since in this case $\min M'_j = \min M_j$ and R_{M_j} is block-admissible. Otherwise, we have $\rho = \min M'_j$. Since by definition block-admissible shift operators do not move the minimal element of a block, we have $\rho > \min R_M(\sigma)_{i_j} = \min(R_{M_{j-1}} \dots R_{M_1}(\sigma))_{i_j}$. Then, by induction, Proposition 6.12 shows that $\rho > \max \sigma_{i_j+1} = \max(R_{M_{j-1}} \dots R_{M_1}(\sigma))_{i_j+1}$, where the equality follows as $i_1 < \dots < i_j$. This proves that $R_{M'_j}$ is block-admissible, completing the inductive proof. \square

6.1.4. Inversions. Our next goal is to prove the equivalence between the m -shift and geometric SU diagonals (Theorem 6.23). As a tool for this proof, we now study *inversions*, or crossings in the partition trees of the geometric SU diagonal.

Definition 6.16. Let σ be an ordered partition.

- The *inversions* of an ordered partition are $I(\sigma) := \{(i, j) : i < j \wedge \sigma^{-1}(j) < \sigma^{-1}(i)\}$.
- The *anti-inversions* of an ordered partition are $J(\sigma) := \{(i, j) : i < j \wedge \sigma^{-1}(i) < \sigma^{-1}(j)\}$.

We then define the *inversions of an ordered partition pair* $I((\sigma, \tau)) := I(\tau) \cap J(\sigma)$.

In words, the inversions of an ordered partition pair are those $i < j$ pairs in which j comes in an earlier block than i in τ , and i comes in an earlier block than j in σ .

Proposition 6.17. *The set of inversions of a facet of the geometric SU diagonal is in bijection with its set of edge crossings. Moreover, under this bijection, strong complementary pairs correspond to facets with no crossings.*

Proof. For the first part of the statement, we note that crossings are clearly produced by both $I(\tau) \cap J(\sigma)$ and $I(\sigma) \cap J(\tau)$ (*i.e.* in the second case j appears before i in σ and i before j in τ). However, the later cannot occur in a facet of the geometric Δ^{SU} ; this follows immediately from the (I, J) -conditions for $\#I = \#J = 1$. The second part of the statement follows from the fact that facets of the diagonal Δ^{SU} with no crossings are in bijection with permutations. By definition (Definition 6.1), from a partition one obtains a SCP, which is in the geometric Δ^{SU} (Proposition 6.4). In the other way around, given a SCP, one can read-off the partition in the associated tree, which has no crossings, by a vertical down-slice of edges (Example 6.2). \square

See Figure 20 for an example of this bijection.

Definition 6.18. We say that an edge crossing is an *adjacent crossing* if the two crossing elements are in adjacent blocks of the partition tree (*i.e.* they are in blocks of the form $\sigma_i | \sigma_{i+1}$ or $\tau_i | \tau_{i+1}$).

Lemma 6.19. *A facet (σ, τ) of the geometric SU diagonal has a crossing if and only if it has an adjacent crossing.*

Proof. An adjacent crossing is clearly a crossing. In the other direction, suppose there is a crossing between an element of σ_i and an element of σ_j . If σ_i and σ_j are not adjacent, then the “triangle” produced by the crossing elements encloses another σ_k such that $i < k < j$, and this produces other crossings. We may repeat this process until an adjacent crossing is found. \square

6.1.5. *Second isomorphism between SU diagonals.* We now aim at showing that the m -shift and the geometric SU diagonal coincide (Theorem 5.13). Recall from Remark 6.7 that left and right path-admissible m -shifts are inverses to one another.

Proposition 6.20. *Let (σ, τ) be a facet of the geometric SU diagonal Δ^{SU} . Then, any pair of ordered partitions obtained by applying a path-admissible m -shift to (σ, τ) is also in the geometric SU diagonal.*

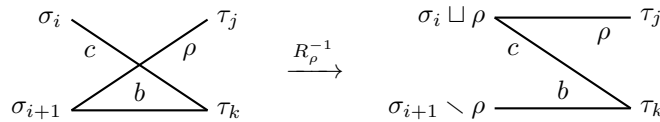
Proof. We consider a right path-admissible shift R_ρ , the left shift and dual result proceeds similarly. Combining Corollary 6.13 and Proposition 6.14, we have that the maxima of paths between consecutive vertices in $(R_\rho(\sigma), \tau)$ are the same as the ones in (σ, τ) , and are moreover traversed in the same direction. Thus, all maxima of paths in $(R_\rho(\sigma), \tau)$ are traversed from right to left, and hence by Theorem 5.17, we have that $(R_\rho(\sigma), \tau)$ is in the geometric SU diagonal. \square

Lemma 6.21. *Any facet (σ, τ) of the geometric SU diagonal Δ^{SU} is mapped to a SCP by a path-admissible sequence of inverse m -shifts.*

Proof. We show that any facet (σ, τ) which has a crossing, and is hence not a SCP, admits an inverse shift operation. This shows that a finite number of inverse shift operations converts any facet to a SCP (if σ is an ordered partition of n with k blocks, then clearly less than n^k inverse shifts are possible). We consider the following partition of the set of facets with crossings, illustrated by example in Example 6.22.

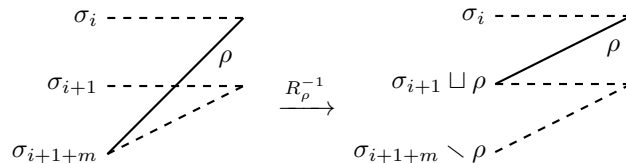
- (1) All adjacent blocks are connected by paths of length 2.
- (2) There exist adjacent blocks which are connected by a path of length $2k$ for $k > 1$.
 - (a) The maximal step of this path is not the last step.
 - (i) The τ block containing the maximal step is not the greatest block.
 - (ii) The τ block containing the maximal step is the greatest block.

In Case (1), as (σ, τ) has a crossing, it has an adjacent crossing by Lemma 6.19. This adjacent crossing is of the following form (we illustrate the case where the crossing happens on the left, the case when it happens on the right is similar):



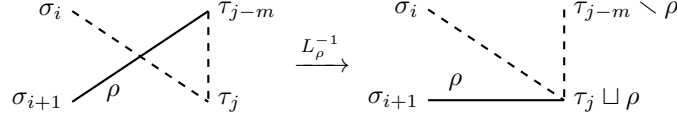
By the path characterization of the geometric SU diagonal (Theorem 5.17), the fact that $\tau_j < \tau_k$ implies that $\rho > b$, and the fact that $\sigma_i < \sigma_{i+1}$ implies that $b > c$. Thus, we have $\rho > \max \sigma_{i,i+1}$, which implies that a path-admissible left shift R_ρ^{-1} can be performed.

In Case (2.a), consider the two adjacent blocks say $\sigma_i | \sigma_{i+1}$ (the τ case is similar), let $\rho := \max \sigma_{i,i+1}$ denote the maximum of the path between them, and let $m \geq 1$ be such that ρ steps into σ_{i+1+m} . Since $\max \sigma_{i,i+1+m} = \max \sigma_{i,i+1} = \rho$ the definition of the geometric SU diagonal implies that the block σ_{i+1+m} comes after the block σ_i , and by assumption after the block σ_{i+1} . Thus, we know that $m > 1$, and using dashed lines to denote paths of length ≥ 1 we have the following picture

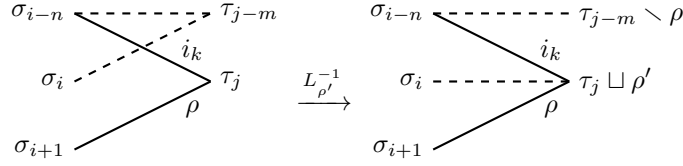


As we have $\rho = \max \sigma_{i,i+1} > \max \sigma_{i+1+m,i+1}$, an inverse m -shift operation can be performed.

In the Case (2.b.i), there exists $j, m > 0$ such that τ_{j-m} is the block of τ which contains the maximal element ρ , and τ_j is any greater block on the path from σ_i to σ_{i+1} . Then we may apply the following inverse m -shift operator.



There remains to be treated Case (2.b.ii). We consider the path $\sigma_{i,i+1} := (i_1, j_1, i_2, \dots, i_k, \rho)$ to be of length $2k$, $k > 1$. We denote by τ_j the block of τ containing the maximal step ρ of this path, which by hypothesis is the last block of τ . Let σ_{i-n} be the last block of σ which is attained by the path $\sigma_{i,i+1}$ before the block σ_{i+1} . We must have $n > 1$, since ρ is the last step and $\sigma_i | \sigma_{i+1}$ are adjacent blocks. The situation can be pictured as on the left.

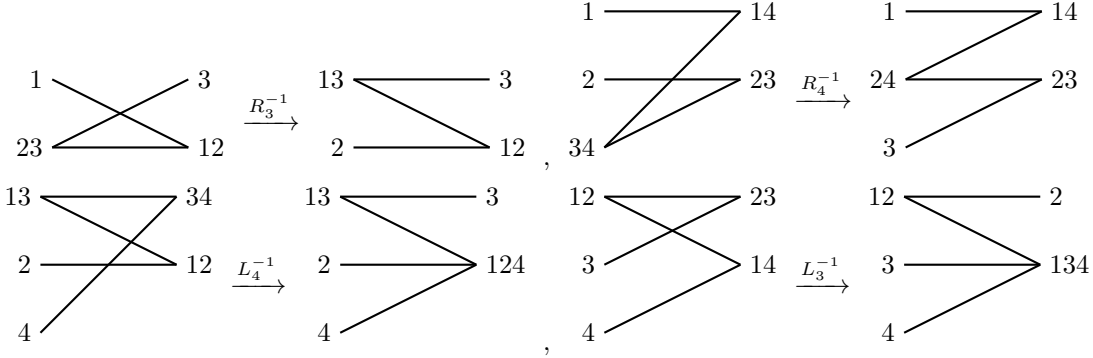


Now let $\rho' := \max \sigma_{i,i-n}$ be the maximum of the path $\sigma_{i,i-n} = (i_1, j_1, i_2, \dots, i_{k-1}, j_{k-1})$, and let τ_{j-m} , $m \geq 1$ be the block of τ containing ρ' . We want to show that an inverse left m -shift can bring ρ' back to τ_j , i.e. we need $\rho' > \max \tau_{j-m,j}$. As $\rho' := \max \sigma_{i,i-n}$, and apart from the step i_k we have $\tau_{j-m,j} \subset \sigma_{i,i-n}$, we just need to show that $\rho' > i_k$. To see that this is indeed the case, it suffices to look at the last steps

$$\tau_l \xrightarrow{j_{k-1}} \sigma_{i-n} \xrightarrow{i_k} \tau_j \xrightarrow{\rho} \sigma_{i+1}$$

of the path $\sigma_{i,i+1}$. By the definition of the geometric SU diagonal, the fact that $\tau_l < \tau_j$ implies that $j_{k-1} > i_k$, and thus that $\rho' > i_k$, which finishes the proof. \square

Example 6.22. Here are examples of each of the cases in the proof of Lemma 6.21. We display cases (1), (2.a), (2.b.i) and, (2.b.ii) respectively, reading the diagrams from top-left to bottom-right.



Note that, as we have chosen minimal illustrative examples, each inverse m -shift is an inverse 1-shift, and after each shift we obtain a SCP. This is not typically the case.

Theorem 6.23. *The m -shift and the geometric SU diagonals coincide.*

Proof. We first note that SCPs are known elements of both the m -shift and the geometric SU diagonals (Proposition 6.4). The proof that every facet of the m -shift Δ^{SU} is in geometric Δ^{SU} follows from the closure of Δ^{SU} under the shift operators (Proposition 6.20). The proof that every facet of geometric Δ^{SU} is in shift Δ^{SU} follows from the closure of Δ^{SU} under the inverse shift operator (Proposition 6.20) and the fact that every facet is sent to a SCP after a finite number of inverse shifts (Lemma 6.21). In particular, for any given facet in geometric Δ^{SU} , this provides a SCP and a sequence of shifts to form it, showing it is a facet of m -shift Δ^{SU} . \square

Combining Theorem 6.15 and Theorem 6.23, we obtain the desired equivalence between the original SU diagonal from [SU04] and the geometric SU diagonal from Definition 5.3.

Theorem 6.24. *The original and geometric SU diagonals coincide.*

6.2. Shifts under the face poset isomorphism. Having proven the equivalence of the original and geometric SU diagonals, we now use the face poset isomorphisms between the geometric LA and SU diagonals from Section 5.3 to translate results and combinatorial descriptions from one to the other. Under the isomorphism $t(r \times r) : \Delta^{\text{LA}} \rightarrow \Delta^{\text{SU}}$ from Remark 5.16, we get a straightforward analogue of Definition 6.9 for the LA diagonal. Firstly, the morphism $r \times r$ exchanges max and min, which yields the following “dual” notions of admissibility.

Definition 6.25. Let σ denote either one of the two ordered partitions of $[n]$ in a $(2, n)$ -partition tree, and let $M \subsetneq \sigma_i$. The right m -shift R_M (resp. the left m -shift L_M) is

- (1) *block-admissible* if $\max \sigma_i \notin M$ and $\max M < \min \sigma_{i+m}$ (resp. $\max M < \min \sigma_{i-m}$),
- (2) *path-admissible* if $\max M < \min \sigma_{i,i+m}$ (resp. $\max M < \min \sigma_{i,i-m}$).

Secondly, as the morphism t switches our ordered partitions, this means that the LA lefts shifts will act on the left ordered partition, and the LA right shifts will act on the right ordered partition. Consequently, admissible sequences of LA shifts are defined similarly to Definition 6.9 (simply replace σ with τ). Which provides an analogue of Definition 6.10 for the LA diagonal.

Definition 6.26. The facets of the *subset shift, 1-shift and m -shift LA diagonals* are given by the formula

$$\Delta^{\text{LA}}([n]) = \bigcup_{(\sigma, \tau)} \bigcup_{\mathbf{M}, \mathbf{N}} L_{\mathbf{M}}(\sigma) \times R_{\mathbf{N}}(\tau)$$

where the unions are taken over all SCPs (σ, τ) of $[n]$, and respectively over all block-admissible sequences of subset 1-shifts \mathbf{M}, \mathbf{N} , over all path-admissible sequences of singleton 1-shifts, and over all path-admissible sequences of singleton m_j -shifts, for various $m_j \geq 1$.

We now formally verify that the isomorphism $t(r \times r)$ relates these shift definitions as claimed.

Proposition 6.27. *Let (σ, τ) be a facet of Δ^{LA} . For each type of LA shift, let \mathbf{M}, \mathbf{N} be admissible sequences of this type, then*

$$t(r, r)(L_{\mathbf{N}}(\sigma), R_{\mathbf{M}}(\tau)) = (R_{r\mathbf{M}}(r\tau), L_{r\mathbf{N}}(r\sigma))$$

where $r\mathbf{M} := (rM_1, \dots, rM_p)$ and $r\mathbf{N}$ (defined similarly) are admissible sequences of SU shifts of the same type.

Proof. As reversing the elements then shifting them is the same as shifting the elements then reversing them, it is clear that the equality holds if $r\mathbf{M}, r\mathbf{N}$ are admissible sequences of SU shifts. As such, we must simply verify the admissibility, and given the equivalence of the various shift definitions, we just do this for path-admissibility of 1-shifts. Consider a right shift R_M , for $M \in \sigma_i$, which is path-admissible in the LA sense (Definition 6.25). Then, we have $\max M < \min \sigma_{i,i+1}$ which implies that $\min rM > \max r\sigma_{i,i+1}$, and thus the right shift R_{rM} is path-admissible in the SU sense (Definition 6.9). Here, $rM \in r\sigma_i$ is interpreted as being in a block of the right partition (τ in the notation of the definition). So, if $\mathbf{M} = (M_{i_1}, \dots, M_{i_p})$, define $r(\mathbf{M}) := (rM_1, \dots, rM_p)$, and from the prior it is clear this is a path-admissible sequence of SU shifts, finishing the proof. \square

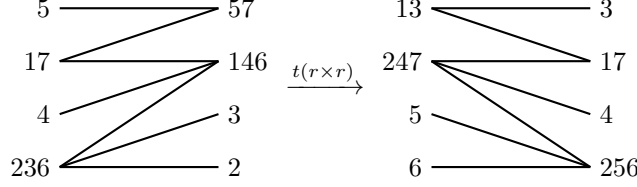
Thus, given $t(r \times r)$ is an isomorphism of the geometric diagonals (Remark 5.16), and the geometric SU diagonal coincides with the shift SU diagonals (Section 6.1.2), we immediately obtain the following statement.

Proposition 6.28. *The geometric LA diagonal and all shift LA diagonals coincide.*

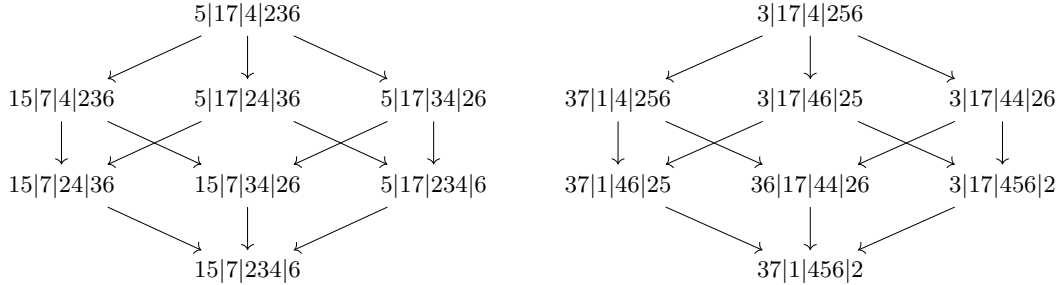
Remark 6.29. The isomorphism $rs \times rs : \Delta^{\text{LA}} \rightarrow \Delta^{\text{SU}}$, identified in Theorem 5.15, also sends shifts operators to shift operators, but it sends left shift operators to right shift operators and vice versa. The LA^{op} and SU^{op} diagonals also admit obvious dual shift descriptions.

We now explore in example how the isomorphism $t(r \times r)$ translates the shift operators.

Example 6.30. The isomorphism $t(r \times r)$ sends the SCP $(\sigma, \tau) := (5|17|4|236, 57|146|3|2)$ to the SCP $(\sigma', \tau') := (13|247|5|6, 3|17|4|256)$. The corresponding $(2, n)$ -partition trees present a clear symmetry



We now illustrate all possible path admissible LA 1-shifts of (σ, τ) and all possible path admissible SU 1-shifts of (σ', τ') . We first display how the LA left shifts act on σ , and the SU left shifts act on τ' . The LA shifts have been drawn so that the leftmost arrow shifts the smallest element, and the SU shifts have been drawn so that the leftmost arrow shifts the largest element. As such, the face poset isomorphism $t(r \times r)$ directly translates one diagram to the other. The specific element being shifted can be inferred by the source and target of the arrow.



We now illustrate all the possible LA right shifts acting on τ

$$\sigma \times 57|146|3|2 \xrightarrow{\rho=1} \sigma \times 57|46|13|2 \xrightarrow{\rho=1} \sigma \times 57|46|3|12$$

and all possible SU right shifts acting on σ'

$$13|247|5|6 \times \tau' \xrightarrow{\rho=7} 13|24|57|6 \times \tau' \xrightarrow{\rho=7} 13|24|5|67 \times \tau'.$$

No other shifts are possible; observe for instance that we cannot perform the LA left shift $15|7|234|6 \times 57|46|13|2 \xrightarrow{\rho=2} 15|27|34|6 \times 57|46|13|2$ as the minimal path connecting 234 and 7 contains 1, which is smaller than 2 (see Example 5.18). We shall see in Section 6.3, that these diagrams are the Hasse diagrams of lattices.

Example 6.31. It was observed in [LA22] that the LA and SU diagonals coincided up until $n = 3$, however due to their dual shift structure they generate the non-SCP pairs in a dual fashion. In particular, the two center faces of the subdivided hexagon of Figure 18 are generated by

$$\begin{array}{ccc} \begin{array}{c} 13 \text{ --- } 3 \\ \diagdown \quad \diagup \\ 2 \text{ --- } 12 \end{array} & \xrightarrow{R_3^{\text{SU}}} & \begin{array}{c} 1 \text{ --- } 3 \\ \diagup \quad \diagdown \\ 23 \text{ --- } 12 \end{array} \end{array} \quad \begin{array}{ccc} \begin{array}{c} 12 \text{ --- } 2 \\ \diagdown \quad \diagup \\ 3 \text{ --- } 13 \end{array} & \xrightarrow{L_3^{\text{SU}}} & \begin{array}{c} 12 \text{ --- } 23 \\ \diagup \quad \diagdown \\ 3 \text{ --- } 1 \end{array} \end{array}$$

and

$$\begin{array}{ccc} \begin{array}{c} 1 \text{ --- } 13 \\ \diagup \quad \diagdown \\ 23 \text{ --- } 2 \end{array} & \xrightarrow{R_1^{\text{LA}}} & \begin{array}{c} 1 \text{ --- } 3 \\ \diagdown \quad \diagup \\ 23 \text{ --- } 12 \end{array} \end{array} \quad \begin{array}{ccc} \begin{array}{c} 2 \text{ --- } 23 \\ \diagdown \quad \diagup \\ 13 \text{ --- } 1 \end{array} & \xrightarrow{L_1^{\text{LA}}} & \begin{array}{c} 12 \text{ --- } 23 \\ \diagup \quad \diagdown \\ 3 \text{ --- } 1 \end{array} \end{array}$$

where we have aligned each element, of each diagonal, vertically with its dual element.

6.3. Shift lattices. In this section, we show that the 1-shifts of the operadic diagonals Δ^{LA} and Δ^{SU} , define the covering relations of a lattice structure on the set of facets. More precisely, we show that each SCP is the minimal element of a lattice isomorphic to a product of chains, where the partial order is given by shifts. Given the bijection between SCPs and permutations, and our prior enumeration of the facets of the diagonal, this produces two new statistics on permutations. In addition, later in Section 6.4, we will use the lattice structure to relate the cubical and shift definitions of the Δ^{SU} diagonal.

Definition 6.32. The LA *shift poset* on the set of facets $(\sigma, \tau) \in \Delta^{\text{LA}}$ is defined to be the transitive closure of the relations $(\sigma, \tau) \prec (L_\rho \sigma, \tau)$ and $(\sigma, \tau) \prec (\sigma, R_\rho \tau)$, for all LA path-admissible 1-shifts L_ρ and R_ρ . The SU *shift poset* is defined similarly. Then, for each permutation v of $[n]$, we define the subposet Σ_v^{LA} (resp. Σ_v^{SU}) to be the set of all admissible LA (resp. SU) shifts of the associated SCP.

Given the shift definitions of Δ^{SU} and Δ^{LA} (Definitions 6.10 and 6.26), the subposets Σ_v^{LA} and Σ_v^{SU} are clearly connected components of their posets, with a unique minimal element corresponding to the SCP. We now aim to prove they are also lattices (Proposition 6.37).

Lemma 6.33. *The m -shift operators defining the facets of an operadic diagonal commute. That is, whenever the successive composition of two m_1, m_2 -shifts is defined on a facet of the LA or SU diagonal, the reverse order of composition is also defined, and the two yield the same facet.*

Proof. A Δ^{SU} (resp. Δ^{LA}) m -shift is defined when ρ is greater (resp. smaller) than the maximal (resp. minimal) element of the connecting path. Combining Corollary 6.13 and Proposition 6.14, we know m -shifts conserve the maximal (minimal) elements of paths and their directions. As such, we can commute any two shift operators. \square

Definition 6.34. Let v be a permutation of $[n]$, and (σ, τ) the SCP corresponding to v . For $\rho \in [n]$, we define the LA *left height* and *right height* of ρ to be

$$\begin{aligned} \ell_v(\rho) &:= \max(\{0\} \cup \{m > 0 : L_\rho(\sigma) \text{ is a path admissible LA } m\text{-shift}\}), \\ r_v(\rho) &:= \max(\{0\} \cup \{m > 0 : R_\rho(\tau) \text{ is a path admissible LA } m\text{-shift}\}). \end{aligned}$$

The left and right heights for the SU diagonal are defined similarly.

The height of an element ρ in a SCP can be explicitly calculated as follows.

Lemma 6.35. *Let (σ, τ) be the SCP corresponding to a permutation v . Then, the right LA height $r_v(\rho)$ (resp. the left LA height $\ell_v(\rho)$) of $\rho \in [n]$ is given by the number of consecutive blocks of σ (resp. of τ) to the right (resp. left) of the one containing ρ whose minima are larger than ρ . The SU heights are obtained similarly by considering blocks whose maxima are smaller than ρ .*

Proof. We consider the right SU height, the other cases are similar. As (σ, τ) is a SCP, we have $\max \sigma_{k,k+1} = \max \sigma_{k+1}$ for all $k \geq 1$. Moreover, from the equivalence between 1-shifts and m -shifts (Proposition 6.14), there exists a m -shift of ρ from σ_i to σ_{i+m} if, and only if, there exists a sequence of m consecutive 1-shifts, each satisfying $\rho > \max \sigma_{j,j+1} = \max \sigma_{j+1}$. Thus, these iterated 1-shifts will be path-admissible until the first failure at $j = r_v(\rho) + 1$. \square

Remark 6.36. The height calculations can also be reformulated directly in terms of the permutation. For instance, for the SU diagonal $r_v(\rho)$ is the number of consecutive descending runs, to the right of the descending run containing ρ , whose maximal element is smaller than ρ .

Proposition 6.37. *The subposets Σ_v^{LA} and Σ_v^{SU} , are lattices isomorphic to products of chains*

$$\Sigma_v^{\text{LA}} \cong \prod_{\rho \in [n]} [0, \ell_v(\rho)] \times \prod_{\rho \in [n]} [0, r_v(\rho)] \quad \text{and} \quad \Sigma_v^{\text{SU}} \cong \prod_{\rho \in [n]} [0, r_v(\rho)] \times \prod_{\rho \in [n]} [0, \ell_v(\rho)],$$

where $[0, k]$ is the chain lattice $0 < 1 < \dots < k$, for $k \geq 0$.

Proof. We denote by L_ρ^m (resp. R_ρ^m) a left (right) m -shift of ρ for $m > 0$, and we let it be the identity if $m = 0$. By the commutativity of m -shift operators (Lemma 6.33), and the existence of unique heights for each element (Lemma 6.35), every element of Σ_v^{LA} admits a unique shift description $(L_n^{\ell_n} \dots L_1^{\ell_1}(\sigma), R_n^{r_n} \dots R_1^{r_1}(\tau))$, where $0 \leq \ell_\rho \leq \ell_v(\rho)$ and $0 \leq r_\rho \leq r_v(\rho)$. Thus, we identify it with the pair of tuples $(\ell_1, \dots, \ell_n) \times (r_1, \dots, r_n)$. This is clearly an isomorphism of lattices. \square

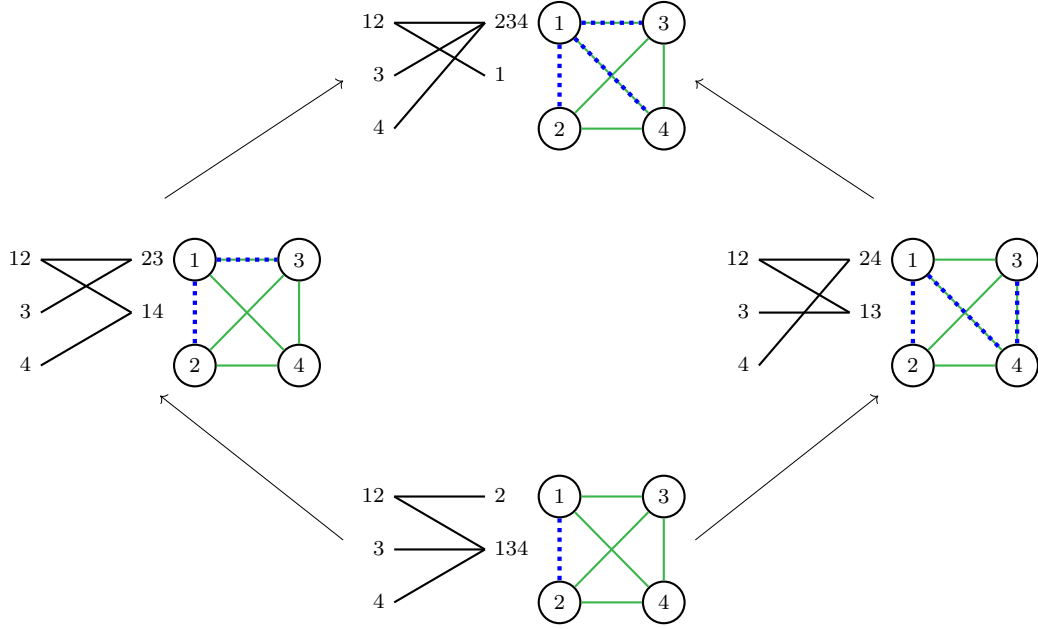


FIGURE 20. The shift lattice $\tilde{\Sigma}_v^{\text{SU}}$ for $v = 4|3|1|2$. Each facet is drawn next to a graph encoding its inversions (Definition 6.16). If $(i, j) \in J(\sigma)$, then a green edge connects (i, j) , and if $(i, j) \in I(\tau)$, then a blue dotted edge connects (i, j) . Consequently, $I((\sigma, \tau))$ is encoded by the presence of both edges, and also the crossings, by Proposition 6.17.

Note that the maximal element of $\tilde{\Sigma}_v$ (for either diagonal) is given by shifting each element of (σ, τ) by its maximal shift. The joins and meets of any two elements are also thus given by isomorphism to the product of chains. For instance, in the case of meets,

$$(\ell_1, \dots, \ell_n, r_1, \dots, r_n) \wedge (\ell'_1, \dots, \ell'_n, r'_1, \dots, r'_n) = (\min\{\ell_1, \ell'_1\}, \dots, \min\{\ell_n, \ell'_n\}, \min\{r_1, r'_1\}, \dots, \min\{r_n, r'_n\})$$

For clear examples of the Hasse diagrams corresponding to our lattices, we direct the reader to Example 6.30, and Figure 20. We note that Figure 20 also illustrates that there is no general relation between the shift lattice structure and inversions sets. In particular, the shift lattices are not sub-lattices of the facial weak order (discussed in Section 5.6), as $24|13$ and $234|1$ are incomparable.

Remark 6.38. As a consequence of Proposition 6.37, the facets of the operadic diagonals are disjoint unions of lattices. However, any lattice L on permutations (such as the weak order) induces a lattice on the facets as follows. For every $v \in L$, we can substitute the lattice $\tilde{\Sigma}_v^{\text{LA}}$ (or $\tilde{\Sigma}_v^{\text{SU}}$) into the permutation v . In particular, every element which was covered by v is now covered by the minimal element of $\tilde{\Sigma}_v^{\text{LA}}$, and every element which was covering v now covers the maximal element of $\tilde{\Sigma}_v^{\text{LA}}$.

Given our previously obtained formulae for the number of elements in the diagonal (Section 4.3), and the results of this section, we obtain the following statistics on permutations.

Corollary 6.39. *Using the heights of either diagonal,*

$$2(n+1)^{n-2} = \sum_{v \in \mathbb{S}_n} \prod_{\rho \in [n]} (\ell_v(\rho) + 1)(r_v(\rho) + 1)$$

Moreover, denoting by $\mathbb{S}_n^{k_1} \subseteq \mathbb{S}_n$ the set of permutations with k_1 ascending runs, and consequently $k_2 = n - 1 - k_1$ descending runs, we have

$$n \binom{n-1}{k_1} (n - k_1)^{k_1-1} (n - k_2)^{k_2-1} = \sum_{v \in \mathbb{S}_n^{k_1}} \prod_{\rho \in [n]} (\ell_v(\rho) + 1)(r_v(\rho) + 1).$$

Proof. This follows directly from Corollary 4.22, with the observation that shifts conserve the number of blocks, and hence the dimensions of the faces. \square

6.4. Cubical description. In this section, we recall the cubical definition of the SU diagonal from [SU22] and explicitly relate it to their shift description, using a new proof that exploits the lattice description of the diagonal (Section 6.3). Then we construct an analogous cubical definition of the LA diagonal, transferring the cubical formulae via isomorphism.

6.4.1. The cubical SU diagonal. We define inductively a subdivision $\square_{n-1}^{\text{SU}}$ of the $(n-1)$ -dimensional cube which is combinatorially isomorphic to the permutahedron $\text{Perm}(n)$ (Proposition 6.42).

Construction 6.40. Given a $(n-k)$ -dimensional face $\sigma = \sigma_1 | \dots | \sigma_k$ of the $(n-1)$ -dimensional permutahedron $\text{Perm}(n)$, we set $n_j := \# \sigma_{k-j+1} \cup \dots \cup \sigma_k$, and define a subdivision $I_\sigma := I_1 \cup \dots \cup I_k$ of the interval $[0, 1]$ by the following formulas

$$I_j := \begin{cases} [0, 1 - 2^{-n_j}] & \text{if } j = 1, \\ [1 - 2^{-n_{j-1}}, 1 - 2^{-n_j}] & \text{if } 1 < j < k, \\ [1 - 2^{-n_{j-1}}, 1] & \text{if } j = k. \end{cases}$$

Let \square_0^{SU} be the 0-dimensional cube (a point), trivially subdivided by the sole element 1 of $\text{Perm}(1)$. Then, assuming we have constructed the subdivision $\square_{n-1}^{\text{SU}}$ of the $(n-1)$ -cube, we construct \square_n^{SU} as the subdivision of $\square_{n-1}^{\text{SU}} \times [0, 1]$ given, for each face σ of $\square_{n-1}^{\text{SU}}$, by the polytopal complex $\sigma \times I_\sigma$. We label the faces $\sigma \times I$ of the subdivided rectangular prism $\sigma \times I_\sigma$ by the following rule

$$(I) \quad \sigma \times I := \begin{cases} \sigma_1 | \dots | \sigma_k | n+1 & \text{if } I = \{0\}, \\ \sigma_1 | \dots | \sigma_j | n+1 | \sigma_{j+1} | \dots | \sigma_k & \text{if } I = I_j \cap I_{j+1} \text{ with } 1 \leq j \leq k-1, \\ n+1 | \sigma_1 | \dots | \sigma_k & \text{if } I = \{1\}, \\ \sigma_1 | \dots | \sigma_j \cup \{n+1\} | \dots | \sigma_k & \text{if } I = I_j \text{ with } 1 \leq j \leq k. \end{cases}$$

This defines a subdivision \square_n^{SU} of the n -cube.

Figure 21 illustrates this subdivision for the first few dimensions. We indicate, in bold, the embedding $\square_{n-1}^{\text{SU}} \hookrightarrow \square_n^{\text{SU}}$ induced by the natural embedding $\mathbb{R}^{n-1} \hookrightarrow \mathbb{R}^n$. Only the vertices of \square_3^{SU} are labelled, but its edges, facets and outer face are all identified with the expected elements of $\text{Perm}(4)$.

Remark 6.41. A consequence of the construction is that each edge of \square_n^{SU} is parallel to one of the canonical basis vectors e_i of \mathbb{R}^n , and corresponds to shifting the element $i+1$ of $[n+1] \setminus \{1\}$.

Proposition 6.42. The polytopal complex \square_n^{SU} is combinatorially isomorphic to the permutahedron $\text{Perm}(n+1)$.

Proof. By construction it is clear that the faces of \square_n^{SU} and $\text{Perm}(n+1)$ are in bijection, and that this bijection preserves the dimension. It remains to show that this bijection is a poset isomorphism. Let $\sigma_1 | \dots | \sigma_i | \sigma_{i+1} | \dots | \sigma_k \prec \sigma_1 | \dots | \sigma_i \cup \sigma_{i+1} | \dots | \sigma_k$ be a covering relation in the face poset of $\text{Perm}(n+1)$. We need to see that the corresponding faces F, G of \square_n^{SU} satisfy $F \prec G$. From Equation (I) this clearly holds for lines. Since any face of \square_n^{SU} is a product of lines, the result follows by induction on the dimension of the faces. \square

We now unpack how certain properties of $\text{Perm}(n)$ have been encoded in the cubical structure of \square_n^{SU} . This will later allow us to construct a cubical formula for the diagonal through maximal pairings of k -subdivision cubes of \square_n^{SU} , which we now introduce.

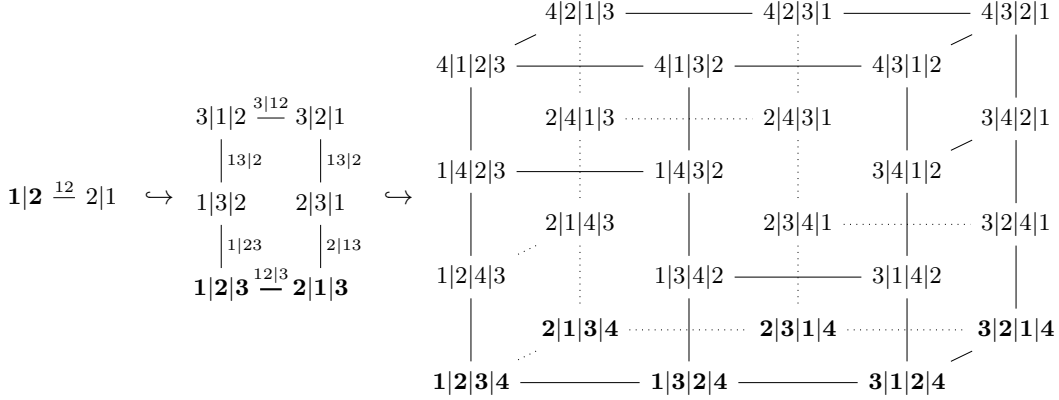


FIGURE 21. Cubical realizations \square_1^{SU} , \square_2^{SU} and \square_3^{SU} of the permutahedra $\text{Perm}(2)$, $\text{Perm}(3)$ and $\text{Perm}(4)$, respectively, from Construction 6.40.

Definition 6.43. For $k \geq 0$, a *k -subdivision cube* of \square_n^{SU} is a union of k -faces of \square_n^{SU} whose underlying set is a k -dimensional rectangular prism.

An important example of a k -subdivision cubes are the k -faces of \square_n^{SU} (other examples are provided in Example 6.48).

Lemma 6.44. A k -subdivision cube has a unique maximal (resp. minimal) vertex with respect to the weak order on permutations.

Proof. By construction, the edges of \square_n^{SU} are parallel to the basis vectors of \mathbb{R}^n (Remark 6.41), and correspond to inversions on permutations. Thus, the vector $\mathbf{v} := (1, \dots, 1)$ induces the weak order on the vertices of \square_n^{SU} . Since each k -subdivision cube is a rectangular prism whose edges are not perpendicular to \mathbf{v} , the scalar product with \mathbf{v} is maximized (resp. minimized) at a unique vertex. \square

Definition 6.45. The *maximal (resp. minimal) k -face* of a k -subdivision cube, with respect to the weak order, is the unique k -face in the subdivision cube which contains the maximal (resp. minimal) vertex.

Construction 6.46. For a k -dimensional face σ of the cubical permutahedron \square_n^{SU} , we construct the unique maximal k -subdivision cube, with respect to inclusion, whose maximal (resp. minimal) k -face with respect to the weak order is σ .

We only treat the case for the maximal k -face σ , the minimal face proceeds similarly. We build the maximal subdivision cubes inductively. Let σ be an edge of \square_n^{SU} , and let v be its maximal vertex. Let $\rho \in [n+1] \setminus \{1\}$ be the element shifted by this edge (Remark 6.41). Shifting this element to the right as far as possible (ρ will be shifted all the way to the right, or be blocked by a larger element), we get the desired 1-subdivision line.

Suppose that we have constructed maximal subdivision cubes up to dimension k , and let σ be a $(k+1)$ -face of \square_n^{SU} , with maximal vertex v . Consider the $k+1$ elements of $[n]$, which correspond to dimensions spanned by σ (Remark 6.41), and let ρ be the largest such element. Let σ_L be the 1-face, with maximal vertex v , whose only non-trivial dimension corresponds to ρ . From the initial step above, there is a unique maximal 1-subdivision line L with maximal 1-face σ_L . Let σ_C be the k -face, with maximal vertex v , spanned by the complement of ρ in $[n+1] \setminus \{1\}$. By induction, there is a maximal k -subdivision cube C with maximal k -face σ_C . Then, it is clear that the product $L \times C$ defines a $(k+1)$ -subdivision cube of \square_n^{SU} , with maximal vertex v . Indeed, as ρ is the maximal element corresponding to dimensions of $L \times C$, the faces of $L \times C$ are the

$(k + 1)$ -dimensional rectangular prisms resulting from shifting ρ through the k -faces of C , as in Equation (I).

Finally, $L \times C$ is maximal under inclusion. If there was a larger $(k + 1)$ -subdivision cube enveloping $L \times C$, then one of its projections would be a 1 or k -subdivision cube enveloping L or C , contradicting the assumption that they are maximal. This finishes the construction.

Definition 6.47. For a vertex v of \square_n^{SU} , the *hourglass* of \square_n^{SU} at v is the maximal pair of subdivision cubes \mathbb{X}_v^{SU} , with respect to inclusion, within the set of all pairs (C, C') of subdivision cubes such that C has maximal vertex v , C' has minimal vertex v , and $\dim C + \dim C' = n$.

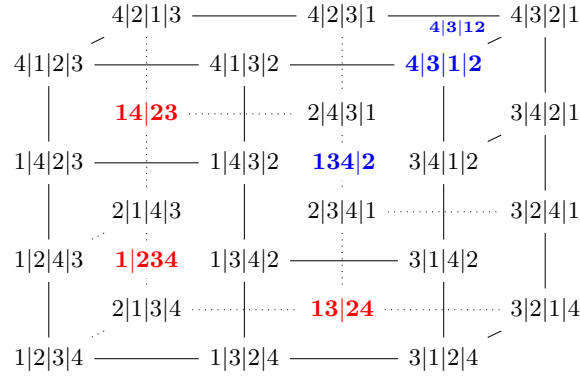


FIGURE 22. The hourglass \mathbb{X}_v^{SU} of \square_3^{SU} at $v = 4|3|1|2$.

The following examples are pictured in Figure 22.

Example 6.48. The sets of faces $\{1234\}$, $\{1|234\}$, $\{1|234, 14|23\}$, and $\{1|3|24, 1|34|2\}$ are all subdivision cubes of \square_3 . In contrast, the sets of faces $\{134|2, 14|23\}$, $\{1|234, 134|2, 14|23\}$, and $\{1|2|34, 1|23|4\}$ are not subdivision cubes of \square_3^{SU} . For $v = 4|3|1|2$, the only 1-subdivision cube with minimal vertex v is $4|3|12$, and the three 2-subdivision cubes with maximal vertex v are $\{134|2\}$, $\{13|24, 134|2\}$, $\{1|234, 13|24, 14|23, 134|2\}$. This defines the hourglass $\mathbb{X}_v^{\text{SU}} = \{1|234, 13|24, 14|23, 134|2\} \times \{4|3|12\}$ of \square_3^{SU} at v .

Let us observe that the SCP corresponding to v is $(\sigma, \tau) := (134|2, 4|3|12)$. The ordered partition σ admits three distinct right shifts, $13|24$, $14|23$, $1|234$, and τ admits no left shifts. Theorem 6.49 shows that \mathbb{X}_v^{SU} is generated by all shifts of the SCP corresponding to v .

Theorem 6.49. Let v be a vertex of the cubical permutahedron \square_n^{SU} , and let (σ, τ) be its associated SCP. Then, we have

$$\mathbb{X}_v^{\text{SU}} = \bigcup_{\mathbf{M}, \mathbf{N}} R_{\mathbf{M}}(\sigma) \times L_{\mathbf{N}}(\tau),$$

where the union is taken over all block-admissible sequences of SU shifts \mathbf{M}, \mathbf{N} .

Proof. We prove the result inductively from lines, and consider the case of σ , τ proceeds similarly. Combining Construction 6.46 with Lemma 6.35, we have that if L is a maximal 1-subdivision cube with maximal 1-face σ , then its faces are generated by the right 1-shifts R_{ρ}^i , for i between 0 and its maximal right height r_{ρ} (Definition 6.34).

Now consider the unique maximal $(k + 1)$ -subdivision cube of \square_n^{SU} with maximal $(k + 1)$ -face σ . By Construction 6.46, this subdivision cube is given by the product $L \times C$ of a line corresponding to the maximal element ρ being shifted, and a k -cube C corresponding to all other elements. By induction hypothesis, both the line L and the cube C are generated by all block-admissible right shifts from their unique maximal faces σ_L and σ_C . Moreover, if ρ is in the i th block of σ_C , then σ is obtained from σ_C by merging the i^{th} and $(i + 1)^{\text{st}}$ blocks.

On the one hand, the right height of any element being shifted in C is the same as its right height in $L \times C$. This follows from the inductive description of \square_n^{SU} (Equation (I)): every k -face in C has ρ in a singleton block, and as ρ is larger than all other elements it blocks all other shifts.

On the other hand, we know from Construction 6.46 that the $(k+1)$ -faces of $L \times C$ are obtained by weaving ρ through the k -faces of C . Indeed, every k -face in C has ρ in a fixed singleton set, and every k -face on the opposite side of $L \times C$ has ρ in another fixed singleton set; given Equation (I), this final singleton block in any k -face of C is either the last block, or is followed by a block containing an element larger than ρ . If we translate this observation back to the $(k+1)$ -faces of $L \times C$ that are adjacent to the boundary of L , then this corresponds to an equivalent calculation of the right height of ρ in σ .

Given the lattice description of the diagonal (Proposition 6.37), we thus have that $L \times C$ is generated by all block-admissible sequences of right shifts of σ , which concludes the proof. \square

This recovers the formulas [SU22, Form. (1) & (3)].

6.4.2. LA cubical description. The LA diagonal also admits a similar cubical description, which we may quickly induce by isomorphism. We first define inductively a subdivision $\square_{n-1}^{\text{LA}}$ of the $(n-1)$ -dimensional cube which is combinatorially isomorphic to the permutahedron $\text{Perm}(n)$, analogous to the one from the preceding sections.

Construction 6.50. Given a $(n-k)$ -dimensional face $\sigma = \sigma_1 | \cdots | \sigma_k$ of the $(n-1)$ -dimensional permutahedron $\text{Perm}(n)$, we set $n_j := \# \sigma_{k-j+1} \cup \cdots \cup \sigma_k$, and define a subdivision $I_\sigma := I_1 \cup \cdots \cup I_k$ of the interval $[0, 1]$ by the same formulas as in Construction 6.40.

Let \square_0^{LA} be the 0-dimensional cube (a point), trivially subdivided by the sole element 1 of $\text{Perm}(1)$. Then, assuming we have constructed the subdivision $\square_{n-1}^{\text{LA}}$ of the $(n-1)$ -cube, we construct \square_n^{LA} as the subdivision of $\square_{n-1}^{\text{LA}} \times [0, 1]$ given, for each face σ of $\square_{n-1}^{\text{LA}}$, by the polytopal complex $\sigma \times I_\sigma$. We label the faces $\sigma \times I$ of the subdivided rectangular prism $\sigma \times I_\sigma$ by the following rule

$$\sigma \times I := \begin{cases} \sigma'_1 | \cdots | \sigma'_k | 1 & \text{if } I = \{0\}, \\ \sigma'_1 | \cdots | \sigma'_j | 1 | \sigma'_{j+1} | \cdots | \sigma'_k & \text{if } I = I_j \cap I_{j+1} \text{ with } 1 \leq j \leq k-1, \\ 1 | \sigma'_1 | \cdots | \sigma'_k & \text{if } I = \{1\}, \\ \sigma'_1 | \cdots | \sigma'_j \cup \{1\} | \cdots | \sigma'_k & \text{if } I = I_j \text{ with } 1 \leq j \leq k, \end{cases}$$

where each block of σ has been renumbered as $\sigma'_i := \{p+1 \mid p \in \sigma_i\}$ for all $1 \leq i \leq k$. We obtain a subdivision \square_n^{LA} of the n -cube isomorphic to the permutahedron $\text{Perm}(n+1)$.

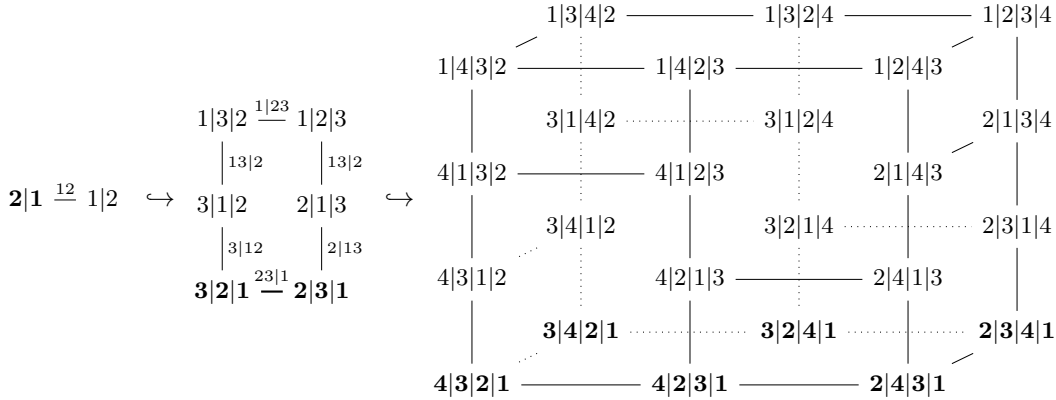


FIGURE 23. Cubical realizations of the permutahedra $\text{Perm}(2)$, $\text{Perm}(3)$ and $\text{Perm}(4)$ from Construction 6.50.

6.5. Matrix description. For completeness, we recall from [SU04] the matrix description of facets of the SU diagonal. We previously saw that SCPs and permutations are in bijection (Definition 6.1). There is also a third equivalent way to encode this data, the *step matrices* of [SU04, Def. 6]. Given a permutation, one defines its associated step matrix by starting in the bottom left corner, writing increasing sequences vertically and decreasing sequences horizontally one after the other, leaving all other entries 0. See Figure 25.

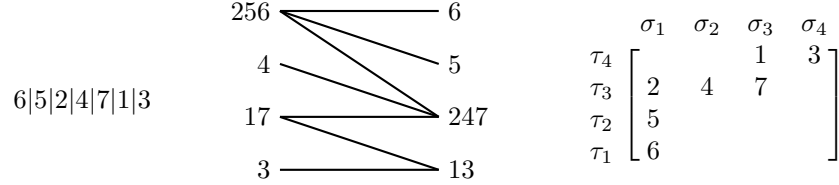


FIGURE 25. A permutation, its associated SCP, and their step matrix.

Given a matrix A whose only non-zero entries are the elements $[n]$, let $\sigma_i(A)$ denote the non-zero entries of the i^{th} column, and $\tau_j(A)$ the non-zero entries of the $(r - j + 1)^{\text{st}}$ row, where r is the number of rows of A . See the labelling in Figure 25. With this identification, the definitions of the shift operators can be translated directly: the right shift operator R_M shifts the elements of a subset $M \subset \sigma_i(A)$ one column to the right, or one row up, replacing only elements of value 0, and leaving 0 elements in their wake, while the left shift operator L_M shifts the elements of M to the left, or down one row.

The fact that the shifts avoid collisions with other elements is a consequence of their admissibility. Recall from Definition 6.6, that a right SU 1-shift R_M is *block-admissible* if $\min \sigma_i \notin M$ and $\min M > \max \sigma_{i+1}$, and that admissible sequence of right shifts proceed in increasing order (Definition 6.9).

Proposition 6.53. *Admissible sequences of matrix shift operators are well-defined.*

Proof. We verify the claim that the admissible sequences of matrix shift operators never replace non-zero elements. It is straightforward to show that this is true when a shift operator is applied to a SCP (σ, τ) . From here we proceed inductively. We assume that all prior shift operators have been well-defined, and we then check that applying another admissible shift operator is also well-defined. Suppose that an admissible right shift R_M is not well-defined, as it tries to move a value m into a non-zero matrix entry n . Then, n must have been placed into that column by a prior left shift operator L_{N_j} , and consequently $n > \min N_j > \max \tau_{j-1} > m$. However, $n \in \sigma_{i+1}$ so $\max \sigma_{i+1} > n > m > \min M_i$ implies that M is not block-admissible, a contradiction. \square

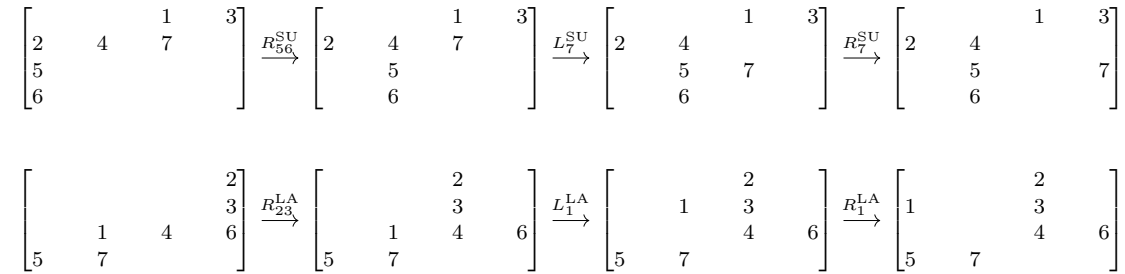


FIGURE 26. Matrix shifts under the isomorphism $t(r \times r)$ between the LA and SU diagonals.

Configuration matrices [SU04, Def. 7] are the matrices corresponding to SCPs and those generated by admissible sequences of shifts. Consequently, they are in bijection with the facets of

the SU diagonal. The translation of these results for the LA diagonal is clear. One can use the isomorphism $t(r \times r)$ as in the following example.

Example 6.54. The first row of Figure 26 contains a sequence of admissible SU subset shifts applied to the matrix encoding of the SCP $256|4|17|3 \times 6|5|147|13$. The second row is the image of these shifts under the isomorphism $t(r \times r)$. Note that the shifts of this example are also isomorphic to those of Example 6.30, under the isomorphism $(rs \times rs)$.

Part III. Higher algebraic structures

In this third part, we derive some higher algebraic consequences of the results obtained in Part II. We first prove in Section 7.1 that there are exactly two topological operad structures on the family of operahedra (resp. multiplihedra) which are compatible with the generalized Tamari order, and thus two geometric universal tensor products of (non-symmetric non-unital) homotopy operads (resp. A_∞ -morphisms). Then, we show that these topological operad structures are isomorphic (Section 7.2). However, these isomorphisms do not commute with the diagonal maps (Examples 7.14 and 7.17). Finally, we show that contrary to the case of permutahedra, the faces of the LA and SU diagonals of the operahedra (resp. multiplihedra) are in general not in bijection (Section 7.3). However, from a homotopical point of view, the two tensor products of homotopy operads (resp. A_∞ -morphisms) that they define are ∞ -isomorphic (Theorems 7.18 and 7.22).

7. HIGHER TENSOR PRODUCTS

7.1. Topological operadic structures. The permutahedra are part of a more general family of polytopes called Loday realizations of the *operahedra* [LA22, Def. 2.9], which encodes the notion of homotopy operad [LA22, Def. 4.11] (we consider here only *non-symmetric non-unital* homotopy operads). Let PT_n be the set of planar trees with n internal edges, which are labelled by $[n]$ using the infix order. For every planar tree t , there is a corresponding operahedron P_t whose codimension k faces are in bijection with nestings of t with k non-trivial nests.

Definition 7.1 ([LA22, Def. 2.1 & 2.22]). A *nest* of $t \in PT_n$ is a subset of internal edges which induce a subtree, and a *nesting* of t is a family of nests which are either included in one another, or disjoint. See Figure 27.

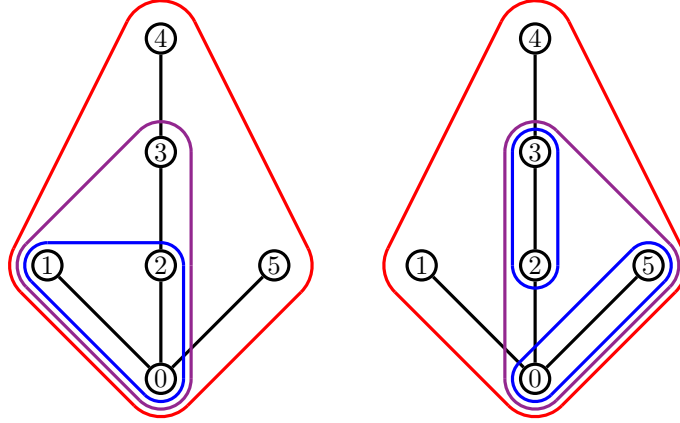


FIGURE 27. Two nestings of a tree with 5 internal edges. These nestings, Definition 7.1, are also 2-colored, Definition 7.6.

Since the operahedra are generalized permutahedra [LA22, Coro. 2.16], a choice of diagonal for the permutahedra induces a choice of diagonal for every operahedron [LA22, Coro. 1.31]. Every face of an operahedron is isomorphic to a product of lower-dimensional operahedra, via an isomorphism Θ which generalizes the one from Section 5.2, see Point (5) of [LA22, Prop. 2.3].

Definition 7.2. An *operadic diagonal* for the operahedra is a choice of diagonal \triangle_t for each Loday operahedron P_t , such that $\triangle := \{\triangle_t\}$ commutes with the map Θ , *i.e.* it satisfies [LA22, Prop. 4.14].

An operadic diagonal gives rise to topological operad structure on the set of Loday operahedra [LA22, Thm 4.18], and via the functor of cellular chains, to a universal tensor product of homotopy operads [LA22, Prop. 4.27]. Here, by *universal*, we mean a formula that applies uniformly to *any*

pair of homotopy operads. Since such an operad structure and tensor product are induced by a geometric diagonal, we shall call them *geometric*.

Theorem 7.3. *There are exactly*

- (1) *two geometric operadic diagonals of the Loday operahedra, the LA and SU diagonals,*
- (2) *two geometric colored topological cellular operad structures on the Loday operahedra,*
- (3) *two geometric universal tensor products of homotopy operads,*

which agree with the generalized Tamari order on fully nested trees.

Proof. Let us first examine Point (1). By Theorem 5.13, we know that if one of the two choices \triangle^{LA} or \triangle^{SU} is made on an operahedron P_t , one has to make the same choice on every lower-dimensional operahedron appearing in the decomposition $P_{t_1} \times \cdots \times P_{t_k} \cong F \subset P_t$ of a face F of P_t . Now suppose that one makes two distinct choices for two operahedra P_t and $P_{t'}$. It is easy to find a bigger tree t'' , of which both t and t' are subtrees. Therefore, P_t and $P_{t'}$ appear as facets of $P_{t''}$ and by the preceding remark, any choice of diagonal for $P_{t''}$ will then contradict our initial two choices. Thus, these had to be the same from the start, which concludes the proof.

Point (2) then follows from the fact that a choice of diagonal for the Loday realizations of the operahedra *forces* a unique topological cellular colored operad structure on them, see [LA22, Thm. 4.18]. Since universal tensor products of homotopy operads are induced by a colored operad structure on the operahedra [LA22, Coro. 4.24], we obtain Point (3). Finally, since only vectors with strictly decreasing coordinates induce the generalized Tamari order on the skeleton of the operahedra [LA22, Prop. 3.11], we get the last part of the statement. \square

This answers a question raised in [LA22, Rem. 3.14].

Example 7.4. The Loday associahedra correspond to the Loday operahedra associated with linear trees [LA22, Sect. 2.2], and define a suboperad. The restriction of the two operad structures of Theorem 7.3 coincide in this case, and both the LA and SU diagonals induce the *magical formula* of [MS06, MTTV21, SU22] defining a universal tensor product of A_∞ -algebras.

Example 7.5. The restriction of Theorem 7.3 to the permutahedra associated with 2-leveled trees gives two distinct universal tensor products of permutadic A_∞ -algebras, as studied in [LR13, Mar20].

Two other important families of operadic polytopes are the *Loday associahedra* and *Forcey multiplihedra*, which encode respectively A_∞ -algebras and A_∞ -morphisms [LAM23, Prop. 4.9], as well as A_∞ -categories and A_∞ -functors [LAM23, Sect. 4.3]. For every linear tree $t \in \text{PT}_n$, there is a corresponding Loday associahedron K_n , whose faces are in bijection with nestings of t , and a Forcey multiplihedron J_n whose faces are in bijection with 2-colored nestings of t .

Definition 7.6 ([LAM23, Def. 3.2]). A *2-colored nesting* is a nesting where each nest N is either blue, red, or blue and red (purple), and which satisfies that if N is blue or purple (resp. red or purple), then all nests contained in N are blue (resp. all nests that contain N are red). See Figure 27.

The Loday associahedra are faces of the Forcey multiplihedra: they correspond to 2-colored nestings where all the nests are of the same color (either blue or red).

Forcey realizations of the multiplihedra are not generalized permutahedra, but they are projections of the Ardila–Doker realizations, which are [LAM23, Prop. 1.16]. A choice of diagonal for the permutahedra thus induces a choice of diagonal for every Ardila–Doker multiplihedron, and a subset of these choices (the ones which satisfy [LAM23, Prop. 2.7 & 2.8]) further induce a choice of diagonal for the Forcey multiplihedra. Every face of a Forcey multiplihedron is isomorphic to a product of a Loday associahedron and possibly many lower-dimensional Forcey multiplihedra, via an isomorphism Θ similar to the one from Section 5.2, see Point (4) of [LAM23, Prop. 1.10].

Definition 7.7. An *operadic diagonal* for the multiplihedra is a choice of diagonal \triangle_n for each multiplihedron J_n , such that $\triangle := \{\triangle_n\}$ commutes with the map Θ .

An operadic diagonal endows the Loday associahedra with a topological operad structure [MTTV21, Thm. 1], and the Forcey multiplihedra with a topological operadic bimodule structure over the operad of Loday associahedra [LAM23, Thm. 1]. Via the functor of cellular chains, it defines universal tensor products of A_∞ -algebras and A_∞ -morphisms [LAM23, Sec. 4.2.1]. Here again, by *universal* we mean a formula that applies uniformly to any pair of A_∞ -algebras or A_∞ -morphisms. We shall call such geometrically defined operadic structures and tensor products *geometric*.

Theorem 7.8. *There are exactly*

- (1) *two geometric operadic diagonals of the Forcey multiplihedra, the LA and SU diagonals,*
- (2) *two geometric topological cellular operadic bimodule structures (over the Loday associahedra) on the Forcey multiplihedra,*
- (3) *two compatible geometric universal tensor products of A_∞ -algebras and A_∞ -morphisms,*

which agree with the Tamari-type order on atomic 2-colored nested linear trees.

Proof. Let us first examine Point (1). Consider the vectors $\mathbf{v}_{\text{LA}} := (1, 2^{-1}, 2^{-2}, \dots, 2^{-n+1})$ and $\mathbf{v}_{\text{SU}} := (2^n - 1, 2^n - 2, 2^n - 2^2, \dots, 2^n - 2^{n-1})$ in \mathbb{R}^n . As previously observed, they induce the LA and SU diagonals on the permutahedra (Definition 5.3). One checks directly that both vectors satisfy [LAM23, Prop. 2.7 & 2.8], and thus define diagonals of the Forcey multiplihedron J_n which agree with the Tamari-type order [LAM23, Prop. 2.10]. Moreover, these diagonals commute with the map Θ for the Forcey multiplihedra [LAM23, Prop. 2.14]; this is because after deleting the last coordinate of \mathbf{v}_{LA} or \mathbf{v}_{SU} , and then applying Θ^{-1} , we still have vectors which induce the LA or SU diagonal, respectively.

By Theorem 5.13, we know that if one of the two choices \triangle^{LA} or \triangle^{SU} is made on a multiplihedron J_n , one has to make the same choice on every lower-dimensional multiplihedra and associahedra appearing in the product decomposition of any face of J_n . Now suppose that one makes two distinct choices for two multiplihedra J_n and $J_{n'}$. It is easy to find a bigger multiplihedron $J_{n''}$, for which J_n and $J_{n'}$ appear in the product decomposition of a face of $J_{n''}$ and by the preceding remark, any choice of diagonal for $J_{n''}$ will then contradict our initial two choices. Thus, these had to be the same from the start, which conclude the proof of Point (1).

Point (2) then follows from the fact that a choice of diagonal for the Loday associahedra and the Forcey multiplihedra *forces* a unique topological cellular colored operad and operadic bimodule structure on them, see [MTTV21, Thm. 1] and [LAM23, Thm. 1]. Since a universal tensor products of A_∞ -algebras, and a compatible universal tensor products of A_∞ -morphisms are induced by an operad and operadic bimodule structures on the associahedra and multiplihedra respectively [LAM23, Sec. 4.2.3], we obtain Point (3). Finally, since only vectors with strictly decreasing coordinates induce the Tamari-type order on the skeleton of the Loday multiplihedra [LAM23, Prop. 2.10], we get the last part of the statement. \square

This answers a question raised in [LAM23, Rem. 3.9].

Remark 7.9. Note that in the case of the Loday associahedra, there is only one geometric operadic diagonal which induces the Tamari order atomic 2-colored nested planar trees (equivalently, binary trees, see [LAM23, Fig. 6]). Therefore, there is only one geometric topological operad structure, and only one geometric universal tensor product. This is because any vector with strictly decreasing coordinates lives in the same chamber of the fundamental hyperplane arrangement of the Loday associahedra (see [LA22, Ex. 1.21]).

Remark 7.10. Considering all 2-colored nested trees instead of only linear trees, one should obtain similar results for tensor products of ∞ -morphisms of homotopy operads.

We shall see now that the two operad (resp. operadic bimodule) structures on the operahedra (resp. multiplihedra) are related to one another in the strongest possible sense: they are isomorphic as topological cellular colored operads (resp. topological operadic bimodule structure over the associahedra).

7.2. Relating operadic structures. Recall that the topological cellular operad structure on the operahedra [LA22, Def. 4.17] is given by a family of partial composition maps

$$\circ_i^{\text{LA}} : P_{t'} \times P_{t''} \xrightarrow{\text{tr} \times \text{id}} P_{(t', \omega)} \times P_{t''} \xrightarrow{\Theta} P_t.$$

Here, the map tr is the *unique* topological cellular map which commutes with the diagonal Δ^{LA} , see [MTTV21, Prop. 7]. This partial composition \circ_i^{LA} is an isomorphism in the category Poly [LA22, Def. 4.13] between the product $P_{t'} \times P_{t''}$ and the facet $t' \circ_i t''$ of P_t . At the level of trees, the composition operation \circ_i is given by *substitution* [LA22, Fig. 14]. Using the SU diagonal Δ^{SU} , one can define similarly a topological operad structure via the same formula, but with a different transition map tr , which commutes with Δ^{SU} .

Recall that a face F of P_t is represented by a nested tree (t, \mathcal{N}) , which can be written uniquely as a sequence of substitution of trivially nested trees $(t, \mathcal{N}) = ((\dots((t_1 \circ_{i_1} t_2) \circ_{i_2} t_3) \dots) \circ_{i_k} t_{k+1})$. Here we use the increasing order on nestings [LA22, Def. 4.5], and observe that any choice of sequence of \circ_i operations yield the same nested tree, since these form an operad [LA22, Def. 4.7]. At the geometric level, we have an isomorphism

$$((\dots((\circ_{i_1}^{\text{LA}}) \circ_{i_2}^{\text{LA}}) \dots) \circ_{i_k}^{\text{LA}}) : P_{t_1} \times P_{t_2} \times \dots \times P_{t_{k+1}} \xrightarrow{\cong} F \subset P_t$$

between a uniquely determined product of lower dimensional operahedra, and the face $F = (t, \mathcal{N})$ of P_t . Note that any choice of sequence of \circ_i^{LA} operations yield the same isomorphism, since they form an operad [LA22, Thm. 4.18]. The same holds when taking the \circ_i^{SU} operations instead of the \circ_i^{LA} .

Construction 7.11. For any operahedron P_t , we define a map $\Psi_t : P_t \rightarrow P_t$

- on the interior of the top face by the identity $\text{id} : \mathring{P}_t \rightarrow \mathring{P}_t$, and
- on the interior of the face $F = ((\dots((t_1 \circ_{i_1} t_2) \circ_{i_2} t_3) \dots) \circ_{i_k} t_{k+1})$ of P_t by the composition of the two isomorphisms

$$((\dots((\circ_{i_1}^{\text{SU}}) \circ_{i_2}^{\text{SU}}) \dots) \circ_{i_k}^{\text{SU}}) ((\dots((\circ_{i_1}^{\text{LA}}) \circ_{i_2}^{\text{LA}}) \dots) \circ_{i_k}^{\text{LA}})^{-1} : F \rightarrow F.$$

Theorem 7.12. The map $\Psi := \{\Psi_t\}$ is an isomorphism of topological cellular symmetric colored operad between the LA and SU operad structures on the operahedra, in the category Poly .

Proof. By definition, we have that Ψ is an isomorphism in the category Poly . It remains to show that it preserves the operad structures, i.e. that the following diagram commutes

$$\begin{array}{ccc} P_{t'} \times P_{t''} & \xrightarrow{\circ_i^{\text{LA}}} & P_t \\ \Psi_{t'} \times \Psi_{t''} \downarrow & & \downarrow \Psi_t \\ P_{t'} \times P_{t''} & \xrightarrow{\circ_i^{\text{SU}}} & P_t \end{array}$$

For two interior points $(x, y) \in \mathring{P}_{t'} \times \mathring{P}_{t''}$, the diagram clearly commutes by definition, since $\Psi_{t'}$ and $\Psi_{t''}$ are the identity in that case. If x is in a face $F = ((\dots((t_1 \circ_{i_1} t_2) \circ_{i_2} t_3) \dots) \circ_{i_k} t_{k+1})$ of the boundary of $P_{t'}$, then the lower composite is equal to $\circ_i^{\text{SU}}(\circ_{i_1}^{\text{SU}} \circ_{i_2}^{\text{SU}} \dots \circ_{i_k}^{\text{SU}} \times \text{id})(\circ_{i_1}^{\text{LA}} \circ_{i_2}^{\text{LA}} \dots \circ_{i_k}^{\text{LA}} \times \text{id})^{-1}$, and so is the upper composite since Ψ_t starts with the inverse $(\circ_i^{\text{LA}})^{-1}$ and the decomposition of F into $P_{t_1} \times \dots \times P_{t_{k+1}} \times P_{t''}$ is unique. The case when y is in the boundary of $P_{t''}$ is similar. Finally, the compatibility of Ψ with units and the symmetric group actions are straightforward to check, see [LA22, Def. 4.17 & Thm. 4.18]. \square

Remark 7.13. Construction 7.11 and Theorem 7.12 do not depend on a specific choice of operadic diagonal. In this case, however, we do not lose any generality by using specifically the LA and SU operad structures.

Example 7.14. Note that Ψ is *not* a morphism of ‘‘Hopf’’ operads, i.e. it does not commute with the respective diagonals Δ^{LA} and Δ^{SU} . Consider the two square faces $F := 12|34$ and $G := 24|13$ of the 3-dimensional permutahedron $\text{Perm}(4)$, and choose a point $z \in (\mathring{F} + \mathring{G})/2$. Then, $\Delta^{\text{LA}}(z)$

and $\Delta^{\text{SU}}(z)$ are two different pair of points on the 1-skeleton of $\text{Perm}(4)$. Since \circ_i^{LA} and \circ_i^{SU} are the identity both on the interior of $\text{Perm}(4)$ (by Construction 7.11) and on the 1-skeleton of $\text{Perm}(4)$ (see the proof of [MTTV21, Prop. 7]), we directly obtain that

$$\Delta^{\text{LA}}(z) = (\Psi \times \Psi) \Delta^{\text{LA}}(z) \neq \Delta^{\text{SU}} \Psi(z) = \Delta^{\text{SU}}(z).$$

Recall that the topological cellular operadic bimodule structure on the Forcey multiplihedra is given by a family of action-composition maps [LAM23, Def. 2.13]

$$\begin{aligned} \circ_{p+1}^{\text{LA}} : J_{p+1+r} \times K_q &\xrightarrow{\text{tr} \times \text{id}} J_{(1, \dots, q, \dots, 1)} \times K_q \xrightarrow{\Theta_{p,q,r}} J_n \text{ and} \\ \gamma_{i_1, \dots, i_k}^{\text{LA}} : K_k \times J_{i_1} \times \dots \times J_{i_k} &\xrightarrow{\text{tr} \times \text{id}} K_{(i_1, \dots, i_k)} \times J_{i_1} \times \dots \times J_{i_k} \xrightarrow{\Theta^{i_1, \dots, i_k}} J_{i_1 + \dots + i_k}. \end{aligned}$$

Here, the map tr is the *unique* topological cellular map which commutes with the diagonal Δ^{LA} , see [MTTV21, Prop. 7]. These action-composition maps \circ_{p+1}^{LA} and $\gamma_{i_1, \dots, i_k}^{\text{LA}}$ are isomorphisms in the category Poly [LAM23, Sec. 2.1] between the products $J_{p+1+r} \times K_q$ and $K_k \times J_{i_1} \times \dots \times J_{i_k}$, and corresponding facets of J_n and $J_{i_1 + \dots + i_k}$, respectively. Using the SU diagonal Δ^{SU} , one defines similarly a topological operadic bimodule structure via the same formula, but with a different transition map tr , which commutes with Δ^{SU} .

There is a bijection between 2-colored planar trees and 2-colored nested linear trees [LAM23, Lem. 3.4 & Fig. 6], which translate grafting of planar trees into substitution at a vertex of nested linear trees. The indices of the \circ_{p+1} and γ_{i_1, \dots, i_k} operations above refer to grafting. Equivalently, a face of J_n is represented by a 2-colored nested tree (t, \mathcal{N}) , which can be written uniquely as a sequence of substitution of trivially nested 2-colored trees $(t, \mathcal{N}) = ((\dots((t_1 \circ_{i_1} t_2) \circ_{i_2} t_3) \dots) \circ_{i_k} t_{k+1})$. Here we use the left-levelwise order on nestings [LAM23, Def. 4.12], and translate tree grafting operations \circ_{p+1} and γ_{i_1, \dots, i_k} into nested tree substitution \circ_{i_j} . Note that any choice of substitutions yield the same 2-colored nested tree, since these form an operadic bimodule.

At the geometric level, we have an isomorphism $((\dots((\circ_{i_1}^{\text{LA}}) \circ_{i_2}^{\text{LA}}) \dots) \circ_{i_k}^{\text{LA}})$ between a uniquely determined product of lower dimensional associahedra and multiplihedra, and the face (t, \mathcal{N}) . Note that any choice of \circ_i^{LA} operations (*i.e.* the \circ_{p+1}^{LA} and $\gamma_{i_1, \dots, i_k}^{\text{LA}}$ action-composition operations) yield the same isomorphism, since they form an operadic bimodule [LAM23, Thm. 1]. The same holds when taking the \circ_i^{SU} (*i.e.* the \circ_{p+1}^{SU} and $\gamma_{i_1, \dots, i_k}^{\text{SU}}$ action-composition) operations instead.

Construction 7.15. For any Forcey multiplihedron J_n , we define a map $\Psi_n : J_n \rightarrow J_n$

- on the interior of the top face by the identity $\text{id} : \overset{\circ}{J}_n \rightarrow \overset{\circ}{J}_n$, and
- on the interior of the face $F = ((\dots((t_1 \circ_{i_1} t_2) \circ_{i_2} t_3) \dots) \circ_{i_k} t_{k+1})$ of J_n by the composition of the two isomorphisms

$$((\dots((\circ_{i_1}^{\text{SU}}) \circ_{i_2}^{\text{SU}}) \dots) \circ_{i_k}^{\text{SU}}) ((\dots((\circ_{i_1}^{\text{LA}}) \circ_{i_2}^{\text{LA}}) \dots) \circ_{i_k}^{\text{LA}})^{-1} : F \rightarrow F.$$

Theorem 7.16. The map $\Psi := \{\Psi_n\}$ is an isomorphism of topological cellular operadic bimodule structure over the Loday associahedra between the LA and SU operadic bimodule structures on the Forcey multiplihedra, in the category Poly .

Proof. The proof is the same as the one of Theorem 7.12, with the multiplihedra \circ_i^{LA} and \circ_i^{SU} operations (that is, the action-composition maps \circ_{p+1}^{LA} and $\gamma_{i_1, \dots, i_k}^{\text{LA}}$, and \circ_{p+1}^{SU} and $\gamma_{i_1, \dots, i_k}^{\text{SU}}$) in place of the operahedra operations. \square

Example 7.17. Note that Ψ does not commute with the respective diagonals Δ^{LA} and Δ^{SU} . Consider the two square faces $F := [(\bullet\bullet\bullet)\bullet]$ and $G := (\bullet[\bullet\bullet]\bullet)$ of the 3-dimensional Forcey multiplihedron J_4 , and choose a point $z \in (\overset{\circ}{F} + \overset{\circ}{G})/2$. Then, $\Delta^{\text{LA}}(z)$ and $\Delta^{\text{SU}}(z)$ are two different pair of points on the 1-skeleton of J_4 (see [LAM23, Ex. 3.7 & Fig. 9]). Since the LA and SU action-composition maps are the identity both on the interior of J_4 (by Construction 7.15) and on the 1-skeleton of J_4 (see the proof of [MTTV21, Prop. 7]), we directly obtain that

$$\Delta^{\text{LA}}(z) = (\Psi \times \Psi) \Delta^{\text{LA}}(z) \neq \Delta^{\text{SU}} \Psi(z) = \Delta^{\text{SU}}(z).$$

7.3. Tensor products. Recall that a homotopy operad \mathcal{P} is a family of vector spaces $\{\mathcal{P}(n)\}_{n \geq 1}$ together with a family of operations $\{\mu_t\}$ indexed by planar trees t [LA22, Def. 4.11]. One can consider the category of homotopy operads with strict morphisms, that is morphisms of the underlying vector spaces which commute strictly with all the higher operations μ_t , or with their ∞ -morphisms, made of a tower of homotopies controlling the lack of commutativity of their first component with the higher operations [LV12, Sec. 10.5.2].

Theorem 7.18. *For any pair of homotopy operads, the two universal tensor products defined by the LA and SU diagonals are not isomorphic in the category of homotopy operads and strict morphisms. However, they are isomorphic in the category of homotopy operads and their ∞ -morphisms.*

Proof. Since the two morphisms of topological operads Δ^{LA} and Δ^{SU} do not have the same cellular image, the tensor products that they define are not strictly isomorphic. However, they are both homotopic to the usual thin diagonal. Recall that homotopy operads are algebras over the colored operad \mathcal{O}_∞ , which is the minimal model of the operad \mathcal{O} encoding (non-symmetric non-unital) operads [LA22, Prop. 4.9]. Using the universal property of the minimal model \mathcal{O}_∞ , one can show that the algebraic diagonals $\Delta^{\text{LA}}, \Delta^{\text{SU}} : \mathcal{O}_\infty \rightarrow \mathcal{O}_\infty \otimes \mathcal{O}_\infty$ are homotopic, in the sense of [MSS02, Sec. 3.10], see [MSS02, Prop. 3.136]. Then, by [DSV16, Cor. 2] there is an ∞ -isotopy, that is an ∞ -isomorphism whose first component is the identity, between the two homotopy operad structures on the tensor product. \square

Remark 7.19. Neither of the two diagonals Δ^{LA} or Δ^{SU} are cocommutative, or coassociative, as they are special cases of A_∞ -algebras [MS06, Thm. 13].

Note that restricting to linear trees, the two tensor products of A_∞ -algebras induced by the LA and SU diagonals coincide (and are thus strictly isomorphic). Restricting to 2-leveled trees, we obtain two tensor product of permutadic A_∞ -algebras whose terms are in bijection. For the operahedra in general, such a bijection does not exist, as the following example demonstrates.

Example 7.20. The LA and SU diagonals of the operahedra associated with trees that have less than 4 internal edges have the same number of facets. However, there are 24 planar trees with 5 internal edges, such that the number of facets of the LA and SU diagonals are distinct, displayed in Figure 28. To compute these numbers, we first computed the facets of the LA and SU diagonals of the permutahedra, and then used the projection from the permutahedra to the operahedra described in [LA22, Prop. 3.20].

Remark 7.21. The lack of symmetry in the trees in Figure 28 arises from the lack of symmetry inherent in the infix order, and in how the LA and SU diagonal treat maximal and minimal elements. A sufficient condition for the diagonals of a tree t to have the same number of facets is to satisfy, N is a nesting of t if and only if rN is a nesting of t . For a tree satisfying this condition, relabelling its edges via the function $r : [n] \rightarrow [n]$ defined by $r(i) := n - i + 1$ exchanges the number of facets between the LA and SU diagonals.

We have an analogous result for universal tensor products of A_∞ -morphisms. Let A_∞^2 denote the 2-colored operad whose algebras are pairs of A_∞ -algebras together with an A_∞ -morphism between them [LAM23, Sec. 4.4.1]. The datum of a diagonal of the operad A_∞ encoding A_∞ -algebras and a diagonal of the operadic bimodule M_∞ encoding A_∞ -morphisms is equivalent to the datum of a morphism of 2-colored operads $A_\infty^2 \rightarrow A_\infty^2 \otimes A_\infty^2$.

Theorem 7.22. *For any pair of A_∞ -morphisms, the two universal tensor products defined by the LA and SU diagonals are not isomorphic in the category of A_∞^2 -algebras and strict morphisms. However, they are isomorphic in the category of A_∞^2 -algebras and their ∞ -morphisms.*

Proof. Since the two morphisms of topological operadic bimodules on the multiplihedra Δ^{LA} and Δ^{SU} do not have the same cellular image, the tensor products that they define are not strictly isomorphic. However, they are both homotopic to the usual thin diagonal. Recall that the operad A_∞^2 is the minimal model of the operad As^2 , whose algebras are pairs of associative algebras together with a morphism between them [LA22, Prop. 4.9]. Using the universal property of the

minimal model A_∞^2 , one can show that the algebraic diagonals $\Delta^{LA}, \Delta^{SU} : A_\infty^2 \rightarrow A_\infty^2 \otimes A_\infty^2$ are homotopic, in the sense of [MSS02, Sec. 3.10]. Then, by [DSV16, Cor. 2] there is an ∞ -isotopy, that is an ∞ -isomorphism whose first component is the identity, between the two tensor products of A_∞ -morphisms. \square

Remark 7.23. As studied in [LAM23, Sec. 4.4], the above tensor products of A_∞ -morphisms are not coassociative, nor cocommutative. Moreover, there *does not exist* a universal tensor product of A_∞ -morphisms which is compatible with composition [LAM23, Prop. 4.23].

Example 7.24. The LA and SU diagonals of the multiplihedra associated with trees that have less than 4 edges have the same number of facets. However, for linear trees with 5 and 6 internal edges, the number of facets of the LA and SU diagonals differ, as displayed in Table 8. To compute these numbers, we first computed the facets of the LA and SU diagonals of the permutahedra, and then used the projection from the permutahedra to the multiplihedra described in the proof of [Dok11, Thm. 3.3.6].

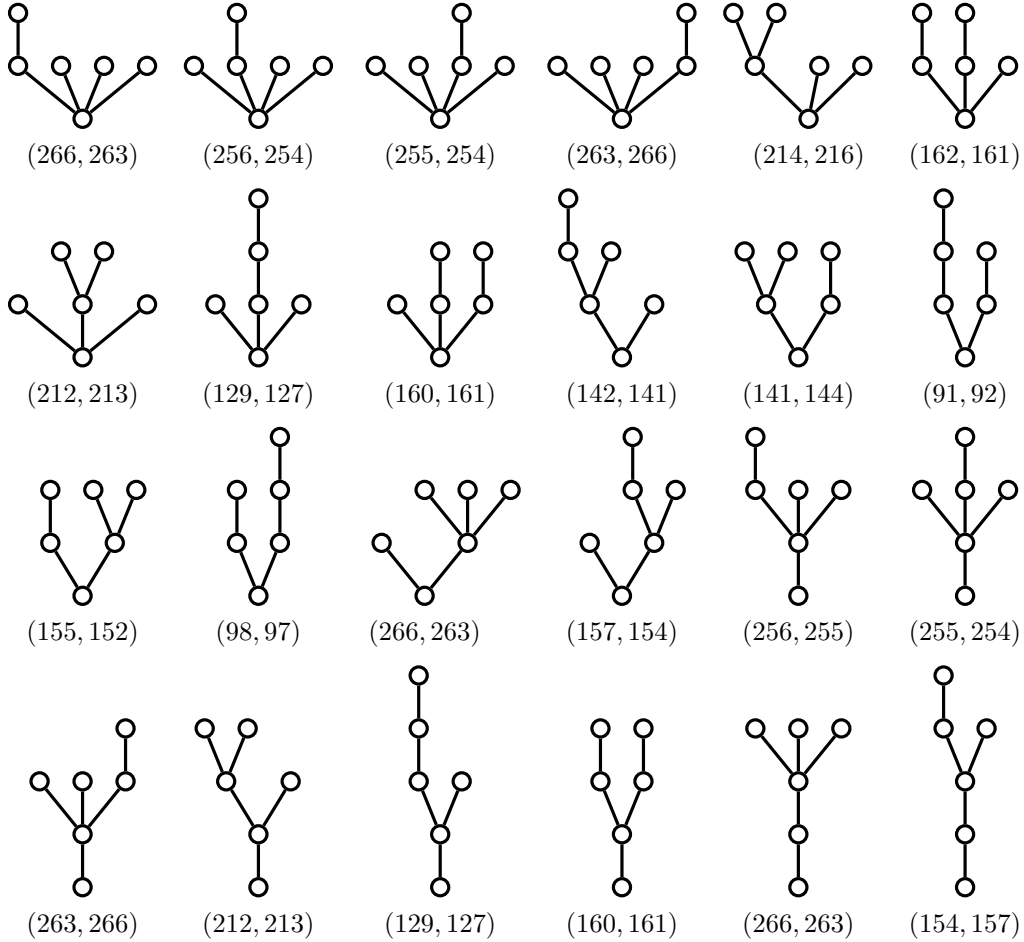


FIGURE 28. The 24 planar trees t with 5 internal edges for which the number of facets in the LA diagonal (left) and the SU diagonal (right) differ.

Internal edges	LA diagonal	LA only	Shared	SU only	SU diagonal
$n = 1$	2	0	2	0	2
$n = 2$	8	0	8	0	8
$n = 3$	42	5	37	5	42
$n = 4$	254	72	182	72	254
$n = 5$	1678	759	919	757	1676
$n = 6$	11790	7076	4714	7024	11738

TABLE 8. Number of facets in the LA and SU diagonals of the multiplihedra, indexed by linear trees with n internal edges.

REFERENCES

- [Bau80] Hans J. Baues. Geometry of loop spaces and the cobar construction. *Mem. Amer. Math. Soc.*, 25(230):ix+171, 1980.
- [BB97] Margaret M. Bayer and Keith A. Brandt. Discriminantal arrangements, fiber polytopes and formality. *J. Algebraic Combin.*, 6(3):229–246, 1997.
- [BCP23] Alin Bostan, Frédéric Chyzak, and Vincent Pilaud. Refined product formulas for Tamari intervals. Preprint, [arXiv:2303.10986](https://arxiv.org/abs/2303.10986), 2023.
- [Ber18] Olivier Bernardi. Deformations of the braid arrangement and trees. *Adv. Math.*, 335:466–518, 2018.
- [Bir95] Garrett Birkhoff. Lattices and their applications. In *Lattice theory and its applications (Darmstadt, 1991)*, volume 23 of *Res. Exp. Math.*, pages 7–25. Heldermann, Lemgo, 1995.
- [BM14] Jonas Bergström and Satoshi Minabe. On the cohomology of the Losev-Manin moduli space. *Manuscripta Math.*, 144(1-2):241–252, 2014.
- [BS92] Louis J. Billera and Bernd Sturmfels. Fiber polytopes. *Ann. of Math. (2)*, 135(3):527–549, 1992.
- [CG71] Wai-Kai Chen and I Goyal. Tables of essential complementary partitions. *IEEE Trans. Circuits and Systems*, 18(5):562–563, 1971.
- [Che69] Wai-kai Chen. Computer generation of trees and co-trees in a cascade of multiterminal networks. *IEEE Trans. Circuit Theory*, CT-16:518–526, 1969.
- [DHP18] Aram Dermenjian, Christophe Hohlweg, and Vincent Pilaud. The facial weak order and its lattice quotients. *Trans. Amer. Math. Soc.*, 370(2):1469–1507, 2018.
- [DKL22] Vladimir Dotsenko, Adam Keilthy, and Denis Lyskov. Reconnectads. Preprint, [arXiv:2211.15754](https://arxiv.org/abs/2211.15754), 2022.
- [Dok11] Jeffrey Samuel Doker. *Geometry of Generalized Permutohedra*. PhD thesis, University of California, Berkeley, 2011.
- [DSV16] Vladimir Dotsenko, Sergey Shadrin, and Bruno Vallette. Pre-Lie deformation theory. *Mosc. Math. J.*, 16(3):505–543, 2016.
- [EM54] Samuel Eilenberg and Saunders MacLane. On the groups $H(\Pi, n)$. III. *Ann. of Math. (2)*, 60:513–557, 1954.
- [FS97] William Fulton and Bernd Sturmfels. Intersection theory on toric varieties. *Topology*, 36(2):335–353, 1997.
- [HP91] Peter Hilton and Jean Pedersen. Catalan numbers, their generalization, and their uses. *Math. Intelligencer*, 13(2):64–75, 1991.
- [Kla70] David A. Klarner. Correspondences between plane trees and binary sequences. *J. Combinatorial Theory*, 9:401–411, 1970.
- [KLN⁺01] Daniel Krob, Matthieu Latapy, Jean-Christophe Novelli, Ha-Duong Phan, and Sylviane Schwer. Pseudo-Permutations I: First Combinatorial and Lattice Properties. 13th International Conference on Formal Power Series and Algebraic Combinatorics (FPSAC 2001), 2001.
- [KUC82] Yoji Kajitani, S. Ueno, and Wai Kai Chen. On the number of essential complementary partitions. *IEEE Trans. Circuits and Systems*, 29(8):572–574, 1982.
- [LA22] Guillaume Laplante-Anfossi. The diagonal of the operahedra. *Adv. Math.*, 405:Paper No. 108494, 50, 2022.
- [LAM23] Guillaume Laplante-Anfossi and Thibaut Mazuir. The diagonal of the multiplihedra and the tensor product of A_∞ -morphisms. *J. Éc. polytech. Math.*, 10:405–446, 2023.
- [Lew99] Richard P. Lewis. The number of spanning trees of a complete multipartite graph. volume 197/198, pages 537–541. 1999. 16th British Combinatorial Conference (London, 1997).
- [Lin16] Matthew Lin. *Graph Cohomology*. PhD thesis, Harvey Mudd College, 2016.
- [LM00] Andrei S. Losev and Yurii I. Manin. New moduli spaces of pointed curves and pencils of flat connections. volume 48, pages 443–472. 2000. Dedicated to William Fulton on the occasion of his 60th birthday.
- [Lod11] Jean-Louis Loday. The diagonal of the Stasheff polytope. In *Higher structures in geometry and physics*, volume 287 of *Progr. Math.*, pages 269–292. Birkhäuser/Springer, New York, 2011.
- [LR13] Jean-Louis Loday and María Ronco. Permutads. *J. Combin. Theory Ser. A*, 120(2):340–365, 2013.
- [LV12] Jean-Louis Loday and Bruno Vallette. *Algebraic operads*, volume 346 of *Grundlehren der mathematischen Wissenschaften [Fundamental Principles of Mathematical Sciences]*. Springer, Heidelberg, 2012.
- [Mar20] Martin Markl. Permutads via operadic categories, and the hidden associahedron. *J. Combin. Theory Ser. A*, 175:105277, 40, 2020.
- [MS89] Yurii I. Manin and V. V. Schechtman. Arrangements of hyperplanes, higher braid groups and higher Bruhat orders. In *Algebraic number theory*, volume 17 of *Adv. Stud. Pure Math.*, pages 289–308. Academic Press, Boston, MA, 1989.
- [MS06] Martin Markl and Steve Shnider. Associahedra, cellular W -construction and products of A_∞ -algebras. *Trans. Amer. Math. Soc.*, 358(6):2353–2372, 2006.
- [MSS02] Martin Markl, Steve Shnider, and Jim Stasheff. *Operads in algebra, topology and physics*, volume 96 of *Mathematical Surveys and Monographs*. American Mathematical Society, Providence, RI, 2002.
- [MTTV21] Naruki Masuda, Hugh Thomas, Andy Tonks, and Bruno Vallette. The diagonal of the associahedra. *J. Éc. polytech. Math.*, 8:121–146, 2021.
- [OEI10] The On-Line Encyclopedia of Integer Sequences. Published electronically at <http://oeis.org>, 2010.

- [Pos09] Alexander Postnikov. Permutohedra, associahedra, and beyond. *Int. Math. Res. Not. IMRN*, (6):1026–1106, 2009.
- [PR06] Patricia Palacios and María O. Ronco. Weak Bruhat order on the set of faces of the permutohedron and the associahedron. *J. Algebra*, 299(2):648–678, 2006.
- [Pro11] Alain Prouté. A_∞ -structures. Modèles minimaux de Baues-Lemaire et Kadeishvili et homologie des fibrations. *Repr. Theory Appl. Categ.*, (21):1–99, 2011. Reprint of the 1986 original, with a preface to the reprint by Jean-Louis Loday.
- [PS00] Alexander Postnikov and Richard P. Stanley. Deformations of Coxeter hyperplane arrangements. volume 91, pages 544–597. 2000. In memory of Gian-Carlo Rota.
- [Rad52] Richard Rado. An inequality. *J. London Math. Soc.*, 27:1–6, 1952.
- [Rot64] Gian-Carlo Rota. On the foundations of combinatorial theory. I. Theory of Möbius functions. *Z. Wahrscheinlichkeitstheorie und Verw. Gebiete*, 2:340–368 (1964), 1964.
- [RS18] Manuel Rivera and Samson Saneblidze. A combinatorial model for the free loop fibration. *Bull. Lond. Math. Soc.*, 50(6):1085–1101, 2018.
- [San09] Samson Saneblidze. The bitwisted Cartesian model for the free loop fibration. *Topology Appl.*, 156(5):897–910, 2009.
- [Sch11] Pieter Hendrik Schoute. *Analytical treatment of the polytopes regularly derived from the regular polytopes. Section I: The simplex.*, volume 11. 1911.
- [Ser51] Jean-Pierre Serre. Homologie singulière des espaces fibrés. Applications. *Ann. of Math. (2)*, 54:425–505, 1951.
- [Shi86] Jian Yi Shi. *The Kazhdan-Lusztig cells in certain affine Weyl groups*, volume 1179 of *Lecture Notes in Mathematics*. Springer-Verlag, Berlin, 1986.
- [Shi87] Jian Yi Shi. Sign types corresponding to an affine Weyl group. *J. London Math. Soc. (2)*, 35(1):56–74, 1987.
- [SU04] Samson Saneblidze and Ronald Umble. Diagonals on the permutahedra, multiplihedra and associahedra. *Homology Homotopy Appl.*, 6(1):363–411, 2004.
- [SU22] Samson Saneblidze and Ronald Umble. Comparing diagonals on the associahedra. Preprint, [arXiv:2207.08543](https://arxiv.org/abs/2207.08543), 2022.
- [Vej07] Mikael Vejdemo-Johansson. Enumerating the Saneblidze-Umbel diagonal terms. Preprint, [arXiv:0707.4399](https://arxiv.org/abs/0707.4399), 2007.
- [Zas75] Thomas Zaslavsky. Facing up to arrangements: face-count formulas for partitions of space by hyperplanes. *Mem. Amer. Math. Soc.*, 1(issue 1, 154):vii+102, 1975.
- [Zie98] Günter M. Ziegler. *Lectures on Polytopes*, volume 152 of *Graduate texts in Mathematics*. Springer-Verlag, New York, 1998.

(Bérénice Delcroix-Oger) INSTITUT MONTPELLIÉRAIN ALEXANDER GROTHENDIECK, UNIVERSITÉ DE MONTPELLIER, FRANCE

Email address: berenice.delcroix-oger@umontpellier.fr

URL: <https://oger.perso.math.cnrs.fr/>

(Guillaume Laplante-Anfossi) SCHOOL OF MATHEMATICS AND STATISTICS, THE UNIVERSITY OF MELBOURNE, VICTORIA, AUSTRALIA

Email address: guillaume.laplanteanfossi@unimelb.edu.au

URL: <https://guillaumelaplante-anfossi.github.io/>

(Vincent Pilaud) CNRS & LIX, ÉCOLE POLYTECHNIQUE, PALAISEAU, FRANCE

Email address: vincent.pilaud@lix.polytechnique.fr

URL: <http://www.lix.polytechnique.fr/~pilaud/>

(Kurt Stoeckl) SCHOOL OF MATHEMATICS AND STATISTICS, THE UNIVERSITY OF MELBOURNE, VICTORIA, AUSTRALIA

Email address: kstoeckl@student.unimelb.edu.au

URL: <https://kstoeckl.github.io/>

REFERENCES

- [AM22] Assar Andersson and Sergei Merkulov. From deformation theory of wheeled props to classification of kontsevich formality maps. *International Mathematics Research Notices*, 2022(12):9275–9307, 2022. arXiv:1911.09089.
- [BD16] Murray R Bremner and Vladimir Dotsenko. *Algebraic operads: an algorithmic companion*. CRC Press, 2016.
- [Ber78] George M Bergman. The diamond lemma for ring theory. *Advances in mathematics*, 29(2):178–218, 1978.
- [BM23] Michael Batanin and Martin Markl. Koszul duality for operadic categories. *Compositionality*, 5(4):56, 2023. arXiv:2105.05198.
- [BV06] John Michael Boardman and Rainer M Vogt. *Homotopy invariant algebraic structures on topological spaces*, volume 347. Springer, 2006.
- [DHR21] Zsuzsanna Dancso, Iva Halacheva, and Marcy Robertson. Circuit algebras are wheeled props. *Journal of Pure and Applied Algebra*, 225(12):106767, 2021. arXiv:2009.09738.
- [DHR23] Zsuzsanna Dancso, Iva Halacheva, and Marcy Robertson. A topological characterisation of the kashiwara–vergne groups. *Transactions of the American Mathematical Society*, 2023. arXiv:2106.02373.
- [DK10] Vladimir Dotsenko and Anton Khoroshkin. Gröbner bases for operads. *Duke Math. J.*, 153(2):363–396, 2010. arXiv:0812.4069.
- [DK13] Vladimir Dotsenko and Anton Khoroshkin. Quillen homology for operads via gröbner bases. *Documenta Mathematica*, 18:707–747, 2013. arXiv:1203.5053.
- [DOLAPS23] Bérénice Delcroix-Oger, Guillaume Laplante-Anfossi, Vincent Pilaud, and Kurt Stoeckl. Cellular diagonals of permutahedra. *arXiv:2308.12119*, 2023.
- [DV21] Malte Dehling and Bruno Vallette. Symmetric homotopy theory for operads. *Algebr. Geom. Topol.*, 21(4):1595–1660, 2021. arXiv:1503.02701.
- [Emp24] Coline Emprin. Kaledin classes and formality criteria. *arXiv preprint arXiv:2404.17529*, 2024.
- [Gal21] Pavel Galashin. P-associahedra. *arXiv preprint arXiv:2110.07257*, 2021.
- [Hof10] Eric Hoffbeck. A poincaré–birkhoff–witt criterion for koszul operads. *manuscripta mathematica*, 131(1):87–110, 2010. arXiv:0709.2286.
- [KW23] Ralph Kaufmann and Benjamin Ward. Koszul Feynman categories. *Proc. Amer. Math. Soc.*, 151(8):3253–3267, 2023. arXiv:2108.09251.
- [LA22] Guillaume Laplante-Anfossi. The diagonal of the operahedra. *Adv. Math.*, 405:Paper No. 108494, 50, 2022. arXiv:2110.14062.
- [LAM23] Guillaume Laplante-Anfossi and Thibaut Mazuir. The diagonal of the multiplihedra and the tensor product of A_∞ -morphisms. *J. Éc. polytech. Math.*, 10:405–446, 2023.
- [Lau24] Paul Laubie. *Combinatorics, homotopy, and embedding of operads*. PhD thesis, Université de Strasbourg, 2024.
- [LV12] Jean-Louis Loday and Bruno Vallette. *Algebraic operads*, volume 346. Springer Science & Business Media, 2012.
- [ML65] Saunders Mac Lane. Categorical algebra. *Bulletin of the American Mathematical Society*, 71(1):40–106, 1965.
- [ML13] Saunders Mac Lane. *Categories for the working mathematician*, volume 5. Springer Science & Business Media, 2013.
- [MMS09] Martin Markl, Sergei Merkulov, and Sergey Shadrin. Wheeled props, graph complexes and the master equation. *Journal of Pure and Applied Algebra*, 213(4):496–535, 2009. arXiv:math/0610683.
- [MPP23] Chiara Mantovani, Arnau Padrol, and Vincent Pilaud. Acyclonestohedra: when oriented matroids meet nestohedra. *in prep*, 2023.
- [MS06] Martin Markl and Steve Shnider. Associahedra, cellular W -construction and products of A_∞ -algebras. *Trans. Amer. Math. Soc.*, 358(6):2353–2372, 2006.
- [MTTV21] Naruki Masuda, Hugh Thomas, Andy Tonks, and Bruno Vallette. The diagonal of the associahedra. *J. Éc. polytech. Math.*, 8:121–146, 2021. arXiv:1902.08059.

- [MV09] Sergeï Merkulov and Bruno Vallette. Deformation theory of representation of prop(erad)s i. *Journal für die reine und angewandte Mathematik*, 634:51–106, 2009. arXiv:0707.0889.
- [Sac23] Andrew Sack. A realization of poset associahedra. *arXiv preprint arXiv:2301.11449*, 2023.
- [Sta63] James Dillon Stasheff. Homotopy associativity of h-spaces. ii. *Transactions of the American Mathematical Society*, 108(2):293–312, 1963.
- [Sto24] Kurt Stoeckl. Koszul operads governing props and wheeled props. *Advances in Mathematics*, 454:109869, 2024.
- [SU04] Samson Sanedidze and Ronald Umble. Diagonals on the permutahedra, multiplihedra and associahedra. *Homology Homotopy Appl.*, 6(1):363–411, 2004. arXiv:0209109.
- [War22] Benjamin Ward. Massey products for graph homology. *International Mathematics Research Notices*, 2022(11):8086–8161, 2022. arXiv:1903.12055.
- [WW16] Nathalie Wahl and Craig Westerland. Hochschild homology of structured algebras. *Advances in Mathematics*, 288:240–307, 2016. arXiv:1110.0651.
- [Zas75] Thomas Zaslavsky. Facing up to arrangements: face-count formulas for partitions of space by hyperplanes. *Mem. Amer. Math. Soc.*, 1(issue 1, 154):vii+102, 1975.